

NASA Contractor Report 3794

NASA-CR-3794 19840018684

Repair Techniques for Celion/LARC-160 Graphite/Polyimide Composite Structures

J. S. Jones and S. R. Graves

**CONTRACT NAS1-16448
JUNE 1984**

LIBRARY COPY

JUL 11 1984

**LANGLEY RESEARCH CENTER
LIBRARY, NASA
HAMPTON, VIRGINIA**

NASA

NASA Contractor Report 3794

**Repair Techniques for
Celion/LARC-160
Graphite/Polyimide
Composite Structures**

J. S. Jones and S. R. Graves
Rockwell International
Downey, California

**Prepared for
Langley Research Center
under Contract NAS1-16448**

NASA
National Aeronautics
and Space Administration
**Scientific and Technical
Information Branch**

1984

FOREWORD

This final report describes the program effort performed by Rockwell International for the National Aeronautics and Space Administration (NASA) Langley Research Center (LaRC) under Contract NAS1-16448 for the development, demonstration, and verification of repair techniques and processes for Celion 6000/LARC-160 graphite/polyimide (GR/PI) composite structures. Viable repair designs and processes were developed for flat laminates, honeycomb sandwich panels, and hat-stiffened skin-stringer panels. The repair methodology was verified through structural element compression tests at room temperature and 315°C (600°F).

The technical monitor for this program was Mr. J. W. Deaton of the NASA LaRC Materials Division. Rockwell performance was under the management of Mr. J. S. Jones (Laboratories and Test) who was also a principal investigator responsible for repair concepts, techniques, materials, and process development and specimen fabrication. Mr. S. R. Graves (Advanced Engineering) was a principal investigator responsible for design, analysis, and data correlation. Major participants in this program were: B. J. Payne, M. Rowley and L. Hegner, specimen fabrication; W. H. Morita, orbiter systems integration; P. J. Hodgetts and F. Roje, NDI techniques development, and R. J. Demonet, S. Collier, and G. Diaz, mechanical properties and structural testing. This report was prepared by the Laboratories and Test and Advanced Engineering Departments of Rockwell's Space Transportation and Systems Group.

Note: Use of commercial products or names of manufacturers in this report does not constitute official endorsement of such products or manufacturer, either expressed or implied, by the National Aeronautics and Space Administration.

CONTENTS

Section		Page
1	INTRODUCTION AND BACKGROUND	1-1
2	TECHNICAL APPROACH	2-1
	2.1 Task 1 — Develop Repair Techniques	2-1
	2.1.1 Subtask 1.1 — Repair Concepts and Analysis	2-1
	2.1.2 Subtask 1.2 — Repair Technique, Process, and NDI Development	2-3
	2.1.3 Subtask 1.3 — Specimen Fabrication NDI and Testing	2-3
	2.1.4 Subtask 1.4 — Verification	2-4
	2.2 Task 2 — Demonstrate Component Repair	2-4
	2.2.1 Subtask 2.1 — Structural Element Repair Verification, NDI, and Testing	2-4
3	DAMAGE CLASSIFICATION AND REPAIR REQUIREMENTS	3-1
4	REPAIR TECHNIQUE, PROCESS, AND NDI DEVELOPMENT	4-1
	4.1 Secondary Midplane Panel Bonding Process Development	4-1
	4.1.1 Midplane Bonding Studies and Adhesive Screening	4-1
	4.1.2 Midplane Bonding Evaluation	4-4
	4.2 Secondary Bond, Flush Scarf Angle Joint Repair Development	4-5
	4.2.1 Specimen Design and Fabrication	4-5
	4.2.2 Flush Scarf Angle Bonding Test and Evaluation	4-11
	4.3 Secondary Bonding Adhesive Selection	4-11
	4.4 Cocure Midplane Panel Bonding Process Development Adhesive Screening, and Evaluation	4-14
	4.4.1 LARC-13 Adhesive/LARC-160 Prepreg Cocure Compatibility Study	4-14
	4.4.2 Initial Midplane Cocure Bonding Process Development	4-16
	4.4.3 In-Situ Imidizing Cocure Process Development	4-16
	4.4.4 Prepreg Resin-Adhesive Cocure Bonding Process Development	4-19
	4.4.5 Process Verification and Lap Shear Testing	4-19
	4.5 Flush Scarf Angle Joint Specimen Cocure Process Development and Verification	4-20

Section

Page

4.5.1	Adhesive Screening and Specimen Fabrication	4-20
4.5.2	Prepreg Adhesive In-Situ Imidize Cocure Process Development	4-25
4.6	Improved Joint Design Process Development	4-25
4.6.1	Improved Joint Design and Process Evaluation	4-28
4.6.2	Tension and NDI Test Results	4-28
4.7	Cocure Bonding Adhesive Process and Design Concept Selection	4-28
4.8	Low Pressure Bonding Study	4-33
4.8.1	Low Pressure Secondary Bonding Development	4-33
4.8.2	Evaluation of Low Pressure Secondary Bonds	4-34
4.8.3	Low Pressure Cocure Bonding Process Development	4-34
5	ANALYTICAL METHODOLOGY DEVELOPMENT	5-1
5.1	Optimum Lap Length — Single Lap Joint	5-1
5.2	Optimum Lap Length — Double Lap Joint	5-8
5.2.1	Double Lap Joint Adhesive Stress Analysis	5-8
5.2.2	Double Lap Joint Peel Stress Analysis	5-12
5.3	Optimum Scarf Angle — Scarf Joint	5-12
5.4	Summary — Analytical Methods Development	5-17
6	FLAT LAMINATE REPAIR	6-1
6.1	Flat Laminate Repair Rationale	6-1
6.2	Flat Laminate Fabrication and Physical Properties Test	6-5
6.3	Flat Laminate Control Element Testing and Results	6-5
6.3.1	Control Element Compression Testing	6-5
6.3.2	Control Element Compression Test Results	6-9
6.4	Analytical Predictions for Flat Laminate Repairs	6-9
6.5	Patch Designs for Repaired Flat Laminate Test Coupons	6-19
6.6	Flat Laminate Repair Methods	6-19
6.7	Repair Installation Results	6-19
6.8	Repaired Element Compression Testing and Results	6-19
6.9	Conclusions — Flat Laminate Repair	6-26

Section		Page
7	HONEYCOMB SANDWICH REPAIR	7-1
7.1	Heavily Loaded Honeycomb Sandwich Repair	7-1
7.1.1	Sandwich Repair Rationale and Concept	7-1
7.1.2	High Temperature Testing Facility	7-4
7.1.3	Heavily Loaded Honeycomb Sandwich Control and Repair Test Methods and Results	7-12
7.1.4	Conclusions - Heavily Loaded Honeycomb Sandwich Repair	7-21
7.2	Lightly Loaded Honeycomb Sandwich Repair	7-21
7.2.1	Baseline Element Fabrication and Prototype Repair	7-27
7.2.2	Maximum Allowable Bonding Pressure Study	7-27
7.2.3	Low Pressure Secondary Bond Repair of Sandwich Panels	7-27
7.2.4	Repair Process Selection	7-31
7.3	Lightly Loaded Honeycomb Sandwich Repair Testing and Results	7-31
7.3.1	Compression Testing	7-31
7.3.2	Control Element Results	7-34
7.3.3	Repaired Element Results	7-34
7.3.4	Conclusions - Lightly Loaded Honeycomb Sandwich Repair	7-41
8	HAT-STIFFENED SKIN-STRINGER REPAIR	8-1
8.1	Hat Stiffened Skin-Stringer Element Repair Development	8-1
8.1.1	Initial Repair Technique and Tooling Approach, Lightly Loaded Skin Stringer	8-1
8.1.2	Improved Repair Techniques and Tooling Concept Development; Repair Technique Approach	8-6
8.1.3	Results of Improved Repair Installations	8-21
8.2	Heavily and Lightly Loaded Hat-Stiffened Skin-Stringer Element Repair Technique and Results	8-21
8.3	Heavily Loaded Hat-Stiffened Element Repair Testing and Results	8-21
8.3.1	Compression Testing	8-21
8.3.2	Control Element Test Results	8-21
8.3.3	Repaired Element Test Results	8-27
8.3.4	Conclusions: Heavily Loaded Hat- Stiffened Panel Repair	8-27

Section		Page
8.4	Lightly Loaded Hat-Stiffened Element	
	Repair Testing and Results	8-32
8.4.1	Control Element Test Results	8-32
8.4.2	Repaired Element Test Results	8-32
8.4.3	Conclusions - Lightly Loaded Hat-Stiffened Panel Repair	8-37
9	SUMMARY AND CONCLUSIONS	9-1
9.1	Adhesive Bonded Joint Processing and Analysis	
	Development	9-1
9.1.1	Secondary Bonding Development	9-1
9.1.2	Cocure Bonding Development	9-2
9.1.3	Concure Scarf Joint Development (Standard and Improved)	9-2
9.1.4	Low Pressure Bonding Development	9-3
9.1.5	Tooling Development	9-3
9.1.6	Analytical Methods Development	9-3
9.2	Flat Laminate Repair	9-4
9.3	Honeycomb Sandwich Repair	9-4
9.4	Hat-Stiffened Skin-Stringer Repair	9-5
10	REFERENCES	10-1
	APPENDIX	
	A. MATERIAL SPECIFICATIONS AND BASELINE LAMINATE FABRICATION PROCESSES	A-1

ILLUSTRATIONS

Figure		Page
1-1	High Temperature Composite Benefits to Orbiter Vehicle. .	1-3
1-2	Orbiter GR/PI Composite Applicants and Potential Weight Savings	1-4
2-1	Technical Approach	2-2
4-1	Midplane Secondary Bonding Process Development Tooling .	4-2
4-2	Midplane Bonded Process Development Panel and Lap Shear Cutting Plan	4-3
4-3	Midplane Bond Panel Specimen Design and Typical Low and High Void Secondary Bond Line Characteristics	4-7
4-4	NDI C-Scan of Typical High and Low Void Midplane Secondary Bonded Laminates	4-8
4-5	Secondary Bonded Flush Scarf Joint Specimen Design and Tooling Concept	4-9
4-6	Adhesive Screening Specimen	4-10
4-7	NDI C-Scans of Secondary Bonded 3-Degree and 4- to 5-Degree Scarf Angle Joint Panels	4-13
4-8	Cross-Section — Cocure Midplane Bonding Tooling and Curing Processes	4-15
4-9	NDI C-Scan Recording of (0, ± 45 , 90), 8-Ply Celion/LARC-160 Imidized Laminate Cocure Bond to Cured Celion/LARC-160 Laminate Using LARC-13 Adhesive	4-17
4-10	Notched Midplane Bonded Test Specimen With Anti-Peel Clamp	4-21
4-11	Cross Sections of Nonadhesive Positive Pressure Cocure Midplane Bonded Panel, EX466	4-22
4-12	NDI C-Scan of Typical Nonadhesive Cocure Bonded Midplane Plane	4-23
4-13	Cross Section of Prepreg Adhesive, In-Situ Imidizing Cocure Scarf Angle Repair Tooling	4-26
4-14	NDI C-Scans of 3-Degree Prepreg Adhesive Cocure Bond Joint	4-27
4-15	Cross Section; Improved Repair Design Concepts 3 Degrees 4.5 Degrees, and 6 Degrees Scarf Angles	4-29
4-16	Average Tensile Strengths of Flush Scarf and Improved Repair Joint Designs	4-30
4-17	NDI C-Scan of Improved Repair 6-Degree Scarf With External Serrated Doublers	4-31
5-1	Lap Joint Geometry	5-3
5-2	Joint Strength Predictions Versus Test Data for LARC-13 .	5-7
5-3	Double Lap Shear Specimen Joint Geometry	5-9
5-4	Theoretical Adhesive Bond Strength Versus Lap Length for Double Lap Joint	5-10
5-5	Scarf-Joint Geometry	5-14
5-6	Scarf-Joint Adhesive and Adherend Potential Strength . .	5-16
6-1	Compression Repair Test Matrix	6-2
6-2	Improved Repair; 6-Degree Scarf Angle With Serrated Octagonal Patch Applied to a Flat Laminate	6-3

Figure		Page
6-3	Flat Laminate Repair 1-Inch Diameter Hole Improved Concept, 6-Degree Scarf With External Octagonal Patch, Serrated Edges	6-4
6-4	NDI C-Scan of Typical (0, ± 45 , 90) 16-Ply Laminate for Flat Panel Repairs	6-6
6-5	NASA LaRC Compression Test Fixture in MTS Machine and Open Fixture With Tested Control Specimen	6-8
6-6	Typical End Failure of Undamaged Control Specimen Without Potted Ends	6-10
6-7	Control Test Coupon With Potted Ends— Typical Failure Mode	6-10
6-8	Control Test Coupon With 2.54 cm (1.00 in.) Hole — Typical Failure Mode	6-11
6-9	Control Test Coupon With 5.08 cm (2.00 in.) Hole — Typical Failure Mode	6-12
6-10	Compression Load/Strain Distribution Through Undamaged Control, Specimen EX425-9	6-13
6-11	Compression Stress/Strain Distribution through Undamaged Control, Specimen EX425-9	6-14
6-12	Compression Load/Strain Distribution Around 2.54 cm (1.00 in.) Diameter Hole, Specimen EX398-3	6-15
6-13	Compression Load/Strain Distribution Around 5.08 cm (2.00 in.) Diameter Hole, Specimen EX397-4	6-16
6-14	Strain Distribution Around 1- and 2-Inch Diameter Holes in a 6-Inch Wide Plate	6-17
6-15	Cross-Sections 1- and 2-Inch Diameter Hole, 3- and 6-Degree Scarf Flush Repairs	6-20
6-16	Cross-Sections, Cocured External Patch Repairs, 1-Inch Diameter Holes	6-21
6-17	Flat Laminate Cocure Repair; 3-Degree Scarf Angle With Prepreg Preform	6-22
6-18	NDI C-Scan of Flat Laminate Cocure 3-Degree Flush Scarf, 2-Inch Hole Repair	6-23
6-19	NDI C-Scan of Flat Laminate Cocure 6-Degree Flush Scarf, 2-Inch Hole Repair	6-24
6-20	NDI C-Scan of Flat Laminate, 6-Degree Scarf Angle With One External Doubler, 1-Inch Diameter Hole Repair	6-25
6-21	3-Degree Scarf Flush Cocure Repair on 5.08 cm (2.00 in.) Diameter Hole; Specimen EX397-5	6-27
6-22	6-Degree Cocure Repair on 5.08 cm (2.00 in.) Diameter Hole; Specimen EX397-3	6-28
6-23	6-Degree Cocure Repair on 2.54 cm (1.00 in.) Diameter Hole; Specimen EX397-X	6-29
6-24	7.62 cm (3.00 in.) Diameter External Cocure Patch on a 2.54 cm (1.00 in.) Diameter Hole; Specimen EX398-5	6-30
6-25	7.62 cm (3.00 in.) Diameter External Cocure Patch 6-Degree Scarf Repair on a 2.54 cm (1.00 in.) Diameter Hole; Specimen EX358-5	6-31

Figure		Page
6-26	Compression Load/Strain Distribution Through Flush Repair Panel, 2-Inch Diameter Hole, 3-Degree Scarf Angle; Specimen EX358-4	6-32
6-27	Compression Load/Strain Distribution Through Flush Repair Panel, 2-Inch Diameter Hole, 3-Degree Scarf Angle; Specimen EX358-8	6-33
6-28	Compression Load/Strain Distribution Through Flush Repair Panel, 2-Inch Hole, 6-Degree Scarf Angle; Specimen EX358-3	6-34
6-29	Compression Load/Strain Distribution through Flush Repair Panel, 1-Inch Diameter Hole, 6-Degree Scarf Angle; Specimen EX358-2	6-35
7-1	Sandwich Panel Baseline Control Compression Subelement Specimen Designs	7-2
7-2	Cocure Repair Design Concept for Heavily Loaded Sandwich Structure Compression Specimen	7-3
7-3	Improved Sandwich Repair Application Technique — Nonadhesive In-Situ Imidize Cocure Process	7-5
7-4	Sandwich Specimen; Heavily Loaded Design Ready for Repair	7-6
7-5	Completed Octagonal Patch Cocure Repair	7-7
7-6	NDI C-Scan of Sandwich Panel Cocure Repair, EX478/484-2	7-8
7-7	Portable Oven, Heat Source and Controls	7-9
7-8	Portable Oven Showing Test Hat-Stringer Element and Base Cooling Plate Details in MTS Test Machine	7-10
7-9	Portable Oven in MTS Test Machine in Test Configuration	7-11
7-10	Heavily Loaded Sandwich Control Specimen EX482/483-4 (0, ± 45 , 90) _{2s} Transverse-Oriented Outer (0) Fibers— Failure Mode	7-14
7-11	Heavily Loaded Sandwich Control Specimen EX482/483-5 (0, ± 45 , 90) _{2s} Transverse-Oriented Outer (0) Fibers— Failure Mode	7-15
7-12	Compression Load/Strain Response of Undamaged Control Specimen at Room Temperature Number 478/484-5	7-16
7-13	Heavily Loaded Sandwich Damaged Control Specimen With 2-Inch Diameter Hole and Parallel Oriented Outer Fibers	7-17
7-14	Compression Load/Strain Distribution Around 5.08 cm (2 in.) Diameter Hole at Room Temperature; Specimen EX478/484-3	7-18
7-15	Compression Load/Strain Distribution Around 5.08 cm (2.00 inch) Diameter Hole; Specimen EX496/494-4 at 600°F	7-19
7-16	Strain Distribution Around 2-Inch Diameter Hole in Specimens EX478/484-3 and EX496/494-4 (Applied Stress 15 ksi)	7-20
7-17	Heavily Loaded Sandwich Specimen Repair EX482/483-3 (0, ± 45 , 90) _{2s} Transverse-Oriented Outer (0) Fibers — Failure Mode	7-22
7-18	Heavily Loaded Sandwich Specimen Repair EX482/483-2 (0, ± 45 , 90) _{2s} Transverse-Oriented Outer (0) Fibers — Failure Mode	7-23

Figure		Page
7-19	Heavily Loaded Sandwich Specimen Repair EX483/483-1 (0, ± 45 , 90) _{2s} Transverse-Oriented Outer (0) Fibers – Failure Mode	7-24
7-20	Heavily Loaded Sandwich Specimen Repair EX478/484-1 – Failure Mode	7-25
7-21	Strain Response of Repaired Heavily Loaded Sandwich Specimens at Room Temperature and 600°F	7-26
7-22	Secondary Bond Repair, Lightly Loaded Sandwich Structure Compression Element Design Concept	7-28
7-23	Cocure Repair, Lightly Loaded Sandwich Structure Compression Element Design Concept	7-29
7-24	Secondary Bond Sandwich Repair Application Technique – Lightly Loaded Design	7-30
7-25	Compression Load/Strain Response of Lightly Loaded Sandwich Panels (Undamaged Control) at Room Temperature and 600°F	7-32
7-26	Strain Response of Cocure Repaired Lightly Loaded Sandwich Panels at Room Temperature and 600°F	7-33
7-27	Lightly Loaded Sandwich Control Specimen EX485/486-3P – Failure Mode	7-36
7-28	Lightly Loaded Sandwich Panel – Room Temperature Control Specimen With a 5.08 cm (2 in.) Diameter Hole Typical Failure Mode (EX485/486-2T)	7-37
7-29	Typical Failure Mode Specimen EX485/485-1T, Room Tempera- ture Test, Secondary Bond Doubler Repair, Lightly Loaded Sandwich Panel	7-40
7-30	Typical Failure Mode Specimen EX485/486-2P Room Temperature Test, Cocure Doubler Repair, Lightly Loaded Sandwich Panel	7-39
7-31	Typical Failure Mode Specimen EX367/368-6, 600°F Test, Cocure Flush Repair, Lightly Loaded Sandwich Panel	7-40
8-1	Hat-Stiffened Skin Subelement Specimen Design	8-2
8-2	Initial Hat-Stringer Repair Bagging Concept	8-3
8-3	Cross-Section – FMC 165 Rubber Bladder Molding Concept	8-5
8-4	Damaged Hat	8-7
8-5	Machined 3-Degree Taper for Scarf Joint	8-8
8-6	Secondary Bond Premolded Internal Support	8-9
8-7	Application of Vacuum Formed Flat Preforms and Cap Elements Repaired Hat Section	8-10
8-8	Lightly Loaded Hat-Stiffened Skin Stringer Element Hat Web Scarf Angle Grinding Operation	8-11
8-9	Lightly Loaded Hat-Stiffened Skin Stringer Element Hat Cap Scarf Angle Grinding Operation	8-12
8-10	Split Internal Hat Support Ready Job Assembly	8-13
8-11	Split Internal Hat Support Installed, Ready to Close	8-14
8-12	Split Internal Hat Support Installation Complete	8-15
8-13	0 Degree Cap Element and Preformed Flat Doubler Ready for Installation	8-16
8-14	Hat Doubler Preform Installed	8-17
8-15		8-18

Figure		Page
8-16	Fluoro Rubber Pressure Caul Being Installed Over Hat Doubler Patch	8-19
8-17	Completed Repair of Hat-Stiffened Element, Lightly Loaded Design	8-20
8-18	Heavily Loaded Stringer Repair — Internal Support and Patch Design	8-22
8-19	Lightly Loaded Stringer Repair — Internal Support and Patch Design	8-23
8-20	Lightly Loaded Hat-Stiffened Skin Stringer Undamaged Control Specimen, Typical Failure Mode	8-24
8-21	Heavily Loaded Hat-Stiffened Skin-Stringer Undamaged Control Specimens — Typical Failure Mode	8-26
8-22	Compression Load/Strain Response of Heavily Loaded Hat- Stiffened Panels (Undamaged Control) at Room Temperature and 600°F	8-28
8-23	Typical Failure Mode — Heavily Loaded Hat-Stiffened Skin Stringer Repaired Panel Tested at Room Temperature, Specimen EX493-2	8-29
8-24	Compression Load/Strain Response of Repaired, Heavily Loaded Hat-Stiffened Panels at Room Temperature and 600°F	8-30
8-25	Failure Mode of Heavily Loaded Repaired Hat Stringer Element Tested at 316°C (600°F)	8-31
8-26	Room Temperature Compression Failure Modes of Repaired Lightly Loaded Hat-Stiffened Skin-Stringer Panel EX247-2	8-34
8-27	Compression Load/Strain Response of Repaired Lightly Loaded Hat-Stiffened Panels at Room Temperature and 600°F	8-35
8-28	Failure Mode of Lightly Loaded Repaired Hat Stringer Element Tested at 316°C (600°F)	8-36

1. The first part of the document is a list of the names of the persons who have been named in the proceedings.

2. The second part of the document is a list of the names of the persons who have been named in the proceedings.

3. The third part of the document is a list of the names of the persons who have been named in the proceedings.

4. The fourth part of the document is a list of the names of the persons who have been named in the proceedings.

5. The fifth part of the document is a list of the names of the persons who have been named in the proceedings.

6. The sixth part of the document is a list of the names of the persons who have been named in the proceedings.

7. The seventh part of the document is a list of the names of the persons who have been named in the proceedings.

8. The eighth part of the document is a list of the names of the persons who have been named in the proceedings.

9. The ninth part of the document is a list of the names of the persons who have been named in the proceedings.

10. The tenth part of the document is a list of the names of the persons who have been named in the proceedings.

11. The eleventh part of the document is a list of the names of the persons who have been named in the proceedings.

12. The twelfth part of the document is a list of the names of the persons who have been named in the proceedings.

13. The thirteenth part of the document is a list of the names of the persons who have been named in the proceedings.

14. The fourteenth part of the document is a list of the names of the persons who have been named in the proceedings.

15. The fifteenth part of the document is a list of the names of the persons who have been named in the proceedings.

16. The sixteenth part of the document is a list of the names of the persons who have been named in the proceedings.

17. The seventeenth part of the document is a list of the names of the persons who have been named in the proceedings.

18. The eighteenth part of the document is a list of the names of the persons who have been named in the proceedings.

19. The nineteenth part of the document is a list of the names of the persons who have been named in the proceedings.

20. The twentieth part of the document is a list of the names of the persons who have been named in the proceedings.

TABLES

Table		Page
3-1	Defects Common to Composite Structures	3-2
3-2	Damage Modes Versus Candidate Repair Methods	3-3
4-1	Cure Cycle Development Matrix and Candidate Adhesives	4-4
4-2	Average Secondary Midplane Adhesive Bonded Tensile Shear Properties at Room Temperature and 316°C	4-6
4-3	Secondary Bonded Flush Scarf Angle Joint Repair Specimen Average Tensile Shear Strengths at Room Temperature and 316°C	4-12
4-4	Average Tensile Shear Properties of Cocure Midplane Bonded Celion/LARC-160 Laminates at Room Temperature and 316°C	4-18
4-5	Cocure Bonded Flush Scarf Joint Angle Repair Specimen Average Tensile Shear Strengths at Room Temperature and 316°C	4-24
4-6	Results of Improved Repair Joint Design Tension Tests at Room Temperature and 600°F	4-32
4-7	Tensile Shear Strengths of Low Pressure Secondary Midplane Bonded Celion/LARC-160 Laminates at Room Temperature and 316°C	4-35
5-1	Effect of Overlap Length on LARC-13 Lap Shear Strength (Room Temperature)	5-2
5-2	Adherend and Adhesive Properties Used in Lap Shear Data Correlation	5-6
5-3	Lap Length Overall Efficiency	5-6
5-4	Adherend and Adhesive Properties Used in Double Lap Joint Analysis	5-12
5-5	Scarf-Joint Test Data - Average Room Temperature	5-14
6-1	Celion/LARC-160 Flat Laminate Repair Room Temperature Compression Test Results	6-7
6-2	Updated Analytical Failure Predictions and Actual Test Results	6-18
7-1	Test Results For Heavily Loaded Honeycomb Sandwich Control and Repaired Elements	7-13
7-2	Test Results For Lightly Loaded Sandwich Control and Repaired Elements	7-35
8-1	Test Results For Heavily Loaded Hat-Stiffened Skin Stringer Control and Repaired Elements	8-25
8-2	Test Results For Lightly Loaded Hat-Stiffened Skin Stringer Control and Repaired Elements	8-33

1. INTRODUCTION AND BACKGROUND

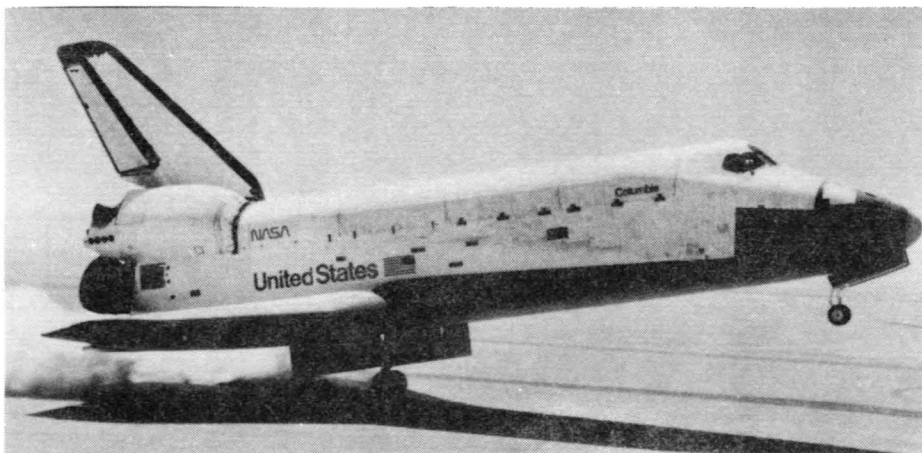
To improve performance and increase recoverable payload capability, the Space Shuttle orbiter and the next generation of reusable space vehicles will require the development of primary and secondary 600°F operational structures that are significantly lighter than those produced from conventional aluminum or titanium alloys. The 600°F operational capability will allow a significant decrease in thermal protection system (TPS) weight.

Continuing research and development programs have demonstrated that the most promising way to achieve the weight-saving goal is by using graphite filament reinforced polyimide matrix composite materials. Structural and thermal analyses show a 25 to 35 percent weight savings can be achieved on Space Shuttle orbiter components and TPS if a graphite/polyimide (GR/PI) composite material system capable of 600°F service could be implemented as a substitute for the baseline aluminum structural material. Predicted weight savings are based on the superior strength and stiffness-to-density ratios of GR/PI composite material over metallic counterparts. Specific strength and stiffness properties of Celion/LARC 160 composite laminates are compared with aluminum and titanium alloys in Figure 1-1. Typical retrofittable and non-retrofittable orbiter component candidates, shown in Figure 1-2, include elevons, aft body flap, landing gear doors, vertical fin, wings, and fuselage sections totaling weight savings greater than 14,000 pounds. To achieve this weight savings goal, the Composites for Advanced Space Transportation Systems (CASTS) project was initiated by NASA-LaRC in 1976 to develop materials, processes, design, manufacturing, and nondestructive inspection (NDI) technologies for a new generation of polyimide resin systems reinforced with graphite fiber.

In order for the GR/PI material system to be acceptable for use in advanced space transportation systems, it is necessary that fabricated components be maintained in both an economical and safe manner. It is inevitable that with planned usage of these structural components, damage will occur either in the form of intrinsic flaw growth, mechanical damage, or in-service deterioration. For example, voids and blisters are classified as intrinsic defects that are built-in during the manufacturing process. Mechanical damage can result from excessive loads, impact during handling, ballistic penetration, overheating, and numerous other causes. In-service deterioration can result from environmental damage such as weathering, moisture, lightning exposure, and rain erosion. The need to develop repair techniques and processes for GR/PI structural components is readily apparent.

This development program is specifically directed toward repairing Celion/LARC-160 GR/PI composite structures representing spacecraft and aircraft component hardware capable of 600°F service. Baseline components requiring repair development include flat laminates and adhesive-bonded sandwich and hat-stiffened skin-stringer components. Operating temperature range of baseline components and repair areas is -78°C (-170°F) to 316°C (600°F) for one orbiter lifetime of 125 hours.

The primary objectives of this research and development program are to develop and document materials, processes, and techniques for making repairs to defects and damage in structural elements fabricated from Celion/LARC-160 composites, which are representative of typical construction details for advanced space transportation systems and aircraft. For these objectives to be accomplished requires the development of repair techniques, processes, and analytical design techniques, and requires the demonstration of the quality of repair concepts of nondestructive evaluation and mechanical and structural tests.



- REDUCE STRUCTURE & TPS WEIGHT
25 TO 35%

- LARGE STRENGTH & STIFFNESS/WT RATIO
- ALLOWS STRUCTURE/TPS INTERFACE TEMPERATURE INCREASE FROM 350 TO 600°F
- ALLOWS DIRECT BOND OF TPS TO STRUCTURE

- MOST IMPORTANT INCREASES ORBITER RECOVERABLE WEIGHT

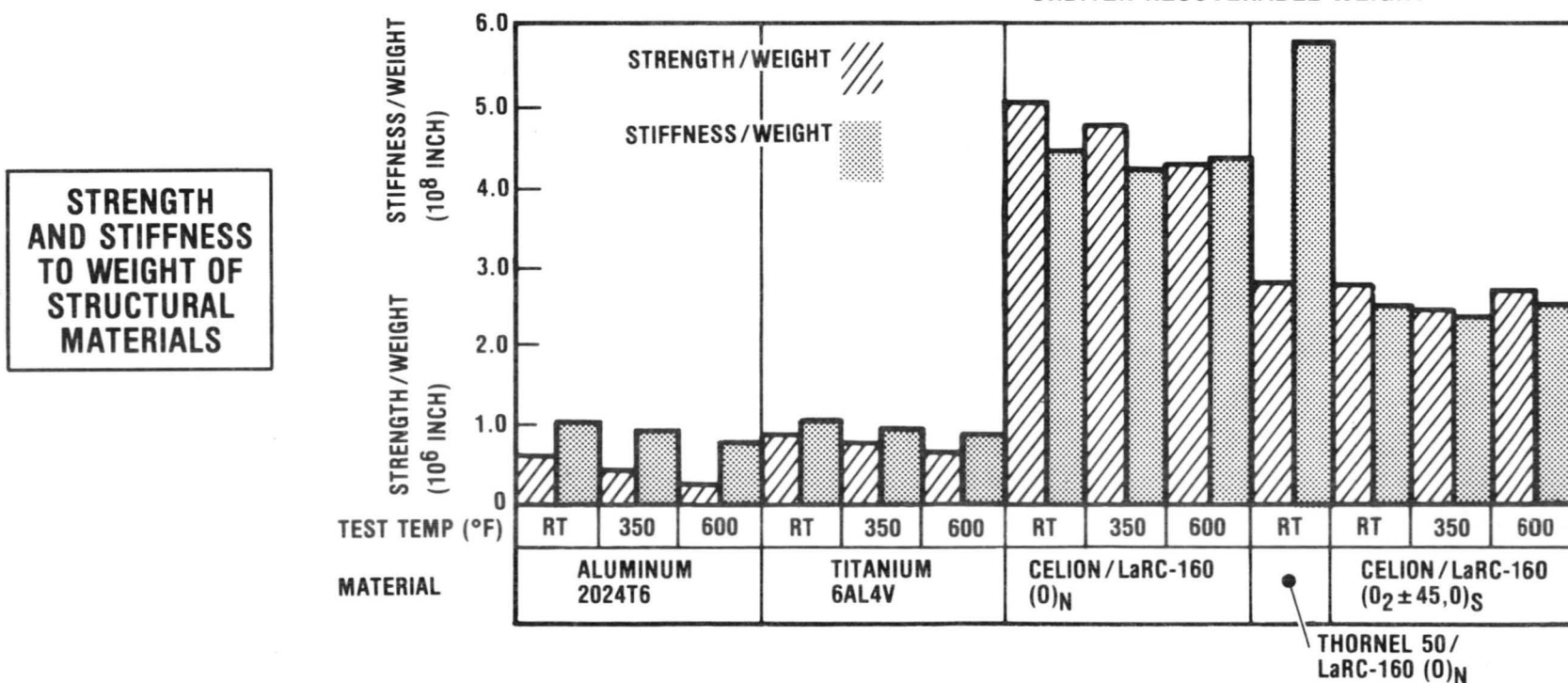


Figure 1-1. High Temperature Composite Benefits to Orbiter Vehicle

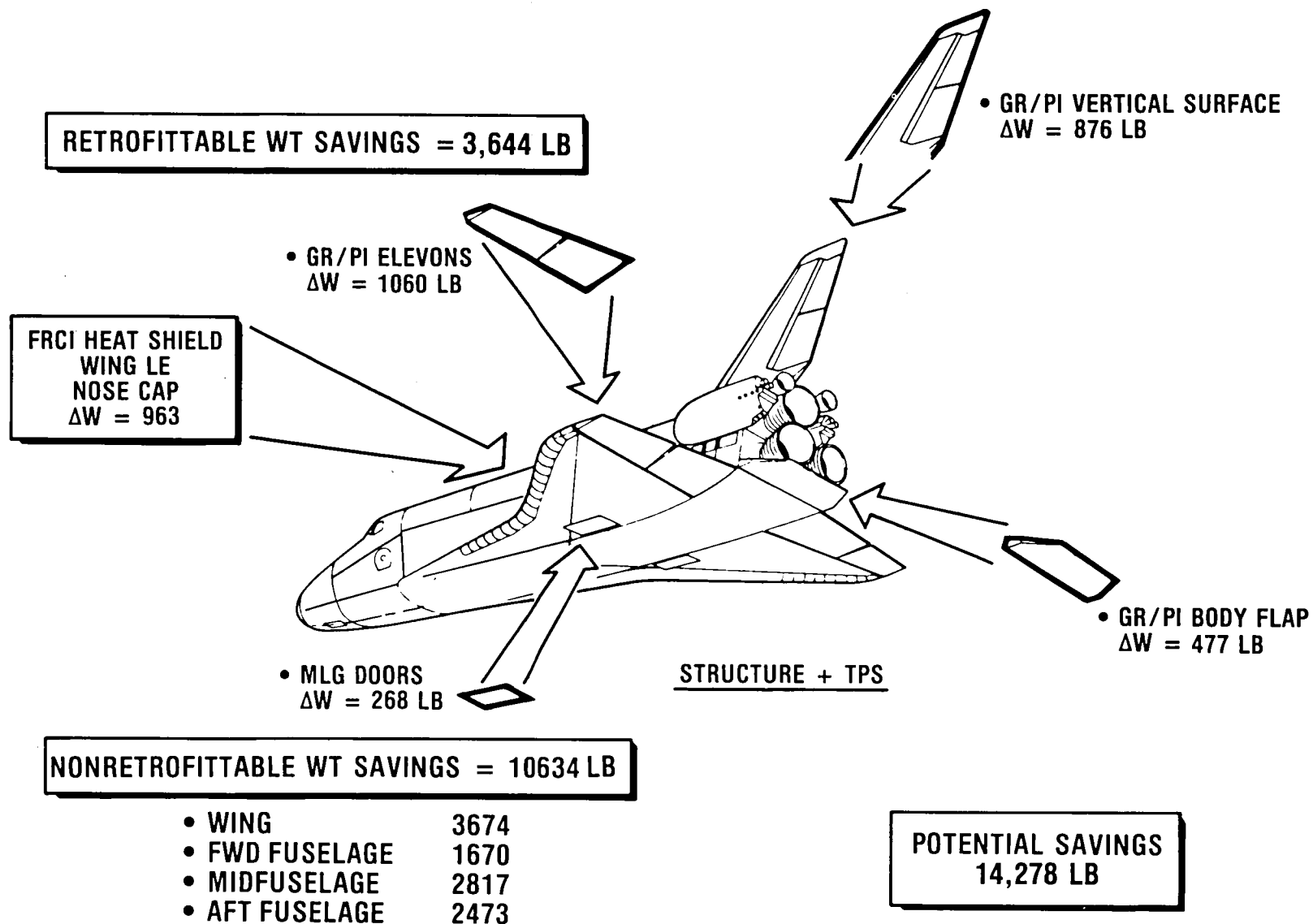


Figure 1-2. Orbiter GR/PI Composite Applicants and Potential Weight Savings

2. TECHNICAL APPROACH

The approach followed in developing repair techniques and processes for Celion/LARC-160 composite structures consists of two tasks: Task 1 — develop repair techniques, and Task 2 — demonstrate component repair. During the program, each subelement repair design concept defined in Task 1.1 was fabricated and tested to confirm the scale-up of the repair technique developed on coupons in Task 1.2. As a result of a program orientation meeting held at NASA LaRC on October 23, 1980, specific guidelines were established for the repair program approach. The same approach specified in the proposal to the development of repair techniques under Task 1 and demonstration of component repair under Task 2 was followed, except that curing processes were performed in an autoclave. All elements were designed for compression loading.

The repair development program addresses both heavily and lightly loaded structural element categories. Selected repair designs and concepts were applied to these structures.

The specific approach followed in developing repair techniques and processes for Celion/LARC-160 structure is illustrated in Figure 2-1 and consisted of two major tasks described in the following.

2.1 TASK 1 — DEVELOP REPAIR TECHNIQUES

This task consisted of the following four subtasks.

2.1.1 Subtask 1.1 — Repair Concepts and Analysis

Under this task, test coupons, subelement repair concepts, and associated analysis techniques were developed. Analysis techniques were based on coupon test data and extended to design of repairs for the subelements.

2.1.2 Subtask 1.2 — Repair Technique, Process, and NDI Development

This subtask was used to develop the basic techniques for repairing flat laminate, honeycomb sandwich, and hat-stringer stiffened skin elements using small specimens representing these structures. Celion/LARC-160 composite fabrication and adhesive bonding technology developed on NASA LaRC Contract NAS1-15371 (Reference 1), and Rockwell IR&D was used as baseline for fabrication of the basic structural laminates, adhesive bonded sandwich, and skin/stringer coupons and elements. Repair quality is of prime importance; therefore, the target was to regain the maximum possible composite structural integrity.

NDI C-scan technology developed by NASA LaRC and Rockwell on the above contracts and IR&D programs, was employed in evaluating the quality of control specimens and repair areas after each operation.

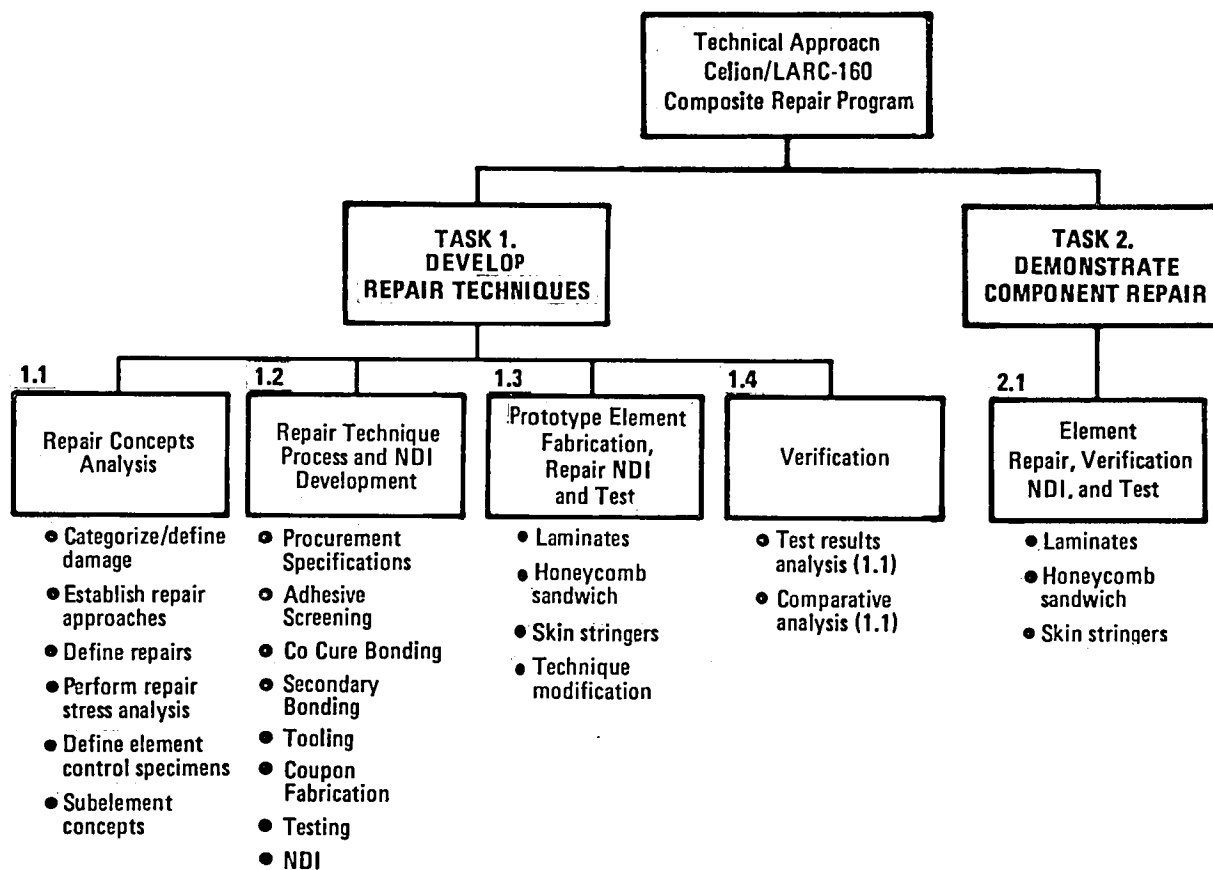


Figure 2-1. Task Breakdown Structure

Preliminary evaluation of repair concepts being developed was accomplished using lap shear type specimens. This series of tests demonstrated compatibility of adhesive materials with Celion/LARC-160 prepreg and laminate stock as employed in cocure and secondary bonding operations.

2.1.3 Subtask 1.3 — Specimen Fabrication, NDI, and Testing

Element specimens representing the three basic structures were fabricated using standard processes. Standard LaRC A-sensitivity NDI C-scan testing was performed on all specimens through the various phases of fabrication to ensure high quality. Target laminate and bond joint C-scan quality is 100 percent sound penetration. Physical properties tests were performed on laminates to determine density, resin content, fiber, and void volumes. Target composite physical properties were less than 1 percent void volume and 60 percent ± 2 fiber volume.

All three element specimens were 6 inches wide and 12 inches long. Repairs were made on structural element specimens using the best procedures developed in Subtask 1.2 studies. NDI testing methods were employed in evaluating repair quality.

Control specimens of each structural type were fabricated and used as baseline comparators for repair analysis and evaluation during development and verification phases.

Back-to-back axial strain gages were installed on repair development element specimens to provide alignment data in adjusting the test fixtures using load/strain data during compression test. Additional strain gages were installed within and around the repair area as required to provide load and strain transfer data.

Compression tests were performed on control and repaired specimens at room temperature and 316°C (600°F). Criteria for evaluation was based on the ability of individual repaired specimens to carry the test load through and around the repair and to attain a load approximating the control specimens.

2.1.4 Subtask 1.4 — Verification

Verification of the repair techniques was made through data correlation of the Subtask 1.3 tests. Test results were analyzed in conjunction with the subelement requirements and compared with the predicted load for verification. Through an iterative process with the above subtasks, design, analysis, and processing techniques were modified to achieve the optimum repair methodology to be used in Task 2.

2.2 TASK 2 — DEMONSTRATE COMPONENT REPAIR

This task consisted of the following two subtasks.

2.2.1 Subtask 2.1 — Structural Element Repair Verification, NDI, and Testing

Flat laminate, honeycomb sandwich, and hat-stringer elements were fabricated and repaired using the best techniques developed under Task 1. These elements were used to verify the repair structural integrity. Single repaired subelements were compression tested at room temperature and 316°C (600°F). Criteria for evaluation of the test data was based on the ability of the repair to approach the ultimate strength of the control elements tested in Subtask 1.3.

3. DAMAGE CLASSIFICATION AND REPAIR REQUIREMENTS

The initial step in the repair process is the classification of the damage type, and an assessment of the extent of the damage. The extent of the damage can be determined by visual inspection in combination with ultrasonic C-scan. Damage or other laminate anomalies are classified as follows:











1. Negligible. Negligible damage is damage that requires no rework other than possible cosmetic surface refinishing. This damage may consist of minor dents, scratches, or voids that will result in no degradation of structural performance, based on damage tolerance studies.
2. Repairable. Repairable damage is damage that requires rework of various degrees to return the component to full flight status. Repairable damage types are defined in Table 3-1, and classified according to damage cause. For example, voids and blisters are classified as intrinsic defects that are built-in during the manufacturing process. Other defects result from mechanical damage during service, or from in-service deterioration. Mechanical damage can result from excessive loads, ballistic penetration, impact during handling, overheating, and numerous other causes. In-service deterioration can result from environmental damage such as lightning exposure, weathering, moisture, and rain erosion.
3. Nonrepairable. Nonrepairable damage is classified as damage in which the structure cannot be restored to a satisfactory condition, whether because of cost considerations or technical limitations. This class of damage requires the removal and replacement of the damaged parts.

During this study, repair concepts were developed and evaluated for three general structural categories: flat laminates, honeycomb sandwich panels, and hat-stiffened panels. The repairs developed for flat laminates are also applicable to the sandwich panel skin and to the hat section. Honeycomb sandwich panels are subject to variable damage situations: core crushing or buckling, node bond separation, skin-to-core debonding, top skin penetration and core breakage, and total penetration through the sandwich structure. The prevalent damage types associated with the three basic structures are given in Table 3-2 along with candidate repair concepts. A particular repair type may apply to many types of damage. The repair concepts for a fracture, gouge, penetration, or splinter of a laminate are identical. Damage to advanced composites may also appear as a combination of several distinct damage modes. For example, laminate penetration is often accompanied by splintering, cracking, or delamination. Note that laminate repairs shown in Table 3-2 also apply to the honeycomb panels and to the hat or skin/stringer panels.

Table 3-1. Defects Common to Composite Structures

Defect	Definition and Probable Cause	Defect Class. ¹
Void	An open area contained within the laminate; no apparent changes in laminate thickness; generally small. Caused by volatile entrapment during cure.	1
Blister	A raised area, pillow-like, soft, can be depressed by light pressure, close to the laminate outer surface. Caused by a partial entrapment of volatiles during cure.	1
Delamination	Separation of adjacent composite plies. Caused by rough handling, poor interlaminar adhesion, or improper machining procedures.	1, 2, 3
Debond	Separation at an adhesive bond line. Caused by improper processing, marginal adhesive, built-in bonding stresses, and, for honeycomb structure, the intrusion and freezing of moisture.	1, 2, 3
Core Damage	Core cell walls wrinkled or buckled. Core cell walls ruptured or split. Debond of core ribbon at the node bond caused by improper processing, design loads exceeded, impact damage.	1, 2, 3
Fracture/ Splintering	Cracks in laminate matrix or matrix and fiber; combined cracking and delaminating of laminate outer fibers caused by improper handling, mechanical minor impact.	2, 3
Abrasion	A wearing away of the laminate surface; may extend into fiber. Caused by environmental conditions (rain, dust, etc.) mechanical (misfit, oversanding, etc.)	1, 2, 3
Recess	Molded in depression in a laminate. Caused by foreign object on mold surface.	1
Scratch	Elongated surface discontinuity that is small in width compared to length. Caused by contact with sharp-edged object.	1, 2, 3
Erosion	Surface abrasion. Caused by natural environment (e.g., rain, dust, dirt, hail, etc.).	3
Porosity	Similar to voids only microscopic in size.	1
Gouge	Elongated surface discontinuity extending through one or several laminate plies removing matrix and fiber. Caused by tool damage in machining or contact with a sharp object.	1, 2, 3
Penetration	Breaking through of a laminate surface or bonded honeycomb panel (top skin into core or totally through the panel). Caused by impact.	1, 2, 3
Matrix Degradation	Breakdown of the matrix material caused by chemical attack or excessive and local exposure to high heat.	2, 3
Matrix/Fiber Degradation	Breakdown of the composite structure due to sonic and/or mechanical fatigue.	3
¹ 1 = intrinsic; 2 = mechanical; 3 = degradation		

Table 3-2. Damage Modes Versus Candidate Repair Methods

			Candidate Repair Concepts									
			Surface Coat/Refinish	Partial Penetration Patch (Flush Surface)	Partial Penetration Patch (Non-Flush Surface)	Full Penetration Patch (Two Flush Surfaces)	Full Penetration Patch (One Flush Surface)	Full Penetration Patch (No Flush Surface)	Partial Core Replacement	Full-Depth Core Replacement	Sandwich Panel Section Replacement	Stringer Rebond
												
Damage Mode												
Skin/Stringer	Stringer Debond											●
	Bond Line Porosity											●
	Sandwich Panel	Abrasion	●									
		Erosion	●									
		Scratch	●									
		Delamination				▲ ▲	▲ ●	●				
		Porosity/Void				▲ ▲	▲ ●	●				
		Recess	▲ □	▲ ●	▲ ●	▲ ▲	▲ ●	●				
		Fracture	▲			▲ ▲	▲ ●	●				
		Gouge		▲ ▲	▲ ▲	▲ ▲	▲ ●	●	●			
		Penetration				▲ ▲	▲ ●	●	●			
		Splintering			▲ ▲	▲ ▲	▲ ●	●				
		Matrix Degradation				▲ ▲	▲ ●	●				
		Core Debond							●	●	●	
		Core Penetration							●	●	●	
		Core Degradation								●	●	
		Bond Line Porosity							●	●	●	
	Laminate											

- △ Thick laminate only
- Feasible repair technique
- No plies fractured
- ▲ Face sheet only involved (honeycomb)

Repair concepts under development are categorized as either one-sided or two-sided, and are either flush or with some protuberance to the surface. The type of repair to be used will be based on criteria to be developed from consideration of several design parameters, many of which are discussed in detail in Reference 2. These parameters are discussed in the following:

1. The primary function of a structural repair is to restore adequate strength and stiffness to allow the damaged component to return to full flight status. In practical aerospace applications many structures are lightly loaded stiffness critical components. Thus, a repair that will return 80 percent of the structure ultimate strength may be considered an adequate repair. The efficiency of the repair should be based not only on strength, but also on added weight to the vehicle. Maximum strength repairs with minimum weight gain are requirements for an optimum design. As outlined in Reference 3, the following criteria can be used in choosing the best candidate design for repairing a structure.

The joint efficiency in terms of load is defined as

$$E_L = \frac{L_j}{L_c}$$

where

L_j is the load capability of the joint
 L_c is the load capability of the continuous member

The joint efficiency in terms of weight is defined as

$$E_w = \frac{W_c}{W_j}$$

where

W_c is the weight of the continuous member
 W_j is the weight of the joint

The overall joint efficiency is given below:

$$E_T = E_L \times E_w$$

An optimum efficiency for the joint would approach 1.0.

2. In many aerospace applications, protuberances on aerodynamic surfaces are undesirable. In these applications flush repairs are required.

3. In general, if enough material is added to the repair area the original strength of the structure can be returned; however, in aerospace applications maximum strength repairs with minimum weight gain are the requirements for an optimum design.
4. Because of the thermal strain incompatibility between GR/PI and metals, metallic patches and bolted repairs are not practical for repairs of GR/PI in -78°C to 316°C (-170°F to 600°F) temperature range applications.
5. Repairs should be designed to last the lifetime of the part. Fatigue, creep, and other time dependent variables should be considered in the repair design.
6. The type of repair to be made will greatly depend on the accessibility of the damaged area, i.e., whether to use a one-sided or two-sided repair.
7. The laminate thickness should be considered in the repair design. Scarf repairs are not practical for very thin laminates, while doublers are very inefficient for thick laminate repair.
8. Cost will be a factor in determining whether or not the structure should be repaired. It could also be a factor in choosing an elaborate but efficient repair, or a less costly but less efficient repair.

4. REPAIR TECHNIQUE, PROCESS, AND NDI DEVELOPMENT

This section addresses the development of basic techniques for repairing flat laminate, honeycomb sandwich, and hat-stringer stiffened skin elements. Celion/LARC-160 composite fabrication and adhesive bonding technology previously developed (Reference 1), and IR&D was used as baseline for fabrication of the basic structural laminate coupons. Basic laminate fabrication procedures and prepreg and laminate quality assurance data are described in Appendix A.

Repair quality is of prime importance; therefore, the target was to regain the maximum possible composite structural integrity. NDI C-scan was employed in evaluating the quality of control specimens and repair areas after each operation. Preliminary mechanical testing of repair concepts being developed were accomplished using lap shear type specimens. This series of tests demonstrated compatibility characteristics of adhesive materials with Celion/LARC 160 prepreg and laminate stock as employed in cocure and secondary bonding operations.

4.1 SECONDARY MIDPLANE PANEL BONDING PROCESS DEVELOPMENT

4.1.1 Midplane Bonding Studies and Adhesive Screening

Processing studies on the candidate adhesives shown in the cure cycle development matrix, Table 4-1 were performed in an autoclave using 84 KN/m^2 (25 in. Hg) vacuum and 689 and $1,378 \text{ KN/m}^2$ (100 and 200 psi) pressures, which simulated, in principle, the repair tooling operating characteristics and application in factory-type facilities. The tooling concept is shown in Figure 4-1.

Secondary bonding process evaluations were performed on 15.2 by 15.2 by 0.165 cm (6 by 6 by 0.065 in.) thick $(0, \pm 45, 90)_S$ quasi-isotropic and $(0_2 \pm 45, 0)_S$ Celion/LARC-160 laminates, representing large faying surface area bonds that will be encountered in repair operations. Faying surfaces were prepared by abrasion, water rinsing, and water breakfree testing in deionized water. Specimens were thoroughly dried prior to applying adhesive materials.

The adhesives under investigation were coated on 104- and 108-style fiberglass fabric carriers, which in turn were applied to one laminate faying surface. The second laminate was then assembled to the adhesive surface of the base laminate, closing the midplane bondline. Adhesive cure and freestanding posture were accomplished per the cycles described in Table 4-1 and Figure 4-1. One slot was cut in each face of the bonded panel, through the adhesive layer, forming a 1.27 cm (0.50-in.) lap shear joint (see Figure 4-2). Slotted panels were then cut into 2.54 cm (1.0 in.) wide lap shear specimens.

VACUUM + POSITIVE PRESSURE SECONDARY BONDING AUTOCLAVE CURE CYCLE
<ol style="list-style-type: none"> 1. APPLY 100 OR 200 PSI AUTOCLAVE PRESSURE 2. RAISE TEMPERATURE TO 550F OR 600F AT 3-5F/MINUTE 3. CURE 3 HOURS AT 550F OR 600F 4. FORCE COOL TO <150F PRIOR TO PRESSURE RELEASE 5. POSTCURE FREESTANDING RT TO 600 F AT ~10 F/MINUTE, POSTCURE 4 HOURS AT 600 F

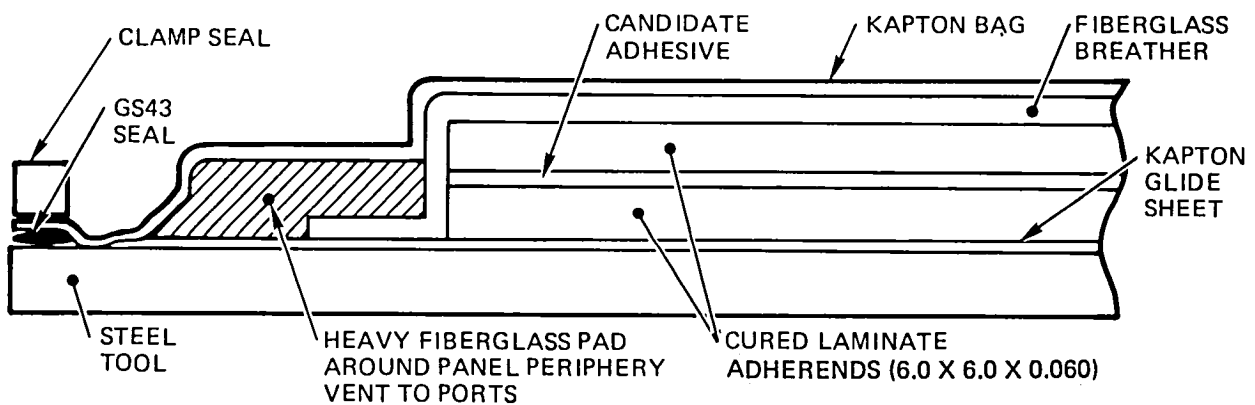


Figure 4-1. Midplane Secondary Bonding Process Development Tooling

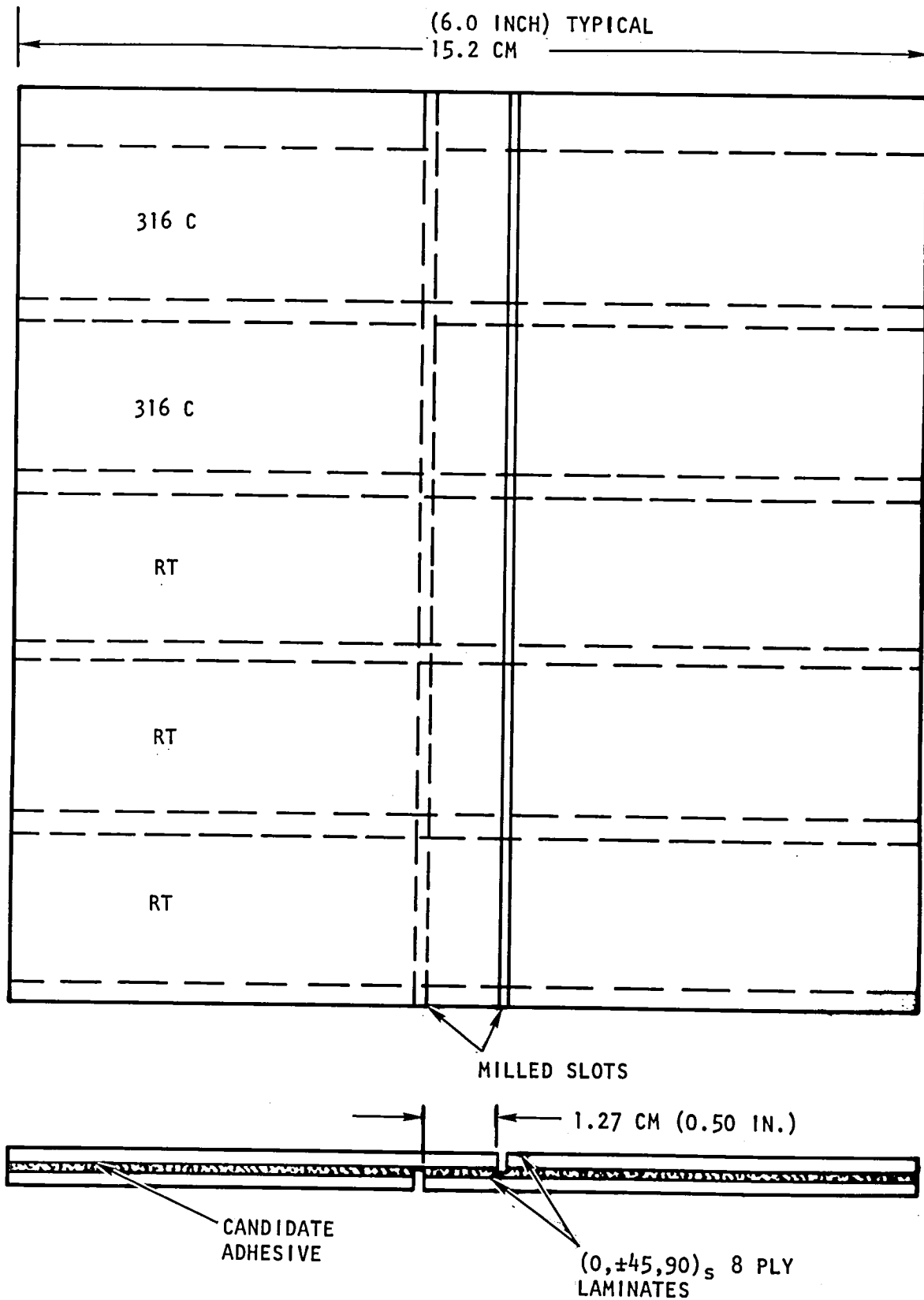


Figure 4-2. Midplane Bonded Process Development Panel and Lap Shear Cutting Plan

Table 4-1. Cure Cycle Development Matrix
and Candidate Adhesives

<div> <div>Process⁽¹⁾ Variable</div> <div>Candidate Adhesive</div> </div>	Cure Temperature 288°C (550°F)				Cure Temperature 316°C (600°F)			
	Cure Pressure		Cure Pressure		Cure Pressure		Cure Pressure	
	KN/m ²	psi	KN/m ²	psi	KN/m ²	psi	KN/m ²	psi
FM34B-18	689	100	1,378	200	689	100	1,378	200
LARC-13 (Peroxide catalyst)	689	100	1,378	200	689	100	1,378	200
LARC-13	689	100	1,378	200	689	100	1,378	200
LARC-160	689	100	1,378	200	689	100	1,378	200
<p>(1) Cure Process</p> <p>Positive pressure plus 84 KN/m² (<25 in.) Hg vacuum were applied at room temperature. Heat rise rate, 1.7°C to 2.8°C (3°F to 5°F) per minute to ultimate cure temperature, and cure for 2 hours. All specimens were postcured freestanding at 316°C (600°F) for 4 hours.</p>								

4.1.2 Midplane Bonding Evaluation

Lap shear tests were performed at room temperature and 316°C (600°F) at a load rate of 0.127 cm (0.05 in.) per minute after stabilizing at 316°C (600°F) for 10 minutes. Initial results of secondary midplane bonded panel processing studies were inconsistent in both NDI C-scan and lap shear values. For example, midplane bonded panels fabricated with LARC-13, LARC-13 (peroxide catalyst), and LARC-160 adhesives cured under the same processing conditions in some cases yielded relatively poor C-scan ultrasound transmission and yet attained superior lap shear strengths to specimen counterparts, which had 99 to 100 percent ultrasound transmission. The FM34B-18 adhesive, because of high condensation volatile activity during cure, resulted in approximately 90 percent void in the midplane bonded panels. The FM34B-18 adhesive was dropped from the program.

The LARC-13 (peroxide catalyst) and LARC-160 adhesives cured under minimum conditions of 288°C (550°F) and 689 KN/m² (100 psi) yielded essentially equivalent lap shear properties to each other at room temperature and 316°C (600°F) and in some tests, yielded superior strength to specimen counterparts cured under higher temperature and pressure. Standard LARC-13 specimens cured under the same minimum conditions tended to yield inferior lap shear results, although 99 to 100 percent ultrasound transmission was attained in some NDI C-scan tests. Low LARC-13 standard adhesive lap shear properties are attributed to insufficient crosslinking attained in the initial cure process. Further processing studies evolved good NDI C-scan through

transmission recordings on all three adhesives. The standard LARC-13 adhesive requires minimum 316°C (600°F), 689 KN/m² (100 psi) processing whereas the LARC-13 (peroxide catalyst) and LARC-160 adhesives require minimum 288°C (550°F), 689 KN/m² (100 psi) processing. Average lap shear properties are presented in Table 4-2. Photomicrographs of typical low and high void secondary bonded specimen adhesive bondlines are shown in Figure 4-3 and C-scan recordings are shown in Figure 4-4.

Relatively low overall room temperature lap shear values that were attained, with any of the candidate adhesives, i.e., 14.35 MN/m², 2,084 psi maximum, are attributed to the thin (0, +45, 90)_s, 0.114 cm (0.045 in.) thick 8-ply laminate adherends offset eccentric design, which in turn forced a high peel moment on the bond joints in test. Additionally, the (0, +45, 90)_s 8-ply per side laminate configuration places only one 0 degree ply next to the bond line. When the test load approaches the tensile strength of the 0 degree ply, combined tension and interlaminar shear failures can occur below the ultimate lap shear strength of the adhesive. This condition is augmented by the peel stresses induced by bending moments. This theory was verified in room temperature lap shear tests where a mix of interlaminar-tensile shear and adhesive type failure modes occurred. In most cases, the 316°C (600°F) tested specimens failed cohesively.

4.2. SECONDARY BOND, FLUSH SCARF ANGLE JOINT REPAIR DEVELOPMENT

4.2.1 Specimen Design and Fabrication

Laminate panels, (0, +45, 90)_{2s} orientation, 16 plies, 0.014 cm (0.0057 in.) per ply faying surfaces were machine ground to 3 degrees, 4.5 degrees, and 6 degrees scarf angle joint configurations per the design shown in Figure 4-5. Laminate scarf angle and faying surfaces were prepared for bonding by abraiding with number 400 emery paper, rinsing with deionized water and checking for a water breakfree surface. Laminates were force dried in an oven at 350°F for 1 hour. Faying surfaces were spray primed with 35 percent solids BR34B-18 primer and staged to 410°F for 30 minutes. Secondary bonding processes that were developed for large area midplane bonded panels were employed in curing the LARC-13 (peroxide catalyst), LARC-13 standard, and LARC-160 adhesives (refer to Figure 4-1 or Table 4-1 for cure-cycle details).

Additional 3-degree, 4.5-degree, and 6-degree scarf angle secondary bonded specimens were made without BR34 primer using standard LARC-160 laminating₂resin as the adhesive coated on unidirectional Celion 3K tape, 152 gm/in.² equivalent to 0.014 cm (0.057 in.) thick. The same cure cycle, using 1378 MN/m² (200 psi) was employed in specimen fabrication.

Scarf angle specimen autoclave cure tooling and design are presented in Figures 4-5 and 4-6.

Table 4-2. Average Secondary Midplane Adhesive Bonded Tensile Shear Properties
at Room Temperature and 316°C

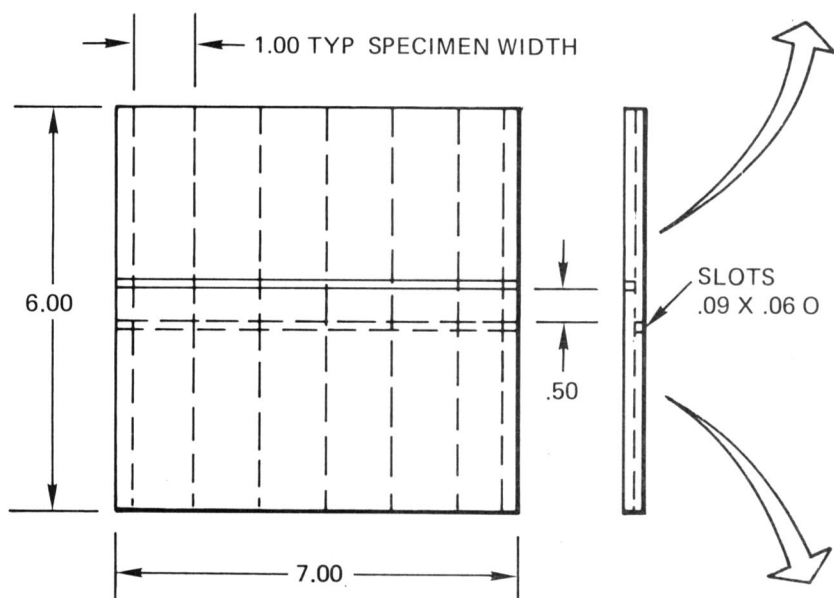
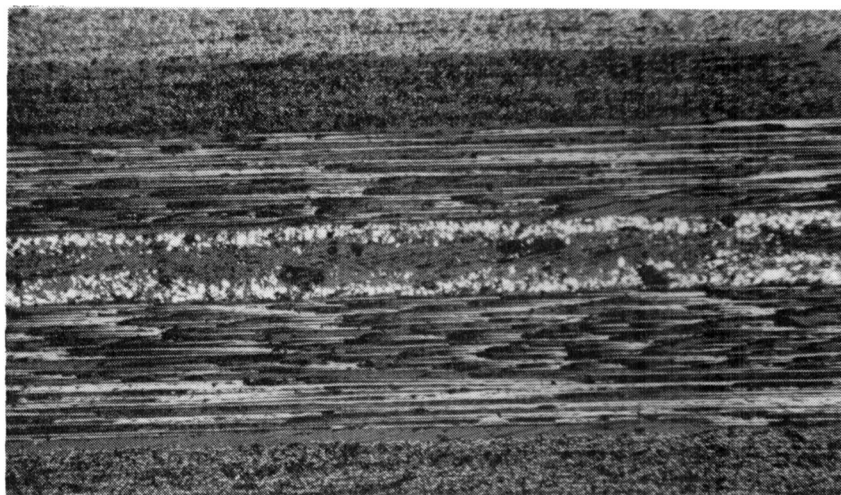
Panel ⁽¹⁾ No.	Adhesive	Bonding Process ⁽¹⁾				Fiber ⁽²⁾ Orientation	C-Scan Transmission (%)	Ult. Strength ⁽³⁾			
		Cure Press.		Cure Temp				RT		316 C (600 F)	
		KN/m ²	(psi)	C	F			MN/m ²	(psi)	MN/m ²	(psi)
EX151-1	LARC 13/108	1,378	(200)	288	(550)	(0,±45,90) _s	80	9.89	(1,436)	7.5	(1,091)
EX151-3		1,378	(200)	288	(550)	(0,±45,90) _s	60	9.77	(1,418)	6.14	(891)
EX288-1		1,378	(200)	316	(600)	(0,±45,90) _s	99	7.31	(1,061)	8.08	(1,173)
EX118-1		689	(100)	316	(600)	(0,±45,90) _s	61	14.35	(2,084)	9.02	(1,309)
EX288-3		1,378	(200)	288	(550)	(0,±45,90) _s	100	8.27	(1,200)	9.02	(1,309)
EX272-6		1,378	(200)	288	(550)	(0 ₂ ,±45,0) _s	98	11.22	(1,629)	9.69	(1,407)
EX197-5		689	(100)	288	(550)	(0,±45,90) _s	99	6.64	(964)	4.57	(664)
EX288-5	LARC 13/108 (peroxide catalyst)	1,378	(200)	288	(550)	(0,±45,90) _s	90	8.89	(1,291)	7.99	(1,159)
EX118-3		689	(100)	288	(550)	(0,±45,90) _s	85	11.31	(1,641)	10.40	(1,509)
EX197-9		689	(100)	288	(550)	(0,±45,90) _s	60	10.94	(1,588)	7.77	(1,128)
EX384-2		689	(100)	288	(550)	(0 ₂ ,±45,0) _s	70	10.74	(1,557)	9.68	(1,405)
EX151-5	LARC 160	1,378	(200)	288	(550)	(0,±45,90) _s	95	8.78	(1,274)	8.71	(1,264)
EX272-8		689	(100)	(316)	(600)	(0 ₂ ,±45,0) _s	65	10.65	(1,546)	10.58	(1,535)
EX197-1		689	(100)	288	(550)	(0,±45,90) _s	95	11.21	(1,627)	10.78	(1,564)
EX384-1		689	(100)	288	(550)	(0 ₂ ,±45,0) _s	96	11.95	(1,735)	10.59	(1,537)
EX272-10		689	(100)	288	(550)	(0 ₂ ,±45,0) _s	95	12.01	(1,743)	12.68	(1,840)

(1) Secondary bonding process: (1) Apply > 25 inches Hg vacuum, and 689 or 1,378 KN/m² (100 or 200 psi) pressure. (2) Raise temperature to 288 or 316 C (550 F or 600 F) at 3 - 5 F/minute. (3) Cure for two hours at specified temperature and pressure. (4) Force cool to < 65.6 C (150 F) prior to pressure release. (5) Tooling concept is shown in Figure 4-1.

(2) Specimen design given in Figure 4-2.

(3) Specimens were tested after stabilizing at 316 C (600 F) for 10 ⁺⁵₋₀ minutes at a load rate of 0.127 cm (0.05 inch)/minute.

EX384-1 60X C-SCAN
SHOWS NO VOID
LARC 160 ADHESIVE
100 PSI, 550 F



EX151-2 60X
C-SCAN SHOWS HIGH VOID
LARC 13 ADHESIVE
200 PSI, 550 F

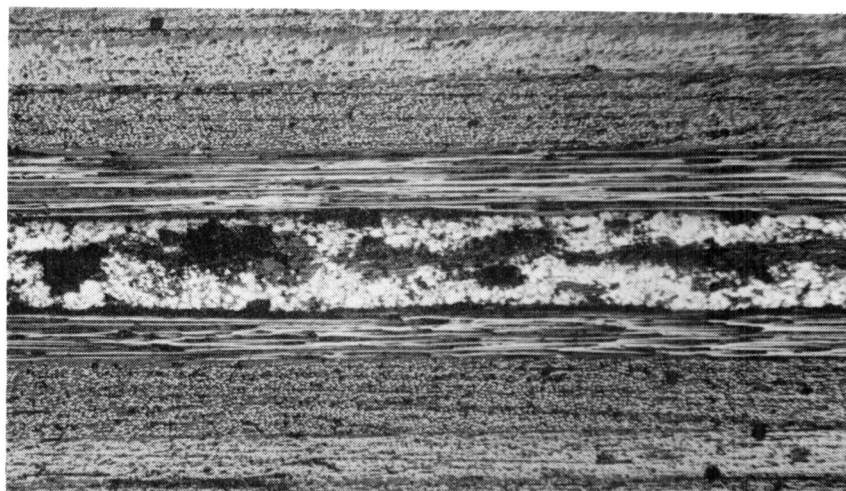
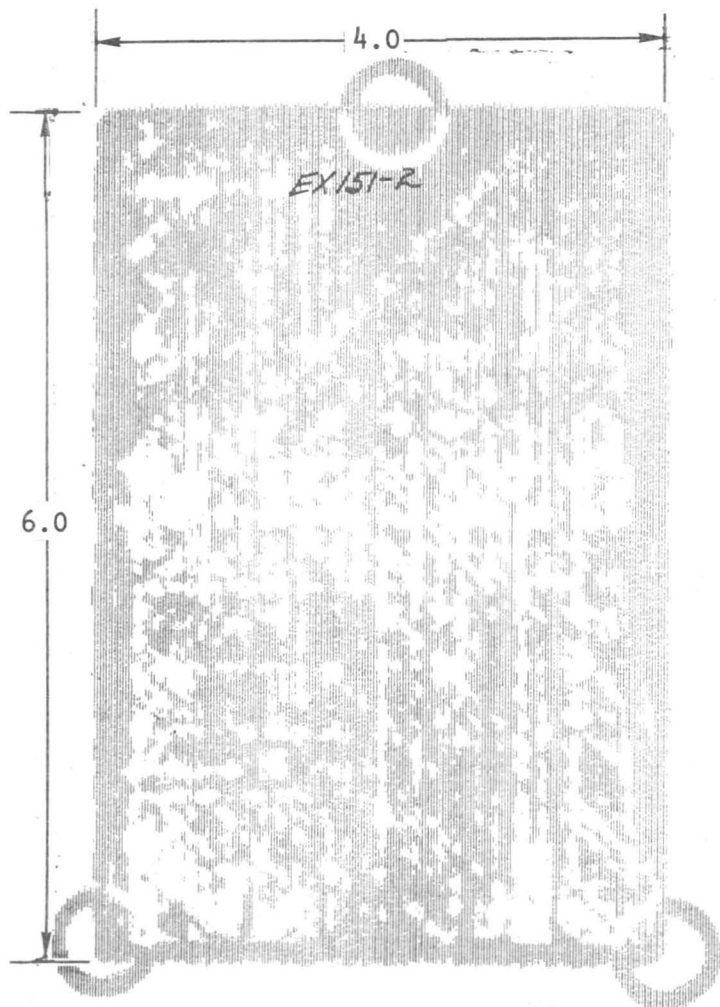
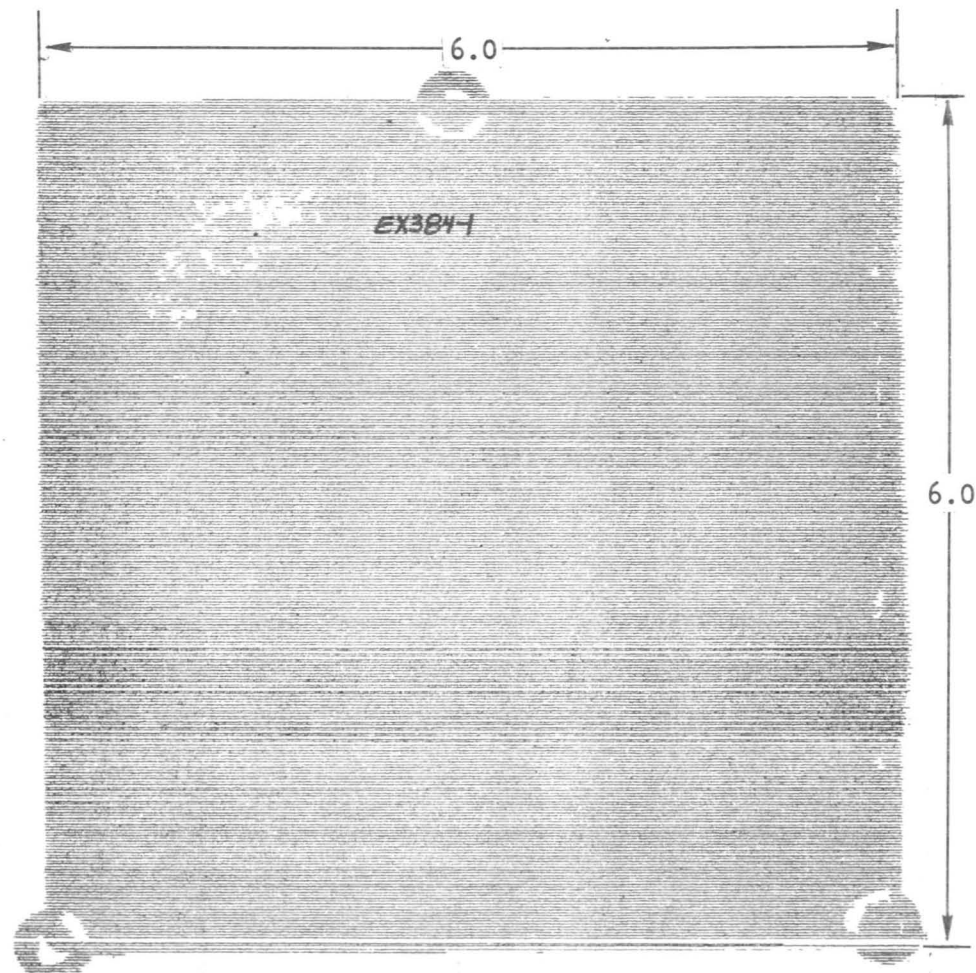


Figure 4-3. Midplane Bond Panel Specimen Design and Typical Low and High Void Secondary Bond Line Characteristics



LARC 13 ADHESIVE CURED
AT 200 PSI, 550 F, POSTCURED
FREESTANDING 4 HOURS AT 600 F



LARC 160 ADHESIVE CURED AT
100 PSI, 550 F, POSTCURED
FREESTANDING 4 HOURS AT 600 F

Figure 4-4. NDI C-Scan of Typical High and Low Void Midplane Secondary Bonded Laminates

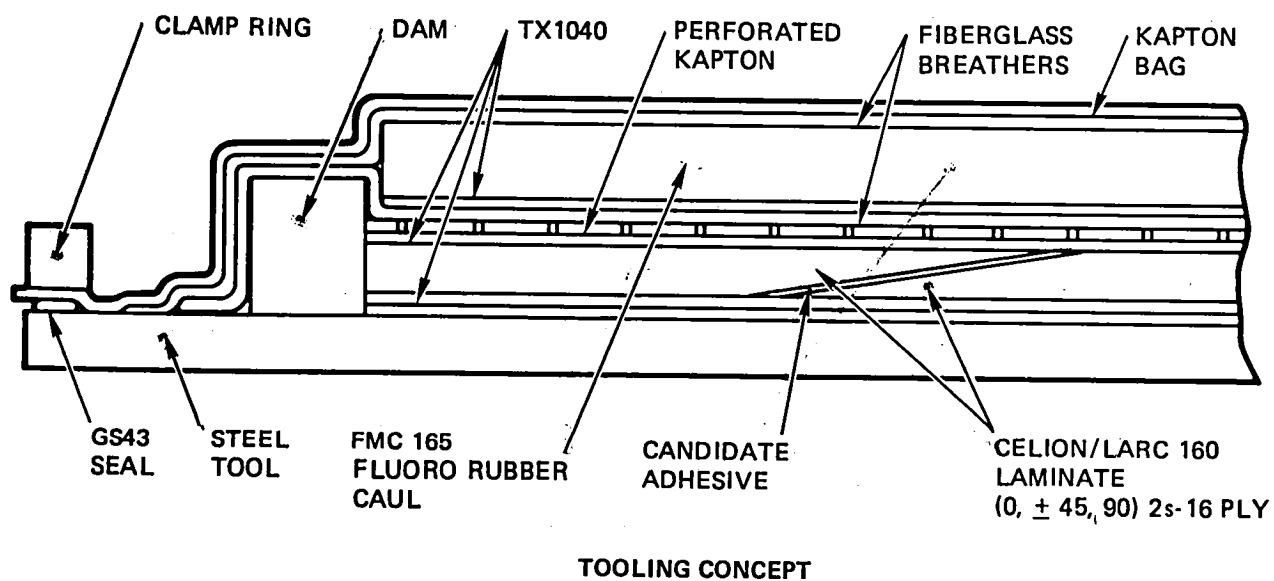
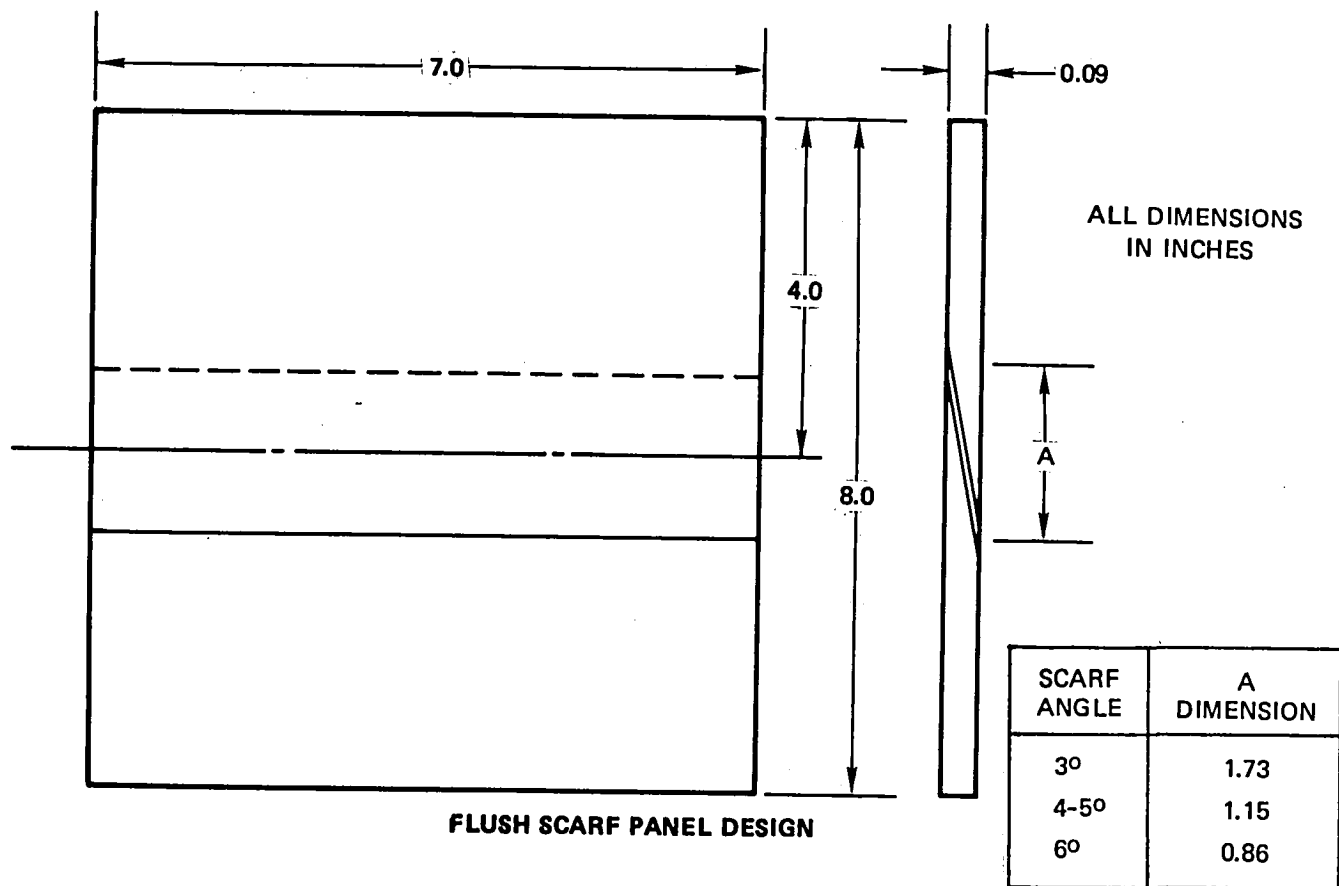


Figure 4-5. Secondary Bonded Flush Scarf Joint Specimen Design and Tooling Concept

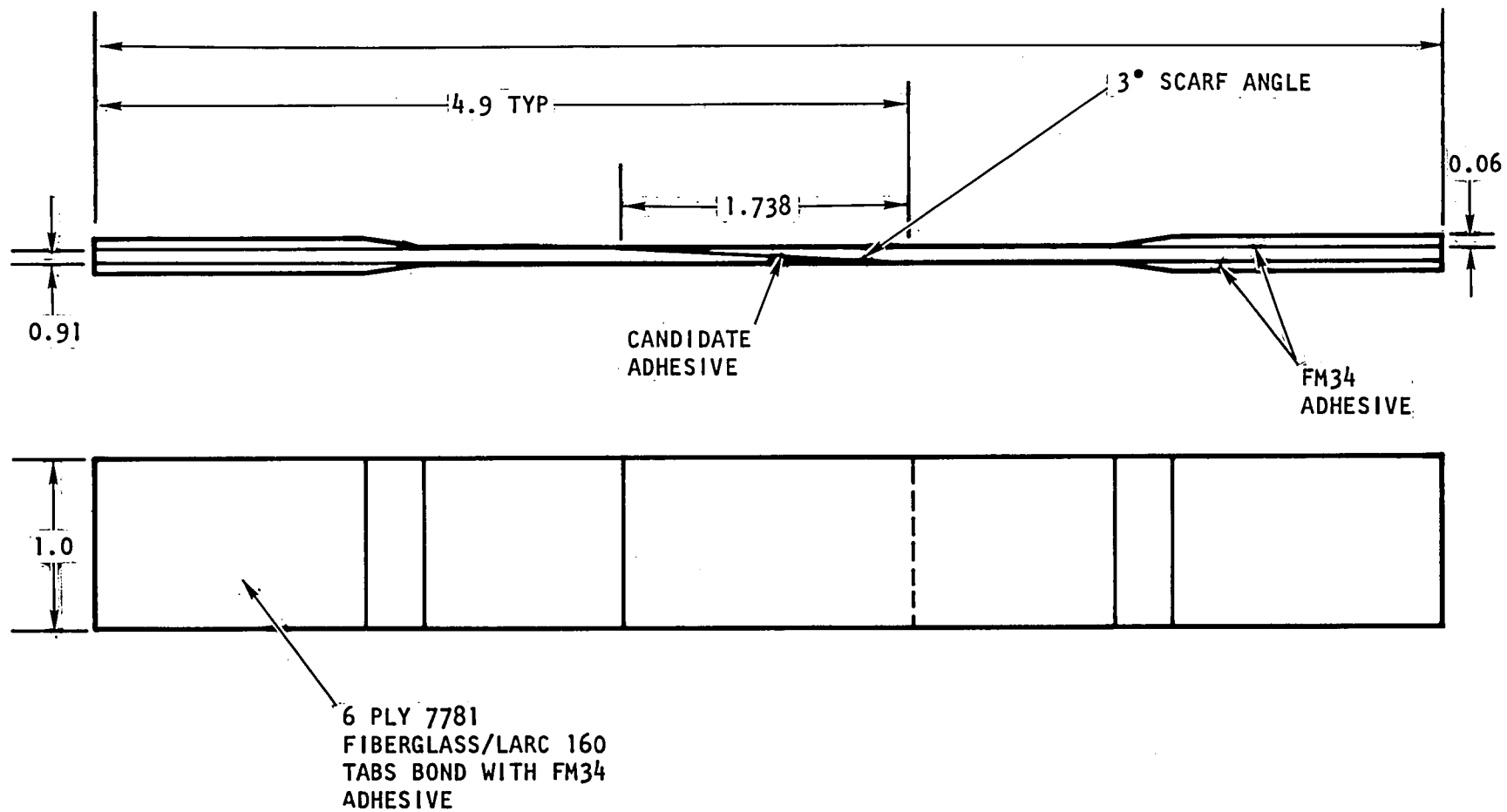


Figure 4-6. Adhesive Screening Specimen

4.2.2 Flush Scarf Angle Bonding Test and Evaluation

Scarf angle secondary bond joints (3 degrees and 6 degrees) made with LARC-13 standard and LARC-160 adhesives were examined by NDI C-scan. Those panels joined with accurately machined and aligned scarf angle adherends achieved 98 percent void free bonds and those showing some mismatch had an approximate 70 percent void free condition.

Specimens were tension tested at room temperature and 316°C (600°F). The 3 degree secondary bonded scarf angle specimens yielded the highest strengths in terms of ultimate load. The LARC-13 and LARC-160 adhesives, 3 degree scarf angle joint specimens were equivalent in strength at room temperature and 316°C (600°F) in terms of stress based on actual overlap length. Joint efficiencies for the 3 degree scarf angle fell short of target parent laminate strength of 945 KN/m (5,400 lb/in.) by 43 percent at room temperature and 59 percent at 316°C (600°F). Failure modes were primarily by cohesive failure of the BR34B-18 primer combined with interlaminar shear of laminar plies. Since specimen failures were predominately cohesive primer failure, the primer was eliminated in fabrication of subsequent specimens.

Specimens made with 3-degree, 4.5-degree, and 6-degree scarf angle joints using the Celion unidirectional tape carrier coated with LARC-160 laminating resin produced excellent 95 to 100 percent void-free bonds as determined by NDI C-scan photomicrographic examinations. Again the 3-degree scarf angle joint proved to be the most efficient in terms of strength. Average secondary bonded scarf angle joint tension test results, bonding process description and quantitative C-scan results are presented in Table 4-3. Typical C-scan recordings of two secondary bonded scarf joint panels are presented in Figure 4-7.

4.3 SECONDARY BONDING ADHESIVE SELECTION

The aluminum filled/diglyme solvent LARC-160 adhesive and prepreg laminating resin were selected as baseline for continuing secondary bonding repair development based on the following rationale.

1. Ability to cure at 288°C, 689 KN/m² (550°F), (100 psi), thus prolonging life of fluoro rubber pressure cauls and vacuum bags and seals
2. Most consistent, low void C-scan through transmission results
3. Equivalent lap shear bond strength to the LARC-13 standard and LARC-13 peroxide catalyst adhesives
4. Lower cost of AP22 diamine component in the LARC-160 adhesive formulations at approximately \$4/lb versus approximately \$300/lb 3-3' diamine MDA used in LARC-13 systems

Table 4-3. Secondary Bonded Flush Scarf Angle Joint Repair Specimen Average Tensile Shear Strengths at Room Temperature and 316°C

Panel No./ Scarf Angle	Bonding Process ⁽¹⁾				Primer	Adhesive	Scarf ⁽³⁾ Length cm/ (inch)	NDI C-Scan Transmission (%)	Tensile Shear Strength/Joint Efficiency					
	Cure Press.		Cure Temp.						Ult Strength ⁽⁴⁾ 24 C (75 F)		Joint (2) Efficiency (%)	Ult Strength ⁽⁴⁾ 316 C (600 F)		Joint (2) Efficiency (%)
	KN/m ²	(psi)	C	F					KN/m	(lb/in.)		KN/m	(lb/in.)	
EX349-1/3°	689	100	316	600	BR34B-18	LARC 13/104	4.32 - 4.45 (1.70 - 1.75)	98	536	(3,061)	56.4	390	(2,228)	41.1
EX384-1/3°	689	100	288	550	BR34B-18	LARC 160/104	3.81 - 3.94 (1.50 - 1.55)	98	486	(2,775)	51.1	371	(2,123)	39.1
EX384-4/3°	689	100	288	550	BR34B-18	LARC 160/104	3.94 - 4.06 (1.55 - 1.60)	70	507	(2,896)	53.3	341	(1,949)	32.3
EX384-3/6°	689	100	288	550	BR34B-18	LARC 160/104	1.90 - 2.03 (0.250 - 0.800)	70	289	(1,655)	30.4	143	(815)	13.5
EX400-9-17/6°	1,378	200	288	550	None	Celion/ LARC 160 tape 152G/m ² 35% R.C.	2.54 - 2.39 (0.85 - 0.94)	100	377	(2,157)	39.7	389	(2,222)	40.9
EX400-7-11/ 4.5°	1,378	200	288	550	None		2.40 - 2.99 (1.14 - 1.18)	100	421	(2,408)	44.4	378	(2,160)	39.8
EX449-6-2/3°	1,378	200	288	550	None		4.45 - 4.83 (1.75 - 1.90)	95	468	(2,677)	49.3	425	(2,428)	44.7

(1) Secondary bond process: (1) Apply > 25 inches Hg vacuum and 689 or 1,378 KN/m² (100 or 200 psi) pressure. (2) Raise temperature to 288 or 316 C (550 F or 600 F) at 3 - 5 F/minute. (3) Cure for two hours at specified temperature and pressure. (4) Force cool to < 65.6 C (< 150 F) prior to pressure release.

(2) Joint efficiency based on percentage of average recoverable strength from baseline control specimen tensile value of 950 KN/m (5,429 lb/in.) at RT.

(3) Specimen design given in Figure 4-2., Fiber Orientation (0, ±45, 90) 2_s - 16 ply ~ 2.31 cm (0.091 inch) thick.

(4) Specimens were tested after stabilizing at 316 C (600 F) for 10₋₀⁺⁵ minutes at a load rate of 0.127 cm (0.05 inch) minute.

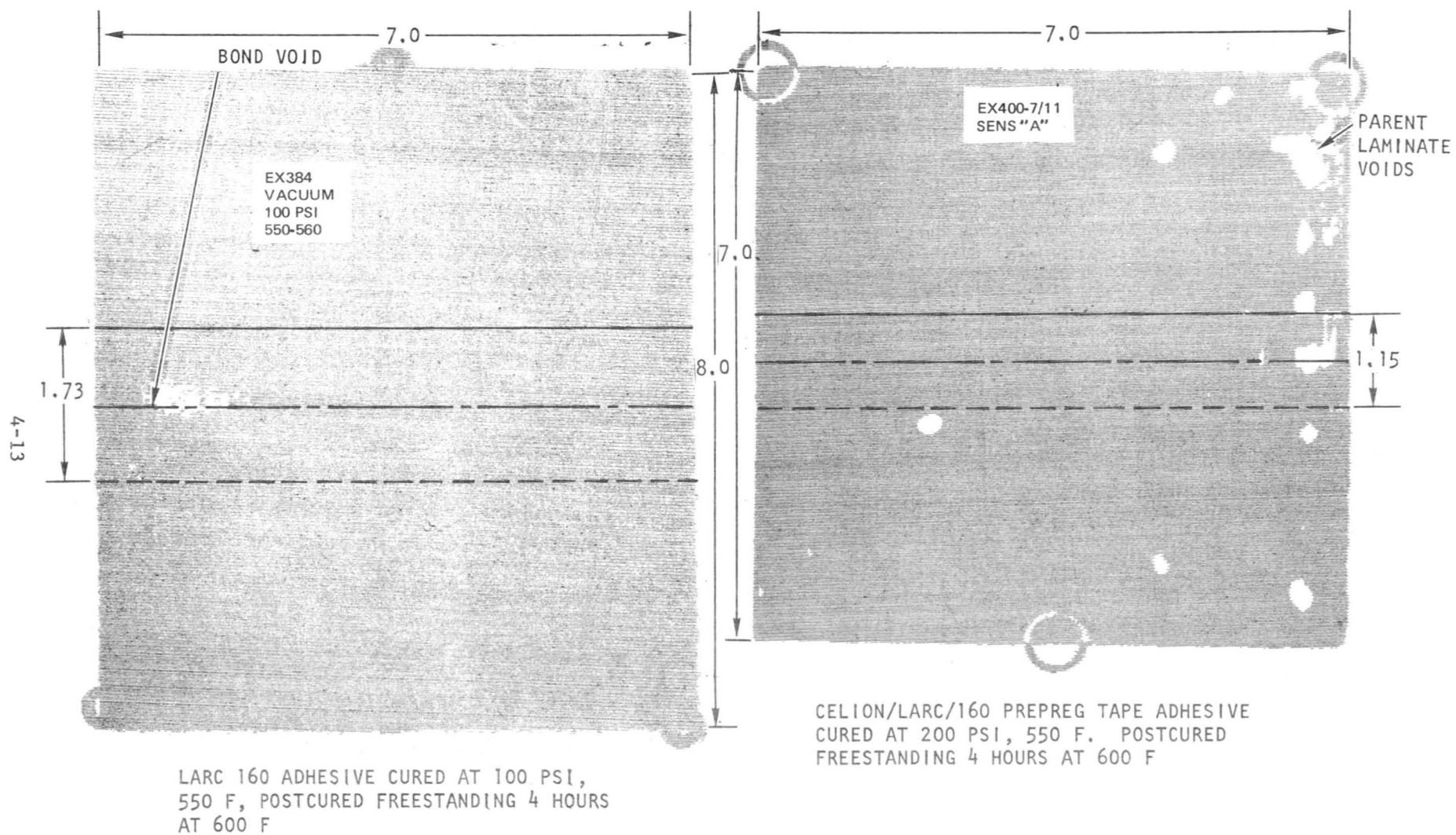


Figure 4-7. NDI C-Scans of Secondary Bonded 3-Degree and 4- to 5-Degree Scarf Angle Joint Panels

4.4 COCURE MIDPLANE PANEL BONDING PROCESS DEVELOPMENT, ADHESIVE SCREENING, AND EVALUATION

The same adhesives employed in the secondary bonding process development studies, with the exception of FM34B-18, were evaluated as auxiliary adhesives in cocure process midplane bonding development in accordance with the matrix defined in Table 4-1. The FM34B-18 condensation reaction polyimide adhesive was not evaluated further because of volatile entrapment problems.

4.4.1 LARC-13 Adhesive/LARC-160 Prepreg Cocure Compatibility Study

Prior to initiation of adhesive screening tests, a preliminary process development panel was cocure-bonded to evaluate the basic compatibility of LARC-13 adhesive and LARC-160 prepreg and establish the need to stage the adhesive prior to bonding using the following procedures.

1. A (0, +45, 0)_s, 8-ply laminate 0.116 cm (0.046 in.) thick, 16 by 17.8 cm (6.5 by 7.0 in.) was used as the base adherend. This adherend was extracted from a 66.0 by 135 cm (26 by 35 in.) laminate number EX151, which had greater than 95 percent C-scan through transmission. The laminate faying surface was prepared by abrasive cleaning to a water breakfree condition and then oven dried at 177°C (350°F) for 30 minutes.
2. Celion/LARC-160 (batch 2W4885) nominal 0.0072 cm (2.85 mils) per ply prepreg was used in making a (0, +45, 90)_s 8-ply preform, which was preimidized at 191°C (375°F) for 1 hour per procedures described in Figure 4-8. Bleeder material was not used.
3. The LARC-13 adhesive was prepared using the ester process, diluted with diglyme solvent and applied to a 108-style fiberglass carrier to 440 gram/m² (0.09 psf) real weight. One section of adhesive was used as is. Two other adhesive sections were staged at 218°C (425°F) for 30 and 60 minutes. Volatile content measurements made at 316°C (600°F) were 15.0, 2.8, and 1.0 percent respectively.
4. Prepared LARC-13 adhesives were affixed to the EX151 panel faying surface and then the Celion/LARC-160 preform was affixed to the adhesive.
5. The assembly was autoclave cured to 288°C (550°F) for 3 hours under 2,378 KN/m (200 psi) pressure 84 KN/m (>25 in. Hg) vacuum using procedures described in Figure 4-8.

4.4.1.1 Results. The cocure laminate-to-cured laminate adhesive bond had good visual appearance with a smooth laminate surface. There was no evidence of LARC-13 adhesive penetration to the outer laminate surface. NDI C-scan A sensitivity tests showed 100 percent ultrasound transmission through the unstaged adhesive bonded section. The 218°C (425°F) 30- and 60-minute staged preforms showed void areas, which increased with staging time at

2 STAGE IMIDIZING & CO CURE BONDING PROCESS	INSTU IMIDIZING & CO CURE BONDING PROCESS
<ol style="list-style-type: none"> 1. IMIDIZING CYCLE (PREPREG PREFORM) <ol style="list-style-type: none"> 1.1 APPLY < 2 INCHES HG VACUUM 1.2 RAISE TEMPERATURE TO 425 F, HOLD FOR 1 HOUR 1.3 FORCE COOL TO < 150 F 2. CO CURE BONDING CYCLE <ol style="list-style-type: none"> 2.1 APPLY > 25 INCHES HG VACUUM 2.2 APPLY 100 OR 200 PSI PRESSURE 2.3 RAISE TEMPERATURE TO 550 OR 600 F 2.4 CURE AT SELECTED PRESSURE & TEMPERATURE 2 HOURS 2.5 FORCE COOL TO < 150 F PRIOR TO PRESSURE RELEASE <p>POSTCURE SPECIMENS AT 600 F FREESTANDING FOR 4 HOURS</p>	<ol style="list-style-type: none"> 1. APPLY < 2 INCHES HG VACUUM 2. RAISE TEMPERATURE TO 425 F, IMIDIZE 1 HOUR 3. APPLY > 25 INCHES HG VACUUM & 100 OR 200 PSI AUTOCLAVE PRESSURE 4. RAISE TEMPERATURE TO 550 F OR 600 F, CURE 2 HOURS 5. FORCE COOL TO < 150 F PRIOR TO PRESSURE RELEASE

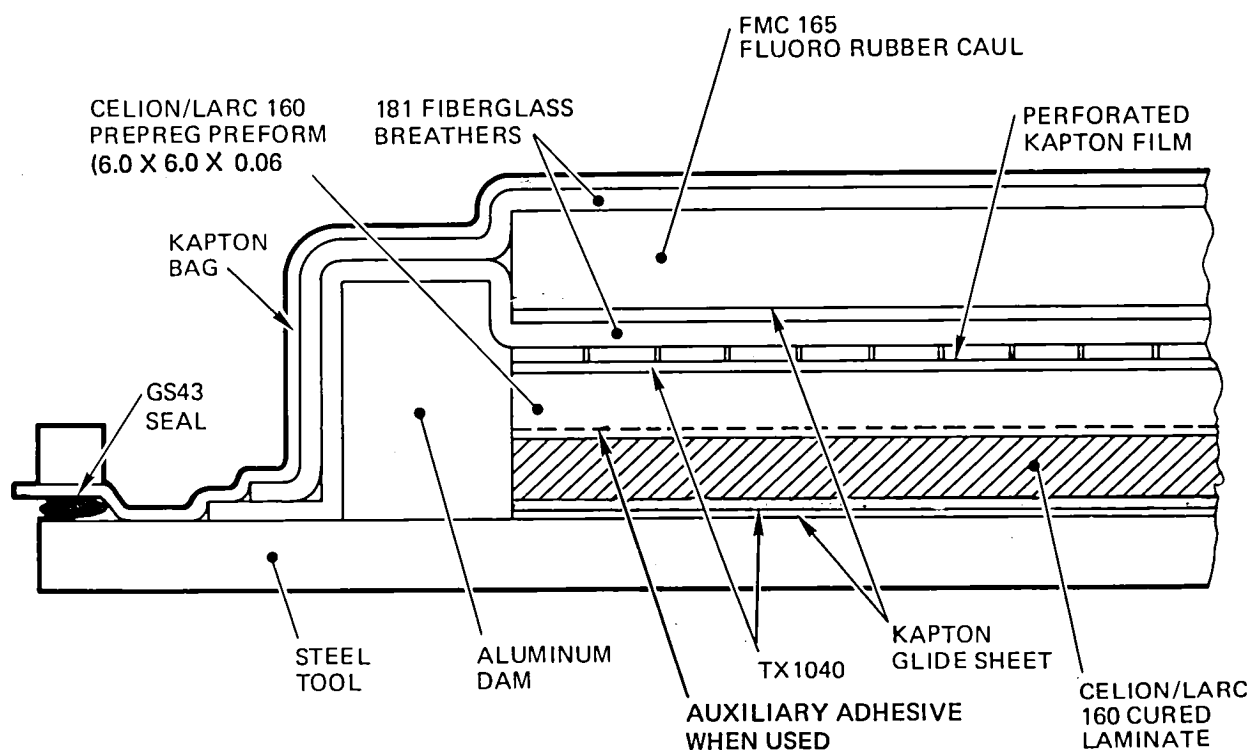


Figure 4-8. Cross-Section - Cocure Midplane Bonding Tooling and Curing Processes

temperature. A C-scan recording of the cocured panel is shown in Figure 4-9. The LARC-13 adhesive film used in the as-coated condition appears satisfactory for accomplishing cocure bonding of staged Celion/LARC-160 prepreg-to-cured Celion/LARC-160 laminates.

4.4.2 Initial Midplane Cocure Bonding Process Development

Cocure bonding experiments representing target processing extremes of 1,378 KN/m² (200 psi) 316°C (600°F) and 689 KN/m² (100 psi), 288°C (550°F) were performed with each of the three candidate auxiliary adhesive systems. The same laminate configurations were employed as cured adherends and prepared for bonding per processes used in secondary bonding operations. The first approach to cocure bonding was to preimidize the Celion/LARC-160 prepreg preform per the imidizing cycle described in Figure 4-8. Aluminum and fluoro rubber pressure cauls were evaluated in the cocure process to impart uniform surfaces to the Celion/LARC-160 prepreg preforms. The fluoro rubber compound is capable of multiple cures in the 288°C to 316°C (550°F to 600°F) temperature range. Several cure trials were performed with both pressure caul materials. The fluoro rubber material was selected for further laminate fabrication because of its ability to conform to any local surface discrepancies or abrupt thickness changes and yet impart the desired surface smoothness to the laminate repair. Aluminum cauls will not conform to local discontinuities, which causes bridging and local high pressure points.

The two-stage cure cycle, tooling, and process described in Figure 4-8 were employed in specimen fabrication. Cured midplane bonded panels were post-cured freestanding at 316°C (600°F) for 4 hours. Panels were slotted and cut into 2.54 cm (1.00 in.) wide lap shear specimens per the design shown in Figure 4-2. Specimens were tested at room temperature and 316°C (600°F). Results of the cocure adhesive midplane bonded laminate lap shear tests closely resembled the peel failure modes and ultimate strengths attained with the secondary bonded specimens. The same analogy as to specimen peel failure mechanism follows the theories described for the secondary midplane bonded specimens.

Correlation of NDI C-scan and lap shear test performed on the midplane cocure bonded panels was inconclusive since some of the highest lap shear strengths in room temperature and 316°C (600°F) tests were achieved on high void specimens. In general, the processes produced cocure midplane bonds with high void contents. Cause of high void was traced to entrapment of the adhesive high temperature boiling diglyme solvent within prepreg preform and bondline during the cure cycle. Average lap shear test results and quantitative C-scan through transmission characteristics are presented in Table 4-4.

4.4.3 In-Situ Imidizing Cocure Process Development

An in-situ prepreg imidizing and cure cycle process, previously developed for Celion/LARC-160 laminates, was evaluated in the cocure application using the three-candidate auxiliary adhesives, and tooling per Figure 4-8. Ultimate cure temperatures and pressures followed the minimum levels previously

LARC 13 ADHESIVE
NO STAGING

EX151/347

LARC 13 ADHESIVE
STAGED 30 MINUTES
AT 218 C (425 F)

LARC 13
ADHESIVE STAGED
60 MINUTES AT
218 C (425 F)

Figure 4-9. NDI C-Scan Recording of $(0, \pm 45, 90)_s$, 8-Ply Celion/LARC-160
Imidized Laminate Cocure Bond to Cured Celion/LARC-160
Laminate Using LARC-13 Adhesive

Table 4-4. Average Tensile Shear Properties of Cocure Midplane Bonded Celion/
LARC-160 Laminates at Room Temperature and 316°C

Panel No.	Adhesive	Imidize ⁽¹⁾ Process	Bonding Process ⁽¹⁾				Fiber ⁽²⁾ Orientation	C-Scan Transmission (%)	Ult. Strength ⁽³⁾			
			Cure Press.		Cure Temp				RT		316 C (600 F)	
			KN/m ²	(psi)	C	(F)			MN/m ²	(psi)	MN/m ²	(psi)
EX118-7	LARC 13/108	In situ	1,378	(200)	316	(600)	(0,±45,90) _s	92	9.48	(1,376)	11.24	(1,632)
DO70X-4		In situ	689	(100)	288	(550)	(0,±45,90) _s	88	8.01	(1,163)	7.90	(1,146)
EX384A-11		Pre	1,378	(200)	288	(550)	(0 ₂ ,±45,0) _s	10	11.87	(1,723)	9.27	(1,346)
EX118-8	LARC 13/108 (peroxide catalyst)	In situ	689	(100)	316	(600)	(0,±45,90) _s	11	12.61	(1,830)	10.90	(1,582)
EX272-1		In situ	689	(100)	288	(550)	(0 ₂ ,±45,0) _s	50	9.10	(1,321)	8.40	(1,219)
EX384A-6		Pre	689	(100)	288	(550)	(0 ₂ ,±45,0) _s	20	13.44	(1,950)	9.78	(1,419)
DO70X-1	LARC 160	In situ	1,378	(200)	316	(600)	(0,±45,90) _s	-	8.23	(1,194)	7.33	(1,064)
EX272-2		In situ	689	(100)	288	(550)	(0,±45,90) _s	68	10.65	(1,545)	8.45	(1,227)
EX384A-5		Pre	689	(100)	288	(550)	(0 ₂ ,±45,0) _s	0	12.45	(1,807)	12.66	(1,837)
EX272-10A		In situ	1,378	(200)	288	(550)	(0 ₂ ,±45,0) _s	40	12.68	(1,840)	12.70	(1,841)
EX424-3	35X34 Celion 1K fabric/ LARC 160 resin	In situ	1,378	(200)	288	(550)	(0) ₈	100	11.68	(1,695)	11.19	(1,624)
EX424-2	No adhesive	In situ	1,378	(200)	288	(550)	(0) ₈	100	9.56	(1,387)	11.22	(1,629)
EX424-1		In situ	1,378	(200)	288	(550)	(0) ₈	100	13.48	(1,957)	7.17	(1,041)
EX466A ⁽⁴⁾		In situ	1,378	(200)	288	(550)	(0) ₈	100	27.41	(3,978)	21.76	(3,158)

(1) Laminate preforms (PRE) were processed by preimidizing per Figure 4-1. Imidized preforms were then assembled to prepared, adhesive coated parent laminate adherends and cured at designated pressures and temperatures per Figure 4-1. Laminate preforms (in situ) were processed using the single stage in situ imidizing and cure process to designated pressure and temperature per Figure 4-1. All specimens were postcured freestanding to 316°C (600°F) for four hours.

(2) Specimen design given in Figure 4-2.

(3) Specimens were tested after stabilizing at 316°C (600°F) for 10^{+5}_{-0} minutes as a load rate of 0.127 cm 0.05 inch/minute.

(4) Specimens were tested using anti-peel clamps per Figure 4-10.

established for the individual adhesive system in the secondary bonding cure cycle study. This process resulted in similar high void preforms and bondlines and lap shear strengths to the preimidized preform process. Average lap shear results are presented in Table 4-4.

Discussions with Mr. J. Deaton, NASA LaRC Contract NAS1-16448 program technical manager, revealed LaRC was experiencing the same cocure bonding problems using the LARC-13 and LARC-160 adhesives. Preliminary work at LaRC had demonstrated that excellent, void-free bonds can be attained using the Celion/LARC-160 laminating resin in the prepreg as the adhesive bonding medium. Midplane cocure bonded flexure specimens demonstrated at least equivalent strength to parent laminate material.

4.4.4 Prepreg Resin-Adhesive Cocure Bonding Process Development

Since excellent zero-void laminates were achieved using the in-situ imidizing cure cycle and tooling previously developed, per Figure 4-8, it was theorized that this processing technology could be employed in cocure bonding of laminates. In this concept, the prepreg preform LARC-160 laminating resin would be utilized as the adhesive medium.

To evaluate this concept, an experiment was devised by preparing a midplane cocure bonded panel. To perform the experiment, an 8-ply, 15.02 by 15.02 by 0.152 cm (6 by 6 by 0.060 in.) thick unidirectional laminate was prepared for bonding as previously described. An 8-ply laminate unidirectional preform was prepared by vacuum bag debulking layers into a consolidated unit. The preform was applied directly to the prepared cured laminate surface and assembled on tooling described in Figure 4-8. Bonding was accomplished per the vacuum plus 1,378 KN/m² (200 psi) autoclave in-situ imidizing and 288°C (550°F) autoclave cure process. The resultant midplane bonded laminate produced using this prepreg resin adhesive cocure process yielded high aesthetic quality and NDI C-scan recordings with 100 percent ultrasound transmission in both cured and postcured conditions. Laminates were slotted and cut into 2.54 cm (1.00 in.) wide lap shear specimens per the specimen design shown in Figure 4-2. Lap shear tests were performed at room temperature and 316°C (600°F) at a load rate of 0.127 cm (0.05 in.) per minute, 10 minutes after attaining 316°C (600°F) test temperature.

Lap shear tests performed at room temperature and 316°C (600°F) yielded only mediocre strength levels, although no evidence of adhesive-type failure occurred; rather interlaminar failures were predominate outside the bondline. Low strength levels were traced to the same peel force problems experienced in secondary bonded specimens because of specimen configuration and resultant loading eccentricity. Average lap shear results are presented in Table 4-4.

4.4.5 Process Verification and Lap Shear Testing

Fabrication of a midplane cocure bonded panel was repeated, this time utilizing the prepreg in-situ imidizing and cocure process without the use of vacuum. Significantly, aesthetic quality of the panel equaled that of the

vacuum bag/autoclave cure processed panel. NDI C-scan through transmission tests also showed equivalent zero-void quality. Lap shear testing was again performed at room temperature and 316°C (600°F). This time, FED STD 406 Method 1042 anti-peel clamps were used during testing, as shown in Figure 4-10 to reduce peel moments caused by specimen configuration and load eccentricity experienced in previous tests. Lap shear test results at room temperature and 316°C (600°F) yielded excellent high strength values with interlaminar failures occurring through the cross-section of both cured and cocured adherends, mainly outside the bondline. Average room temperature and 316°C (600°F) tensile shear strengths were 22.4 MN/m² and 21.8 MN/m² (3,978 psi and 3,158 psi).

The anti-peel clamps reduced peel forces sufficiently to yield approximately true interlaminar shear properties of the laminate and cocured bondline. These initial tests clearly illustrate the potential of the prepreg resin adhesive, cocure bonding concept with and without the use of vacuum in the process. Average lap shear results are presented in Table 4-4.

A photograph of a room temperature tested specimen and a 32.5X photomicrograph cross-section of the specimen are illustrated in Figure 4-11. A typical C-scan recording is shown in Figure 4-12.

4.5 FLUSH SCARF ANGLE-JOINT SPECIMEN COCURE PROCESS DEVELOPMENT AND VERIFICATION

The purpose of these tests was to establish maximum joint efficiency that could be achieved with the individual scarf angle cocured bond joints. Target tensile load was 946 KN/m (5,400 lb/in.) width, 413 MN/m² (60 ksi) established in testing tensile specimens comprised of the same (0, ±45, 90)_{2S} 0.231 cm (0.091 in.) thick cross section as the lap shear specimen parent material (refer to Appendix A).

4.5.1 Adhesive Screening and Specimen Fabrication

Parent laminate material (0, ±45, 90)_{2S}, 16-ply 0.014 cm (5.7 mils per ply), 0.231 m (0.091 in.) thick was diamond ground into nominal 3-degree, 4.5-degree, and 6-degree scarf angle panels. Panel stock was sized to yield six 2.54 cm (1.00 in.) wide lap shear specimens. Faying surfaces were prepared for bonding per processes previously employed.

Candidate auxiliary adhesives, LARC-13 standard, LARC-13 (peroxide catalyst) and LARC-160 coated on Type 104 glass carriers were fabricated concurrently with cocure midplane bonding studies, following the same two-stage preimidizing and cocure process Figure 4-8. During the adhesive screening portion of the program only 3-degree flush scarf cocure bond joints were evaluated. The same problems related to adhesive solvent compatibility were experienced in high void volumes detected in NDI C-scan tests. High void levels did not affect bond strengths significantly at room temperature or 316°C (600°F) test temperatures. Refer to Table 4-5 for average tensile shear strengths and quantitative NDI C-scan results.

A single 3-degree scarf joint panel (EX384-5) was made using the prepreg adhesive cocure bonding process developed in midplane cocure bonding studies.

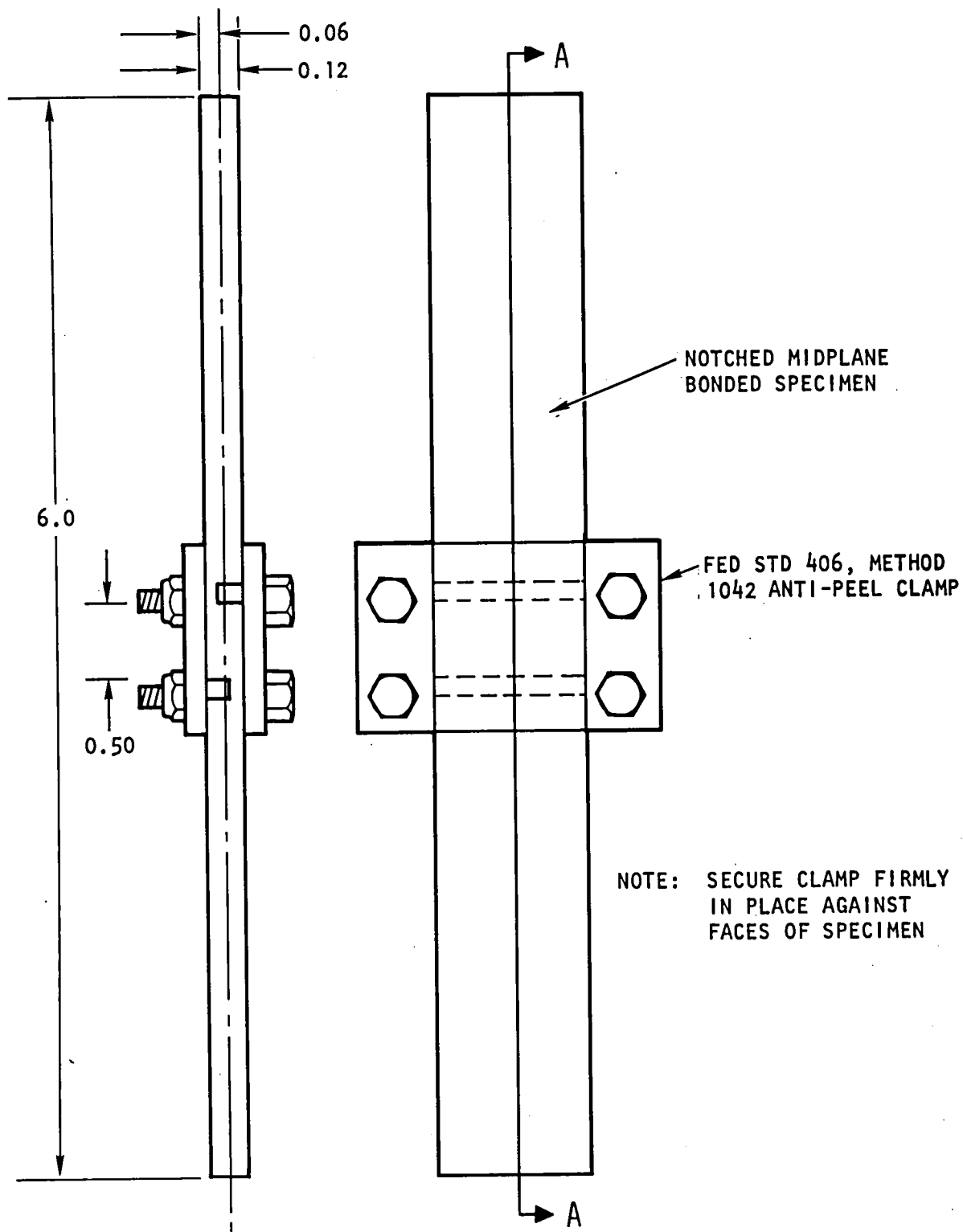


Figure 4-10. Notched Midplane Bonded Test Specimen With Anti-Peel Clamp

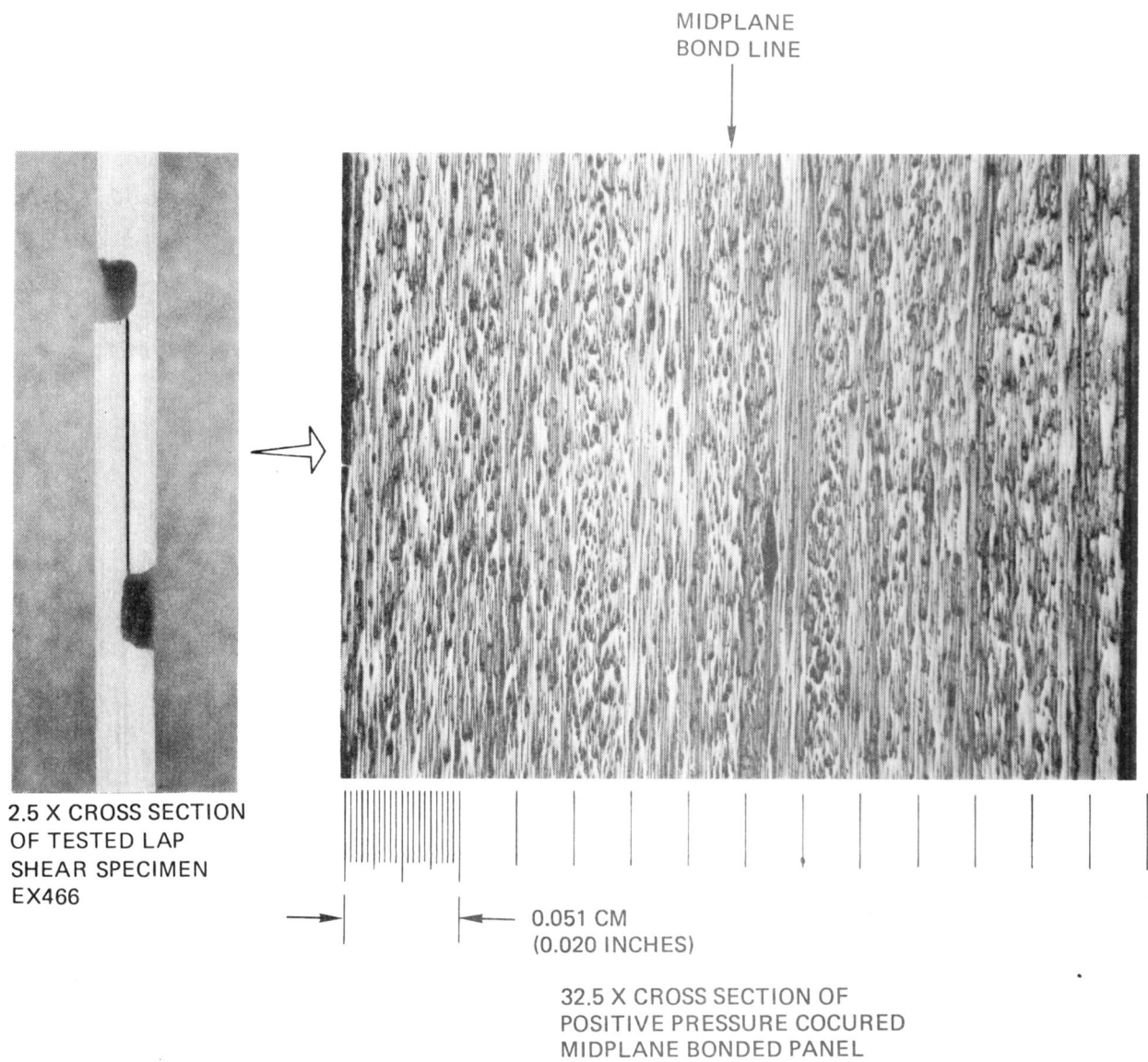


Figure 4-11. Cross Sections of Nonadhesive Positive Pressure Cocure Midplane Bonded Panel, EX466

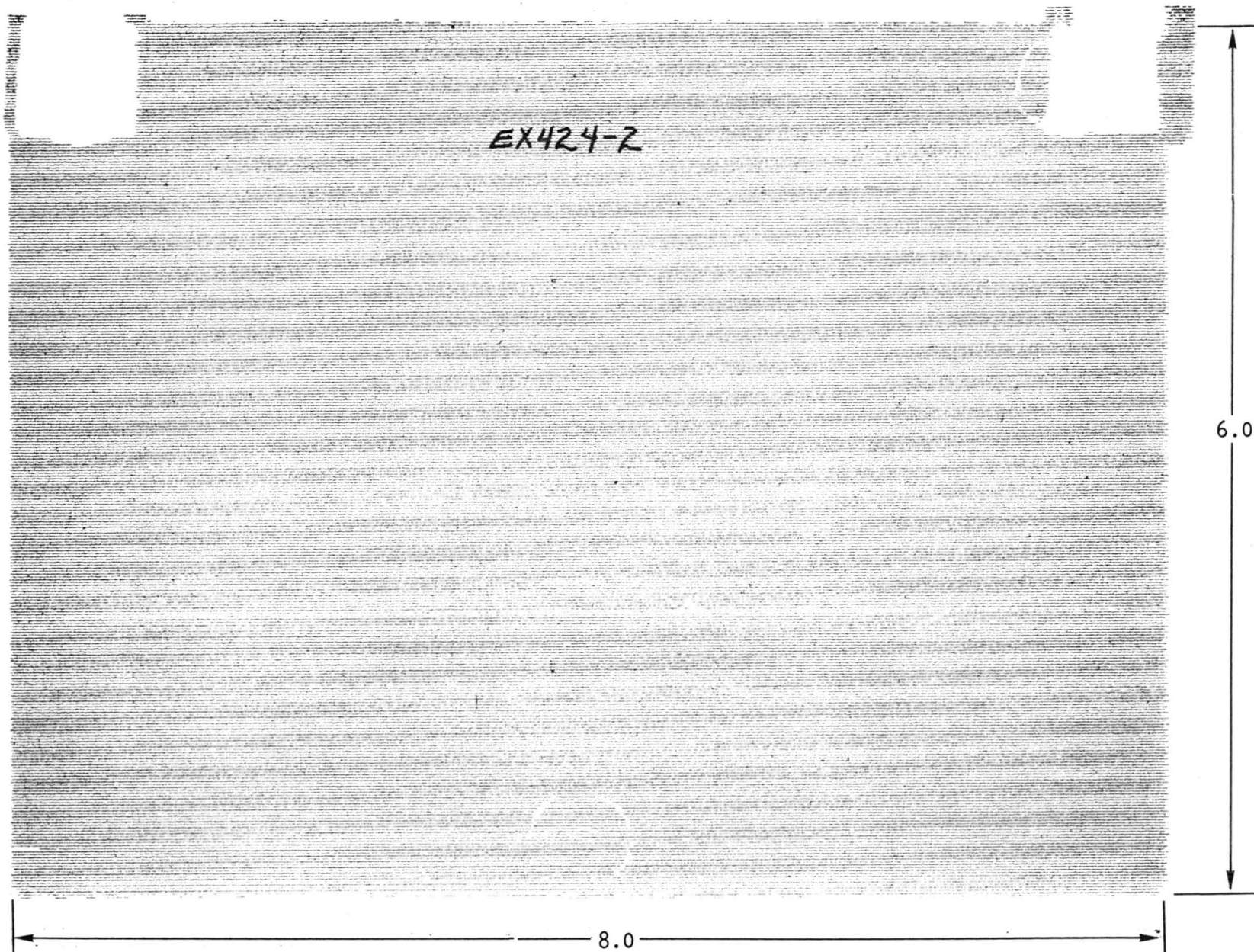


Figure 4-12. NDI C-Scan of Typical Nonadhesive Cocure Bonded Midplane Panel

Table 4-5. Cocure Bonded Flush Scarf Angle Joint Repair Specimen Average Tensile Shear Strengths at Room Temperature and 316°C

Panel No./ Scarf Angle	Bonding Process ⁽¹⁾				Primer	Adhesive	Scarf Length cm/(Inch)	NDI C-Scan Transmission (%)	Tensile-Shear Strength/Joint Efficiency					
	Cure Press.		Cure Temp.						Ult Strength 24 C (75 F)		Joint(2) Efficiency (%)	Ult Strength ⁽⁴⁾ 316 C (600 F)		Joint(2) Efficiency (%)
	KN/m ²	(psi)	C	F					KN/m	(lb/in.)		KN/m	(lb/in.)	
EX349-3/3°	1,378	(200)	316	(600)	BR34B-18	LARC 13/104	4.06 (1.60)	50	557	(3,182)	58.6	401	(2,294)	42.2
EX349-6/3°	1,378	(200)	316	(600)	BR34B-18	LARC 13/104	4.19-4.32 (1.65-1.70)	30	486	(2,778)	51.2	441	(2,523)	46.5
EX349-8/3°	1,378	(200)	316	(600)	BR34B-18	LARC 13/104	4.06 (1.60)	0	445	(2,544)	46.9	399	(2,282)	42.0
EX349-8A/3°	689	(100)	288	(550)	BR34B-18	LARC 160/104	4.45 (1.75)	5	567	(3,240)	59.7	356	(2,033)	33.2
EX349-9/3°	689	(100)	288	(550)	BR34B-18	LARC 13 (peroxide catalyst)/104	4.45 (1.75)	50	541	(3,100)	57.1	293	(1,672)	27.2
EX384-5/3°	689	(100)	288	(550)	BR34B-18	None	1.94-4.06 (1.55-1.60)	98 Bond 80 Laminate	625	(3,574)	65.8	222	(1,271)	21.1
EX384-6/6°	1,378	(200)	288	(550)	None	None	1.65-1.78 (0.65-0.70)	100	418	(2,390)	44.0	378	(2,158)	39.7
EX400-21/6°	1,378	(200)	288	(550)	None	None	2.03 - 2.11 (0.800-0.830)	100	408	(2,330)	51.0	341	(1,950)	35.9
EX400-14/3°	1,378	(200)	288	(550)	None	None	4.57 (1.800)	100	513	(2,932)	54.0	431	(2,462)	45.3
EX450-1/3°	1,378	(200)	288	(550)	None	None	4.45-4.55 (1.75-1.79)	100	566	(3,233)	59.6	556	(3,178)	58.5
EX450-4/3°	1,378	(200)	288	(550)	None	None	4.45 (1.75)	100	548	(3,129)	57.6	512	(2,924)	53.9
EX400-18/3°	1,378	(200)	288	(550)	None	None	4.45 (1.75)	100	459	(2,626)	48.4	427	(2,439)	44.9
EX400-15/4.5°	1,378	(200)	288	(550)	None	None	(2.82-2.84) (1.11-1.12)	100	515	(2,941)	54.2	460	(2,629)	48.4
EX384-20/6°	1,378	(200)	288	(550)	None	None	(2.03-2.16) (0.80-0.85)	100	447	(2,533)	47.0	404	(2,310)	42.5
EX451-20/6°	1,378	(200)	288	(550)	None	None	2.03 (0.80)	100	388	(2,218)	40.9	403	(2,305)	42.5
EX400-22/3°	1,378	(200)	288	(550)	None	Celion 35 x 34 fabric/ LARC 160 resin	4.19 (1.65)	100	454	(2,592)	47.7	407	(2,322)	38.5
EX384-X/6°	1,378	(200)	288	(550)	None		2.11 (0.83)	100	339	(1,936)	35.7	268	(1,531)	25.4

- (1) Specimens EX349-3/3° through EX384-5/3° were processed by pre-impregnating the scarfed preform per Figure 4-8. Impregnated preforms were then assembled to prepared, adhesive coated parent laminate adherends and cured at designated pressures and temperatures per Figure 4-8. Specimens were postcured freestanding at 316°C (600°F) for 4 hours.
- Specimens EX384-6/6° through EX384-X/6° were cured using the nonadhesive, in situ impregnating and cure process to designated pressure and temperature levels per Figure 4-8. Specimens were postcured freestanding to 316°C (600°F) for 4 hours.
- (2) Joint efficiency based on percentage of average recoverable strength from baseline control specimen tensile values of 950 KN/m (5,429 lb/in.) at RT.
- (3) Specimen design given in Figure 4-6, fiber orientation (0, ±45, 90)_{2s} -16 ply 0.231 cm (0.091 inch) thick.
- (4) Specimens were tested after stabilizing at 316°C (600°F) for 10⁺⁵₋₀ minutes at a load rate of 0.127 cm (0.05 inch)/minute.

Bond joint quality was significantly improved as indicated by C-scan recordings of 98 percent ultrasound through transmission through the bond areas: however, portions of the cocure laminate outside the bond area showed about 20 percent void.

Relatively high laminate void can be attributed to the low, 689 KN/m^2 (100 psi) autoclave molding pressure used in the process. Bond strengths at room temperature were also improved, while 316°C (600°F) properties showed a significant loss from previous auxiliary adhesive bonded specimens. Average data points are presented in Table 4-5.

4.5.2 Prepreg Adhesive In-Situ Imidize Cocure Process Development

The prepreg adhesive in-situ imidize cocure process development effort was continued from midplane bonding studies in application of the process to 3-degree, 4.5-degree, and 6-degree flush scarf angle tensile shear specimens following the secondary bond design, shown in Figure 4-6. Specimens were prepared without BR34B-18 primer on faying surfaces. The in-situ imidizing autoclave cocure process was performed on stepped scarf angle preforms at 288°C (550°F) and $1,378 \text{ KN/m}^2$ (200 psi) per the cycle shown in Figure 4-8. Specimens were postcured free-standing at 316°C (600°F) for 4 hours. The tooling concept is shown in Figure 4-13. NDI C-scan test results indicated excellent void-free bonds and laminates were attained. Tensile shear strength of the 3-degree scarf angle joint specimens at room temperature and 316°C (600°F) was fairly consistent with previous auxiliary adhesive cocure bonded specimens. The 3-degree scarf angle bonds demonstrated superior joint efficiency to 4.5-degree and 6-degree scarf angle joint specimens, however, bond strength efficiencies of the 3-degree scarf angle joint specimens fell short of the target tensile strength by approximately 40 percent. Relatively low strength efficiency is traced to peel moments initiated at the scarf joint adherend thin leading edges. Average tensile shear properties at room temperature and 316°C (600°F) and quantitative NDI C-scan recording data are given in Table 4-5. A typical NDI C-scan recording of a cocured specimen bond joint and laminate areas is presented in Figure 4-14.

4.6 IMPROVED JOINT DESIGN PROCESS DEVELOPMENT

Since target tensile shear load could not be achieved with the basic flush scarf joint concepts, alternate repair techniques and joint concepts were evaluated. The improved repair joint design evaluated is based on a concept developed by Northrop Corp. for graphite/epoxy composite repair under Air Force Contract, and reported in Reference 2. The concept follows the basic parent material scarf angle joint approach but adds three external stepped doubler plies to top and bottom parent laminate surfaces that extend beyond the edge of the scarf portion of the patch. Terminating doubler ply edges are serrated with conventional 0.30 cm (0.12 in.) by 45 degrees pinking shears. Northrop tests showed the stepped external doublers with serrated edge feature reduces peel forces in the joint under tension and compression stress and repair joint efficiency using this approach was increased to 100 percent of parent graphite/epoxy laminate strength.

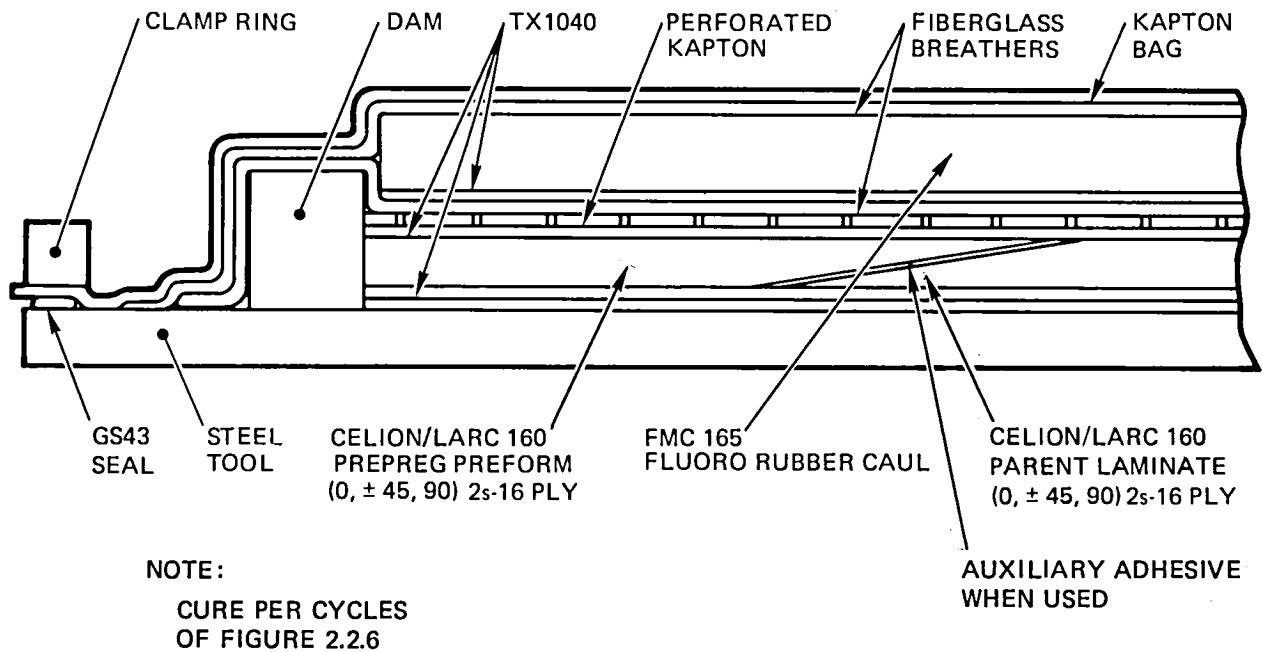


Figure 4-13. Cross Section of Prepreg Adhesive, In-Situ Imidizing
Cocure Scarf Angle Repair Tooling

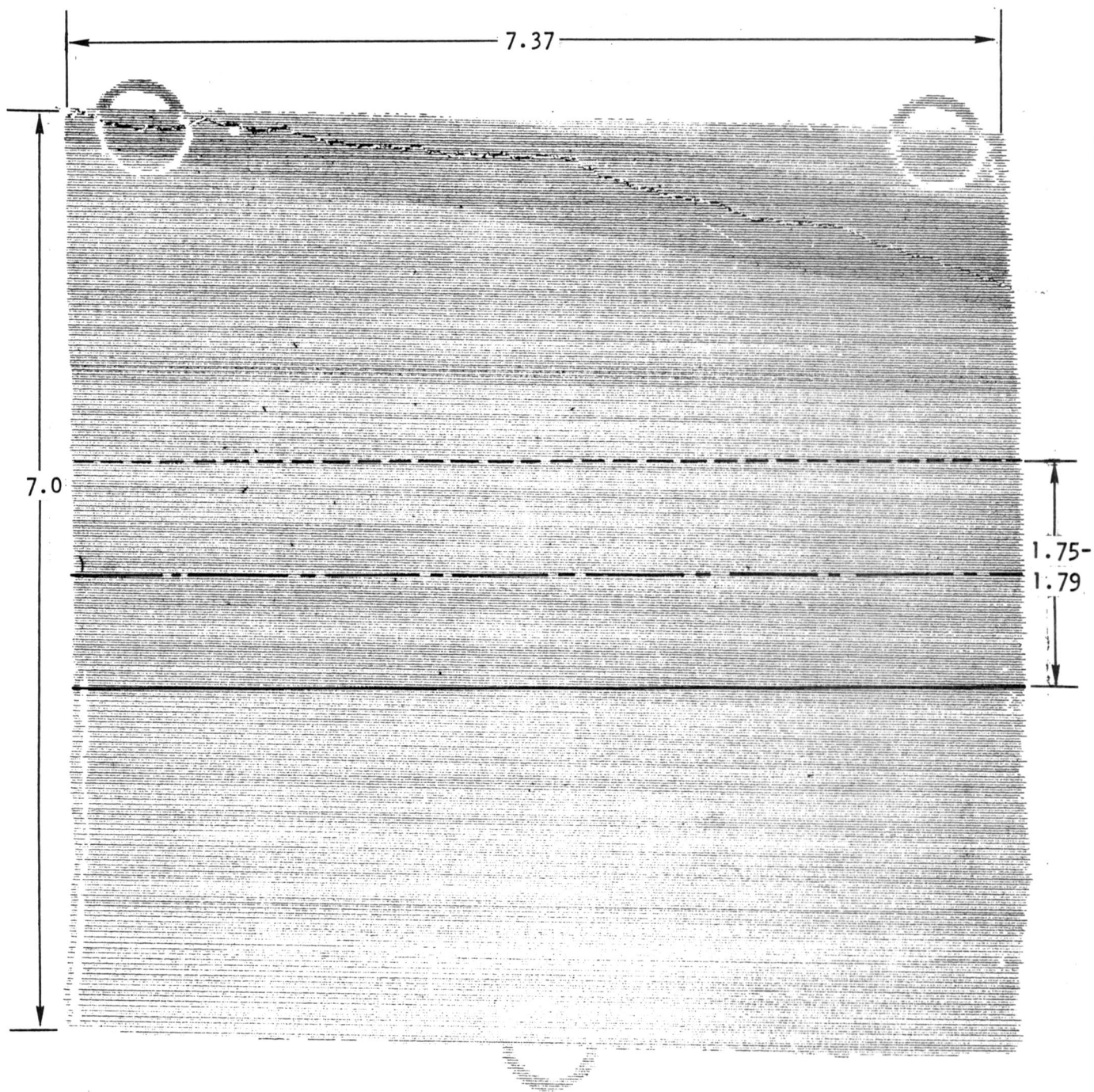


Figure 4-14. NDI C-Scans of 3-Degree Prepreg Adhesive Cocure Bond Joint

4.6.1 Improved Joint Design and Process Evaluation

The joint design, Figure 4-15, was evaluated in application of Celion/LARC-160 prepreg to parent composite laminates with 3-degree, 4.5-degree, 6-degree scarf angle joints. The prepreg adhesive in-situ imidizing cocure process, Figure 4-8, and tooling, Figure 4-13 were employed in the repair operations. Parent laminate stock (0, ± 45 , 90)_{2s} was sized to yield six, 2.54 cm (1.00 in.) wide tensile specimens. Tensile specimens were trimmed on a diamond saw to 17.8 cm (7.00 in.) long by 2.54 cm (1.00 in.) wide test configuration. Specimens were tested in tension at room temperature and 316°C (600°F) at 0.127 cm (0.05 in.) per minute, 10 minutes after attaining test temperature.

4.6.2 Tension and NDI Test Results

Results of tension tests were extremely encouraging with the three scarf angle configurations evaluated. Joint efficiencies at room temperature ranged between 89 and 99 percent of parent laminate baseline strength of 946 KN/m (5,400 lb/in.) with some tension failures occurring in the parent laminate. Specimens tested at 316°C (600°F) yielded 80.2 to 90.5 percent room temperature joint efficiency, with some parent laminate tension failures. Improved joint strength efficiency is compared graphically with flush scarf angle secondary and cocure bonded joints in Figure 4-16. NDI C-scan tests performed on repair joints showed 100 percent ultrasound through transmission indicating zero-void bonds were achieved, as shown in Figure 4-17. Photomicrographs of 4.5 degree scarf angle specimen joint areas verify the high quality of the laminate in Figure 4-15. Tensile strengths achieved on the three configurations at room temperature and 316°C (600°F) are presented in Table 4-6.

4.7 COCURE BONDING ADHESIVE PROCESS AND DESIGN CONCEPT SELECTION

The Celion LARC-160 unidirectional tape, 152 gram/m² areal weight prepreg was selected for cocure repair of flat laminate, honeycomb sandwich, and hat-stringer stiffened skin elements. This selection was based on the following test results and rationale.

1. Cocured midplane bonded notched lap shear specimens (with anti-peel clamps) yielded the highest bond strengths with failure modes predominately outside the bondline.
2. NDI C-scan tests on midplane, various scarf angle, and improved serrated edge doubler patch cocure bonds yielded recordings of consistent low or zero void.
3. Cocure prepreg preform patches will conform to any machined surface, without forming voids caused by mismatch.
4. The prepreg adhesive, in-situ imidizing cocure process allows integral molded and bonded repair patches to be applied to cured laminate structure using proven standard laminate autoclave molding procedures.

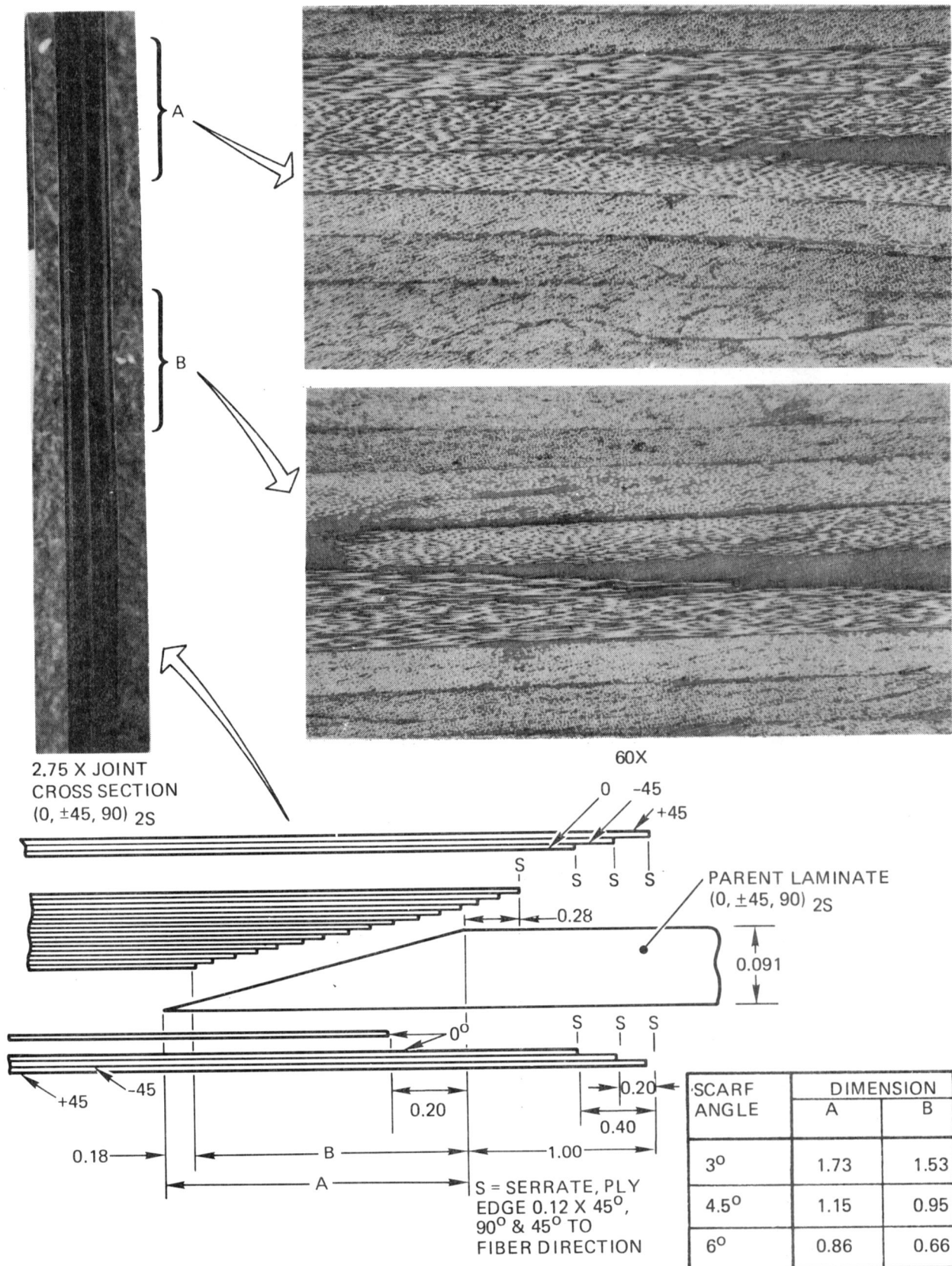


Figure 4-15. Cross Section; Improved Repair Design Concepts 3-Degree, 4.5-Degree, and 6-Degree Scarf Angles

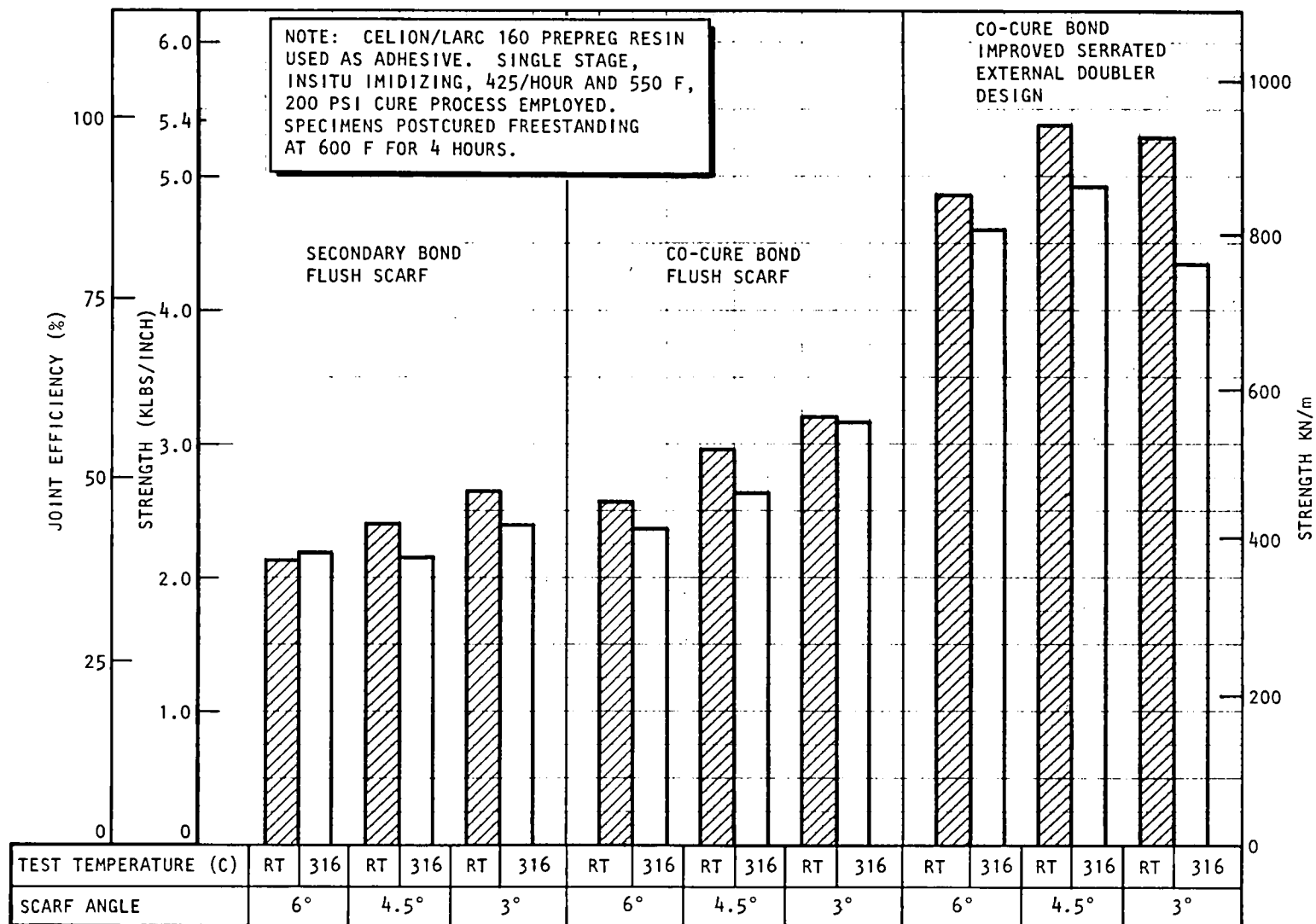


Figure 4-16. Average Tensile Strengths of Flush Scarf and Improved Repair Joint Designs

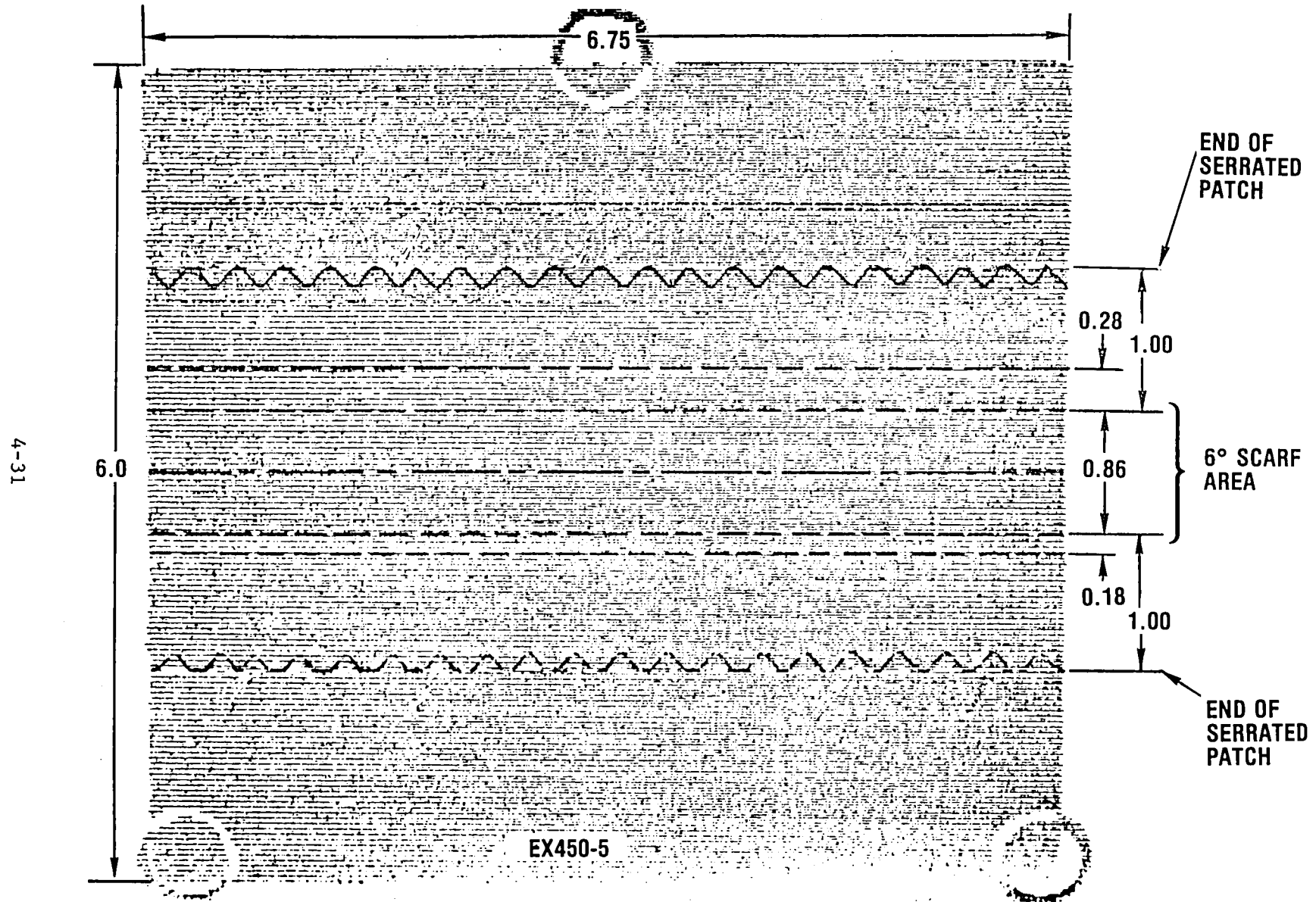


Figure 4-17. NDI C-Scan of Improved Repair 6-Degree Scarf With External Serrated Doublers

Table 4-6. Results of Improved Repair Joint Design
Tension Tests at Room Temperature and 600°F

Panel No.	Scarf(1) Angle	NDI C-Scan Transmission (%)	Tensile Shear Strength/Joint Efficiency					
			Ultimate Strength ⁽²⁾ RT		Joint (3) Efficiency (%)	Ultimate Strength ⁽²⁾ 316°C (600°F)		Joint (3) Efficiency (%)
			KN/m	lb/in.		KN/m	lb/in.	
EX450-2	3°	100		4,720 5,376 <u>5,183</u>	97.4		4,585 4,286 <u>4,179</u>	80.2
			Avg 926	5,290		769	4,350	
EX400-40	4.5	100		5,471 5,314 <u>5,325</u>	98.9		4,801 4,620 <u>5,275</u>	90.5
			Avg 946	5,370		861	4,915	
EX450-5	6°	100		4,529 4,965 <u>5,066</u>	89.4		4,752 4,533 <u>4,470</u>	84.5
			Avg 850	4,853		803	4,585	
<p>(1) Specimen joint design is given in Figure 4-15. Specimen repair was performed using the non-adhesive, in-situ imidizing cocure cycle per Figure 4-8. Specimens post-cured at 316°C (600°F) for 4 hours.</p> <p>(2) Specimens were tested after stabilizing at 316°C (600°F) for 10⁺⁵₋₀ minutes at a load rate of 0.127 cm (0.05 in.) per minute.</p> <p>(3) Joint efficiency based on percentage of average recoverable strength from baseline control tensile values of 950 KN/m (5,429 lb/in.) at room temperature.</p>								

5. The improved, external octagonal doubler repair concept can be applied integrally with scarfed prepreg preforms. This concept has demonstrated 99 percent recoverable parent laminate strength by reducing peel forces under tensile stress.

4.8 LOW PRESSURE BONDING STUDY

As discussed in Section 7, an autoclave isostatic flatwise compression pressure of 689 KN/m^2 (150 psi) will crush the HRH 327-3/16-3.5 pcf fiberglass/polyimide honeycomb (stabilized) during sandwich repair cures at 288°C (550°F). Midplane secondary bonded and single-stage in-situ imidized, cocure bonded panels were made to evaluate the effects of reduced pressure levels on cocure bond line and laminate quality. Standard NDI C-scan techniques were employed to establish quality.

4.8.1 Low Pressure Secondary Bonding Development

Secondary midplane bonding pressure of 689 KN/m^2 (100 psi) was verified in early bonding studies to yield fairly consistent void-free bonds using LARC-160 adhesive based on diglyme solvent; therefore, only 689 and 516 KN/m^2 (100 and 75 psi) pressures were evaluated in secondary bonding studies in support of Rockwell design sandwich repair operations. The standard single-stage in-situ 218°C (425°F) imidizing 288°C (550°F) cure cycle per Figure 4-8 was employed in all secondary bonding operations. Midplane-bonded unidirectional panels and lap shear specimens were fabricated as per the design shown in Figure 4-2.

An improved LARC-160 adhesive diluted with ETOH solvent was evaluated in these low pressure bonding studies. The ETOH solvent carrier boils at 78.3°C (173°F) and, therefore, should afford lower void bonds with these low bonding pressures than the 160°C (320°F) boiling point diglyme solvent presently used in the standard LARC-160 adhesive.

The three adhesive systems evaluated were:

1. LARC-160/AL123/ETOH/108 fiberglass carrier, approximately 440 grams/ m^2 (0.09 psf)
2. Celion 6K/LARC-160 unidirectional tape, 152 grams/ m^2 , 34.5 percent resin solids.
3. Celion 1K/LARC-160, 34 by 35, 5-harness satin weave, 6.5 mils per ply 36 percent resin solids

4.8.2 Evaluation of Low Pressure Secondary Bonds

NDI C-scan tests showed varying degrees of void in all 517 KN/m² (75 psi) bonded panels. the 689 KN/m² (100 psi LARC-160/AL123/ETOH/108) fiberglass adhesive-bonded panel had 100 percent through transmission. The two prepreg adhesives were not evaluated at 689 KN/m² (100 psi) bonding pressure since it was later determined the HRH-317 - 3/16 - 3.5 pcf honeycomb core would crush at this pressure level. Approximate bondline void yield levels for each adhesive system are given in Table 4-7. Midplane-bonded panels were notched and cut into 2.54 cm (1.0 in.) wide tensile shear specimens, per the design shown in Figure 4-2. The FED STD 406 Method 1042 anti-peel clamp was employed in room temperature and 316°C (600°F) tests to eliminate peel forces.

Tensile shear strengths of all specimens tested at room temperature and 316°C (600°F) exceeded values attained previously in adhesive screening studies where anti-peel clamps were not employed. The best balance of properties was achieved in the 35 by 34, five-harness satin weave Celion 1K/LARC-160 fabric prepreg adhesive with average room temperature and 316°C (600°F) values of 18.9 and 16.3 KN/m² (2,745 and 2,383 ksi). This adhesive system was selected for secondary bonding repair of a lightly loaded sandwich element.

4.8.3 Low Pressure Cocure Bonding Process Development

Cocure midplane bonded 0.16 cm (0.065 in.) thick laminates were fabricated using two prepreg adhesive, in-situ imidizing and cure cycles. The first process evaluated was the standard 218°C (425°F), 1 hour imidizing cure with cure at 288°C (550°F) using 517 KN/m² (75 psi) autoclave pressure for 2 hours. High voids were detected in NDI C-scan tests and cocured laminates indicated a visual lack of compaction. The second process evaluated was an imidizing cycle of 325°F for 1 hour followed by curing at 288°C (550°F) 517 KN/m² (75 psi) for 2 hours. This cycle also produced cocure laminates with high void as indicated by C-scan recordings. Notched interlaminar shear specimens were not machined from panel stock or tested because of high void levels.

Table 4-7. Tensile Shear Strengths of Low Pressure Secondary Midplane Bonded Celion/LARC-160 Laminates at Room Temperature and 316°C

Specimen No.	Adhesive	Cure Pressure ⁽¹⁾		C-Scan Transmission (%)	Ultimate Strength ⁽²⁾					
		KN/m ²	(psi)		RT		316°C (600°F)			
					MN/m ²	(psi)	MN/m ²	(psi)		
EX516-1	LARC-160/AL123/ ETOH/108 Carrier staged 150°F, 1 hr	689	100	85	<u>216</u>	3,095 3,259 <u>3,066</u> (3,140)	<u>145</u>	2,065 2,086 <u>2,162</u> (2,104)		
EX516-2	LARC-160/AL123/ ETOH/108 Carrier no stage	689	100	100		2,631 2,933 <u>3,144</u> (2,903)		<u>151</u>	--- 2,118 <u>2,282</u> (2,198)	
EX516-5	LARC-160/AL123/ ETOH/108 Carrier no stage	516	75	50		2,509 2,801 <u>3,119</u> (2,810)			<u>104</u>	1,850 1,182 --- (1,516)
EX516-7	152g/m ² Celion/ LARC-160 tape, 34.0 percent Resin cont	516	75	20		2,561 1,923 <u>2,522</u> (2,335)				<u>134</u>
EX516-8	35 x 34 - 5 Harness Satin weave Celion 1K/ LARC-160	516	75	85	2,509 3,152 <u>2,570</u> (2,745)	<u>164</u>	2,807 2,179 <u>2,162</u> (2,383)			

(1) Autoclave cure process: apply <2 inches Hg vacuum, raise temperature from room temperature to 425°F at 3 to 8°F/minute; apply pressure, imidize at 425°F, 1 hour; raise temperature to 550°F at 3 to 5°F/minute; cure at 550°F, 2 hours; force cool to <250°F prior to pressure release.

(2) Specimens were tested at 0.05 inch/minute after stabilizing at 600°F for 10 minutes. FED STD 406, Method 1042 anti-peel clamps were used in testing

5. ANALYTICAL METHODOLOGY DEVELOPMENT

The repairs are idealized in the analytical models as a type of bonded joint, i.e., single lap, double lap, or scarf. Simple analytical models were developed for sizing of optimum doubler lap lengths and scarf angles. These simple models allow design of the repairs without the need for a sophisticated computer program. Because the test data generally have considerable scatter because of processing and other variations, the simple models provide as much accuracy as the more sophisticated models. Comparison of the analytical models with coupon test data developed confidence in the design methodology. These results were then extrapolated for the design of the subelement repairs discussed in subsequent sections.

Repair concepts are categorized as either one-sided or two-sided, and either flush or with some surface protuberance. Repairs with a doubler on one side are analytically idealized as adhesively bonded single lap joints, while repairs with doublers on both sides are idealized as double lap joints. Flush repairs are idealized as scarf joints. The analytical models developed to determine the stress state associated with the repair concepts were based on the work done by Hart-Smith (References 4 through 7) on adhesively bonded composite joints.

5.1 OPTIMUM LAP LENGTH--SINGLE LAP JOINT

A flat laminate repaired by a single doubler is idealized as a single lap joint in the analysis, which is based on the formulation presented in Reference 4. The accuracy of the analysis is determined by a comparison of the lap shear data in Table 5-1 (Reference 8). The analysis examines the three primary modes of failure of the bonded lap joint with filamentary composite adherends:

1. Interlaminar transverse tension failure caused by peel stresses
2. Adherend failure caused by a combination of axial loads and bending stress from the eccentricity of the loads
3. Adhesive failure in shear

Except for very short lap lengths, the thickness of the laminate dictates the most probable failure mode. Short lap lengths generally fail in adhesive shear (Mode 3) in combination with some interlaminar transverse tension failure (Mode 1) independent of laminate thickness. Thin laminates with moderate lap lengths will fail because of inplane loads (Mode 2), while thick laminates will fail because of transverse tension (Mode 1). Analysis of the adhesive shear stress predicts a potentially high shear strength for lap joints of practical length; however, failure of the filamentary composite adherends under inter-laminar transverse tension because of the peel stresses prevents the attainment of the potentially high shear strength. Because of the eccentricity of the load path, the single lap joint efficiency is always less than unity. Lap lengths needed to develop peak efficiencies are so great as to impose a significant weight penalty for single lap joints.

Table 5-1. Effect of Overlap Length on LARC-13 Lap Shear Strength (Room Temperature)

Length ₁ Overlap cm (in.)	Lap Shear Strength				Mode of Failure ² (%)
	MN/m ²	psi	KN/m	lb/in.	
0.64 (0.25)	43.3	6285	275	1571	L75, C25
1.27 (0.5)	25.4	3690	323	1845	L60, C40
2.54 (1.0)	14.1	2045	358	2045	L100
5.08 (2.0)	9.8	1425	499	2850	L100
10.16 (4.0)	5.9	860	602	3440	L95
¹ All specimens were 2.54 cm (1 in.) wide Adherends: Celion/PMR-15, 16 ply (0.20 cm, 0.08 in.), unidirectional ² L = Laminate failure; C = Cohesive failure in adhesive					

The geometry for the single lap joint analysis is shown in Figure 5-1. A list of symbols to be used in the analysis is given in the following. All derivations of the formulas used are given in Reference 4.

In order of appearance

σ_p	Peel stress N/cm ² (psi)
K _p	Peel stress concentration factor
σ_{avg}	Average adherend stress N/cm ² (psi)
P	Applied load N (lb)
t	Laminate thickness cm (in.)
k	Eccentricity factor
t _a	Adhesive thickness cm (in.)
E' _c	Transverse tension modulus N/cm ² (psi)
ν	Poissons ratio
k _b	Bending stiffness parameter
E	Laminate longitudinal modulus N/cm ² (psi)
E _c	Adhesive peel modulus N/cm ² (psi)
E _n	Laminate transverse tensile modulus N/cm ² (psi)

D	Flexural rigidity of adherends $N\text{-cm}^2$ (lb-in.^2)
ℓ	Lap length cm (in.)
K_B	Bending stress concentration factor
τ_{avg}	Average shear stress N/cm^2 (psi)
τ_{max}	Maximum shear stress N/cm^2 (psi)
K_s	Shear stress concentration factor
λ, λ'	Exponents of elastic shear stress distribution cm^{-1} (in.^{-1})
G	Adhesive shear modulus N/cm^2 (psi)

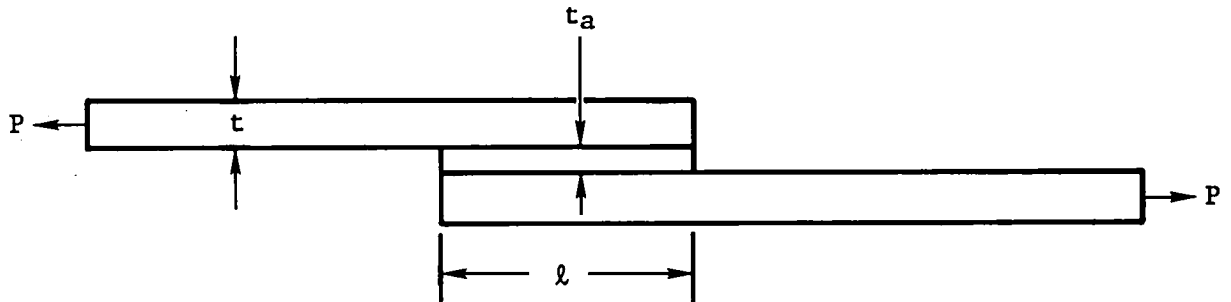


Figure 5-1. Lap Joint Geometry

The primary modes of failure are discussed in the following.

Failure Mode 1. The most prominent failure mode for single lap joints with composite adherends is the interlaminar transverse tensile failure caused by the peel stresses. Because of the assumption made in its derivation, the formula given here applies only for thick laminates with long lap lengths. The peel stress is given by

$$\sigma_p = K_p \sigma_{\text{avg}} \quad (1)$$

where

$$\sigma_{\text{avg}} = P/t \quad (2)$$

and

$$K_p = k(1 + \frac{t_a}{t}) \left[\frac{3 E'_c (1 - \nu^2) t}{2 k_b E t_a} \right]^{1/2} \quad (3)$$

where

$$\frac{1}{E'_c} = \frac{1}{E_c} + \frac{4}{E_n} \quad (4)$$

$$k_b = \frac{D}{[Et^3/12(1 - \nu^2)]} \quad (5)$$

and

$$k = \frac{1}{1 + \frac{\ell\sqrt{P}}{2\sqrt{D}} + \frac{P\ell^2}{24D}} \quad (6)$$

From laminate theory in the notation of Reference 9, the laminate bending stiffness is

$$D = 1/3 \sum_{k=1}^n (\bar{Q}_{11}) (h_k^3 - h_{k-1}^3) \quad (7)$$

which simplifies to the following for unidirectional laminates:

$$D = \frac{Et^3}{12(1 - \nu_{xy}\nu_{yx})}, \text{ thus } k_b = 1.0 \quad (8)$$

Failure Mode 2. The adherend failure just outside the joint area is the predominate failure mode for thin laminates with moderate lap lengths. The adherend stress distribution resulting from the combined axial stresses and the bending stresses caused by the eccentricity of the load path is given as follows:

$$\sigma_{\max} = K_B \sigma_{\text{avg}} \quad (9)$$

where

$$K_B = [1 + 3k(1 - \frac{t_a}{t})] \quad (10)$$

Failure Mode 3. Except for short lap lengths, the adhesive shear failure is not of major concern in the design of lap joints with composite adherends. The adhesive shear distribution is given as follows:

$$\tau_{avg} = P/\ell \quad (11)$$

and

$$\tau_{max} = K_s \tau_{avg} \quad (12)$$

where

$$K_s = 1 + \left[1 + \frac{3k(1 - \nu^2)}{k_b} \left(1 + \frac{t_a}{t} \right) \right] \left[\frac{\lambda^2}{4(\lambda')^2} \right] \left[\frac{\lambda' \ell}{2 \tanh(\lambda' \ell)} - 1 \right] \quad (13)$$

where

$$\lambda^2 = \frac{2G}{Et} \frac{1}{t_a} \quad (14)$$

and

$$(\lambda')^2 = \left[1 + \frac{3(1 - \nu^2)}{k_b} \right] \frac{\lambda^2}{4} \quad (15)$$

Analytical Correlation of Lap Shear Data. To assess the accuracy of the analytical models presented, the formulas were used to correlate the room temperature lap shear data for LARC-13 adhesive, reference 8. The effect of lap length on the lap shear strength of LARC-13 is presented in Table 5-1. The material properties used in the analysis are given in Table 5-2. Because bulk adhesive properties for LARC-13 were not available, properties of a brittle high modulus epoxy were assumed. The predicted adhesive shear failure levels and the predicted peel failure levels are shown with the lap shear test data in Figure 5-2. Because of the high strength of the unidirectional laminate adherends, the inplane loads (Failure Mode 2) were negligible.

The predicted adhesive shear failure fit the data well for lap lengths up to 2 inches, but did not predict failure for longer lap lengths. The analytical model for peel failure, which is the dominate failure mode, does not fit the test data. A more accurate model of the peel stress state in single lap joints should be developed. For practical repair designs, the ends of the doublers will be beveled to reduce the peel stresses. An analytical model is necessary to assess the effect of the beveled edges.

The optimum lap length for a single lap joint is determined by applying the efficiency criteria presented in Section 3. As shown in Table 5-3, the overall efficiency of a particular lap length depends on the total length of

Table 5-2. Adherend and Adhesive Properties Used in Lap Shear Data Correlation

⁰ 16 Celion/PMR-15 Adherends $E = 138 \text{ GN/m}^2 \text{ (20.0 ksi)}$ $E_n = 11 \text{ GN/m}^2 \text{ (1.6 ksi)}$ $\nu_{xy} = 0.275$ $\nu_{yx} = 0.022$ $t = 0.20 \text{ cm (0.08 in.)}$ $\sigma_{\max} = 1.93 \text{ GN/m}^2 \text{ (280 ksi)}$ $\sigma_p = 0.02 \text{ GN/m}^2 \text{ (3.4 ksi)}$	LARC-13 adhesive (estimated) $G = 2.24 \text{ GN/m}^2 \text{ (325 ksi)}$ $\tau_{\max} = 50.5 \text{ MN/m}^2 \text{ (7320 psi)}$ $E_c = 8.3 \text{ GN/m}^2 \text{ (1.2 ksi)}$ $t_a = 0.0127 \text{ cm (0.005 in.)}$
----------------------------------------------------------------------------------------------------------------------------------------------------------------------------------------------------------------------------------------------------------------------------------------------------------------------------------------	--------------------------------------------------------------------------------------------------------------------------------------------------------------------------------------------------------------------------------

Table 5-3. Lap Length Overall Efficiency

Lap Length cm (in.)	15 cm (6 in.)* Efficiency	183 cm (6 ft)* Efficiency
0.64 (0.25)	0.072	0.078
1.27 (0.5)	0.078	0.091
2.54 (1.0)	0.075	0.099
5.08 (2.0)	0.084	0.135
10.16 (4.0)	0.071	0.154
*Length of parent laminate		

the parent laminate. If the parent laminate is relatively short (15 cm [6 in.]), the added strength of a 10 cm (4 in.) lap is offset by the added weight; however, if the parent laminate is relatively long (183 cm [6 ft]), the weight added by a 4-inch lap doubler is negligible. When the weight impact of a doubler repair is evaluated on a local scale, the optimum doubler lap length is 5.08 cm (2 in.).

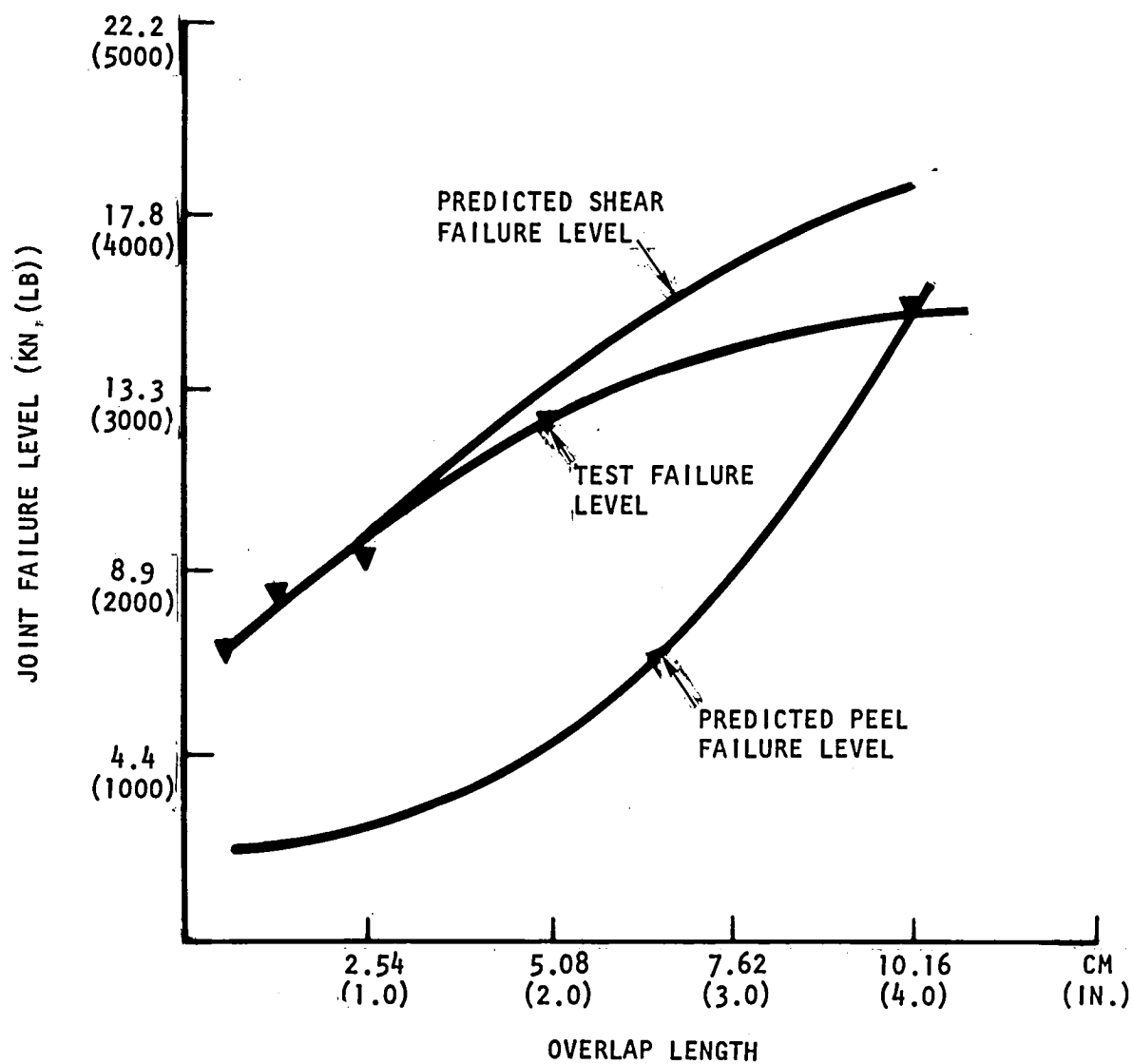


Figure 5-2. Joint Strength Predictions Versus Test Data for LARC-13

5.2 OPTIMUM LAP LENGTH - DOUBLE LAP JOINT

Because of its symmetric load path and reduced peel stresses, the double lap joint is an improvement over the single lap joint in terms of load efficiency (60 percent more efficient for a 1/2-inch lap length). Double lap failure modes are dependent upon the adherend thickness. For joints with thin adherends, adherend tensile failure predominates since the adhesive strength is greater and the peel stresses are negligible. For thick adherends, adhesive shear failure is possible. For thicker adherends, failures occur because of peel stresses. Because of the relatively low flatwise tensile strength of GR/PI composites, peel failure is much more of a problem than adhesive failure; however, adhesive failure will predominate for most laminate configurations and joint geometries in 316°C (600°F) applications. An analysis of the failure modes is presented in the following paragraphs. The objective of the analysis is to define the optimum joint configuration for maximum strength.

5.2.1 Double Lap Joint Adhesive Stress Analysis.

The following solution for the load transfer across a double lap joint is taken from Reference 5. It is assumed that the adhesive is brittle ($\gamma^P = 1.5 \gamma^e$, see Figure 5-3). Increasing the lap length for double lap joints increases the strength in the initial small range of overlap values, after which the strength reaches a constant value. The solution predicts the minimum overlap required for maximum bond strength (see Figure 5-4). The solution is not valid for adhesive stresses for shorter lap lengths, and longer lap lengths do not result in additional joint strength.

The geometry and definition of symbols for the double lap joint is shown in Figure 5-3. The average shear stress is

$$\tau_{avg} = \frac{P}{2\ell}$$

The maximum adhesive shear stress is

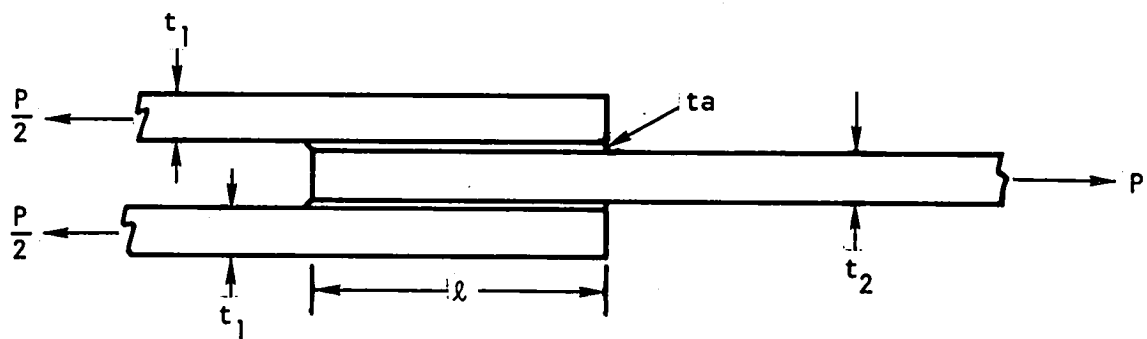
$$\tau_{max} = K \tau_{avg}$$

where

$$K^2 = \frac{G\ell^2}{t_a C}$$

and C equals the lesser of

$$\left[4E_1 t_1 \left(1 + \frac{2E_1 t_1}{E_2 t_2} \right) \right]$$



LIST OF SYMBOLS

τ_{avg}	Avg adhesive shear stress
P	Applied load
l	Lap length
τ_{max}	Max adhesive shear stress
K	Stress concentration factor
G	Adhesive shear modulus
t_a	Adhesive thickness
C	Factor
E	Adherend tensile modulus
t_1	Adherend thickness
t_2	Parent thickness
P_{max}	Maximum possible load
σ_p	Maximum peel stress
E_p	Modified peel modulus
ν	Poissons ratio
γ^p	Adhesive plastic strain
γ^e	Adhesive elastic strain

Figure 5-3. Double Lap Shear Specimen Joint Geometry

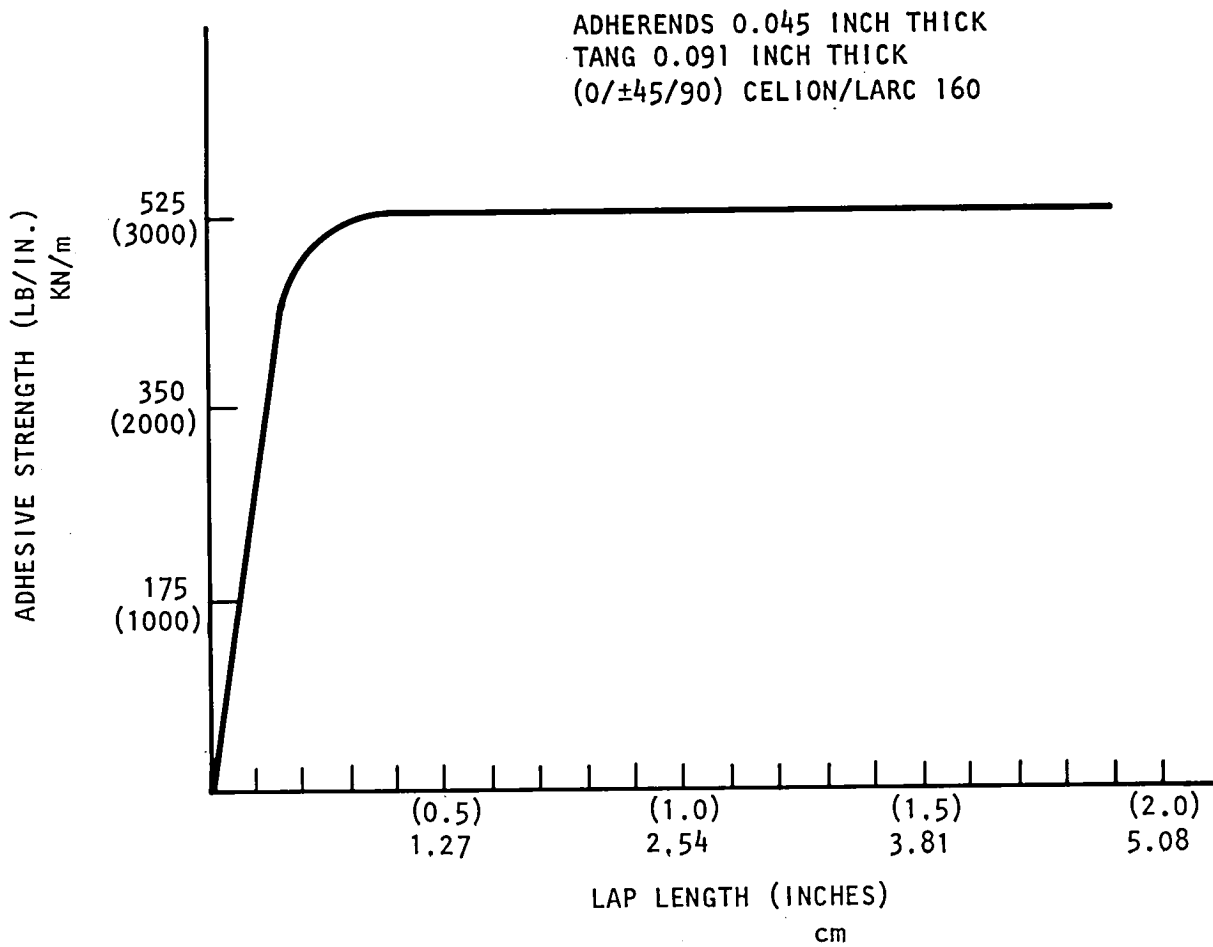


Figure 5-4. Theoretical Adhesive Bond Strength Versus Lap Length for Double Lap Joint

or

$$\left[2E_2 t_2 \left(1 + \frac{E_2 t_2}{2E_1 t_1} \right) \right]$$

Rearranging the above equations

$$P_{\max} = 2 \sqrt{\frac{t_a C}{G}} \tau_{\max}$$

The optimum lap length is defined in Reference 5 as

$$\ell = \frac{P_{\max}}{2 \tau_{\max}} + \frac{2}{\lambda}$$

where

$$\lambda^2 = \frac{G}{t_a} \left(\frac{1}{E_1 t_1} + \frac{2}{E_2 t_2} \right)$$

For the special case where $E_1 = E_2 = E$, and $t_2 = 2t_1$

$$P_{\max} = 8 \sqrt{\frac{E t_1 t_a}{2G}} \tau_{\max} \quad (16)$$

and

$$\ell = \frac{P_{\max}}{2 \tau_{\max}} + 2 \sqrt{\frac{E t_1 t_a}{2G}} \quad (17)$$

Inserting the assumed properties from Table 5-4 yields

$$P_{\max} = 530 \frac{\text{KN}}{\text{m}} \left(3,023 \frac{\text{lb}}{\text{in.}} \right)$$

and

$$\ell = 0.787 \text{ cm (0.31 in.)}$$

A factor should be added to this length in a practical design to account for manufacturing anomalies and to provide better fatigue life. Also, the analysis used room temperature adhesive properties. For applications up to 315°C (600°F) another factor should be added to the lap length; however, increasing the lap length past 1.27 cm (0.5 in.) for room temperature applications or 2.54 cm (1.0 in.) for elevated temperature applications would in theory not be effective in transferring additional shear load.

Table 5-4. Adherend and Adhesive Properties Used
in Double Lap Joint Analysis

Adherends (0/±45/90) _{2s} Celion/LARC 160	Adhesive (estimated) FM-34
$t_1 = 0.045 \text{ in. (0.114 cm)}$	$G = 325 \text{ ksi (2.2 GN/m}^2\text{)}$
$t_2 = 0.091 \text{ in. (0.231 cm)}$	$\tau_{\max} = 7,320 \text{ psi (50.5 MN/m}^2\text{)}$
$E = 7.7 \text{ msi (53 GN/m}^2\text{)}$	$t_a = 0.005 \text{ in. (0.0129 cm)}$
$E_p = 0.3 \text{ msi (2.1 GN/m}^2\text{)}$	
$\sigma_p = 3.4 \text{ ksi (23. MN/M}^2\text{)}$	
$\sigma_{\max} = 82.5 \text{ ksi (569 MN/m}^2\text{)}$	
$\nu = 0.295$	

5.2.2 Double Lap Joint Peel Stress Analysis

As discussed, peel stresses can become significant in double lap joints with thick adherends. The maximum peel stress in the adhesive and adjacent adherend at the end of the joint is given below. Because the flatwise tensile allowable for the adherends is less than that for the adhesive, failure will initiate in the adherend.

$$\sigma_p = \tau_{\max} \left(\frac{3E_p (1-\nu^2)t_1}{E t_a} \right)^{1/4} \quad (18)$$

The simultaneous solution of equations (16) and (17) yields a predicted peel failure load of 249 KN/m (1,420 lb/in.). The low flatwise tensile allowable 23.4 MN/m² (3,400 psi) of GR/PI laminates makes failure caused by peel stresses likely. To reduce the peel stresses, the ends of the adherends should be tapered at least 15 degrees, per Reference 5. The amount of peel stress reduction is difficult to assess analytically, but most of the potential adhesive strength should be realized.

5.3 OPTIMUM SCARF ANGLE - SCARF JOINT

The load carrying capability of scarf joints has been evaluated to determine an optimum scarf angle for flush repairs. The analytical models developed in Reference 6 for scarf joints include the effects of dissimilar adherends and the plasticity of the adhesive. The scarf repairs of interest have identical adherends, use a relatively brittle adhesive, and have small scarf angles. For this latter simple case, the solution of Reference 6

predicts uniform adhesive shear stresses. For preliminary sizing of the scarf joint, the optimum scarf angle (θ) for a maximum strength joint is given as

$$\theta = \text{Arctan } \frac{\tau_{\max}}{\sigma_{\max}} \quad (19)$$

where τ_{\max} is the maximum allowable adhesive shear stress, σ_{\max} is the maximum allowable adherend stress, and θ is defined in Figure 5-5.

From Table 5-1, the bulk adhesive shear strength for LARC-13 adhesive is estimated to be 50.5 MN/m^2 (7,320 psi). The tensile allowable for a quasi-isotropic Celion/LARC-160 laminate is 569 MN/m^2 (82.5 ksi) (Reference 10). Thus the optimum scarf angle is about 5 degrees.

Because the analysis of Reference 6 neglects the heterogeneous laminar nature of the adherends, an analysis was performed based on the methodology outlined in Reference 11 and the scarf joint test data presented in Table 5-5. Stress concentrations in the adhesive caused by the stiffness differences between the individual plies have been experimentally evaluated (Reference 11). Based on these data, an adhesive shear stress concentration factor of 2.88 is used to account for the heterogeneity of the adherends.

The symbols used in the following analysis are defined below in the order of appearance.

τ_{\max}	Maximum adhesive shear stress
τ_{avg}	Average adhesive shear stress
K_a	Stress concentration factor - adhesive
P	Total load applied to joint
w	Width of joint
t	Laminate thickness
θ	Scarf angle
σ_{\max}	Maximum adherend tensile stress
K_l	Stress concentration factor - laminate

The maximum adhesive shear stress is

$$\tau_{\max} = K_a \tau_{\text{avg}}$$

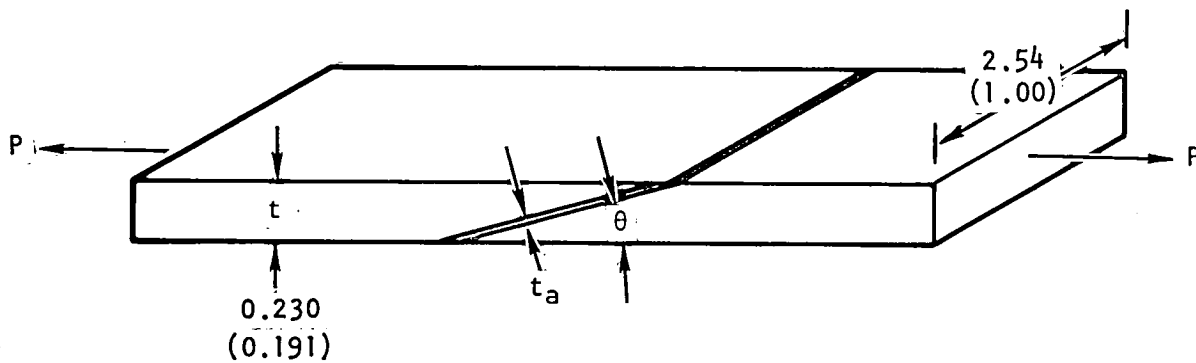


Figure 5-5. Scarf Joint Geometry

Table 5-5. Average Room Temperature Scarf Joint Test Data

Scarf Angle	Secondary Bond (1)		Cocure (2)		Improved (3)	
	LB/IN	KN/m	LB/IN	KN/m	LB/IN	KN/m
3°	2650	464	3200	560	5300	928
4.5°	2440	427	2950	516	5400	946
6°	2175	381	2600	455	4900	858
(1) See Figure 4-16						
(2) See Figure 4-16						
(3) See Figure 4-16						

where

$$\tau_{avg} = \frac{P}{wt} \cos \theta \sin \theta$$

$$K_a = 2.88$$

Therefore,

$$\tau_{max} = \frac{2.88P}{wt} \cos \theta \sin \theta \quad (20)$$

for small angles (less than 10°)

$$\tau_{max} = \frac{2.88P}{wt} \cos \theta \quad (21)$$

The maximum tensile stress in the adherends is

$$\sigma_{max} = K_\ell \frac{P}{wt} \quad (22)$$

where

$$K_\ell = 1.35 \cos^2 \theta + 1$$

For small angles (less than 10°)

$$\sigma_{max} = \frac{2.35P}{wt}$$

Solving equations (19) and (20) simultaneously for P and θ yields (for small angles)

$$\theta = \text{Arctan} \left(0.81 \frac{\tau_{max}}{\sigma_{max}} \right) \quad (24)$$

and

$$P_{max} = \frac{\tau_{max} wt}{2.88 \theta} \quad (25)$$

The load carrying capability of scarf joints has been analytically evaluated to determine the optimum scarf angle for flush repairs. The potential load carrying capability of the adhesive and the adherends in the joint as a function of scarf angle is shown in Figure 5-6 (derived by plotting Equations (20) and (22)). The strength of the adherend in the joint area decreases with decreasing scarf angle caused by: reduction in the

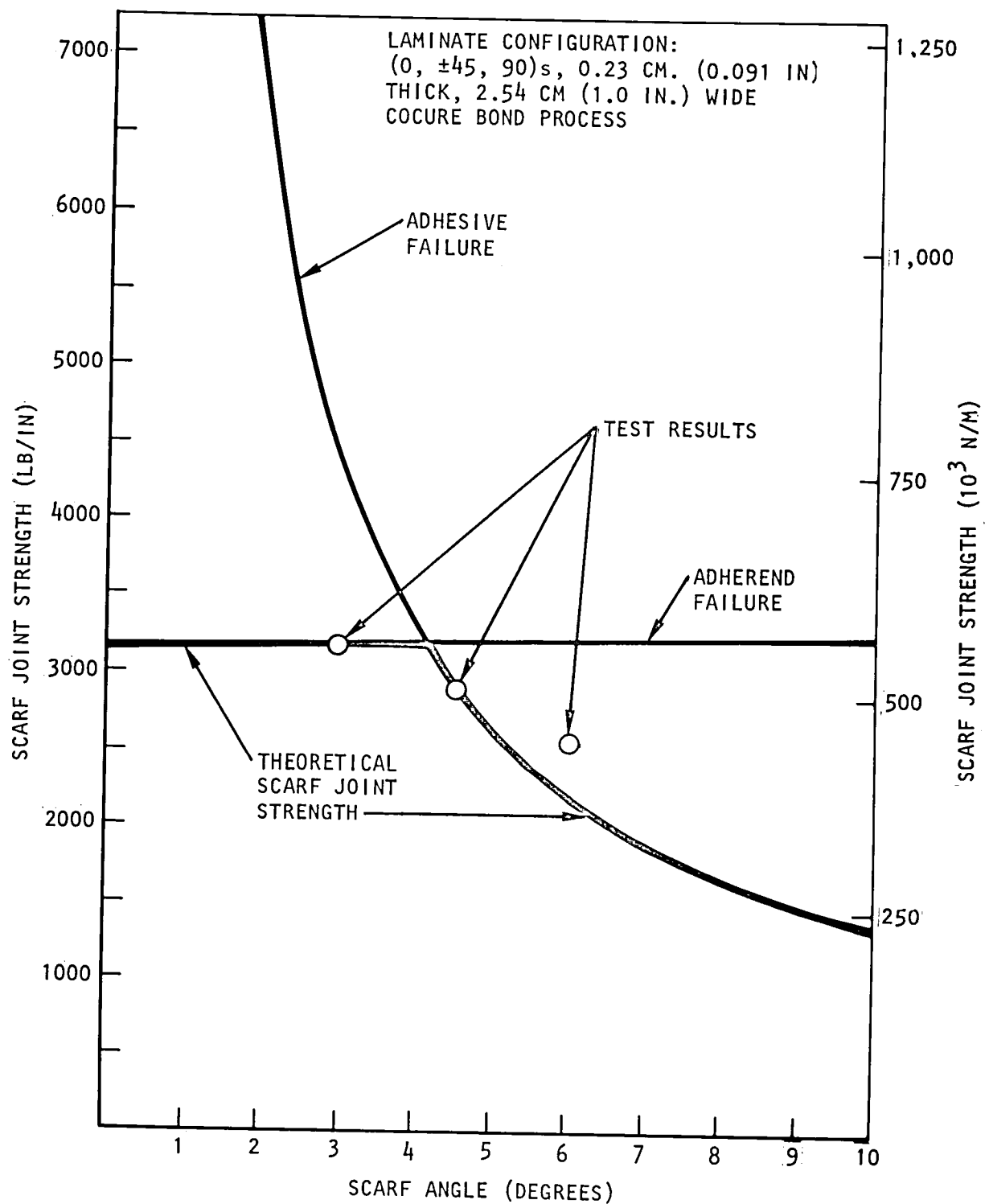


Figure 5-6. Scarf-Joint Adhesive and Adherend Potential Strength

cross-sectional thickness and increasing stresses at the scarf tip (stress concentration at the end of the joint increases with decreasing scarf angles) making the joint tension failure critical in the laminate. The load carried by the adhesive increases with decreasing scarf angle because the bond area increases. The optimum scarf angle occurs when the adhesive failure load is equal to the adherend failure load.

As shown in Figure 5-6, the theoretical optimum scarf angle is 4.1 degrees, which is very similar to that predicted by Equation (19). The maximum predicted load (560 KN/m, [3,200 lb/in.]) agrees with the cocure development test specimens (Table 5-5), but does not agree with the secondary bond data. The improved scarf joint design relieves the stress concentrations and increases the strength of the joint.

5.4 SUMMARY - ANALYTICAL METHODS DEVELOPMENT

Analytical models developed in previous sections were used to predict optimum doubler overlaps, and optimum scarf angles for flush repairs. The analysis used room temperature adhesive properties, which would not be conservative at elevated temperatures. Factors have been added to the theoretical design parameters to account for temperature effects, manufacturing anomalies, analytical approximations, fatigue, and endurance life. For the 0.23 cm (0.091 in.) thick $(0, \pm 45, 90)_{2S}$ isotropic Celion/LARC-160 laminates used in this study the following recommendations are made.

- | | |
|----------------------|-------------------|
| 1. Single lap length | 5.08 cm (2.0 in.) |
| 2. Scarf angle | 3 degrees |
| 3. Double lap length | 2.54 cm (1.0 in.) |

To reduce peel stresses, the ends of doublers should be tapered at least 15 degrees. Additional literature on repair of composite materials and related subjects are listed in References 12 through 33.

6. FLAT LAMINATE REPAIR

Flat laminate element specimens were fabricated and repair design, processes, and techniques developed in Section 4 were implemented to evaluate the repair concepts. Since encouraging results were obtained using the prepreg adhesive in-situ imidizing cocure process the same basic techniques were employed in repair of flat laminate elements. Control specimens with and without simulated damage were tested as baseline comparators. The flat laminate repair development program involved compression testing of 15.2 by 30.5 by 0.23 cm (6 by 12 by 0.091 in.) 16-ply (0/±45/90)_{2s} Celion/LARC-160 laminates. As shown in Figure 6-1, the flat laminate repair development involved three types of specimens:

1. Control specimens, undamaged, and with 2.54 and 5.08 cm (1 and 2 in.) diameter holes
2. Flush repairs with 3- and 6-degree scarf repairs
3. External patch repairs

6.1 FLAT LAMINATE REPAIR RATIONALE

Process development studies performed in Section 4 demonstrated that superior repair joints could be made using the cocure bonding techniques over secondary bonding methods. The scarf angle joint-type repairs with 3-ply stepped, serrated edge top and bottom surface external doublers yielded close to 100 percent parent laminate strength in tension tests. Unfortunately, the exterior octagonal patch design feature, as applied to flat laminates, was not compatible with the NASA-LaRC supplied compression fixture; therefore, the flush scarf angle nonadhesive cocure repair technique was selected for flat laminates.

Prototype specimens representing nonflush repairs were fabricated per the design in Figure 4-15 and cast in place using Hysol EA934 adhesive in the LaRC compression test fixture to immobilize the specimen. Provisions were made using a parting agent to release the specimen from the fixture to prevent binding during compression test. Because of the complexity of the casting material, binding did occur and inconsistent load/deflections and ultimate strengths resulted in the specimen during test within the compression fixture; therefore, it was concluded the fixture could not be used beyond its original design intent without extensive modification.

Although the flush scarf angle joint designs yielded relatively low values in process development tensile shear tests, they provide a good basis for direct comparison of ultimate achievable loads between varying scarf angles in tension and compression test. The improved octagonal exterior patch concept was evaluated in cocure sandwich panel repairs which are analogous to flat laminates. A photograph of octagonal patch installation on a flat laminate panel is shown in Figure 6-2 and NDI C-scan recording in Figure 6-3.


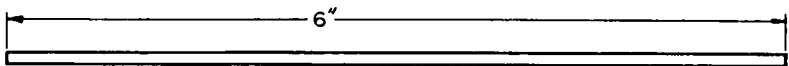
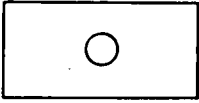
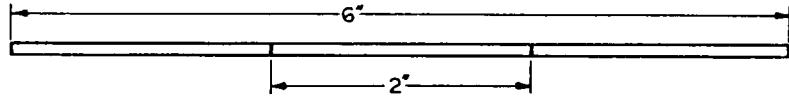
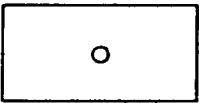
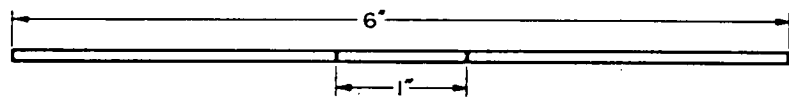
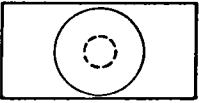
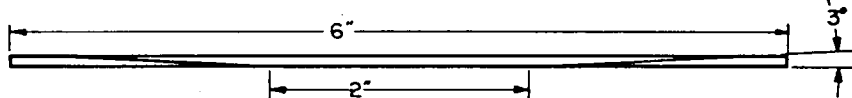
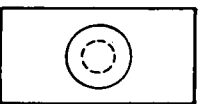
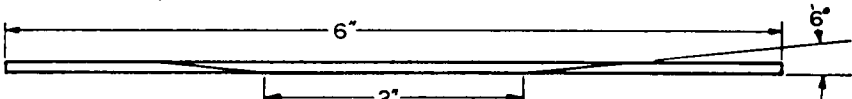
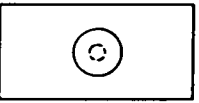
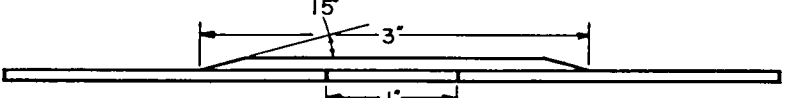
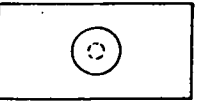
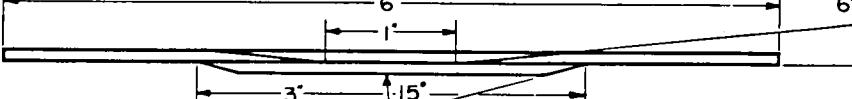
DESCRIPTION		NO. OF SPECIMENS	PLAN VIEW ALL SPECIMENS 6" X 12"	CROSS-SECTION
CONTROL	CONTROL	2 AT R.T.		
	2 INCH HOLE	2 AT R.T.		
	1 INCH HOLE	2 AT R.T.		
FLUSH	2 INCH HOLE 3° SCARF	2 AT R.T.		
	2 INCH HOLE 6° SCARF	2 AT R.T.		
DOUBLER	1 INCH HOLE 3 INCH PATCH PLUG HOLE	2 AT R.T.		
	1 INCH HOLE FLUSH SCARF ON ONE SIDE 3 INCH PATCH OTHER SIDE	2 AT R.T.		

Figure 6-1. Compression Repair Test Matrix

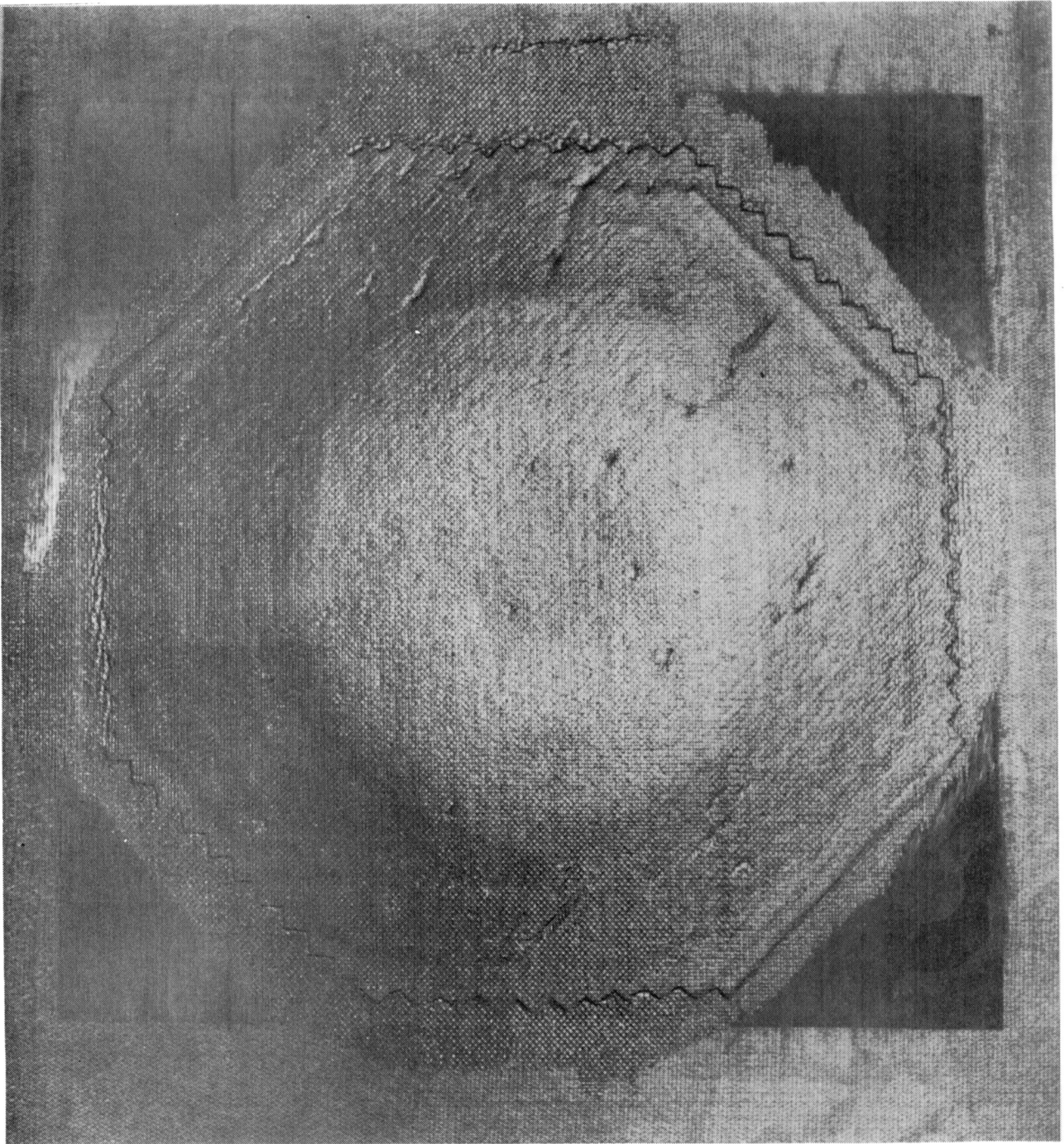


Figure 6-2. Improved Repair; 6-Degree Scarf Angle With Serrated Octagonal Patch Applied to a Flat Laminate

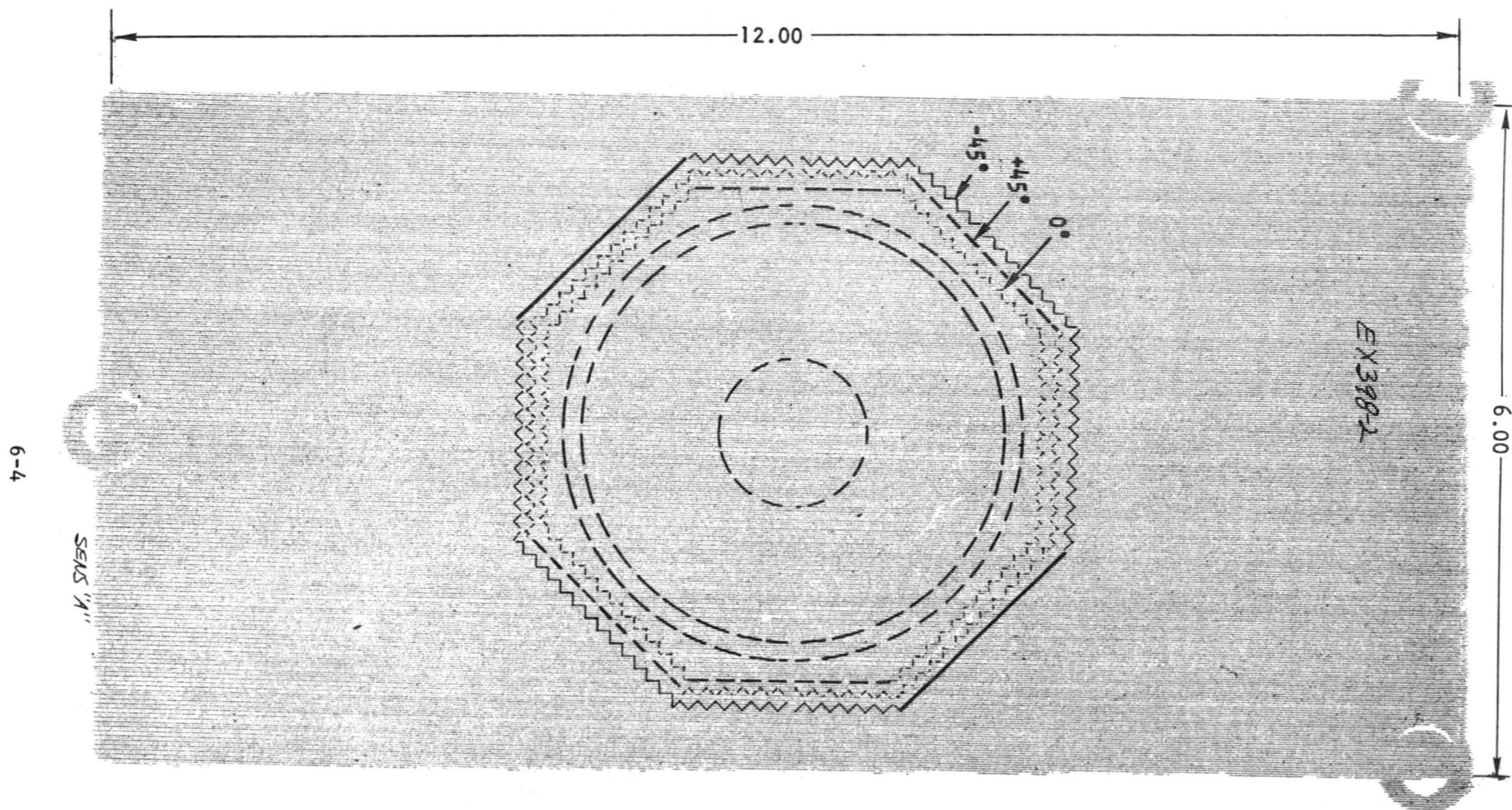


Figure 6-3. Flat Laminate Repair 1-Inch Diameter Hole Improved Concept,
6-Degree Scarf With External Octagonal Patch, Serrated Edges

6.2 FLAT LAMINATE FABRICATION AND PHYSICAL PROPERTIES TEST

Flat laminate stock for making elements for repair was fabricated using the tooling and two-stage imidizing and cure cycle illustrated in Appendix A, Figure A-1. Standard size laminates were fabricated 66.04 by 68.58 cm (26 by 27 in.), 16-ply, 0.231 cm (0.091 in.) thick, (0, ± 45 , 90)_{2s} fiber orientation. Laminates were postcured at 316°C (600°F) for 4 hours. NDI C-scan tests were performed on laminates and were found to be essentially void-free except for some minor tow splice voids in some panels. A typical NDI C-scan recording is shown in Figure 6-4. Physical properties measurements and calculations yielded target (less than 0.5 percent void volume, and 60 percent ± 2 fiber volume on all laminates).

6.3 FLAT LAMINATE CONTROL ELEMENT TESTING AND RESULTS

6.3.1 Control Element Compression Testing

The control elements defined in Figure 6-1 were used as a baseline for comparison to assess the degradation associated with defects and to assess the efficiency of the repairs. The test results for the control laminates are presented in Table 6-1. Three types of coupons were tested at room temperature in the special compression test fixture provided by NASA, as shown in Figure 6-5. The fixture is designed to provide uniform support of the 30.04 by 15.02 by 0.23 cm (12.00 by 6.00 by 0.09 in.) laminate specimens during test. Testing of nonflush repairs up to 7.62 cm (3.00 in.) diameter is made possible by an adjustable window that provides local support to the protruding repair patch. The fixture is supported during test on an adjustable spherical seat that provides accurate alignment during test in a 2,224 KN (500 K lb) capacity MTS closed-loop electrohydraulic test system. Specimens were tested at a load rate of 133 KN (30,000 lb) per minute.

The three types of 15.24 by 30.48 by 0.23 cm control elements tested included an undamaged laminate, a laminate with a 2.54 cm (1.00 in.) hole, and a laminate with a 5.08 cm (2.00 in.) hole. Compression testing of flat laminate control and repaired elements at 316°C (600°F) was not performed because of problems associated with heating the large NASA-LaRC steel test fixture mass. Potential binding and damage of the fixture caused by coefficient of thermal expansion (CTE) differences between materials can occur; therefore, it was recommended that the 316°C (600°F) flat laminate element compression tests in the NASA test fixture be deleted from the program. Flat laminate control and repair compression tests at 316°C (600°F) can be accomplished using the NASA-LaRC sandwich design specimen. Rationale to substantiate this approach is based on a comparison of flat laminate and sandwich element control specimen compression test data that shows both specimen configurations yield essentially equivalent room temperature strengths. The sandwich specimen allows implementation of the 4.5-degree scarf angle--serrated edged doubler improved repair technique developed for sandwich structures (refer to Section 7, Figure 7-2). This repair design has demonstrated a significant improvement over the 3-degree scarf angle flush repair for flat laminates tested in the NASA-LaRC fixture. The improved repair design demonstrated in sandwich element tests cannot be evaluated in flat laminate tests even at room temperature

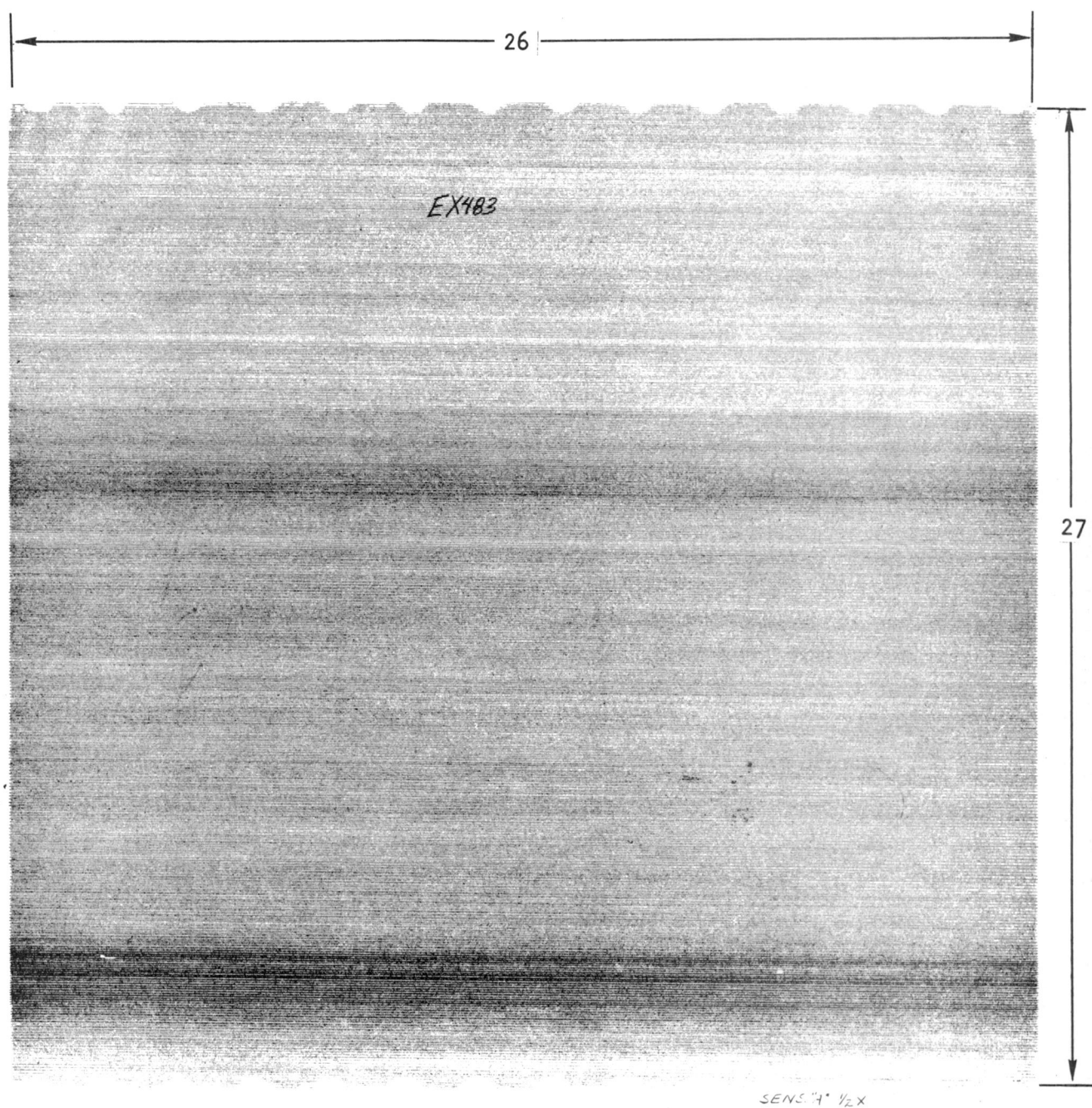
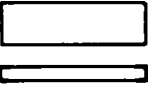
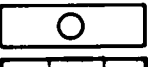








Figure 6-4. NDI C-Scan of Typical $(0, \pm 45, 90)_{28}$ 16-Ply Laminate for Flat Panel Repairs

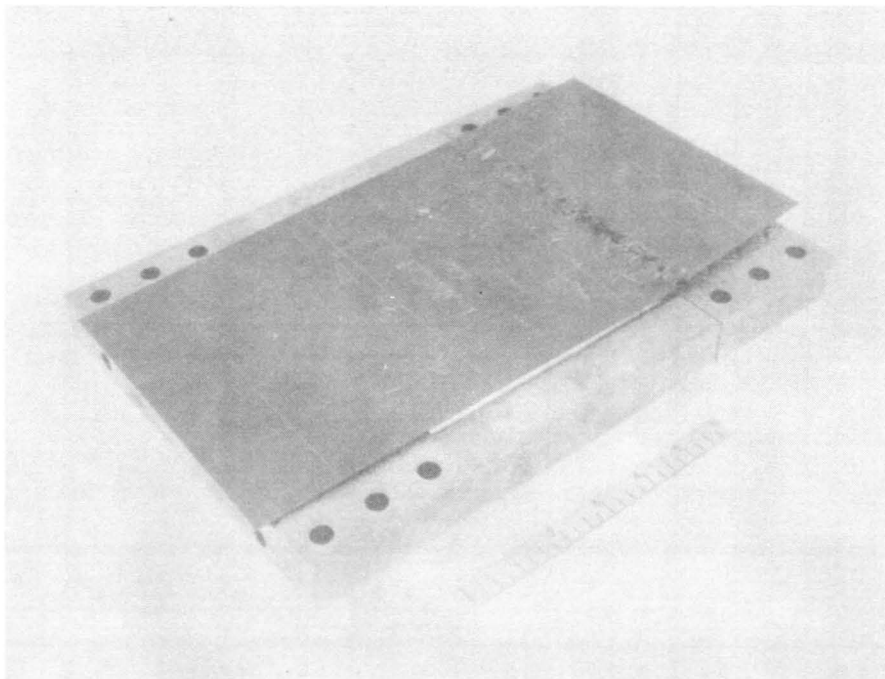
**Table 6-1. Celion/LARC-160 Flat Laminate Repair Room Temperature
Compression Test Results**

Repair Description		Configuration 6.0 x 12.0 in.	Specimen No.	Thickness		R. T. Compressive Properties								
						Net Section Stress		Total Section Stress		Ultimate Load		Joint (1) Efficiency (%)	Δ% Over Damaged Specimen	Failure Mode
				cm	(in.)	MN/m ²	(Ksi)	MN/m ²	(Ksi)	KN/m	lbs/in.			
Control	Undamaged		EX398-1*	0.236	0.093		—	>415	>60.2*	>980	>5597*	100	2.0 in. dia hole	End failure
			EX425-1*	0.236	0.093		—	>398	>57.8*	>940	>5371*			End failure
			EX425-2*	0.231	0.091		—	>358	>52.0*	>829	>4733*		240	End failure
			EX425-6	0.227	0.090		—	>458	>66.5	>1048	>5983			End failure
			EX425-4	0.227	0.090		—	475	69.3	1091	6233		1.0 in. dia hole	Compression gap area
			EX425-3	0.226	0.089	—	—	449	65.2	1021	5833			Compression gap area
			EX425-9	0.227	0.090	—	—	435	63.1	995	5683		180	Compression gap area
					Avg			454	(66.0)	1039	(5933)			
	2.0 in. hole		EX397-1	0.236	0.093	279	40.5	186	27.0	440	2512	41.7	100	Compression net section
			EX397-7	0.227	0.090	277	40.2	187	26.8	423	2413			Compression net section
			EX397-4	0.224	0.088	293	42.5	195	28.3	437	2494			Compression net section
					Avg	283	(41.1)	189	(27.4)	433	(2473)			
	1.0 in. hole		EX408-1	0.234	0.092	307	44.5	254	36.9	596	3401	55.5	100	Compression net section
			EX408-5	0.241	0.095	291	42.2	242	35.1	584	3333			Compression net section
			EX398-3	0.227	0.090	292	42.4	240	34.9	549	3138			Compression net section
					Avg	297	(43.0)	245	(35.6)	576	(3291)			
Flush Scarf	2.0 in. hole, 3° scarf angle		EX358-7	0.216	0.085			364	52.9	788	4500	78.9	189	Compression net section outside hole, patch shear
			EX397-5	0.227	0.090			368	53.4	841	4805			Compression net section thru thin area of patch
			EX358-8	0.234	0.092			344	49.9	707	4040			Compression net section, patch shear
			EX358-4	0.239	0.094			394	57.2	941	5372			End failure (not cast)
					Avg			368	(53.4)	819	(4679)			
	2.0 in. hole, 6° scarf angle		EX358-3	0.239	0.094			283	41.1	669	3819	66.1	158	Compression net, section, outside of hole, patch shear
			EX397-3	0.203	0.080			347	50.3	705	4027			Compression net section, outside hole, patch shear
					Avg			315	(45.7)	687	(3923)			
	1.0 in. hole, 6° scarf angle		EX397-X	0.218	0.086			370	53.7	809	4620	78.0	140	Compression net section outside hole patch shear
			EX358-2	0.299	0.096			343	49.8	812	4632			Compression net section outside hole patch shear
					Avg			357	51.8	810	(4628)			
External Doubler	1.0 in. hole, 3.0 in., 16 ply doubler patch 1 side, cured plug hole		EX398-4	0.227	0.090			320	(46.5)	757	4325	78.0	130	Compression net section thru center of hole shear of external patch
			EX398-5	0.231	0.091			321	46.6	742	4237			Compression net section outside hole, shear of external patch
					Avg			321	(46.6)	750	(4281)			
	1.0 in. hole, 6° scarf angle, 16 ply doubler patch 1 side		EX358-5	0.239	0.094			305	(44.3)	729	(4164)	70.2	127	Compression net section shear in patch areas

(1) Specimens were tested in the NASA-LaRC compression fixture at a load rate of 133 kn 30,000 lbs/minute.

*Undamaged control specimens had end mushroom failures, due to load concentration, therefore data were not used in averaging. All other undamaged control specimens were cast flush with the fixture in base areas with EA934 adhesive for uniform support during test.

A810813 G-4C



A810813 G-3C

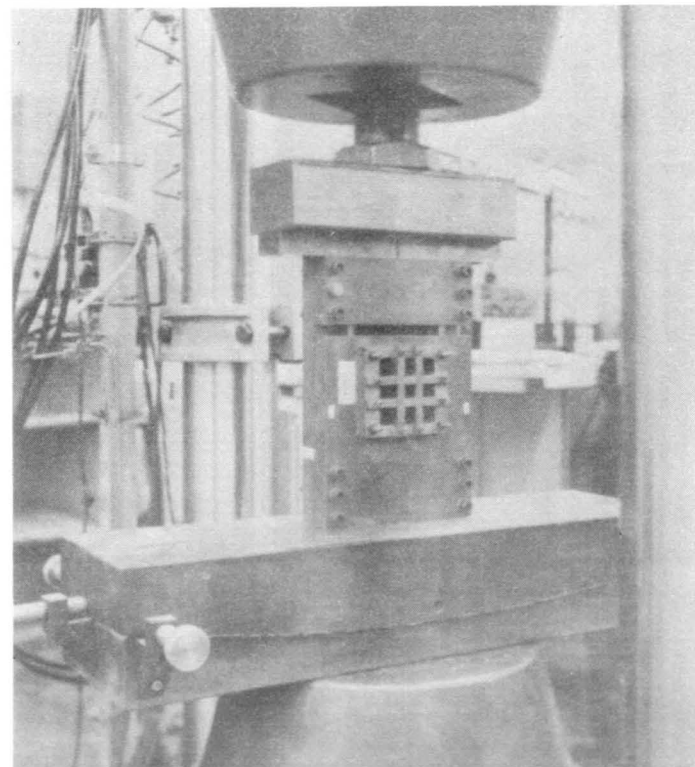


Figure 6-5. NASA LaRC Compression Test Fixture in MTS Machine and Open Fixture With Tested Control Specimen

because of test fixture constraints. The sandwich element provides an improved test bed for implementing optimized flat laminate repairs and has been demonstrated in both room temperature and 316°C (600°F) compression tests.

6.3.2 Control Element Compression Test Results

As shown in Figure 6-6 initial undamaged control specimen tests resulted in end failure caused by uneven load introduction in the test fixture base grip area. To resolve this problem, the ends of the specimens were potted as shown in Figure 6-7, resulting in failure in the slotted area of the test fixture, as shown in Figures 6-5 and 6-7. Undamaged control specimens failed at an average 1,039 KN/m (5,933 lb/in.).

Next, specimens with 2.54 cm (1.00 in.) and 5.08 cm (2.00 in.) holes were tested. The specimen with the 2.54 cm (1.00 in.) diameter hole (Figure 6-8) failed at an average 576 KN/m (3,291 lb/in.), or at 55 percent of the undamaged strength. The specimen with the 5.08 cm (2.00 in.) diameter hole (Figure 6-9) failed at an average 433 KN/m (2,473 lb/in.), or at 42 percent of the undamaged strength.

Typical load-strain and stress-strain curves for the undamaged control laminates are shown in Figures 6-10 and 6-11. The back-to-back rosette strain gages have a baseline for the undamaged laminate behavior. Also, the rosette yields the tensile modulus, 48.3 GN/m² (7.0 msi), and Poisson's ratio (0.285) for the quasi-isotropic test laminate. Note that the strain plots were cut off before the failure load, and thus do not yield ultimate strain-to-failure.

Typical load-strain curves for test laminates with 2.54 and 5.08 cm (1.00 and 2.00 in.) diameter holes are shown in Figures 6-12 and 6-13, respectively. The strain distribution around the holes along the horizontal axis through the hole center is shown in Figure 6-14. At an equivalent applied stress level, the test laminate with the 5.08 cm (2.00 in.) diameter hole had a much higher stress level at the hole edge. By projecting the curves, stress concentrations at the hole edges can be estimated: 2.6 for the 2.54 cm (1.00 in.), and 3.6 for the 5.08 cm (2.00 in.) diameter hole.

6.4 ANALYTICAL PREDICTIONS FOR FLAT LAMINATE REPAIRS

Analytical strength predictions for the flat laminate repair specimens are presented in Table 6-2. The predictions are based on the control laminate strengths discussed in Section 6.3, and the various analytical models presented in Section 5. In most cases, the analytical predictions were 15 to 25 percent higher than the actual test values. It was assumed that the repairs would relieve the stress concentrations around the hole (Figure 6-14). The stress concentrations were not totally relieved, which is why the test results are less than expected. The exception was the 3-degree scarf flush repair on a 5.08 cm (2 in.) diameter hole. Even though the 3-degree scarf will carry more load, it was anticipated that the small scarf angle would remove too much undamaged material and weaken the test specimen. Thus, it was predicted that the 6-degree scarf repair would result in a stronger specimen, which was not supported by the test results.

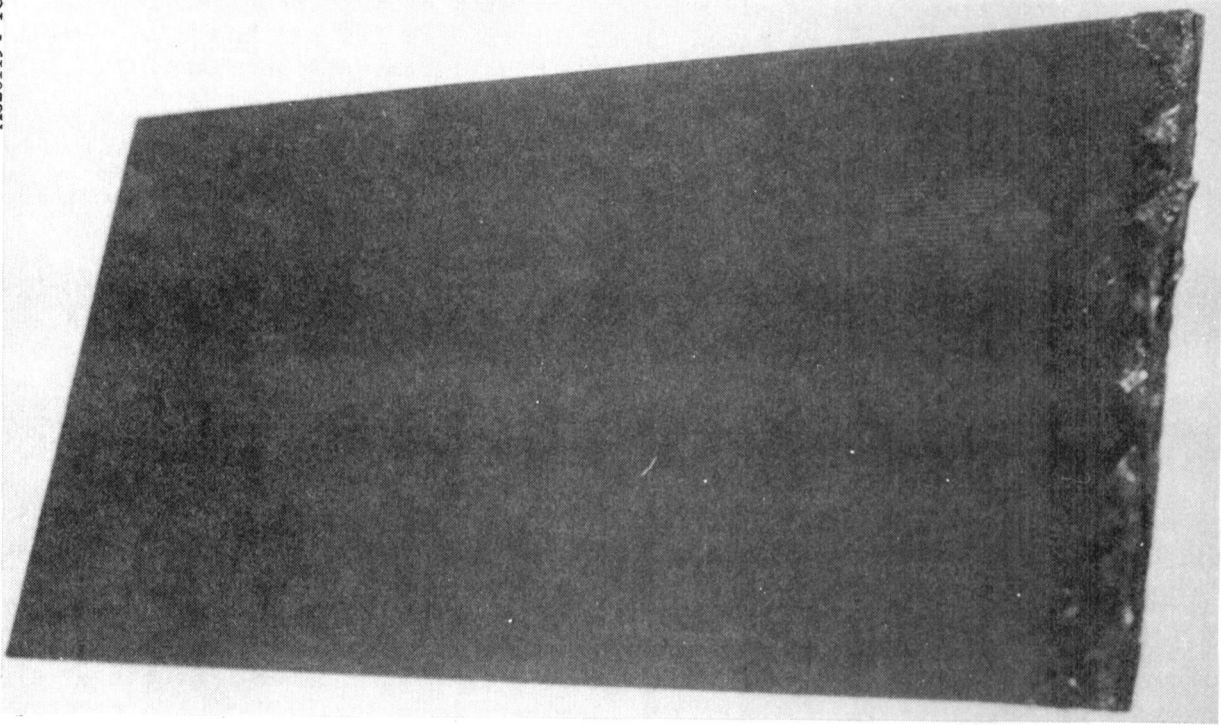


Figure 6-6. Typical End Failure of Undamaged Control Specimen Without Potted Ends

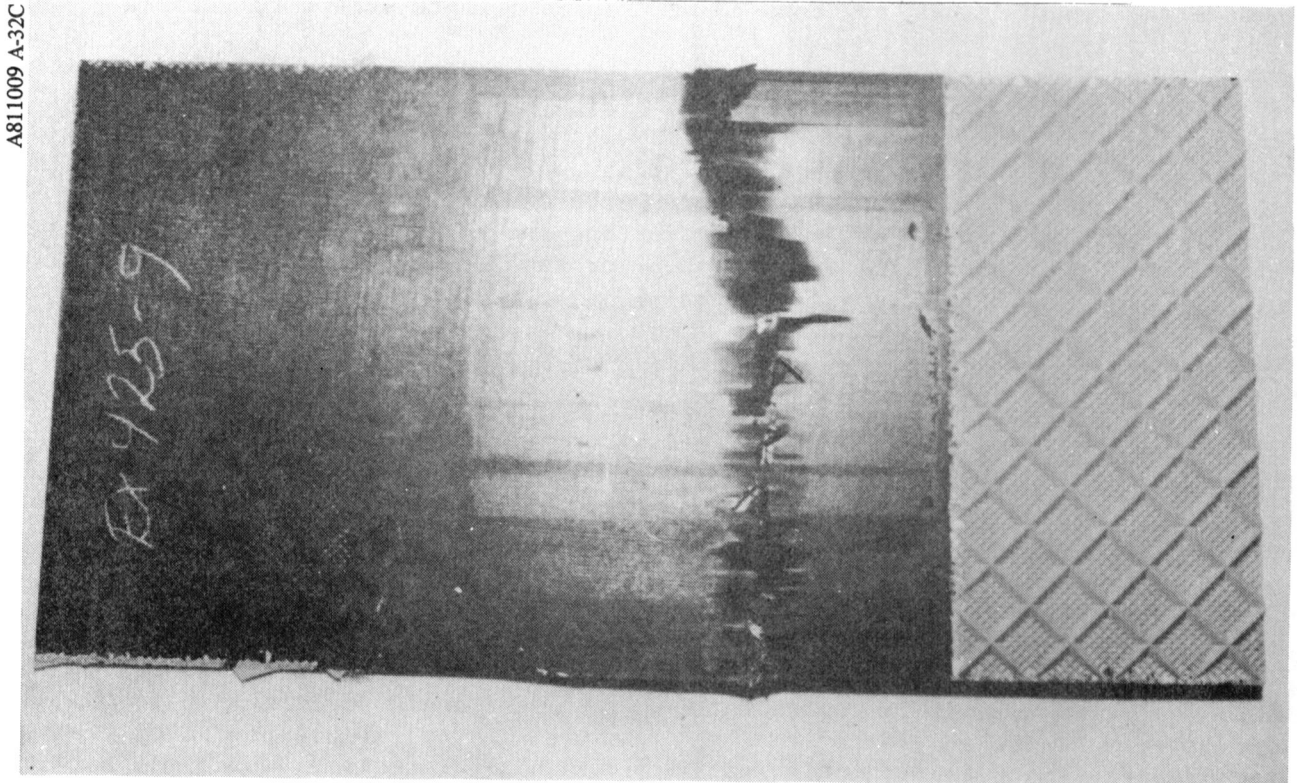


Figure 6-7. Control Test Coupon With Potted Ends--Typical Failure Mode

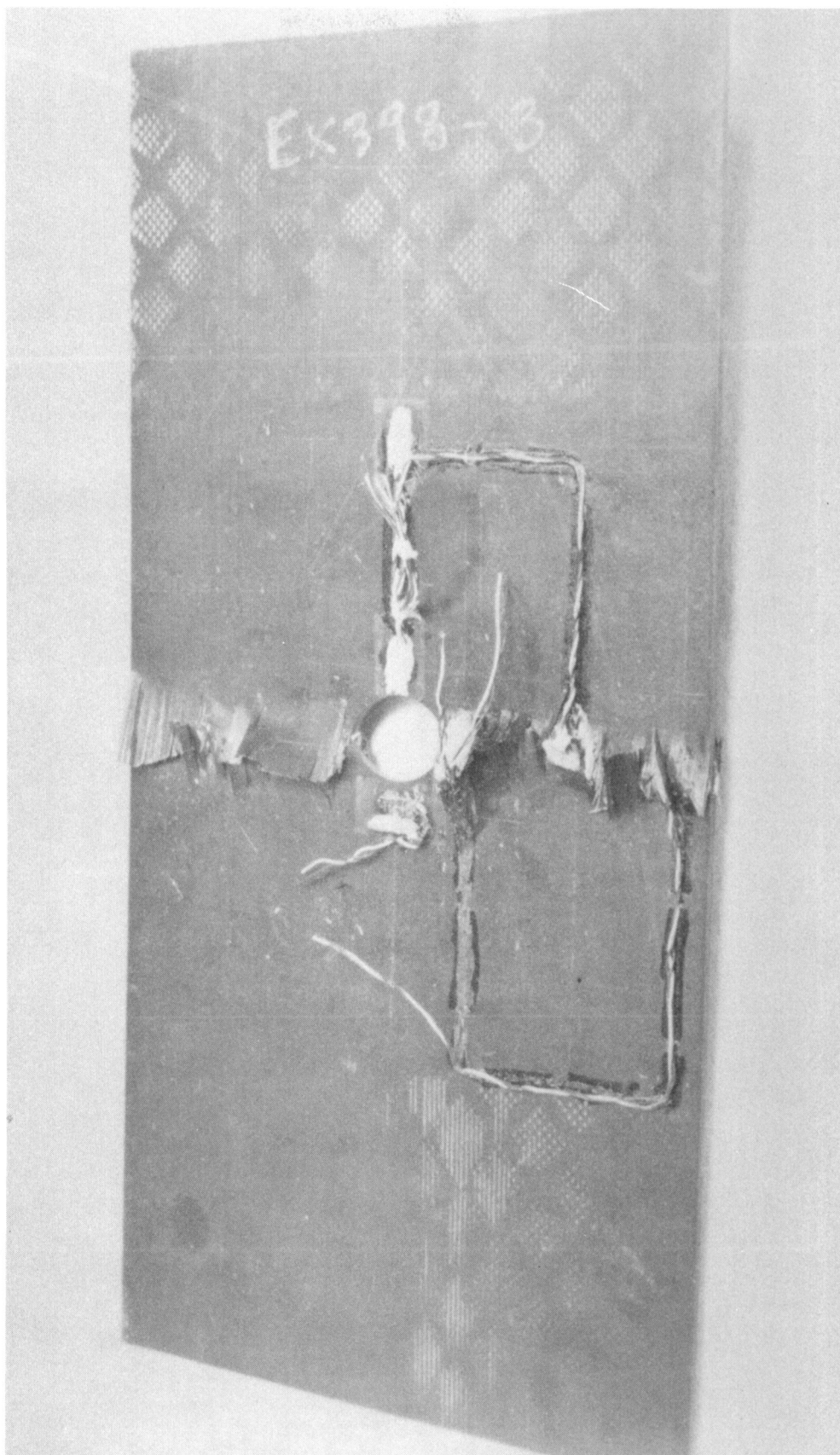


Figure 6-8. Control Test Coupon With 2.54 cm (1.00 in.) Hole--
Typical Failure Mode

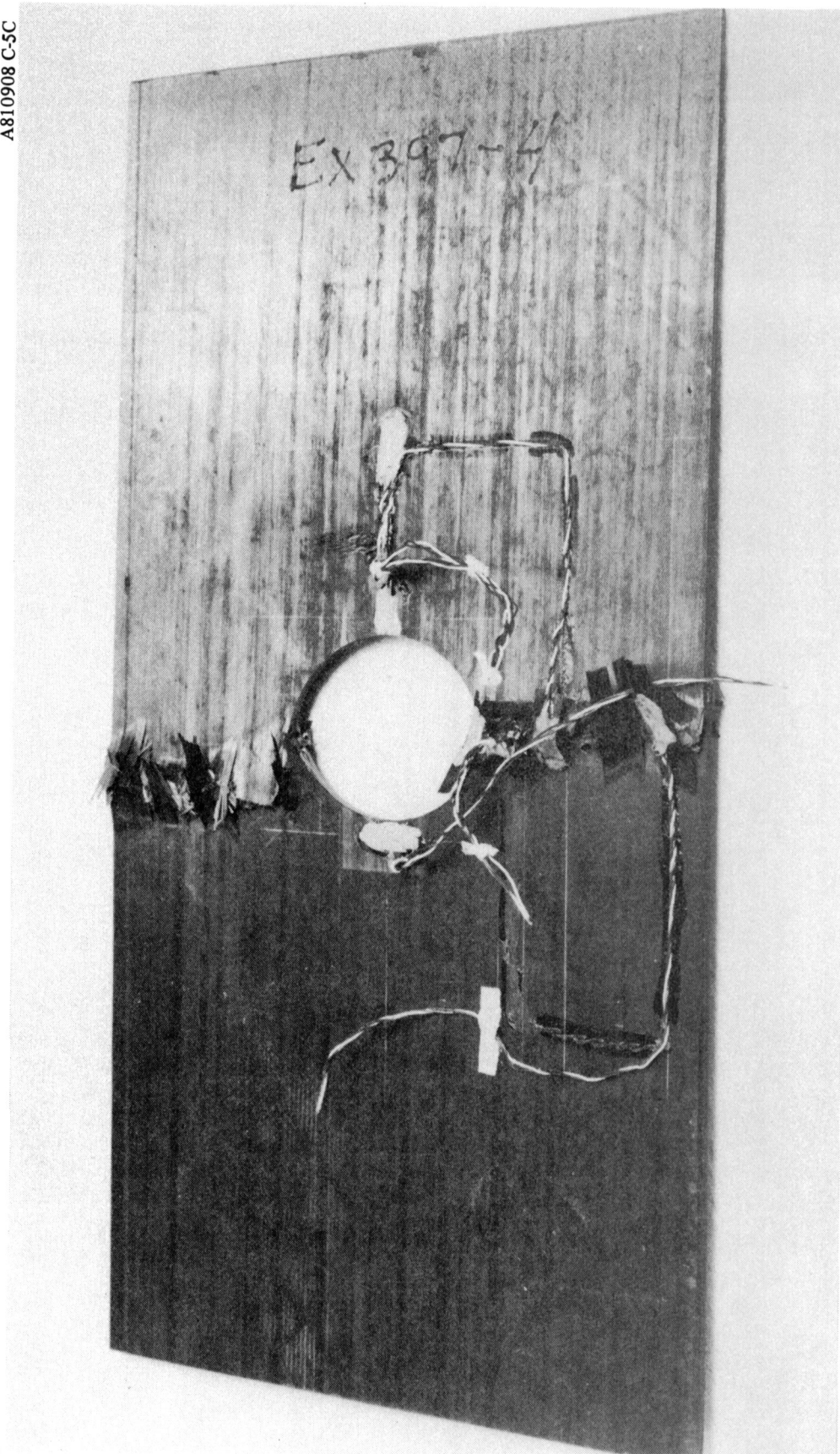


Figure 6-9. Control Test Coupon With 5.08 cm (2.00 in.) Hole--
Typical Failure Mode

ULTIMATE LOAD: 152 KN (34,100 LB)
 ULTIMATE LOAD: 995 KN/m (5,683 LB/IN.)

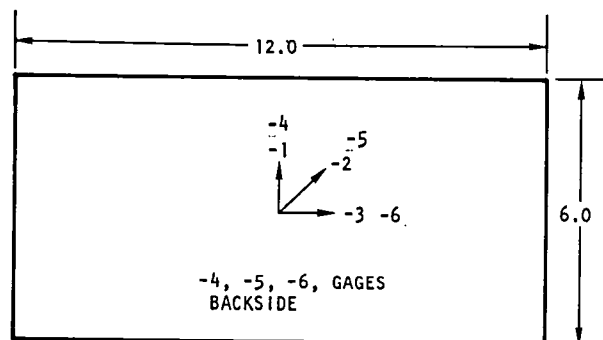
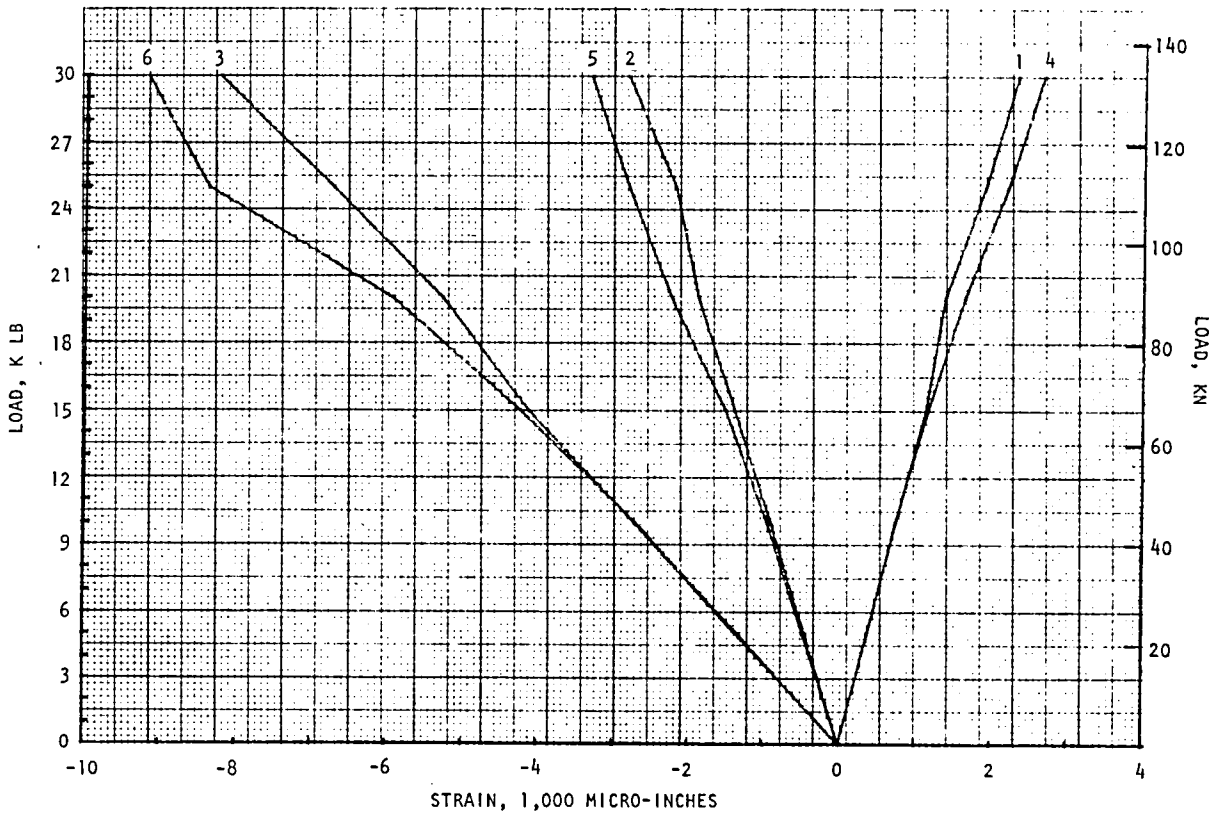


Figure 6-10. Compression Load/Strain Distribution Through Undamaged Control, Specimen EX425-9

ULT STRESS: 434 MN/m^2 (63.1 KSI)

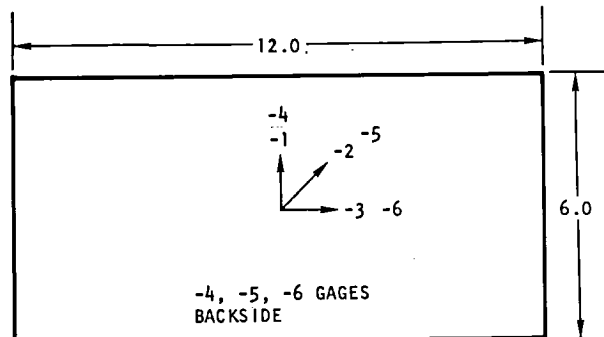
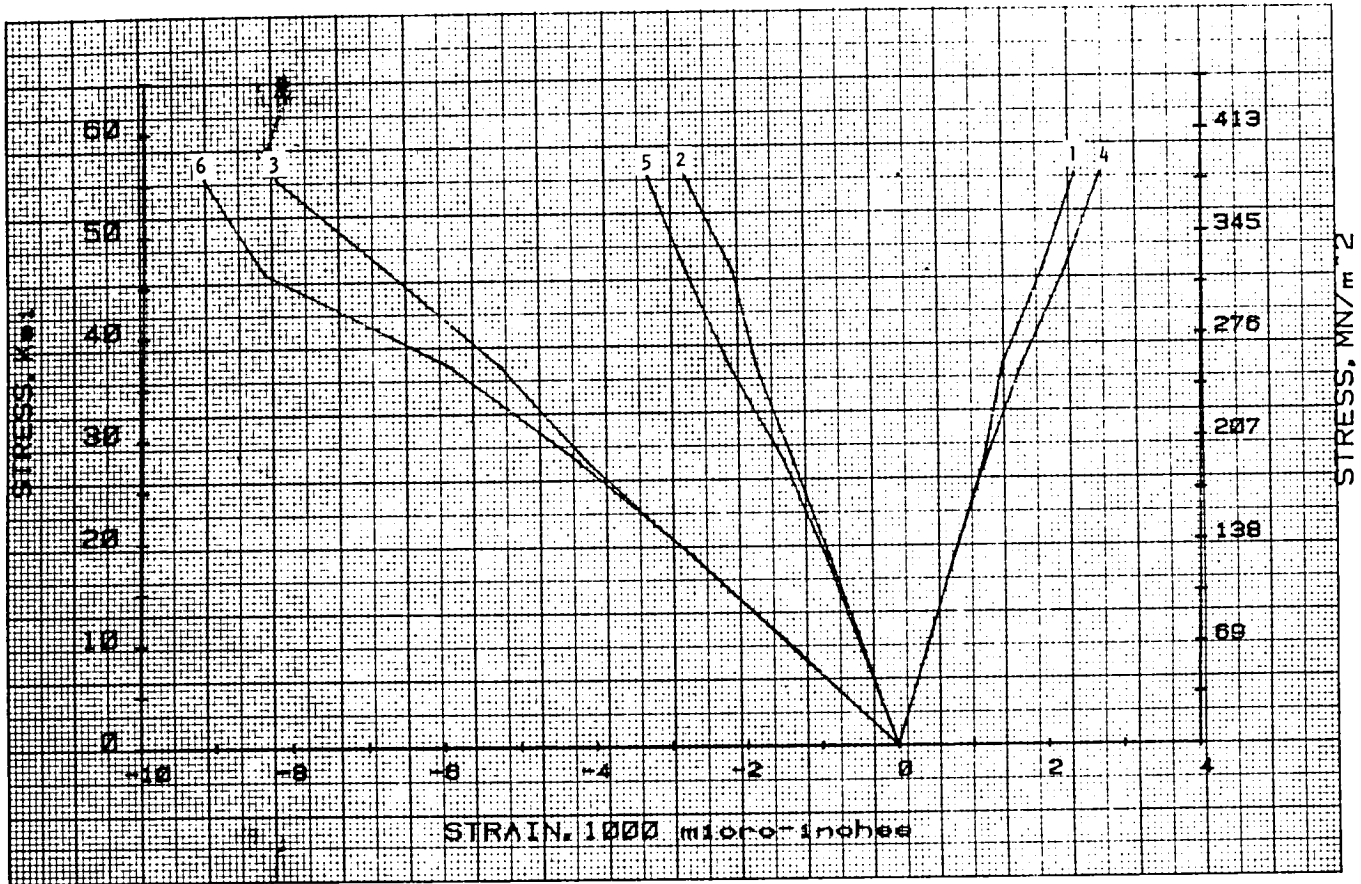


Figure 6-11. Compression Stress/Strain Distribution Through Undamaged Control, Specimen EX425-9

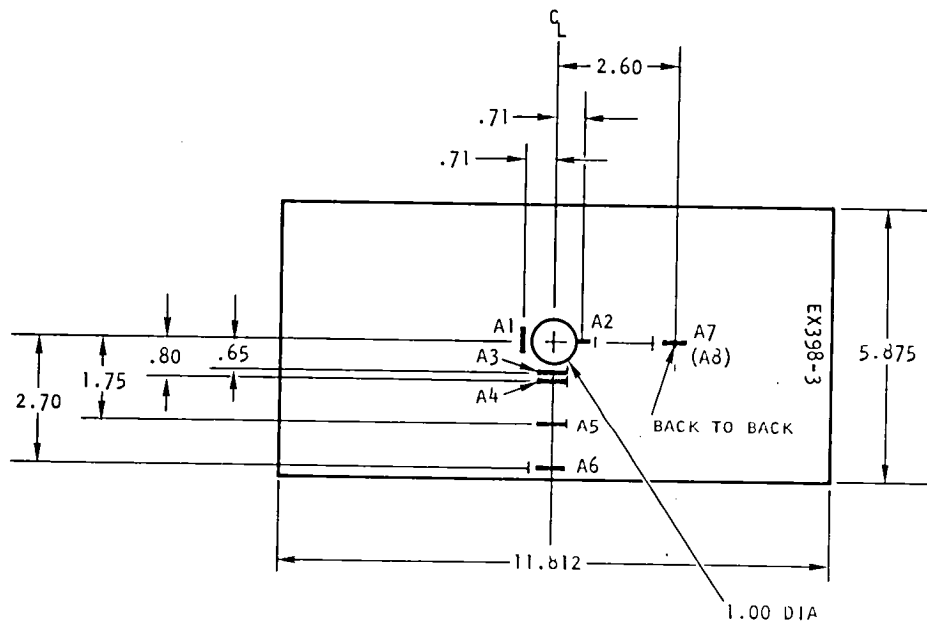
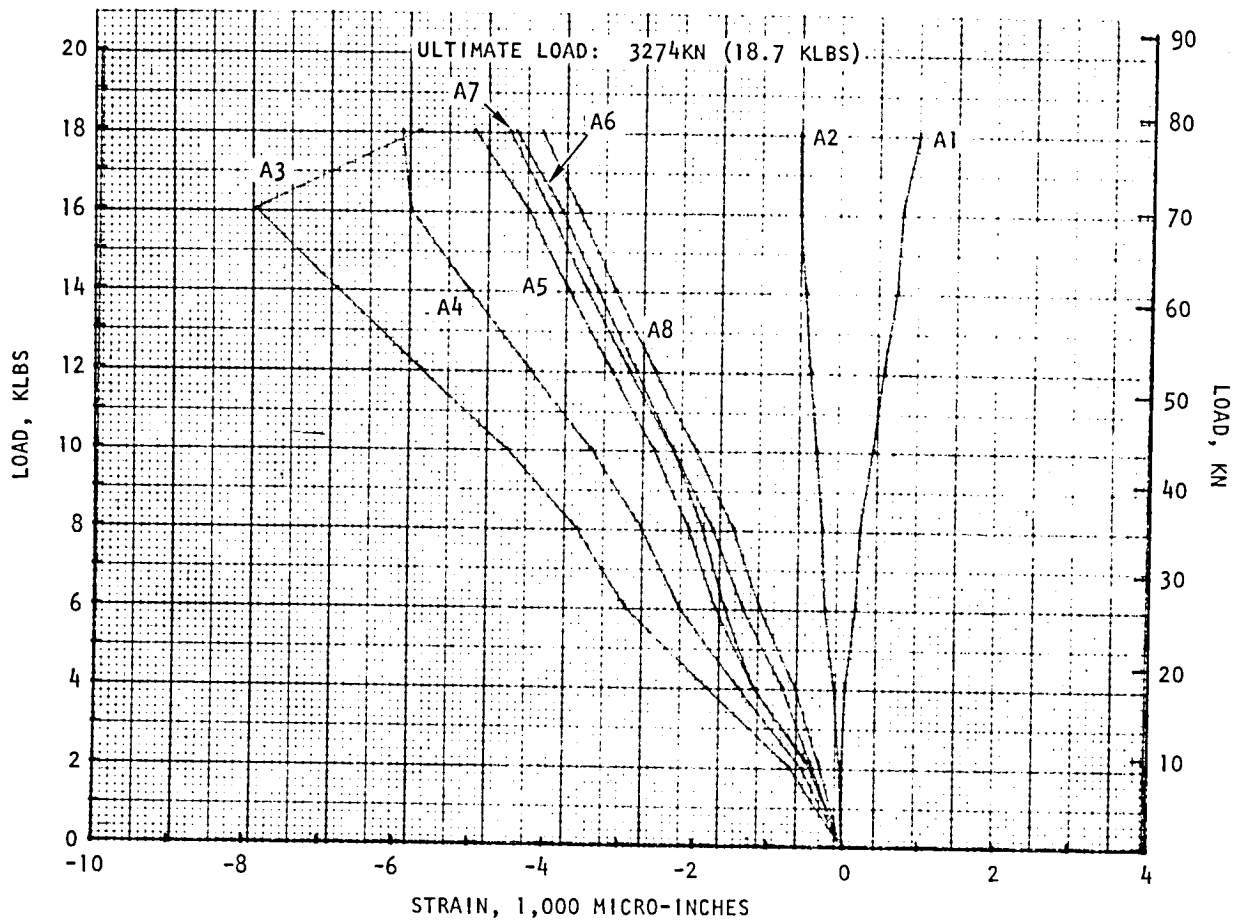


Figure 6-12. Compression Load/Strain Distribution Around 2.54 cm (1.00 in.) Diameter Hole, Specimen EX398-3

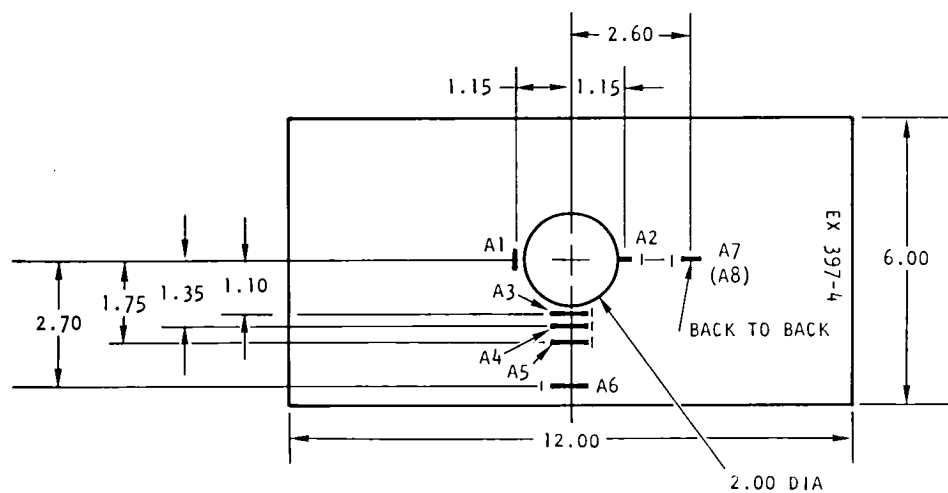
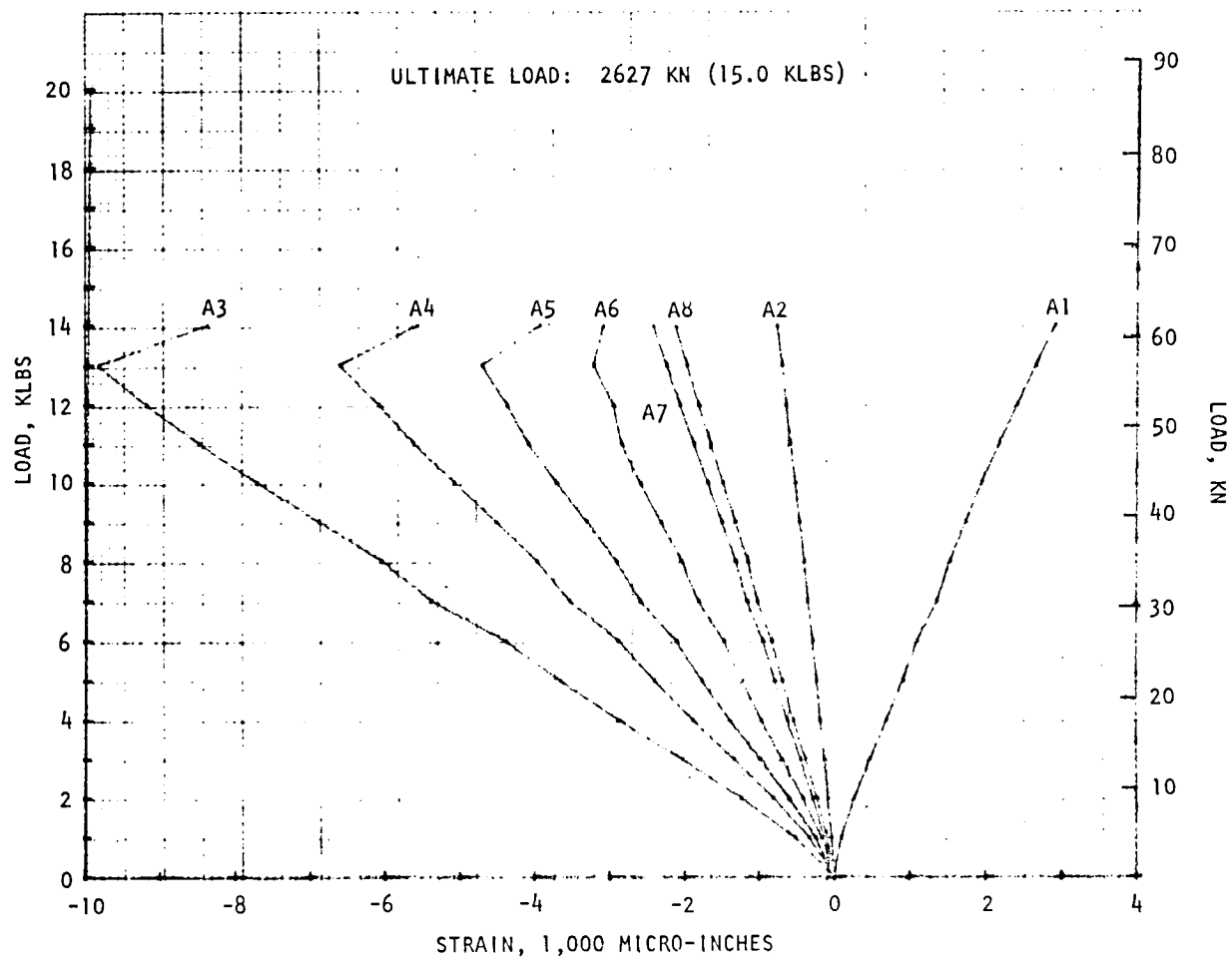


Figure 6-13. Compression Load/Strain Distribution Around 5.08 cm (2.00 in.) Diameter Hole, Specimen EX397-4

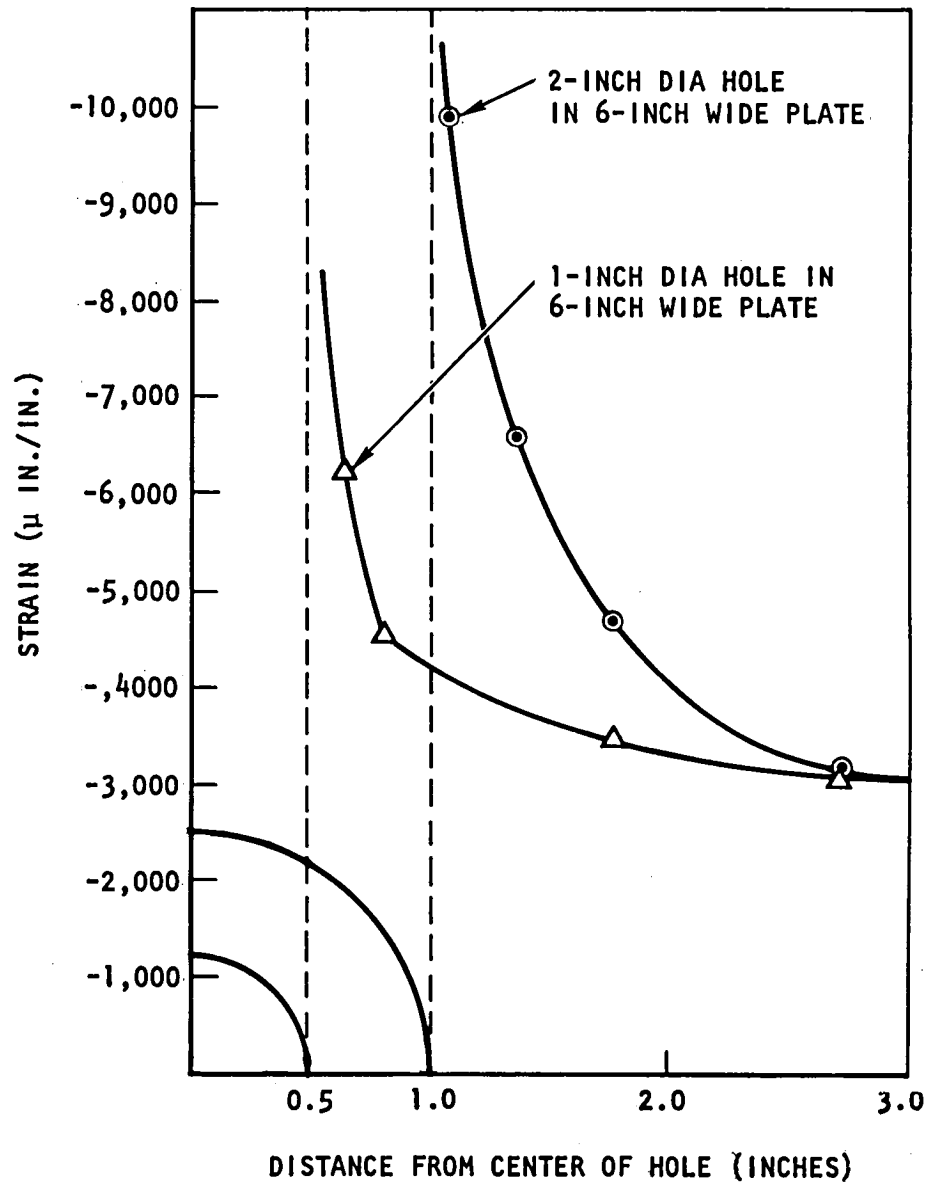
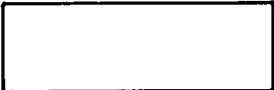

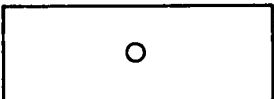

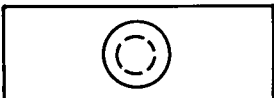




Figure 6-14. Strain Distribution Around 1- and 2-Inch Diameter Holes in a 6-Inch Wide Plate

Table 6-2. Updated Analytical Failure Predictions
and Actual Test Results

Description		Plan View All Specimens 6 in. x 12 in.	Predicted Failure Load		Actual Failure Load	
			Lb/In.	KN/m	Lb/In.	KN/m
CONTROL	Control		5,933	1,039	5,933	1,039
	2 inch hole		2,750	481	2,473	433
	1 inch hole		3,433	601	3,291	576
FLUSH	2 inch hole 3° scarf		4,130	723	4,679	819
	2 inch hole 6° scarf		4,510	790	3,923	687
DOUBLER	1 inch hole 3 inch patch plug hole		5,160	904	4,281	750
	1 inch hole flush scarf on one side 3 inch patch other side		5,220	914	4,164	729

6.5 PATCH DESIGNS FOR REPAIRED FLAT LAMINATE TEST COUPONS

Patch designs for the various flush and external patch repairs are presented in Figures 6-15 and 6-16. Figure 6-15(A) presents a cocured flush repair for a 5.08 cm (2.00 in.) diameter hole with a 3-degree scarf angle. Figures 6-15(B) and (C) present cocured flush repairs for 2.54 cm and 5.08 cm (1.00 in. and 2.00 in.) diameter holes with a 6-degree scarf angle. Figure 6-16(A) presents a cocure bonded external patch one-sided repair for a 2.54 cm (1.00 in.) diameter hole. The repair has a 7.62 cm (3.00 in.) diameter external patch with beveled edges, and a precured secondary bonded plug in the hole. Figure 6-16(B) presents a cocure bonded external patch/flush repair combination for a 2.54 cm (1.00 in.) hole. The flush portion has a 6-degree scarf angle cocure bonded patch and the external doubler has a 7.62 cm (3.00 in.) diameter.

6.6 FLAT LAMINATE REPAIR METHODS

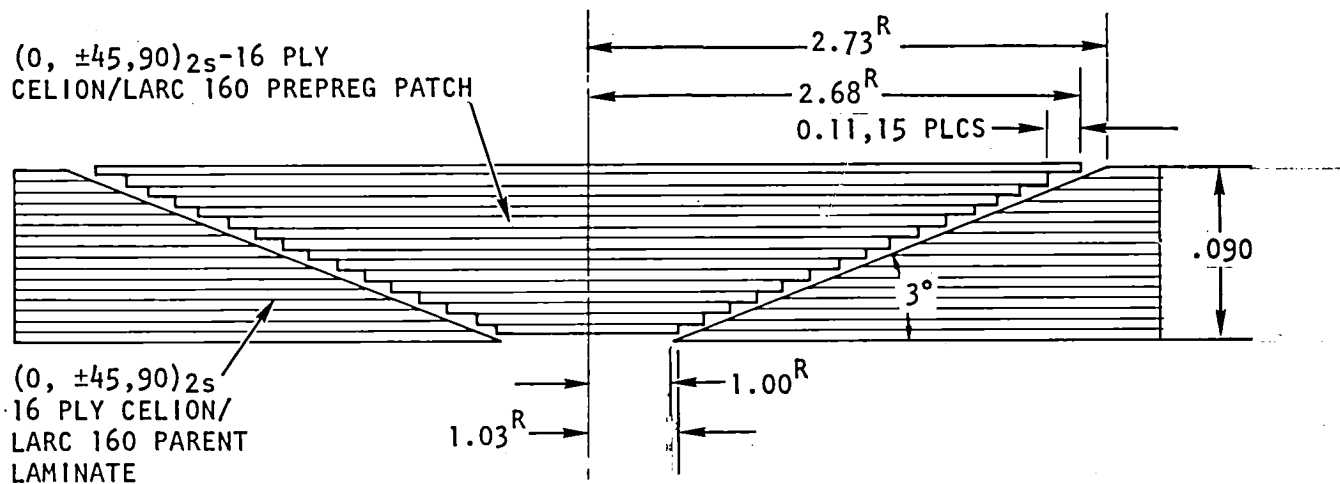
Laminate stock described in Section 6.2, was diamond-saw cut into 30.9 by 15.7 cm (12.2 by 6.2 in.) specimens. Holes were bored 7.54 and 5.08 cm (1.00 and 2.00 in.) diameter on center with diamond core drills and grinder. Scarf angles, nominal 3 degree and 6 degree, were machined to specific 4.4 and 2.19 cm (1.73 and 0.866 in.) scarf lengths to fit the nominal panel thickness of 0.226 to 0.231 cm (0.088 to 0.091 in.). Scarf angle machining operations were successfully performed on a lathe using carbide cutters, mounted stones, and diamond grinders. Laminate faying surfaces were prepared per standard procedure and were not primed. Repair concepts described in Figures 6-15 and 6-16 were implemented on five of six sets of specimens using the prepreg adhesive in-situ imidizing cocure cycle, and tooling concepts, Figures 4-8 and 4-13. A photograph of a typical scarf angle machined in a laminate and stepped-flush (0, ± 45 , 90) 16-ply debulked Celion/LARC-160 prepreg patch is presented in Figure 6-17. Fluoro rubber (FMC 165) pressure cauls were employed in all cure operations over flush and external doubler repairs.

6.7 REPAIR INSTALLATION RESULTS

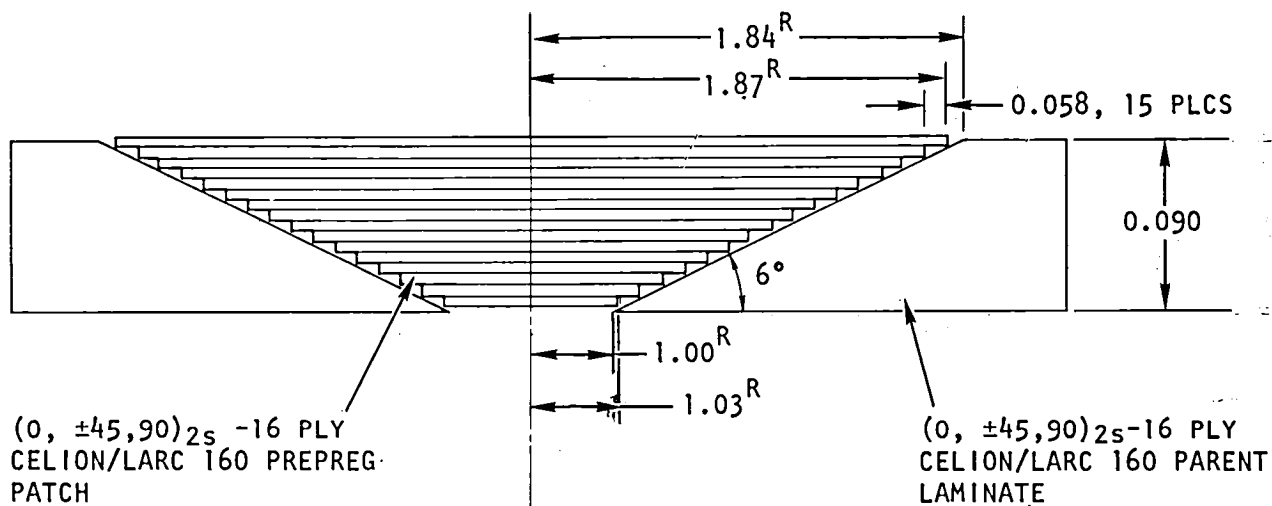
Aesthetic quality of all repair installations was very good. The fluoro rubber pressure cauls imparted smooth, wrinkle-free surfaces on most installations, with the exception of some minor fiber washing on some external doublers. NDI C-scan recordings of flush scarf angle repairs showed 98 percent to 100 percent ultrasound through transmission indicating low void bonds were attained. The external doubler repairs also demonstrated fair C-scan recordings on most panels; however, showed blank spots in some tapered external doubler areas. Typical C-scan recordings are shown in Figures 6-18, 6-19 and 6-20.

6.8 REPAIRED ELEMENT COMPRESSION TESTING AND RESULTS

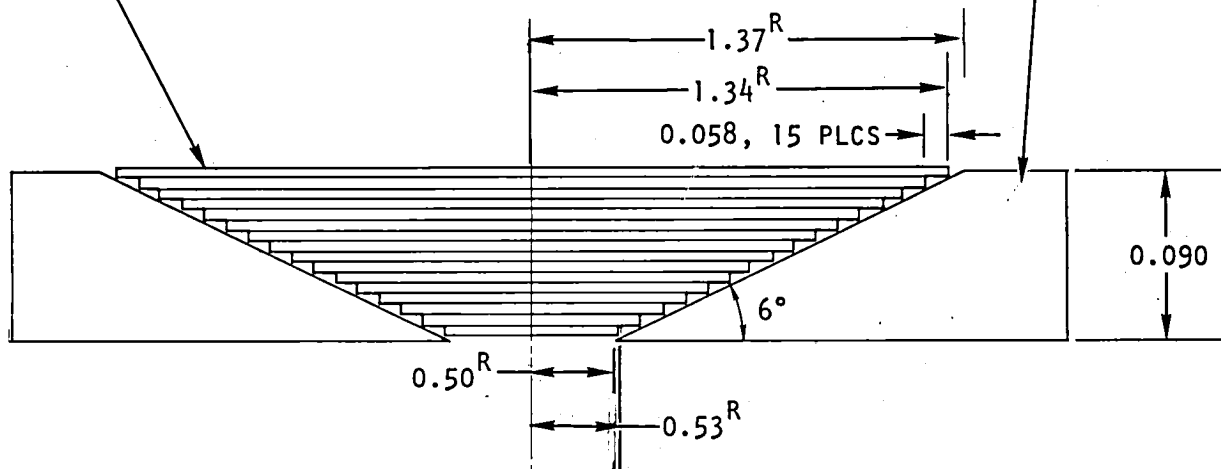
Repaired elements were tested at room temperature in the NASA LaRC supplied compression fixture, using procedures employed for control elements. The test results for the various flush and external patch repairs are presented in Table 6-1. The failure mode for each repair type is given in



A. 2.00 INCH DIAMETER HOLE, 3° SCARF FLUSH REPAIR

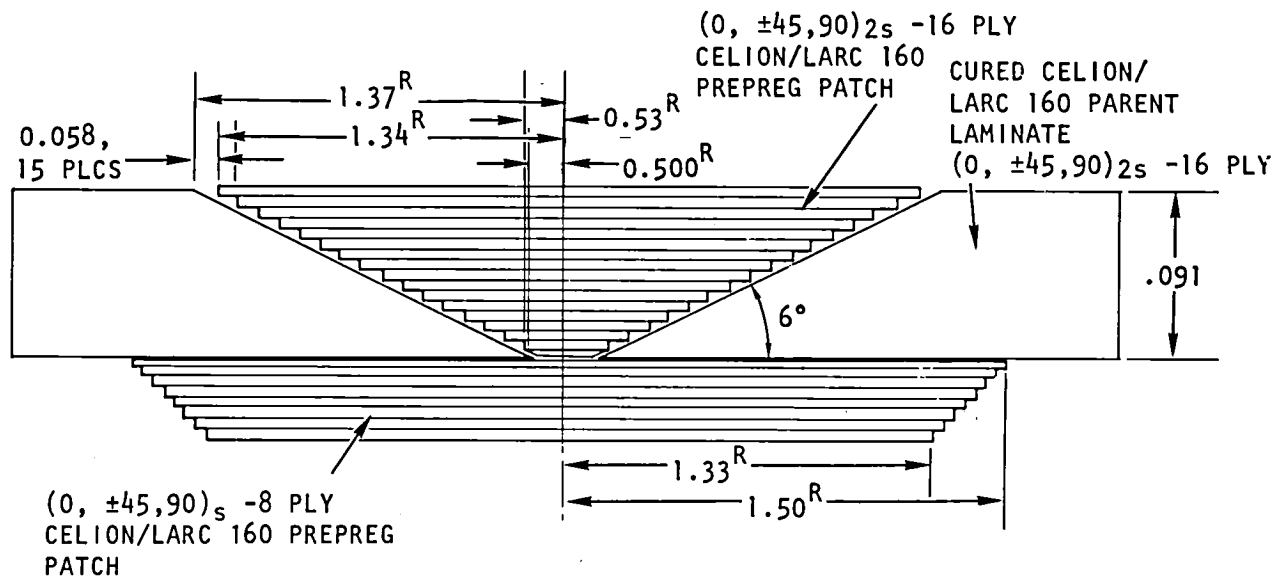


B. 2.00 INCH DIAMETER HOLE, 6° SCARF FLUSH REPAIR



C. 1.00 INCH DIAMETER HOLE, 6° SCARF FLUSH REPAIR

Figure 6-15. Cross-Sections 1- and 2-Inch Diameter Hole, 3- and 6-Degree Scarf Flush Repairs



(B) 1.00 INCH
DIAMETER HOLE
CO-CURE 6° FLUSH
SCARF WITH EXTERNAL
DOUBLER PATCH

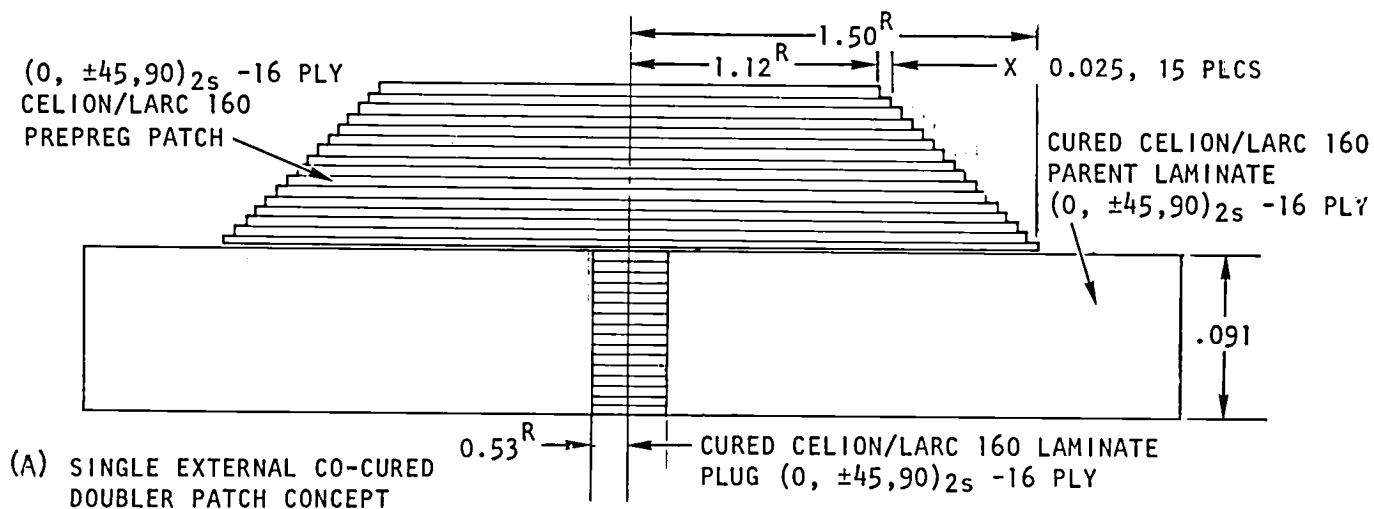


Figure 6-16. Cross-Sections, Cocured External Patch Repairs,
1-Inch Diameter Holes

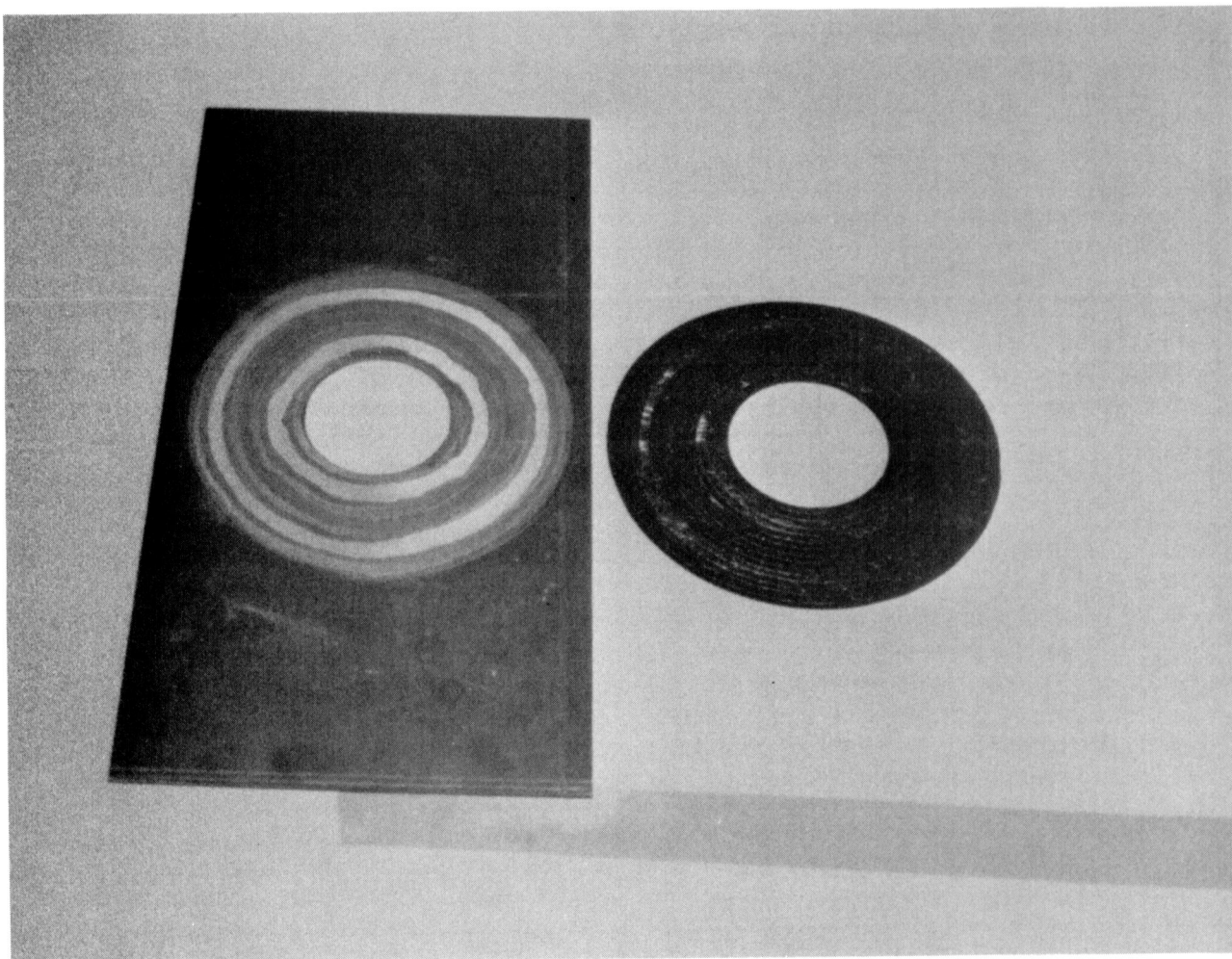


Figure 6-17. Flat Laminate Cocure Repair; 3-Degree Scarf Angle
With Prepreg Preform

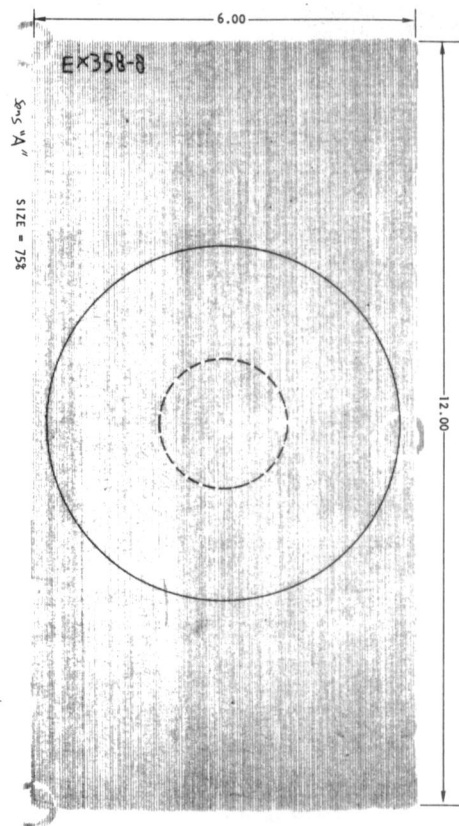
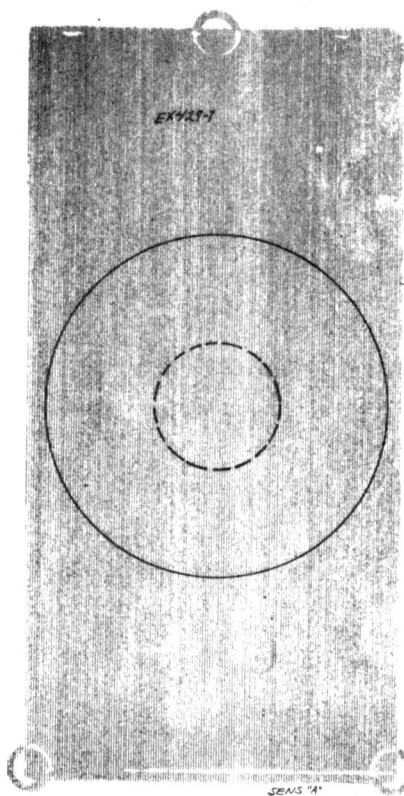
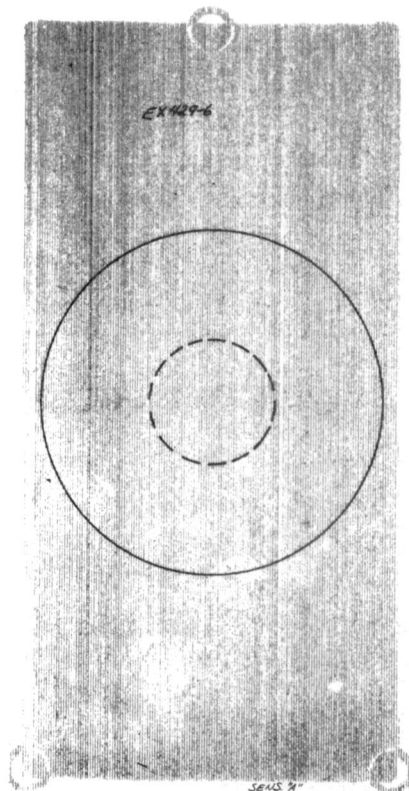
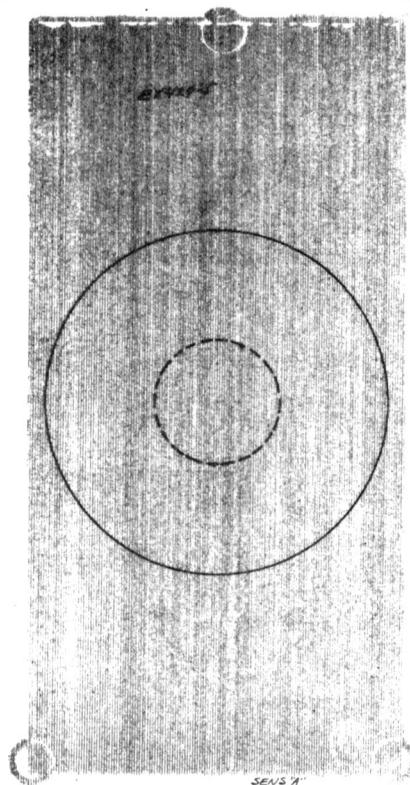


Figure 6-18. NDI C-Scan of Flat Laminate Cocure 3-Degree Flush Scarf, 2-Inch Hole Repair

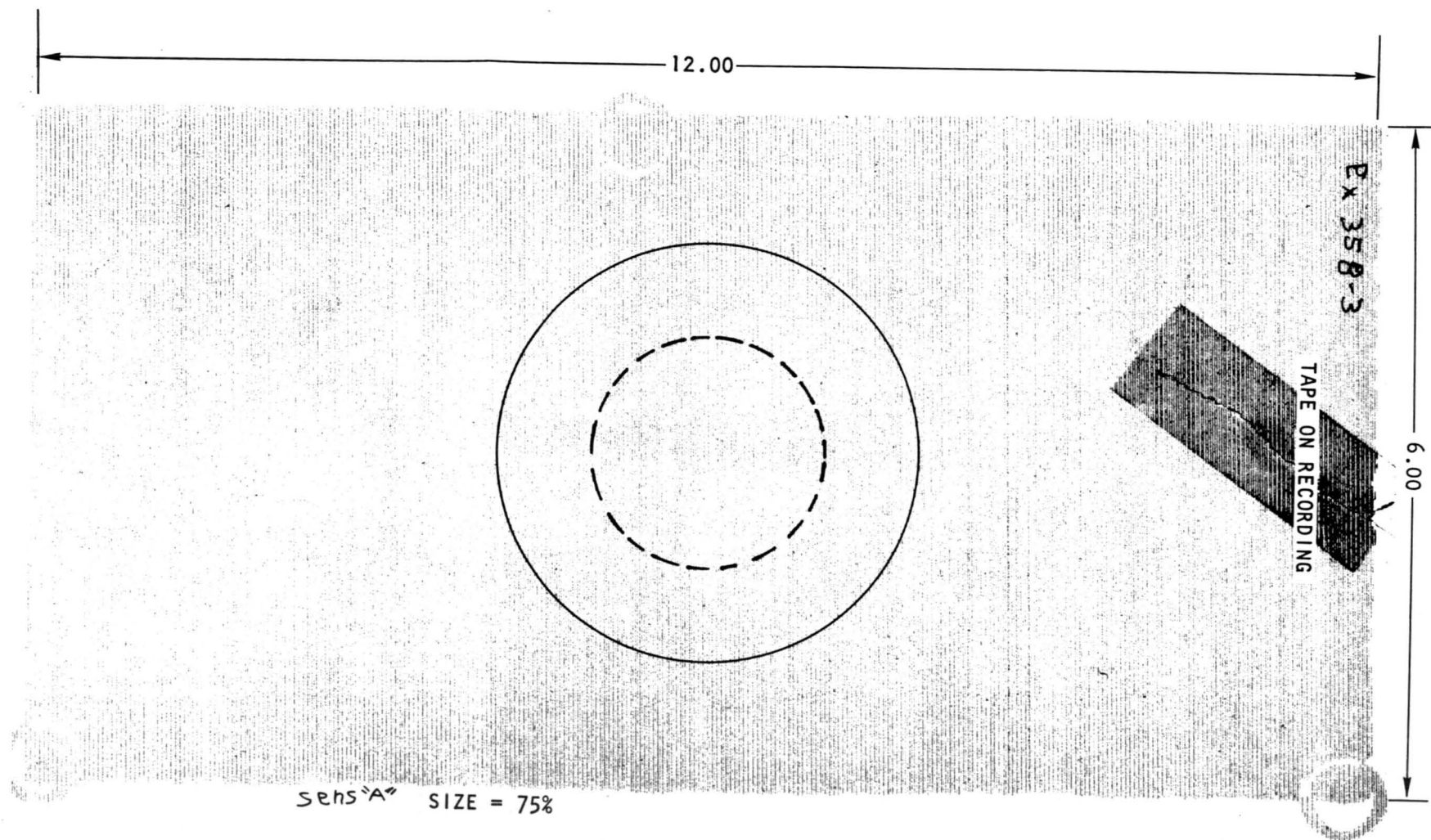


Figure 6-19. NDI C-Scan of Flat Laminate Cocure 6-Degree Flush Scarf,
2-Inch Hole Repair

6-25.

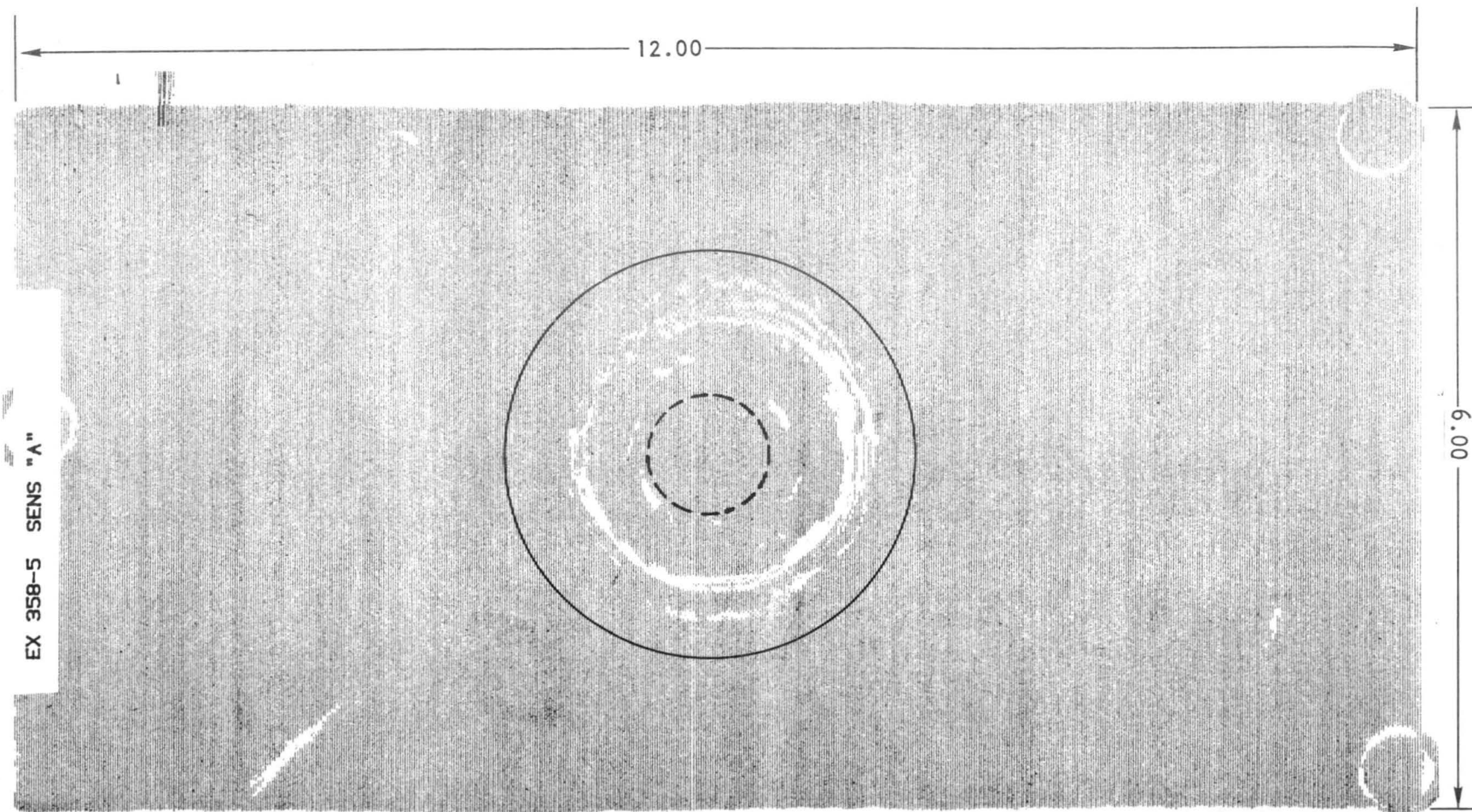


Figure 6-20. NDI C-Scan of Flat Laminate, 6-Degree Scarf Angle With One External Doubler, 1-Inch Diameter Hole Repair

Table 6-1 and can be seen typically in the photographs of the failed specimens in Figures 6-21 through 6-25. These photographs show both the patch side and the back side of the test specimens. The 3-degree scarf flush repair resulted in the greatest load transfer, and greatest strength increase over the damaged laminate strength. The load transfer by the external patch repairs is somewhat less than anticipated. Test specimens EX358-2 and EX358-5 are identical except that the latter has an external patch and had a much lower failure level. Only a few external patch specimens were fabricated. It is anticipated that current improvements in repair processes could result in higher failure levels for future external patch repairs.

Typical load-strain for test specimens with a 3-degree scarf repair on a 5.08 cm (2.00 in.) hole, a 6-degree scarf repair on a 5.08 cm (2.00 in.) hole, and a 6-degree scarf repair on a 2.54 cm (1.00 in.) diameter hole, are shown in Figures 6-26 through 6-29, respectively. Referring to Figure 6-26, the stress concentration around the hole has been greatly relieved as can be seen by the uniform response of gages 13, 14, and 15, and gages 20, 21, 22, and 23. The control laminate with a 5.08 cm (2.00 in.) hole (see Figure 6-13) had a local stress concentration of 3.6 at the edge of the hole.

Undamaged control specimen failure loads averaged 1,039 KN/m (5,933 lb/in.), which established the baseline target load for repair concepts. Compression failures occurred in one gap area of the test fixture.

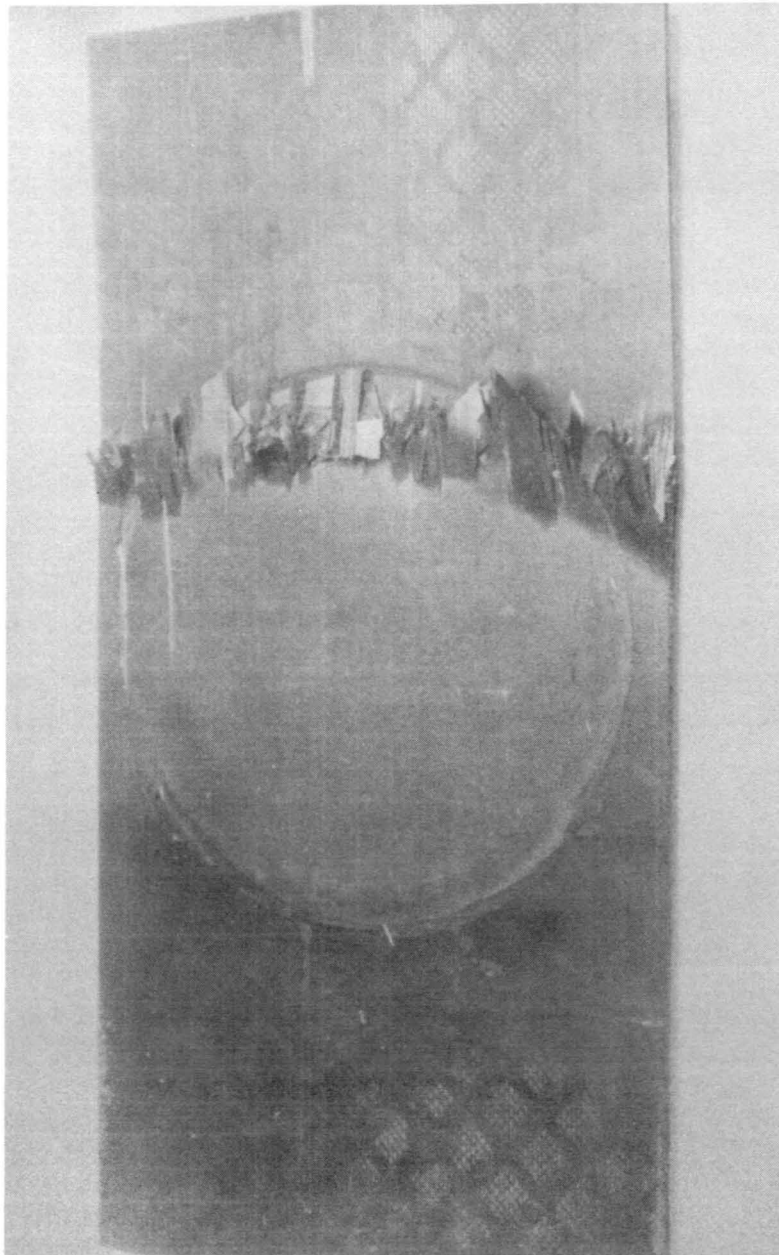
Simulated damaged specimens with 2.54 and 5.08 cm (1.00 and 2.00 in.) holes averaged 576 and 433 KN/m (3,291 and 2,473 lb/in.), respectively. These loads represent 44.5 and 58.3 percent loss in parent laminate strength because of simulated specimen damage. Compression failures occurred through the net section of the specimen between the hole and side edges.

Flush 3-degree scarf angle 4.08 cm (2.00 in.) diameter repairs demonstrated the highest average recoverable strength at 78.9 percent of parent laminate strength. Ultimate failing loads ranged between 707 and 941 KN/m (4,040 and 5,372 lb/in.) on the four specimens tested, averaging 819 KN/m (4,679 lb/in.). Failure modes varied from parent laminate compression with patch shear out to combined laminate and patch compression with minor patch shear out.

6.9 CONCLUSIONS — FLAT LAMINATE REPAIR

A 5.08 cm (2 in.) diameter hole was found to reduce the test laminate strength to 42 percent of the undamaged value. Simple scarf flush repairs returned the damaged laminate to nearly 80 percent of the undamaged strength. Early in the program, a few repairs were fabricated and tested with external doublers. These specimens did not perform as well as predicted. It is anticipated that these doubler repair strengths could be greatly increased with the improved processes developed as the program matured. It is expected that the improved serrated patch flush repairs will return at least 90 percent of the undamaged strength based on tensile coupon tests; however, this design could not be tested in the compression test fixture.

A810908 C-11C



A810908 C-10C

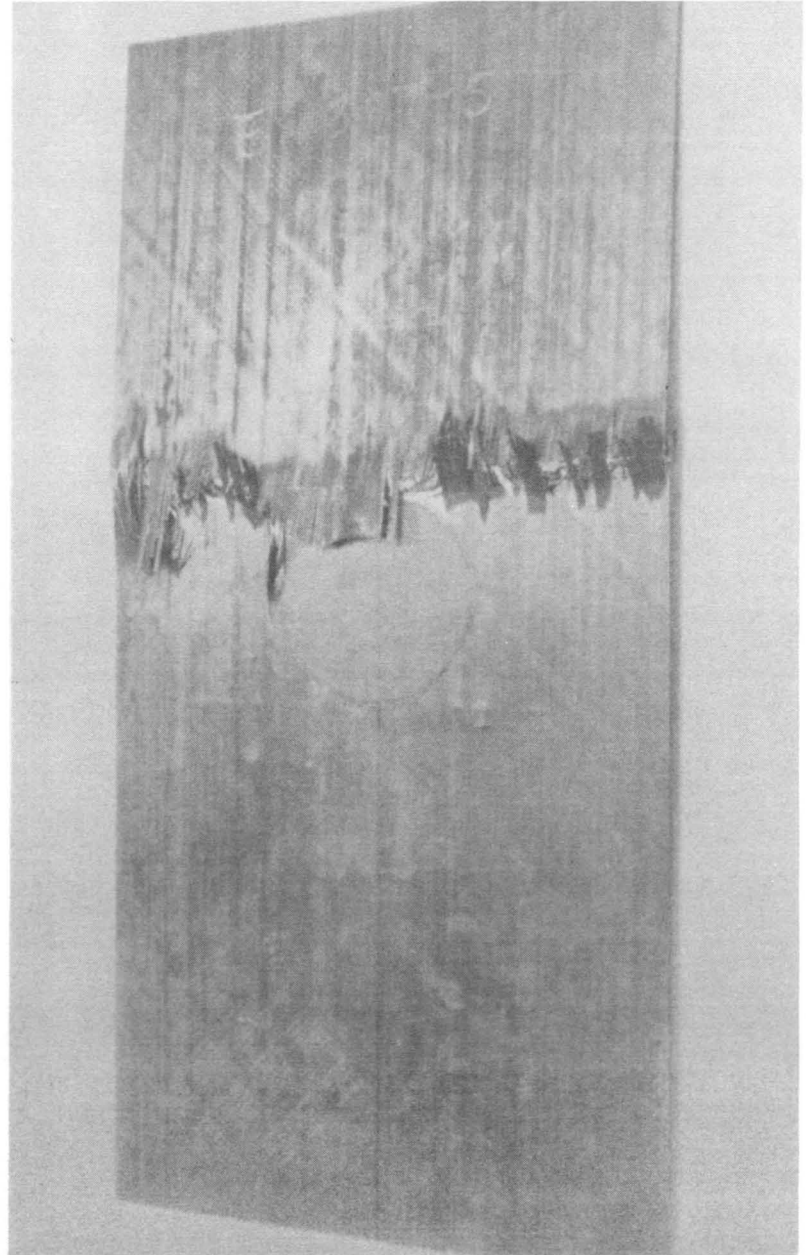
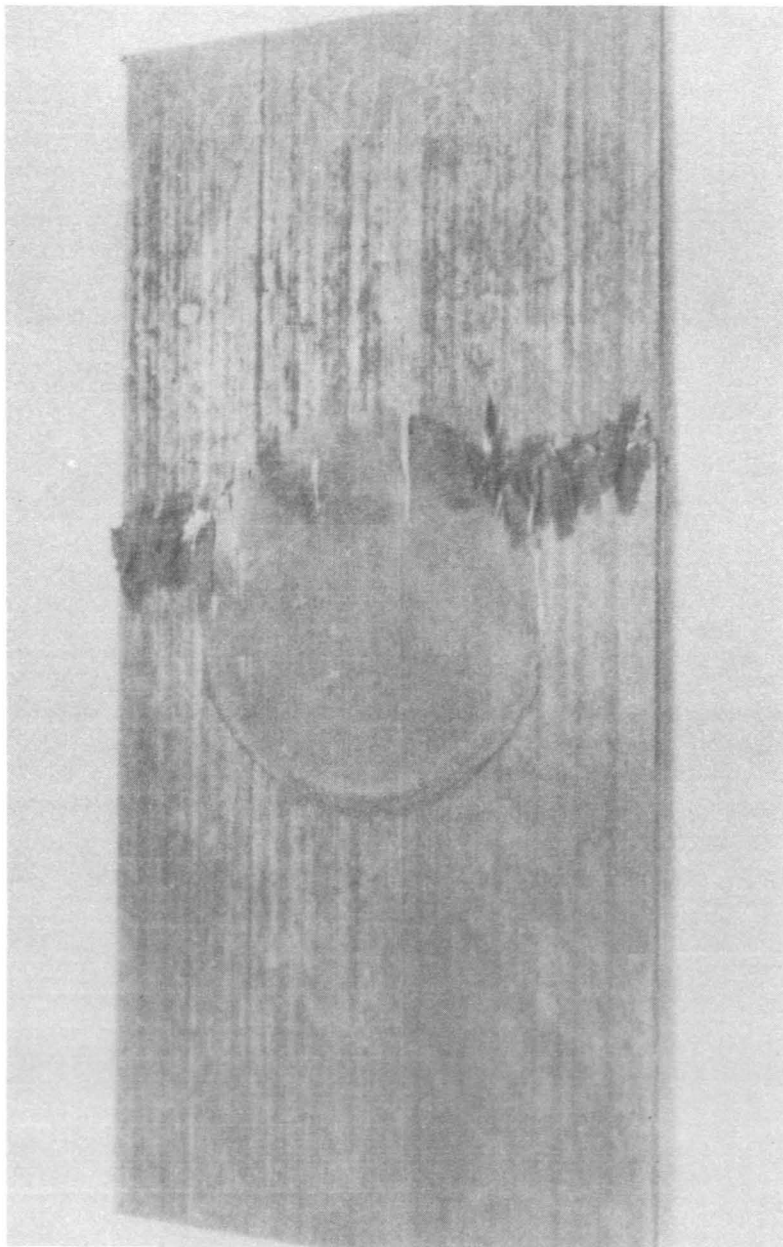
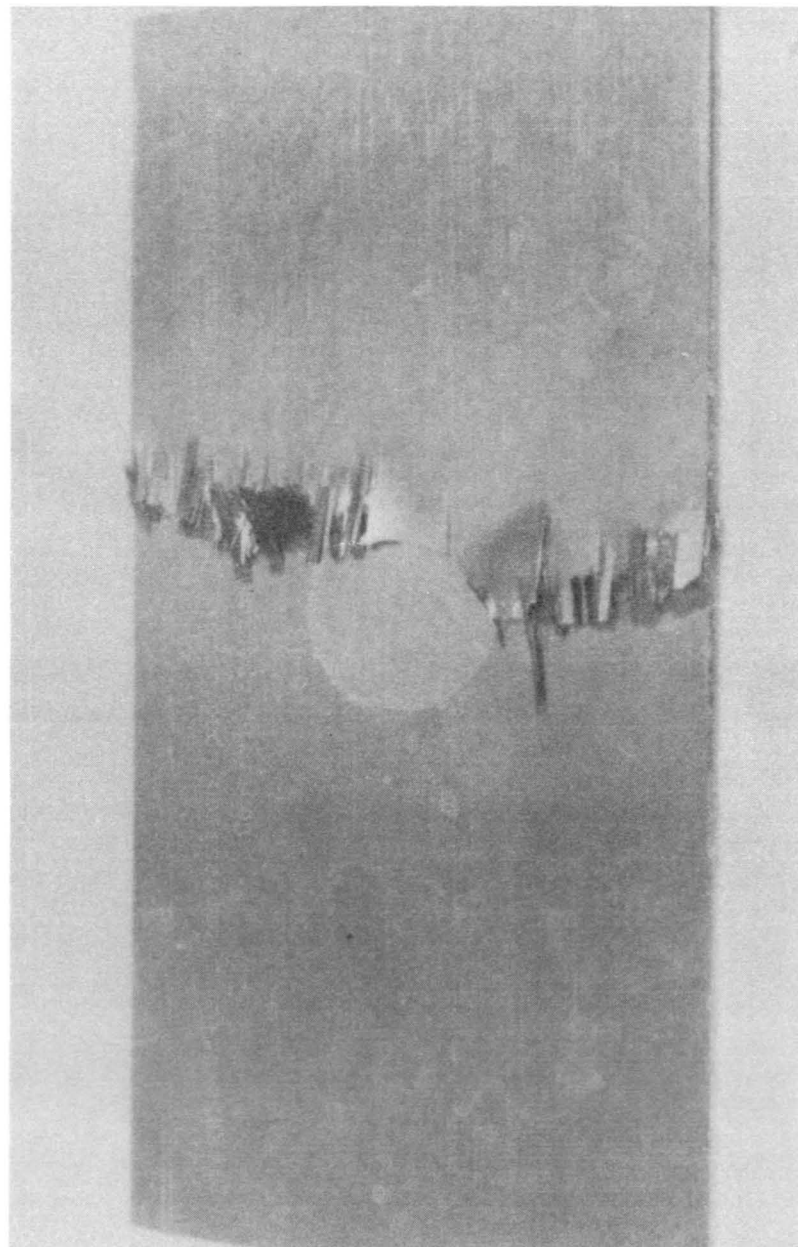


Figure 6-21. 3-Degree Scarf Flush Cocure Repair on 5.08 cm (2.00 in.) Diameter Hole; Specimen EX397-5

A810908 C-9C



A810908 C-8C



6-28

Figure 6-22. 6-Degree Cocure Repair on 5.08 cm (2.00 in.) Diameter Hole; Specimen EX397-3

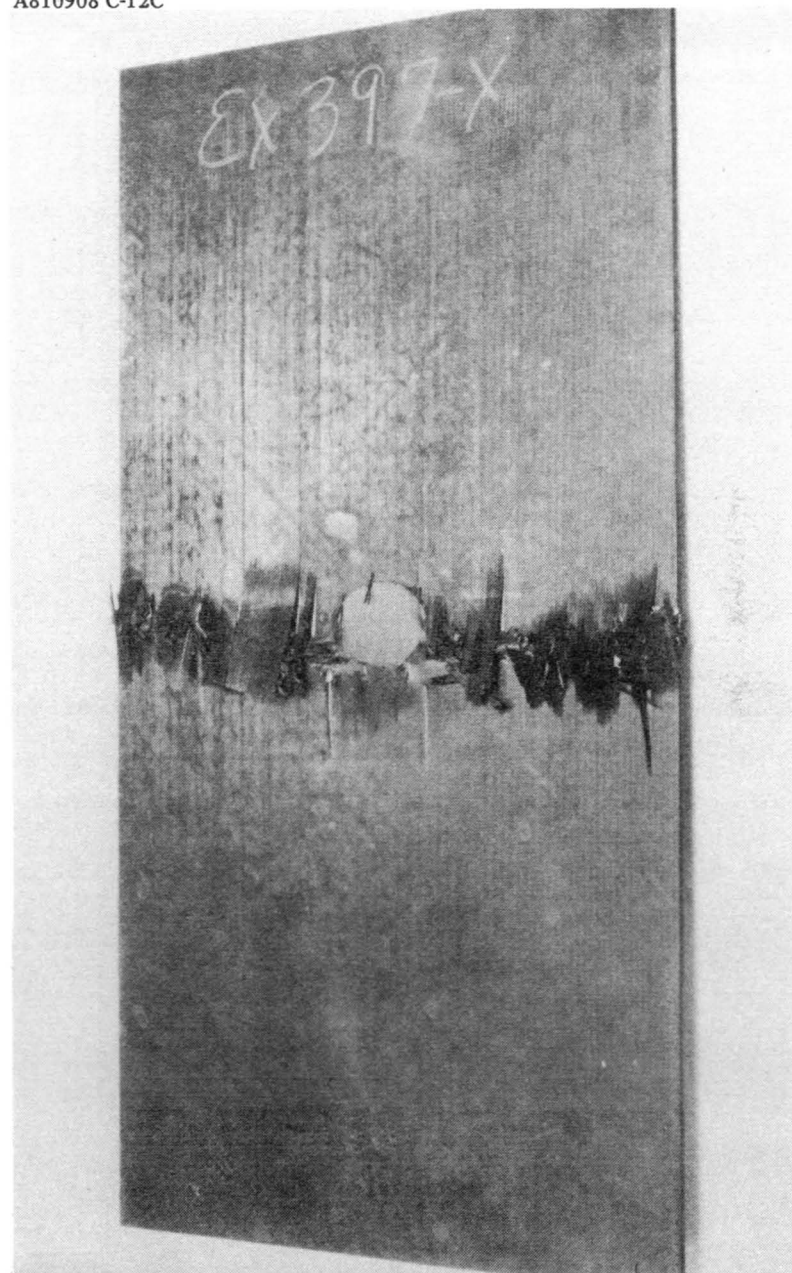
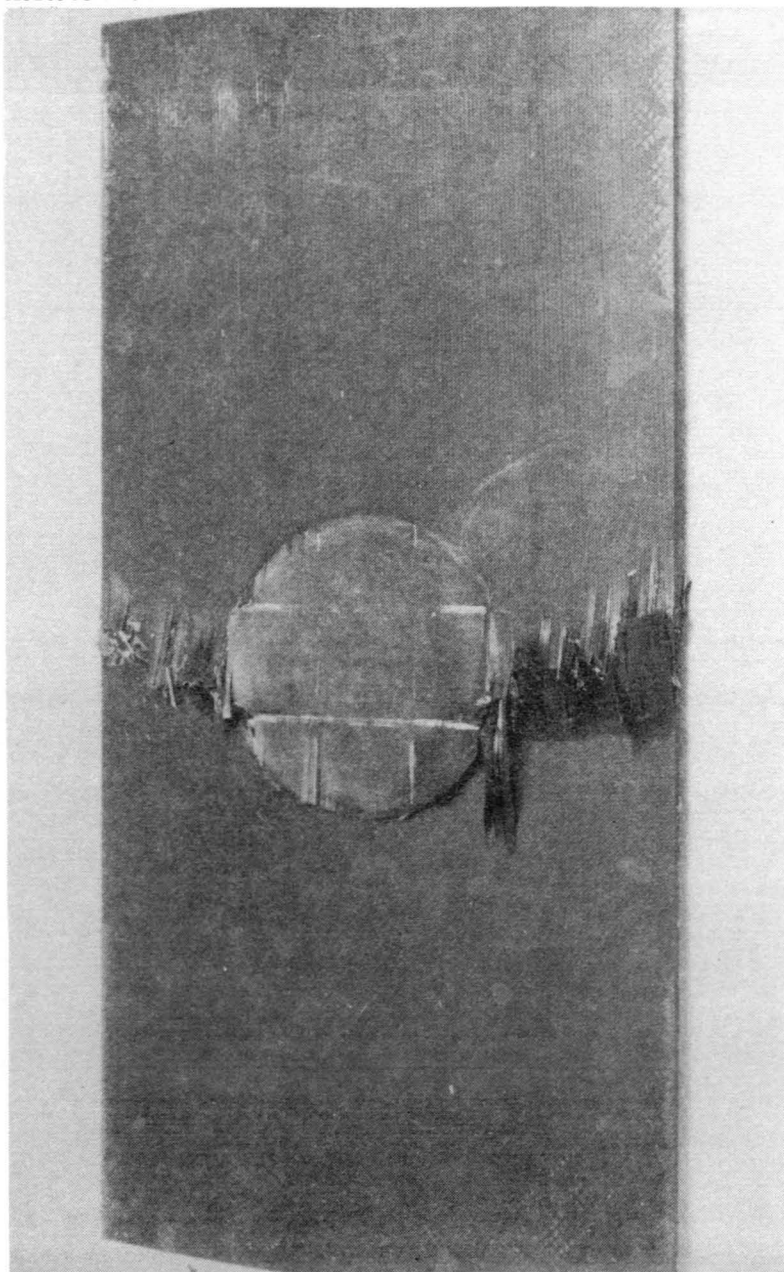
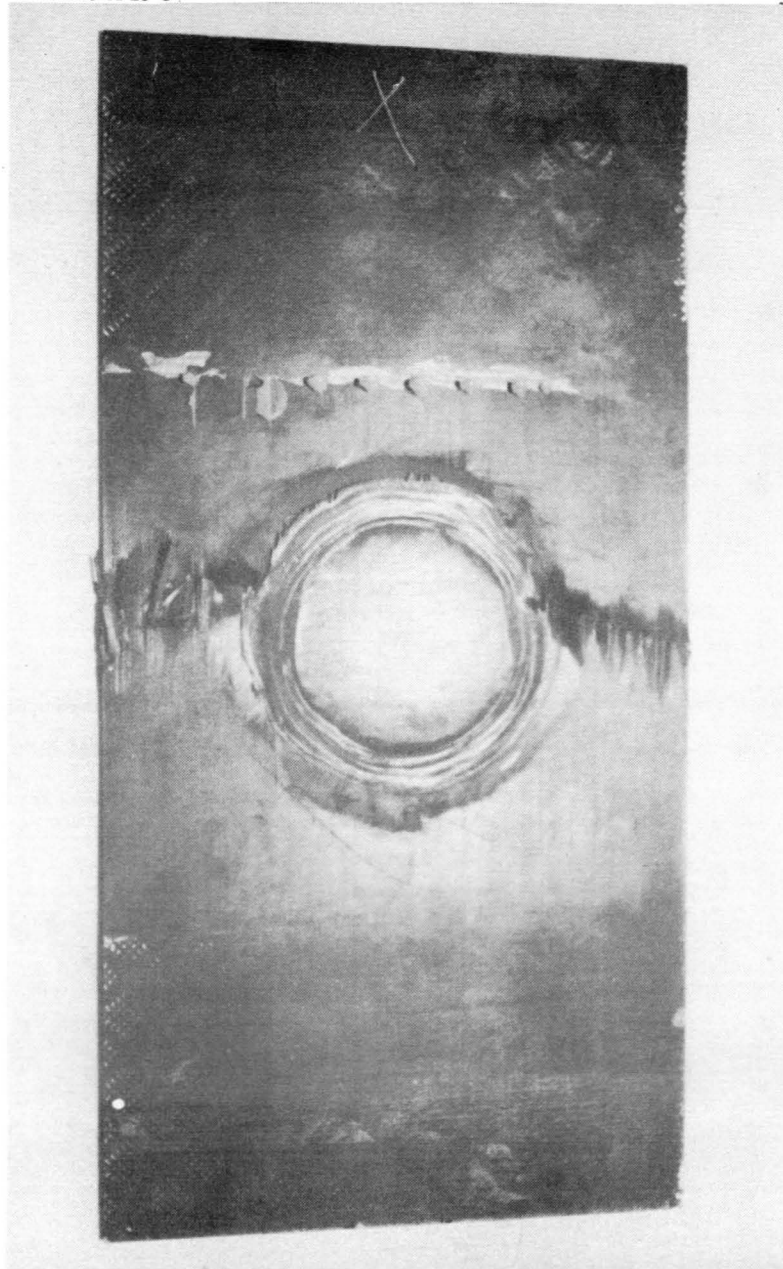


Figure 6-23. 6-Degree Cocure Repair on 2.54 cm (1.00 in.) Diameter Hole; Specimen EX397-X

A811009 A-25 C



6-30

A811009 A-24 C

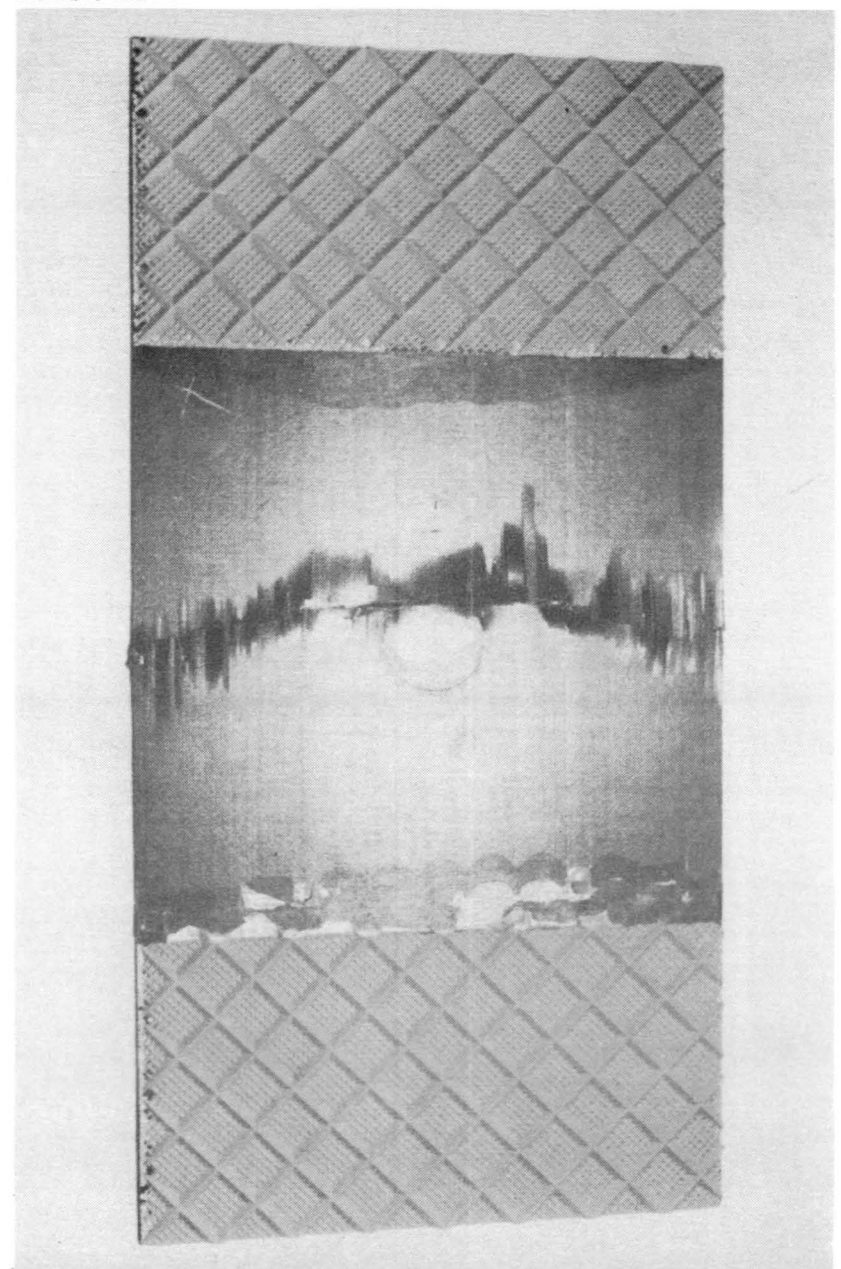


Figure 6-24. 7.62 cm (3.00 in.) Diameter External Cocure Patch on a
2.54 cm (1.00 in.) Diameter Hole; Specimen EX398-5

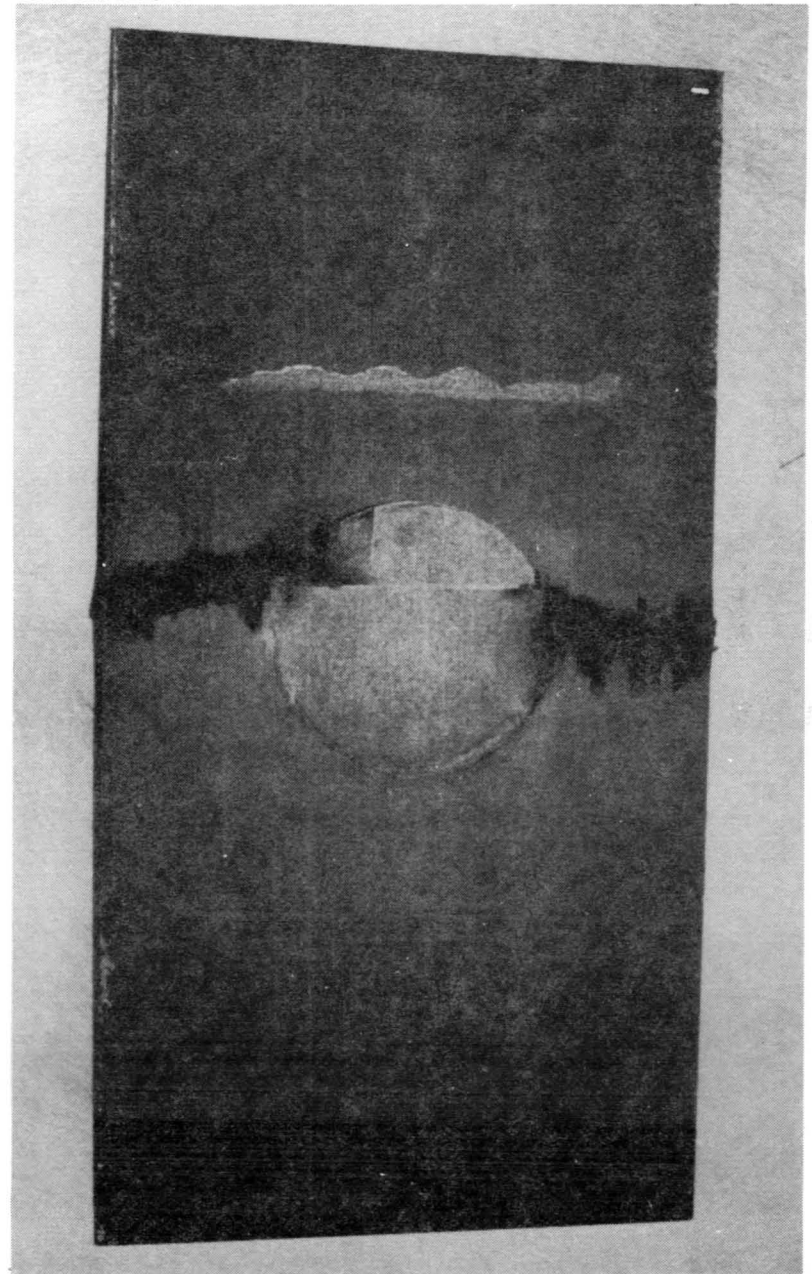
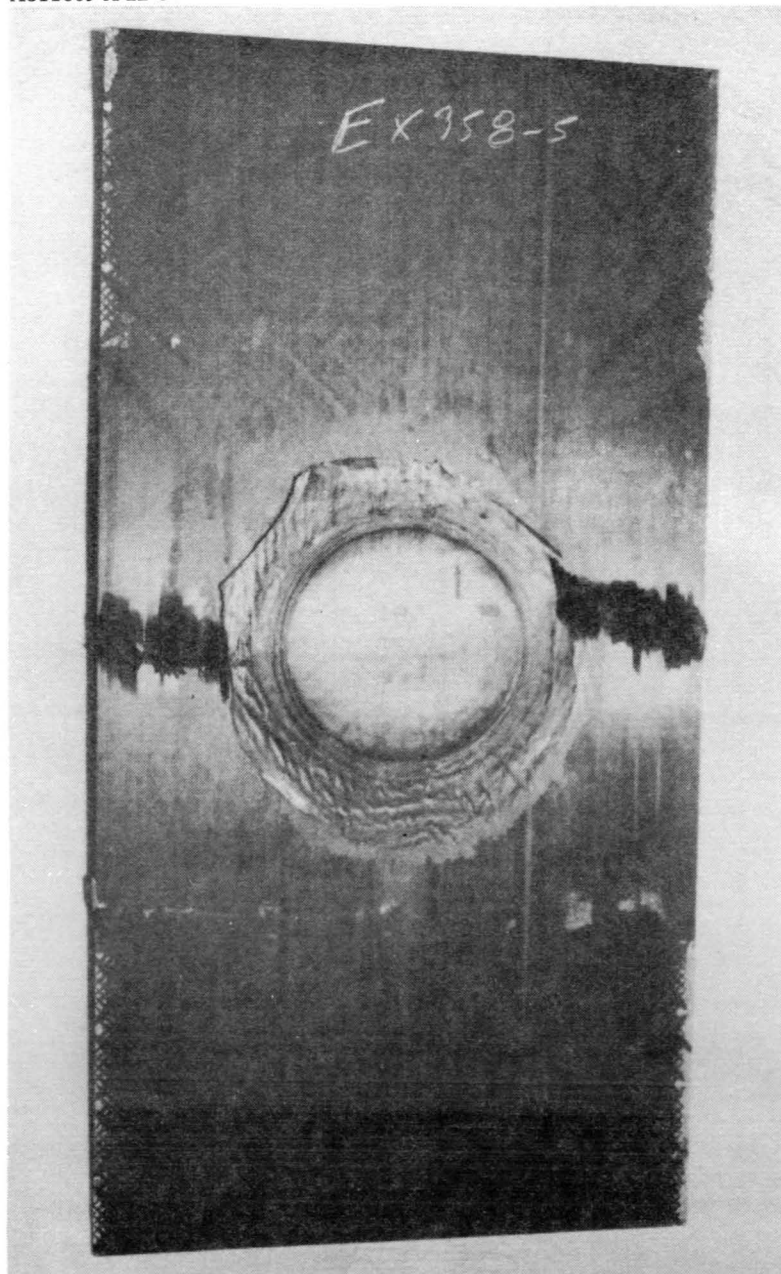


Figure 6-25. 7.62 cm (3.00 in.) Diameter External Cocure Patch 6-Degree Scarf Repair on a 2.54 cm (1.00 in.) Diameter Hole; Specimen EX358-5

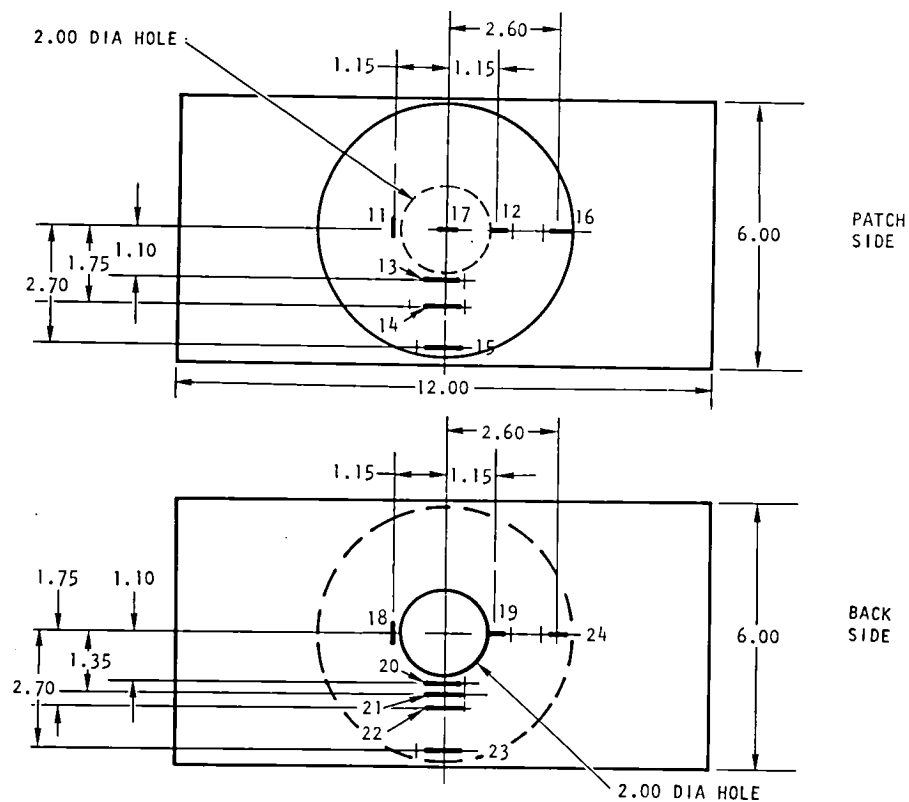
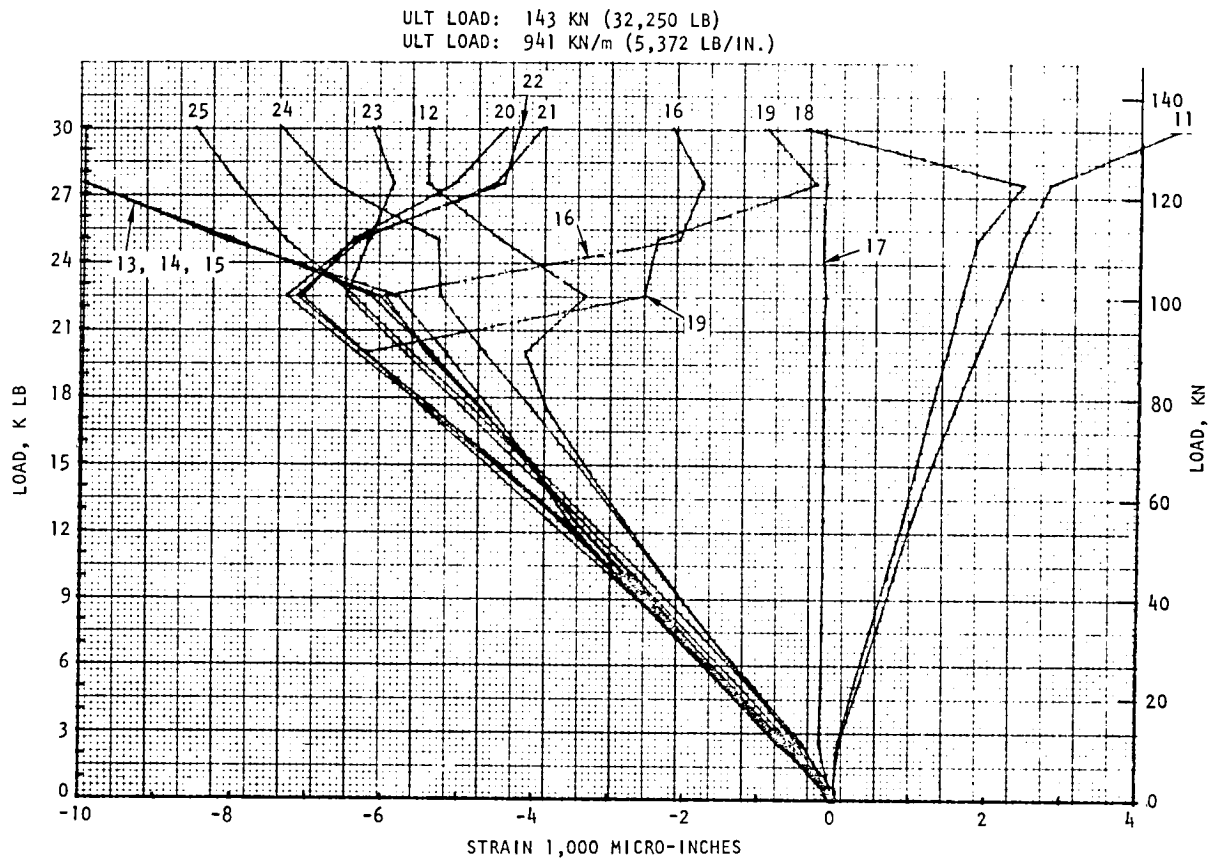


Figure 6-26. Compression Load/Strain Distribution Through Flush Repair Panel, 2-Inch Diameter Hole, 3-Degree Scarf Angle; Specimen EX358-4

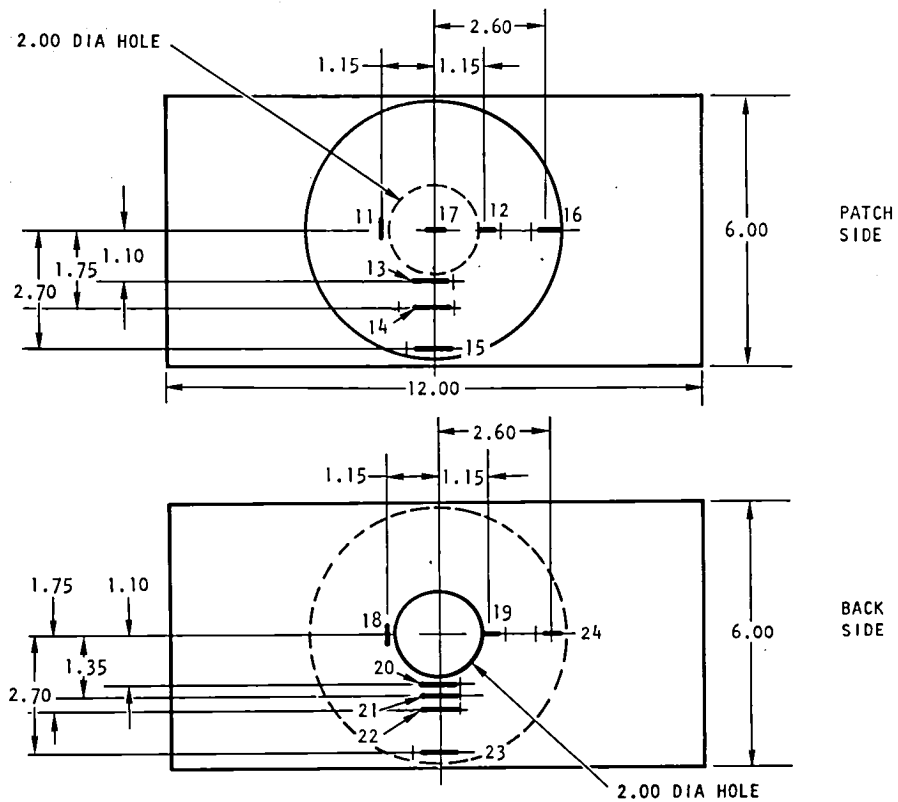
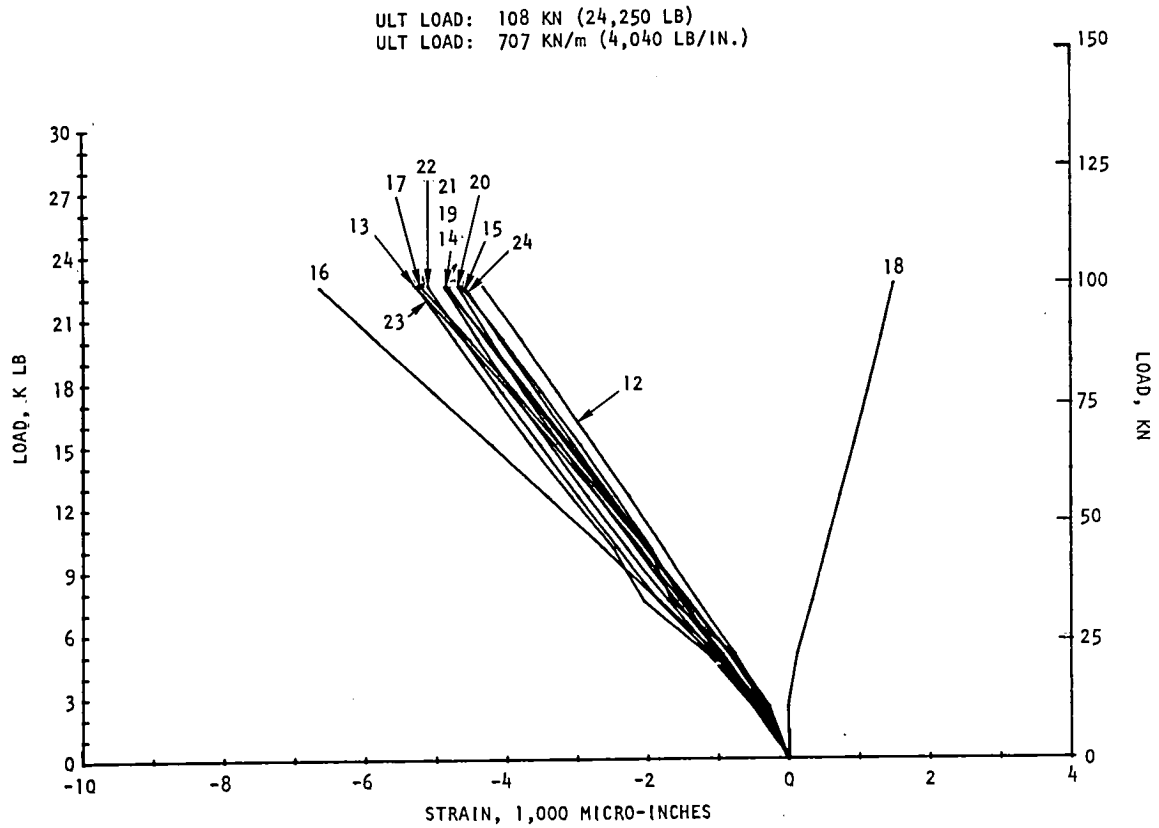


Figure 6-27. Compression Load/Strain Distribution Through Flush Repair Panel, 2-Inch Diameter Hole, 3-Degree Scarf Angle; Specimen EX358-8

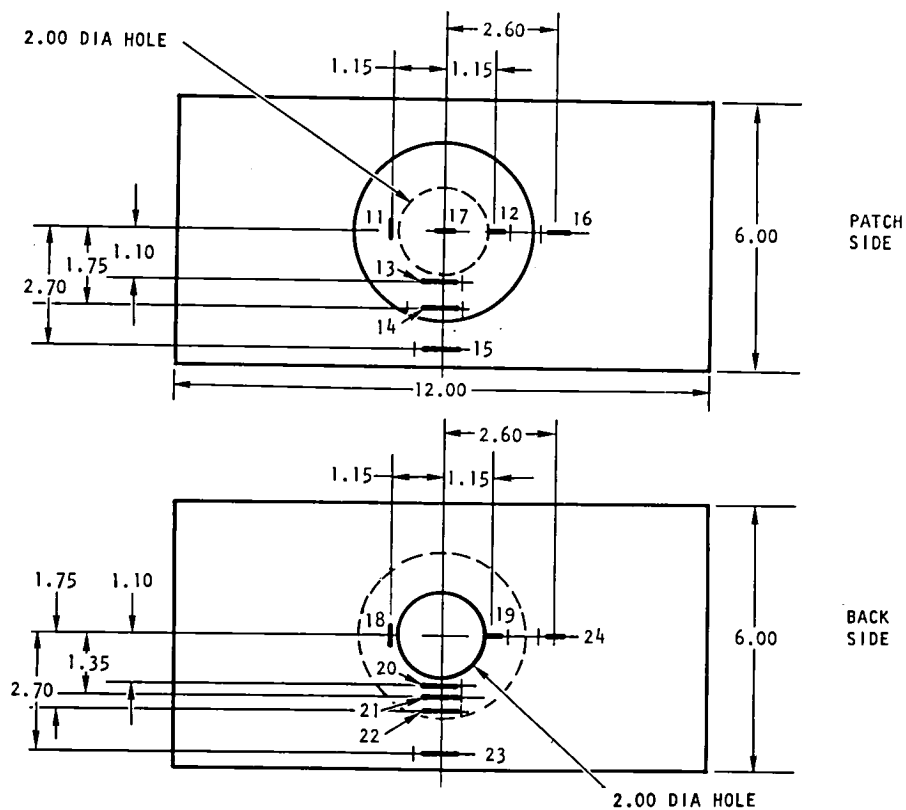
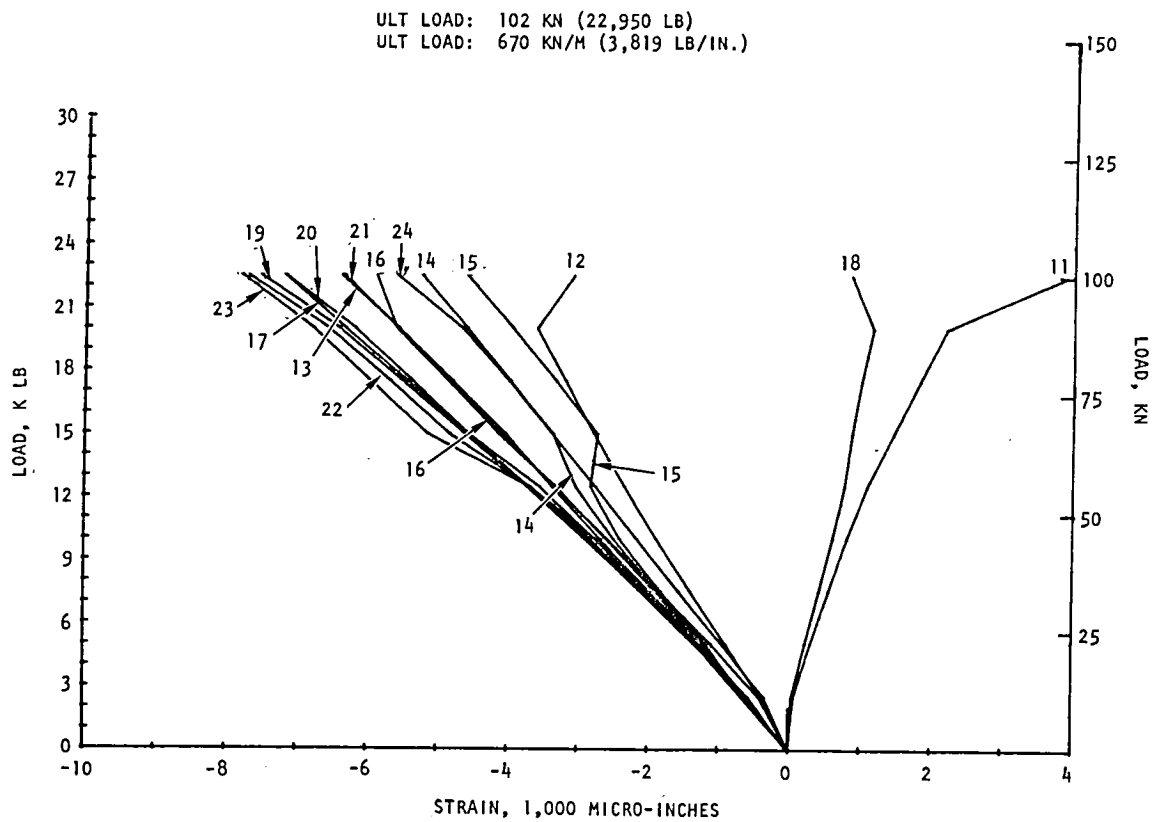


Figure 6-28. Compression Load/Strain Distribution Through Flush Repair Panel, 2-Inch Hole, 6-Degree Scarf Angle; Specimen EX358-3

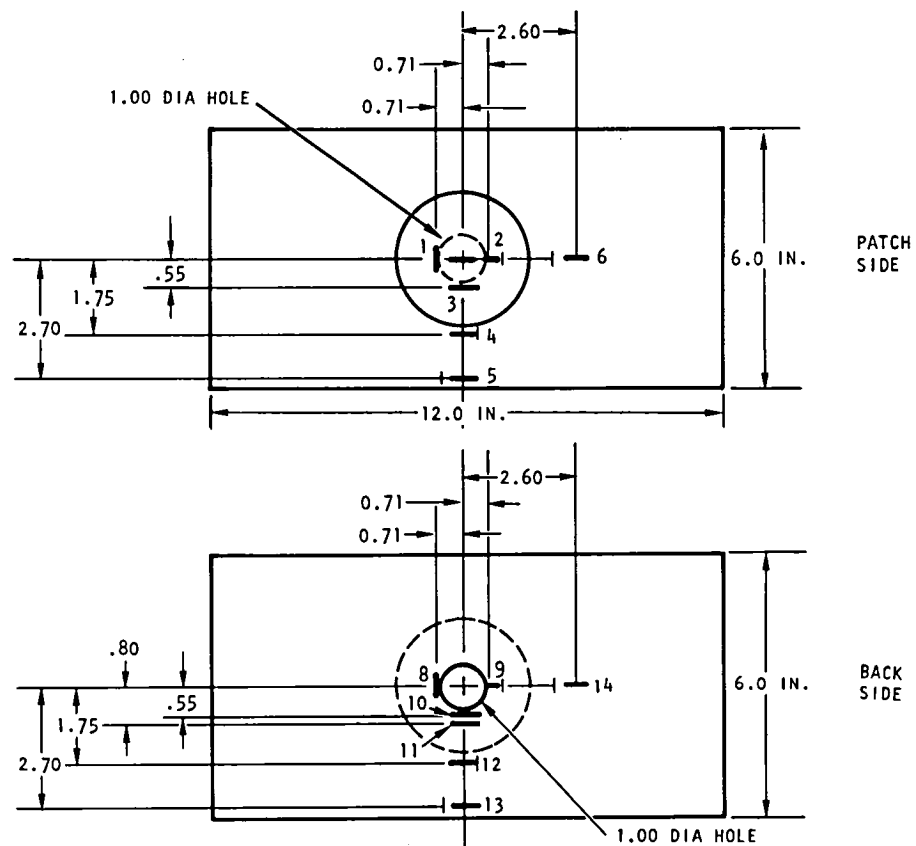
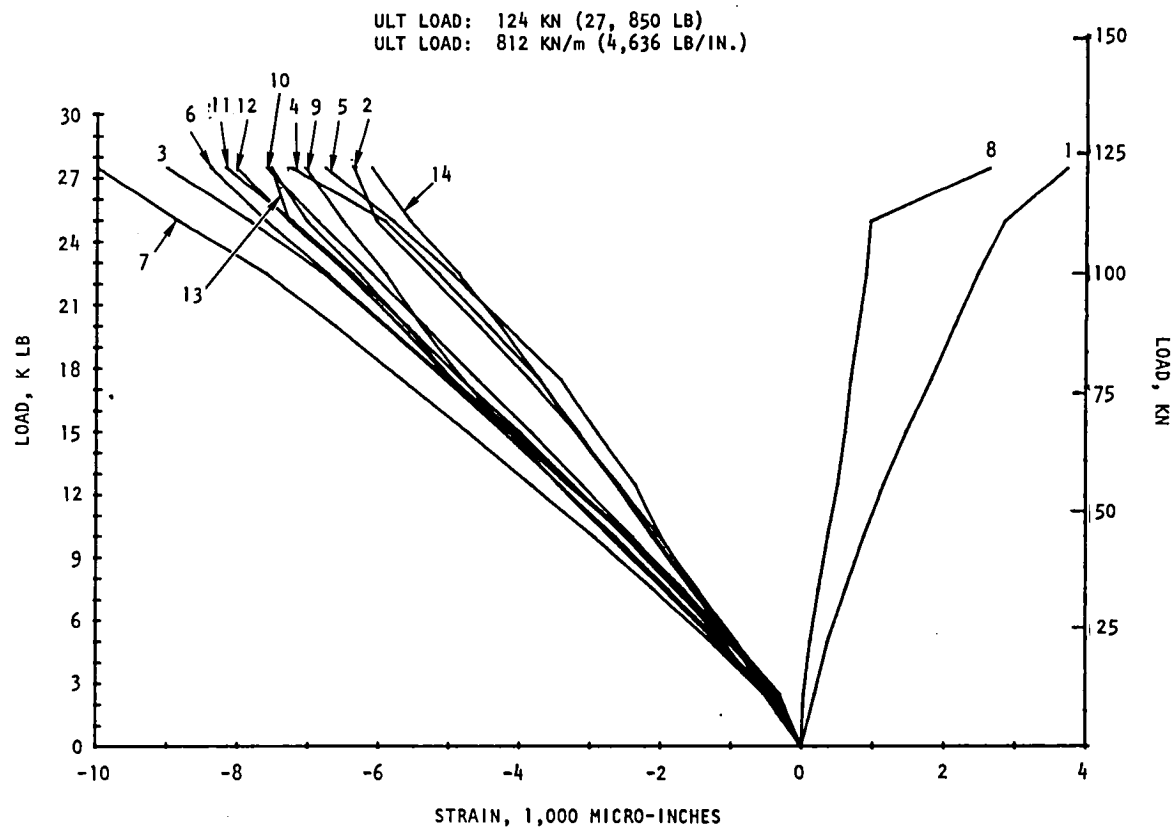


Figure 6-29. Compression Load/Strain Distribution Through Flush Repair Panel, 1-Inch Diameter Hole, 6-Degree Scarf Angle; Specimen EX358-2

7. HONEYCOMB SANDWICH REPAIR

Two types of honeycomb sandwich panel configurations were used for repair development and demonstration. The first type is a heavily loaded panel designed by NASA LaRC to carry a compression load of 2.1 MN/m (12,000 lb/in.). The second type is a lightly loaded panel designed by Rockwell to withstand 0.53 MN/m (3,000 lb/in.). The baseline control compression subelement design concepts are presented in Figure 7-1.

7.1 HEAVILY LOADED HONEYCOMB SANDWICH REPAIR

The heavily loaded honeycomb sandwich repair program involved testing of three types of specimens: undamaged control laminates, damaged control laminates with a 5.08 cm (2 in.) diameter hole, and repaired specimens. The repair design was selected from the most efficient repair developed for flat laminates (Section 6.8) and is presented in Figure 7-2. The test specimen measures 20.7 by 30.5 cm (8.15 by 12.00 in.) with 16-ply (0,+45, 90)_{2s 3} Celion/LARC-160 face sheets bonded to 2.54 cm (1.00 in.) thick 96.1 g/m³ (6.0 pcf) HRH-327 core. The laminates used as face sheets on the honeycomb sandwich test panels are identical to the flat laminates discussed in previous sections. Based directly upon the compression test results for flat laminates presented in Table 6-1, the predictions for the strengths of the sandwich panels are as follows: the undamaged control specimens were expected to fail at 2.1 MN/m (12 K lb/in.), the damaged control specimen with a 5.08 cm (2 in.) diameter hole was expected to fail at 0.876 MN/m (5 K lb/in.) or 41 percent of the undamaged strength, and the repaired specimens were expected to fail at 1.89 MN/m (10.8 K lb/in.) or 90 percent of the undamaged strength.

In the sandwich repair development phase of this study, the processes developed for the repair of flat laminates were directly extended to the repair of honeycomb sandwich panels. The repair consists of a precured solid laminate plug bonded into a recess in the core. This plug provides the base for cocuring the patch plies on the face sheet laminate. The patch has a 4.5-degree scarf with three external serrated octagonal patch plies added. The 4.5 degree scarf angle was selected on the basis of Figure 5-6 and tension test results, refer to Table 4-6 and Figure 4-16.

7.1.1 Sandwich Repair Rationale and Concept

The initial approach to preparing sandwich structure where either the skin or skin and core were damaged was to remove the damaged skin and or core, replace the core, and cocure or secondary bond a replacement skin flush patch and external doubler. Shortcomings to this approach occur in the cocure process resulting in severe laminate dimpling and high void areas when the patch is applied directly over the core. Laminate dimpling and void areas can cause loss of composite mechanical properties.

In the case of secondary bonded repairs, difficulty in attaining an accurate fit-up between the cured-tapered composite patch in a tapered hole poses a problem in resultant bondline voids.

V

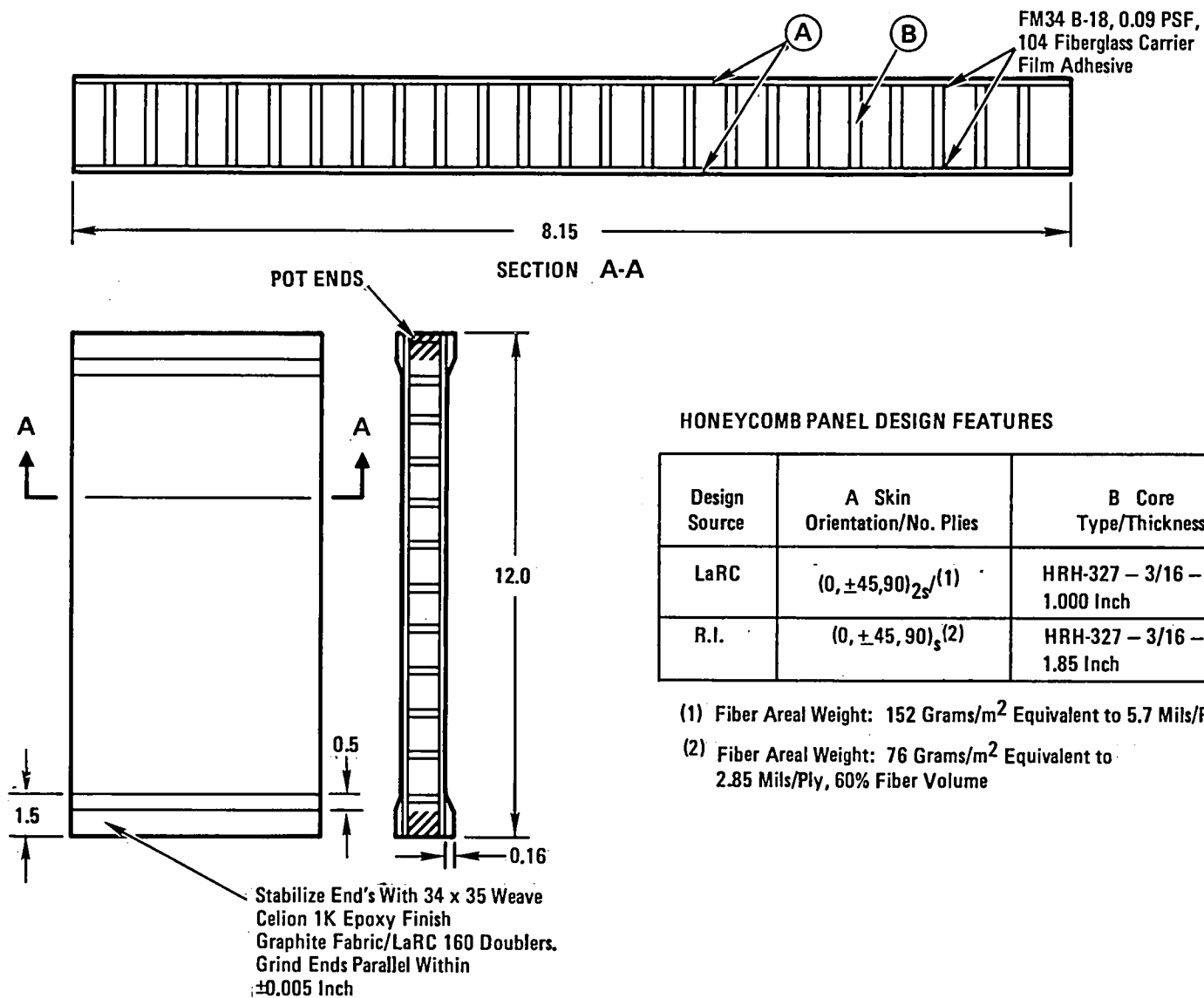


Figure 7-1. Sandwich Panel Baseline Control Compression Subelement Specimen Designs

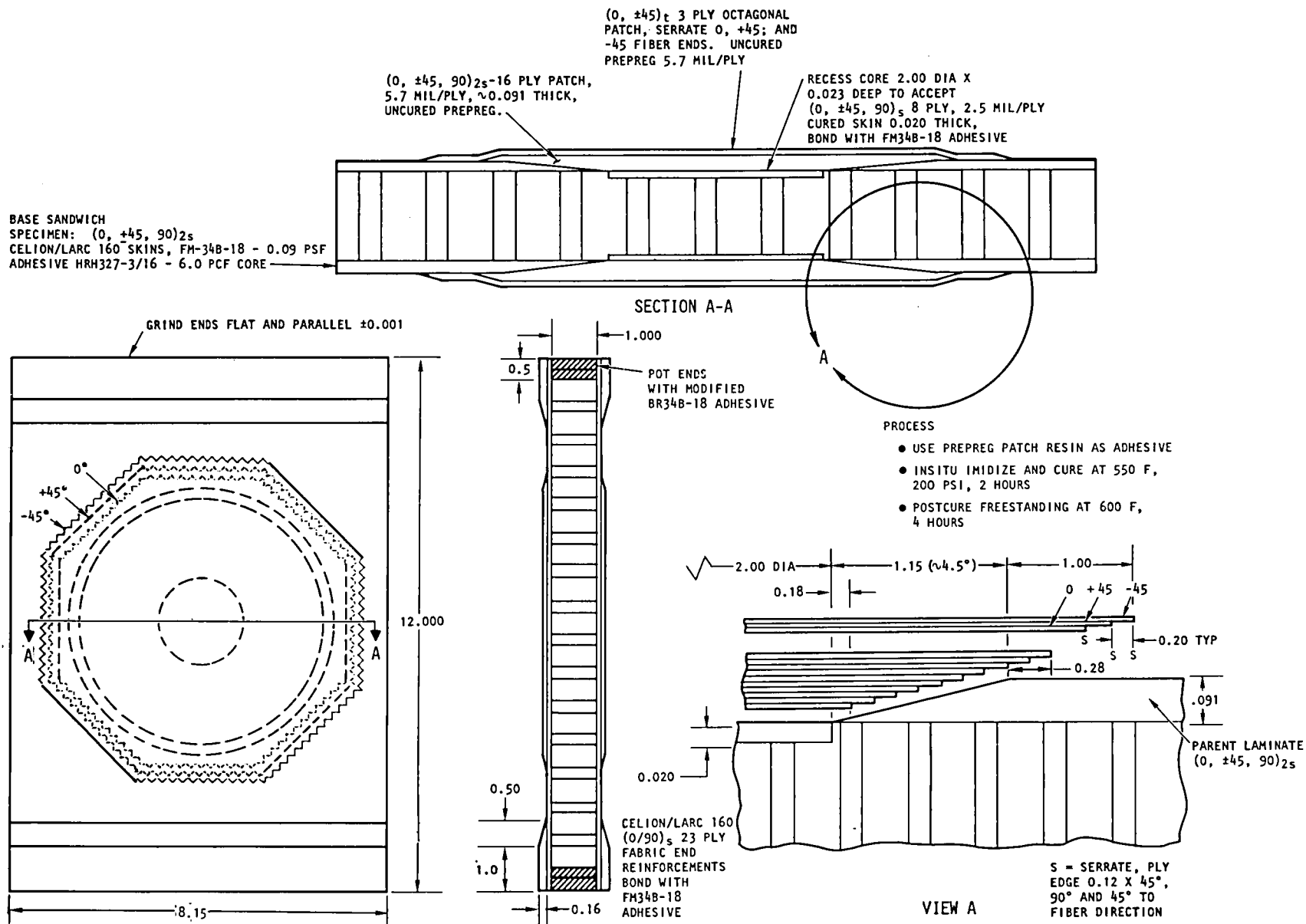


Figure 7-2. Cocure Repair Design Concept for Heavily Loaded Sandwich Structure Compression Specimen

An improved sandwich repair concept was conceived that allows the application of the prepreg adhesive, in-situ imidizing cocure bonding technique developed for flat laminates, Section 4.5. The concept uses a scarf angle joint in the parent laminate with an external octagonal 3-ply patch with serrated edges which proved successful in flat laminate repair. Prepreg dimpling problems are resolved by bonding a pre-cured laminate facing over the exposed core to provide a backup for the prepreg patch during the cocure bonding process.

The tooling approach also follows the approach used for flat laminates. The FMC165 fluoro rubber is employed as a flexible pressure caul to impart uniform pressure and smooth surfaces to each patch side of the sandwich panel. The tooling concept is illustrated in Figure 7-3.

Repair of the first two prototype specimens showed an excellent aesthetic, smooth appearance of the octagonal patches with serrated edges was imparted by the fluoro rubber pressure cauls. NDI C-scan recordings also indicated near zero void cocure bonds were achieved. Photographs of a specimen in the process of repair with patch preforms ready for assembly and a completed repair are shown in Figures 7-4 and 7-5. A NDI C-scan of a typical repaired 30.48 by 20.62 cm (12.00 by 8.12 in.) specimen is shown in Figure 7-6.

Inadvertently, six specimens, 30.48 by 15.24 cm (12.00 by 6.00 in.), were trimmed from the 66.04 by 68.58 by 3.00 cm (26.00 by 27.00 by 1.18 in.) sandwich panel stock with outer 0-degree fiber orientation transverse to the specimen length and load directions. Although not in the original test plan, these specimens provide useful data in comparing load transfer efficiency of the repair into the transverse-oriented (0 degree) outer plies of the sandwich skin. Test results are compared with specimens having parallel-oriented (0 degree) outer fibers.

7.1.2 High Temperature Testing Facility

A special portable oven for heating sandwich, and hat stringer stiffened skin specimens on the spherical seat test bed of the MTS test machine was designed and fabricated for testing at 316°C (600°F). Test temperature was achieved by passing low pressure air through a resistance-heated corrosion resistant steel (CRES) pipe into the oven. Power to the resistance heater was supplied by a 20:1, 130 kilovolt-ampere (KVA) transformer, which was powered by a 440-volt, 60-ampere source. Temperature was controlled by varying the voltage through the transformer using a Thermac 625 power controller. Hot air was dispersed in the oven through perforated tubes, two each located either side of the specimen. Perforations dispersed hot air against the sides of the oven to prevent locally overheating the specimen. Twelve thermocouples were taped, six each to front and back surfaces of the specimen and were used to monitor specimen temperature distribution. Watercooled compression plates were used on top and bottom of the specimen to prevent overheating the test machine. Photographs of the heating device are presented in Figures 7-7, 7-8, and 7-9.

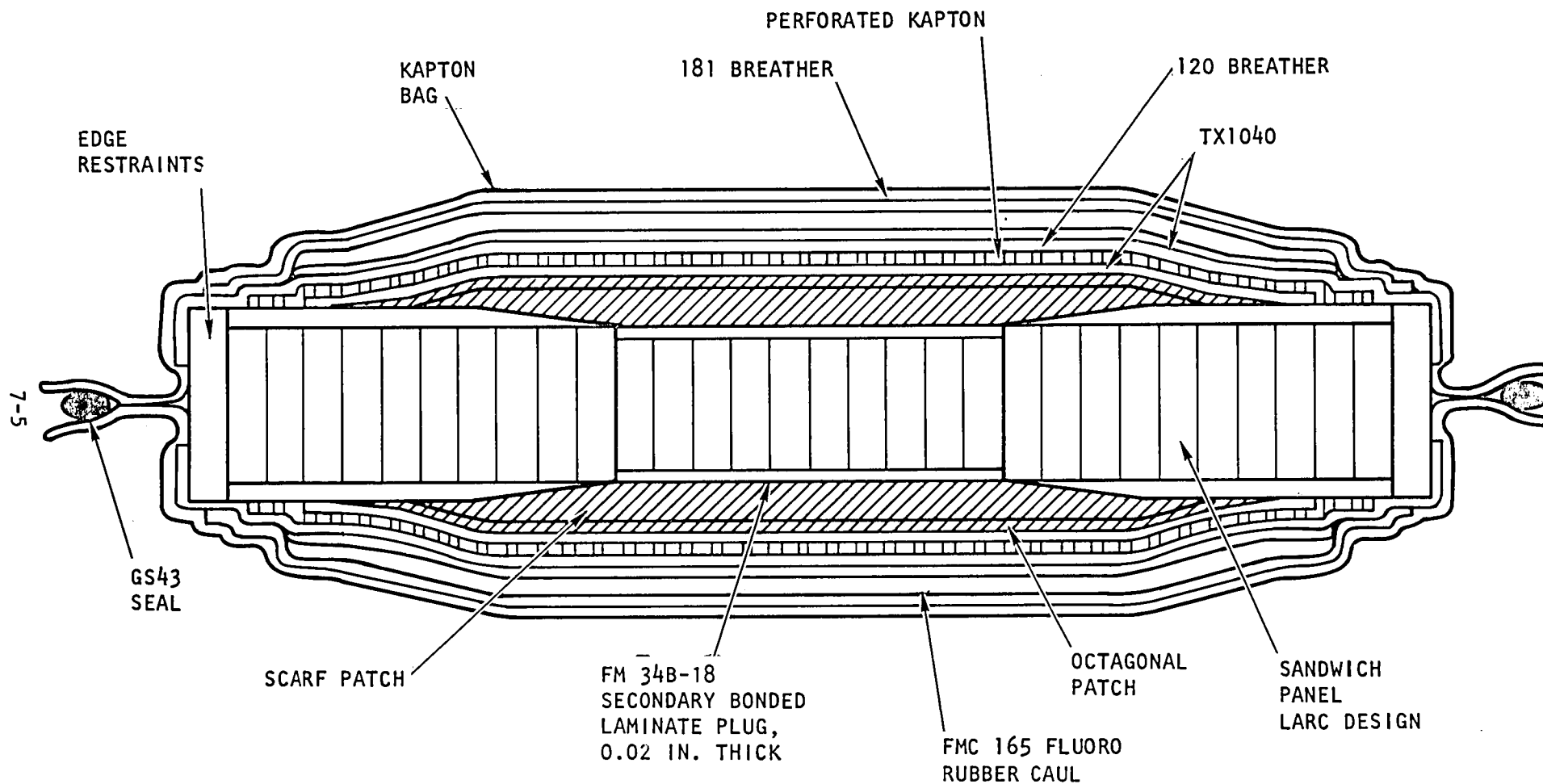


Figure 7-3. Improved Sandwich Repair Application Technique - Prepreg
Adhesive In-Situ Imidize Cocure Process

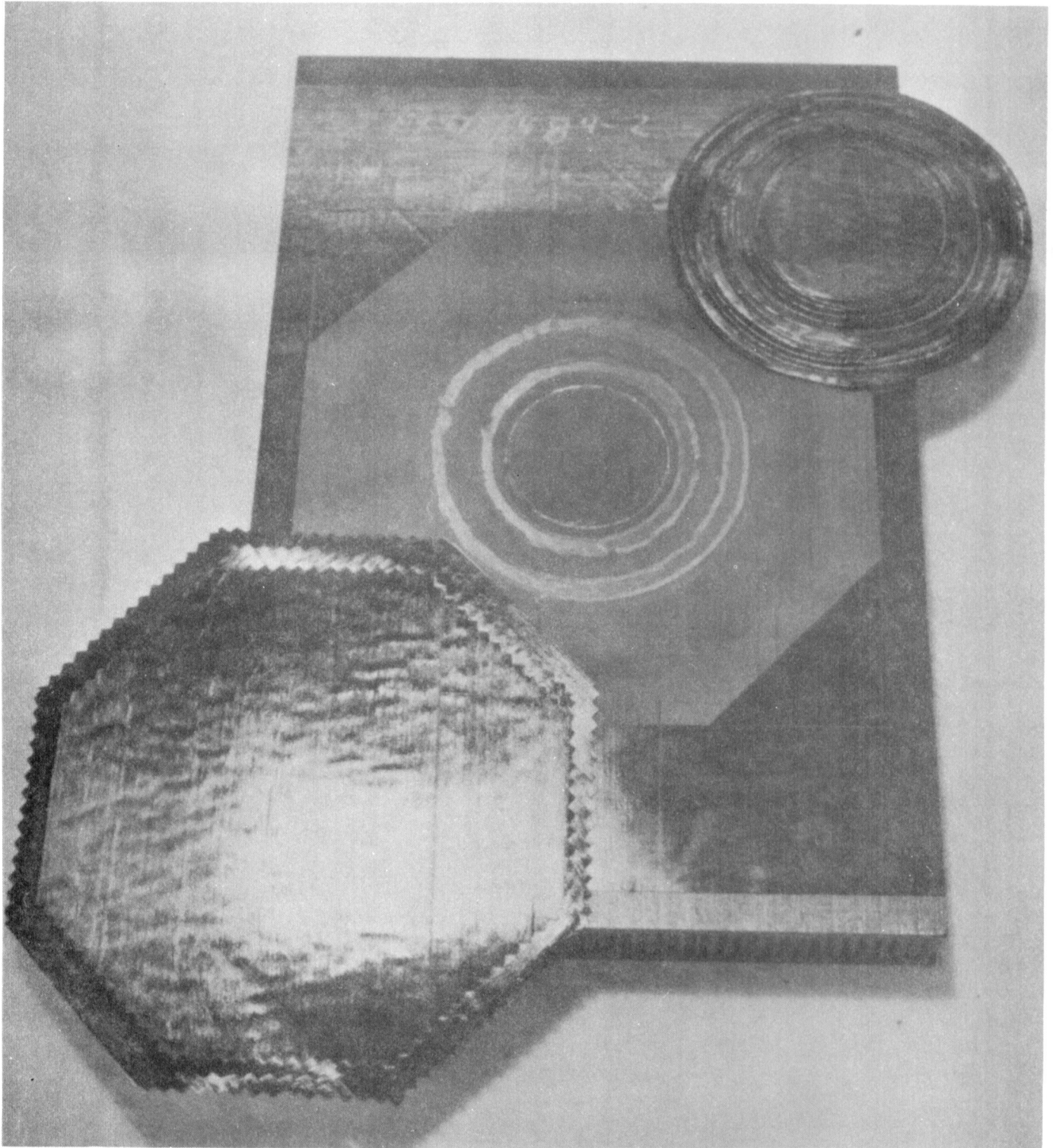


Figure 7-4. Sandwich Specimen; Heavily Loaded Design Ready for Repair

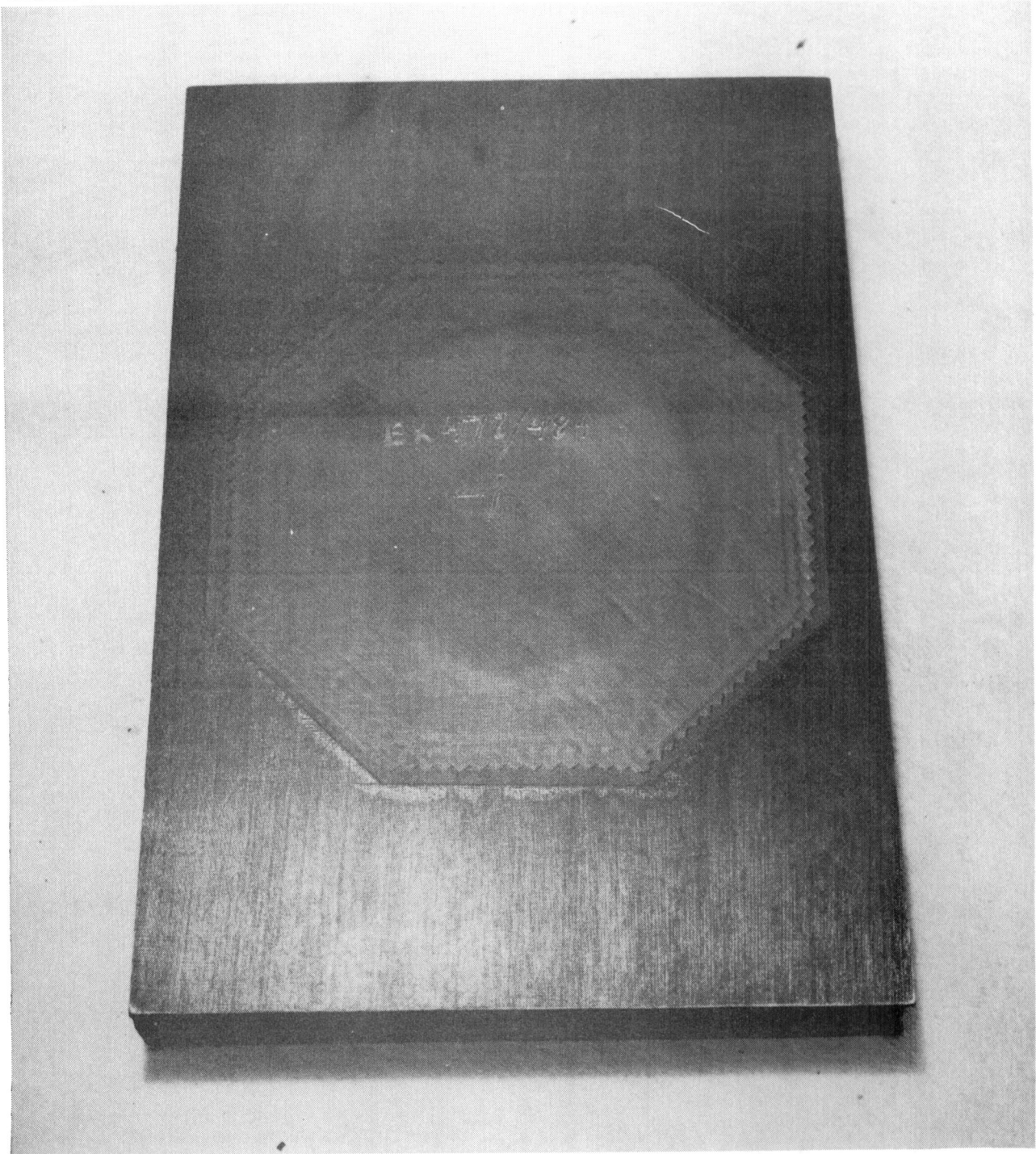


Figure 7-5. Completed Octagonal Patch Cocure Repair

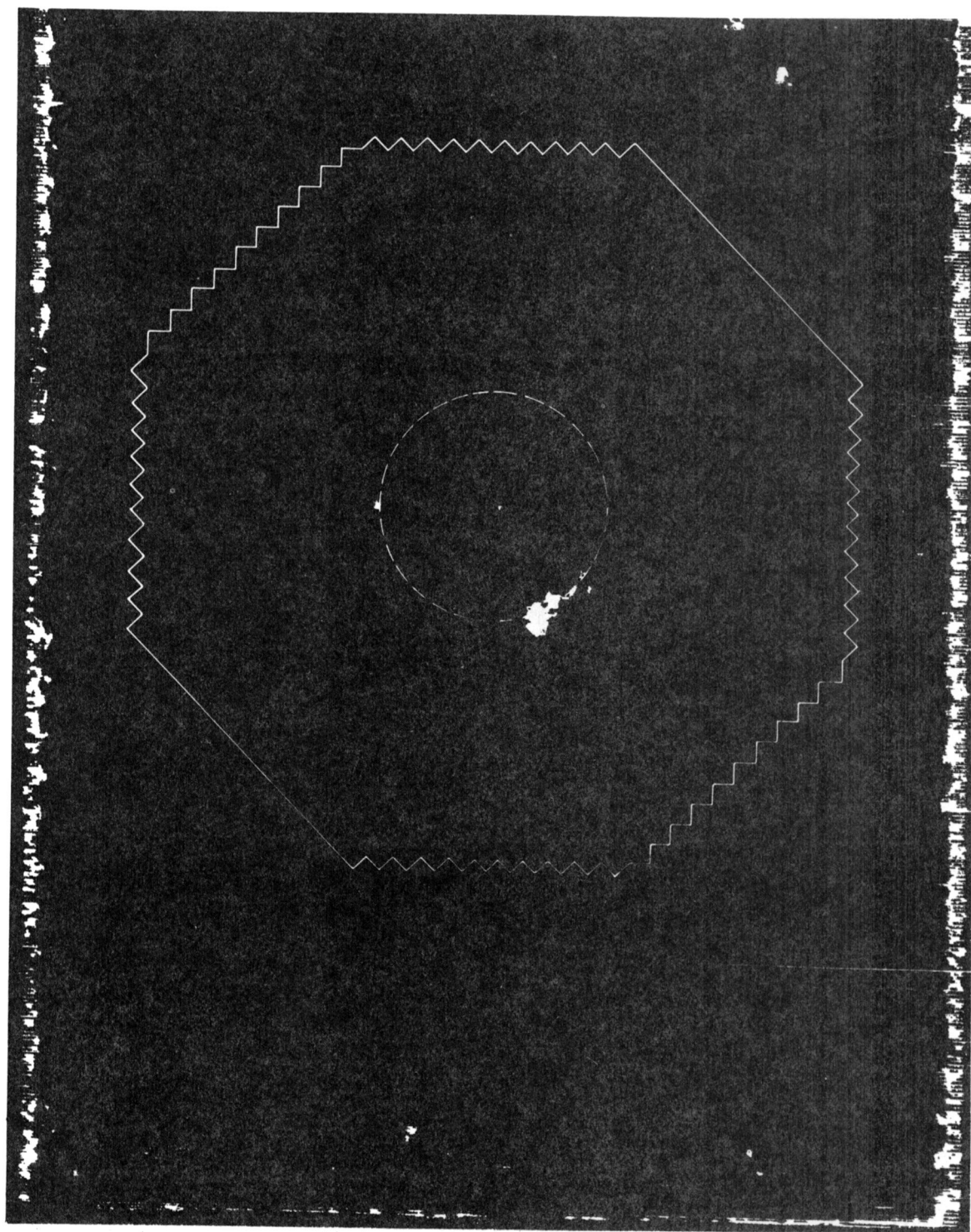


Figure 7-6. NDI C-Scan of Sandwich Panel Cocure Repair,
EX478/484-2

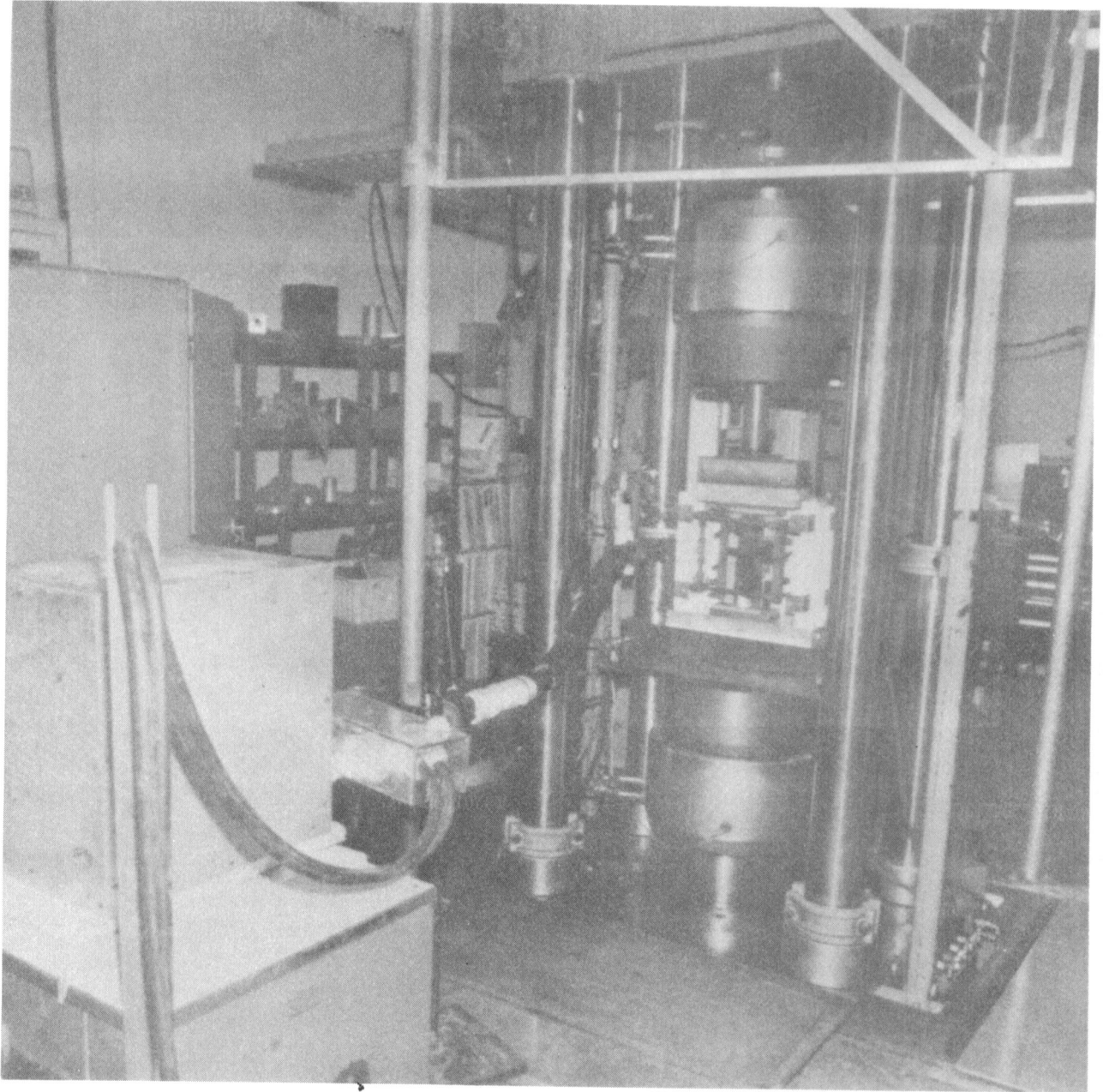


Figure 7-7. Portable Oven, Heat Source, and Controls

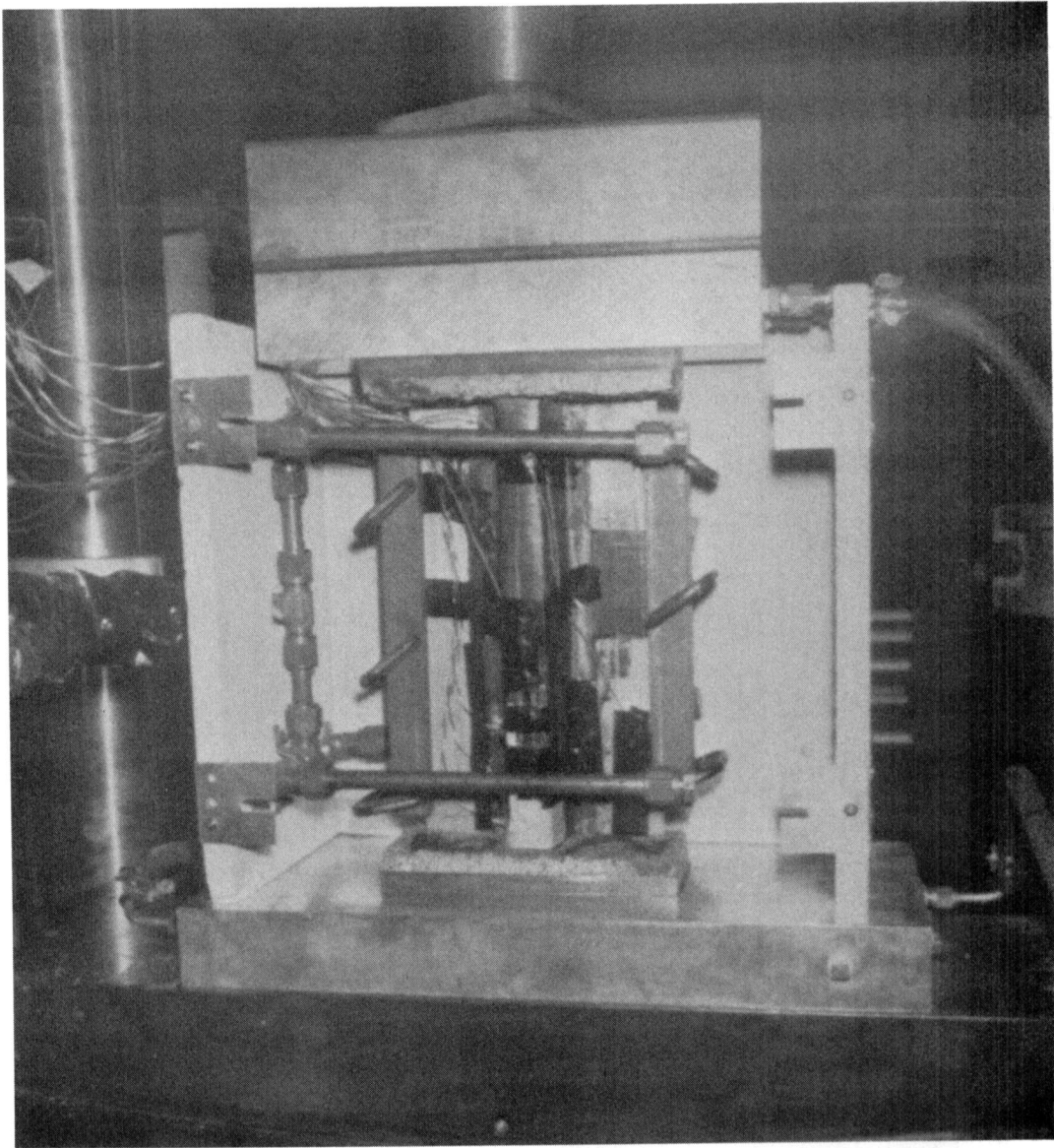


Figure 7-8. Portable Oven Showing Test Hat-Stringer Element and Base Cooling Plate Details in MTS Test Machine

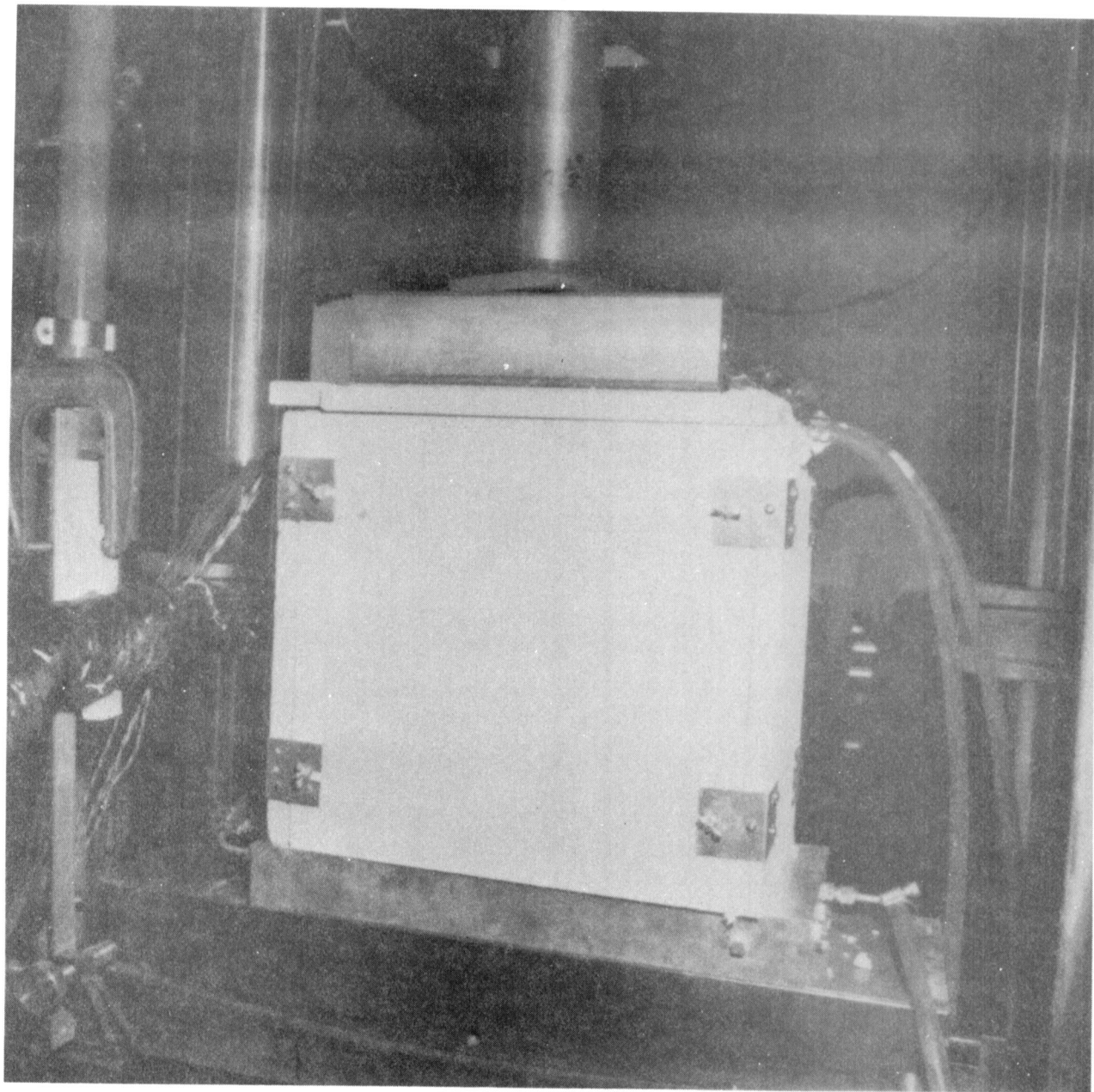


Figure 7-9. Portable Oven in MTS Test Machine in Test Configuration

7.1.3 Heavily Loaded Honeycomb Sandwich Control and Repair Test Methods and Results

The test results for the heavily loaded honeycomb sandwich panels are presented in Table 7-1. Testing was accomplished in a 2,224 KN (500 Kips) MTS closed loop electro-hydraulic test system. Accurate alignment in the test machine was provided by an adjustable spherical seat that supported the specimen during test.

Two control elements with outer 0-degree fibers oriented transverse to compression load were tested at room temperature. Three parallel 0-degree outer fiber control elements were tested: two at room temperature and one at 316°C (600°F). The two transverse-oriented fiber specimens average failure load was 2,026 KN/m (11,650 lb/in.), while one parallel fiber specimen failed at 1,744 KN/m (9,966 lb/in.). The lower ultimate load of this specimen was probably caused by eccentric load introduction, resulting in a failure mode inside one of the base load pads. The other parallel-oriented specimen failed at 1,841 KN/m (10,512 lb/in.). Compression fracture of both faces occurred approximately 2.5 cm (1.0 in.) above the bottom load pads. The 316°C (600°F) tested specimen failed at 1,203 KN/m (6,871 lb/in.) through the center area of both face sheets. Baseline target strength recovery for repair was established by averaging the transverse and parallel-oriented control specimen room temperature strengths, which equalled 1,915 KN/m (10,944 lb/in.). Photographs showing specimens after testing and failure modes are presented in Figures 7-10 and 7-11.

Typical load-strain curves for the undamaged control specimen EX478/484-5 are shown in Figure 7-12. The back-to-back strain rosettes give a baseline for the undamaged laminate behavior. A compression modulus of 46.9 GN/m² (6.8 msi) and a Poisson's ratio of 0.313 for the quasi-isotropic test laminate was obtained from the strain data. Note that the strain plots were cut-off before the ultimate failure load, and thus do not yield ultimate strain-to-failure.

Three control specimens with simulated damage (5.08 cm [2.0 in.] diameter hole) were tested. The two specimens tested at room temperature failed at an average of 53 percent of the undamaged laminate strength. The specimen tested at 316°C (600°F) failed at 47 percent of the undamaged laminate strength. Compression failures occurred simultaneously through the net composite areas on either side of the hole in each skin. Photographs showing typical failure modes are presented in Figure 7-13.

Typical load strain curves for control laminates with 5.08 cm (2 in.) diameter holes are shown in Figures 7-14 and 7-15. Figure 7-14 presents the load strain response of Specimen EX478/484-3, which was tested at room temperature, and Figure 7-15 presents the response of Specimen EX496/494-4, which was tested at 316°C (600°F). The strain distribution around the holes along a horizontal axis through the hole center is presented in Figure 7-16. The stress concentration factors are 2.7 at room temperature, and 3.3 at elevated temperature. This compares to a stress concentration factor of 3.6 for a 5.08 cm (2 in.) diameter hole in the flat laminate test at room temperature (Figure 6-11).

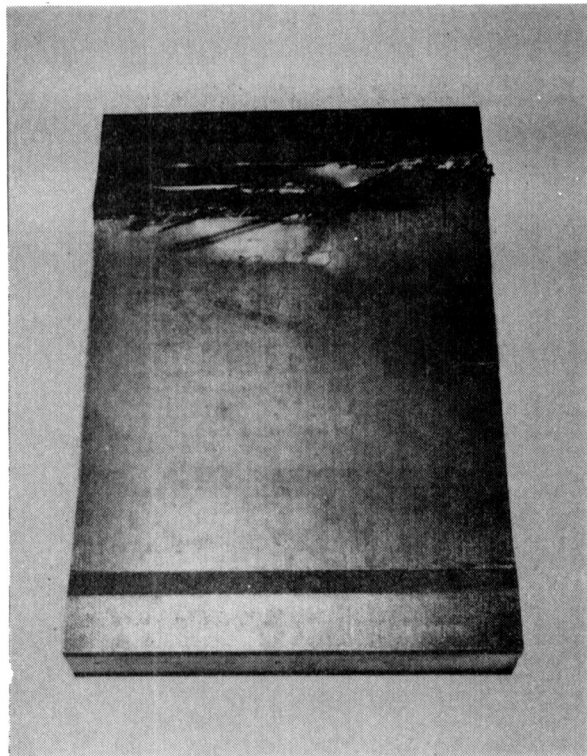
Table 7-1. Test Results for Heavily Loaded Honeycomb Sandwich Control and Repaired Elements

Specimen Configuration		Specimen No.	Skin (2) Orientation	Test Temperature C (F)		Compressive Properties ⁽¹⁾								Repair Efficiency (%)	Δ% of Damaged Specimen	Failure Mode/ Remarks
						Net Section Stress		Total Section Stress		Ultimate Load						
						MN/m ²	(Ksi)	MN/m ²	(Ksi)	KN/m	lbs/in.					
Control	Undamaged	EX482/483-5	Transverse	23	75			443	64.3	2,026	11,576	100% (10,944 lb/inch avg)	190 (Avg of EX478/484-4 and -3 specimens)		Compression failure both skins next to end tab one side, inside end tab other side. Minor skin to core failure.	
		EX482/483-4	Transverse	23	75			449	65.1	2,052	11,723				Compression failure both skins next to end tabs. Minor skin to core failure.	
		EX478/484-6	Parallel	23	75			380	55.1	1,744	9,966				Compression both skins next to end tab one side, inside end tab other side. No skin to core failure. Core shear indicates high loading in one skin.	
		EX478/484-5	Parallel	23	75	--	--	402	58.3	1,841	10,512				Compression failure, both skins 1.0 inch above 2 bottom load pads. No skin to core failure.	
		EX496/494-2	Parallel	316	600	--	--	260	37.7	1,205	6,871				100	212
	2.0 inch diameter hole damaged	EX478/484-4	Parallel	23	75	303	44.0	227	32.9	1,036	5,919	54.1	--		Compression failure both skins through net section.	
		EX478/484-3	Parallel	23	75	284	41.1	211	30.6	977	5,580	51.0	--		Compression net section no debond.	
		EX496/496-4	Parallel	316	600	163	23.7	151	21.9	567	3,239	47.0	--		Compression net section no debond.	
		Repair	Co-cure repair of 2.0 inch diameter hole	EX482/483-3	Transverse	23	75	--	--	371	53.8	1,670	9,544	87.2	166	
EX482/483-1	Transverse			23	75	--	--	315	45.7	1,449	8,282	75.7	144		Shear failure in repair and skin compression under patch.	
EX482/483-2	Transverse			23	75	--	--	380	55.1	1,735	9,914	90.6	172		Compression both skins outside repair with skin to core debond.	
EX478/484-2	Parallel			23	75	--	--	388	56.1	1,724	9,846	90.0	171		Compression inside load tabs, 1 end no bond failure.	
EX478/484-1	Parallel			316	600	--	--	202	29.4	908	5,182	75.4	160		Compression failure 0.75 - 1.00 inch above centerline of repair, one skin only, no bond failures.	

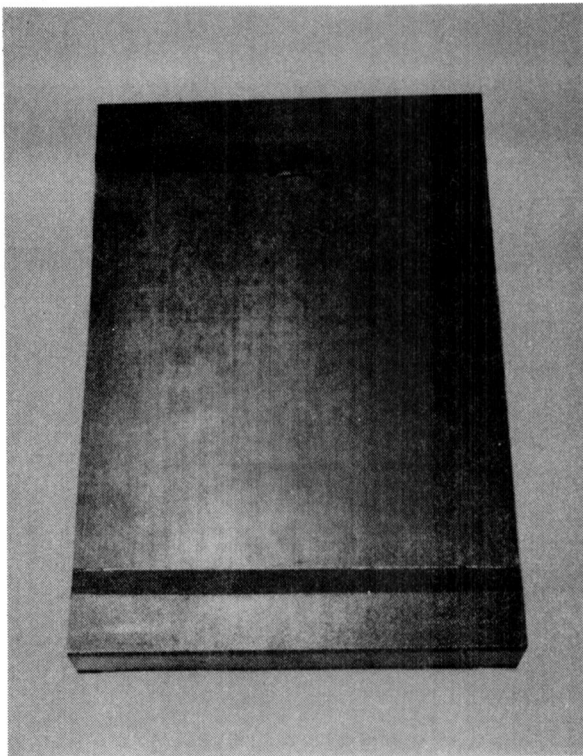
(1) Specimens were tested in a MTS 500 Kips test machine on a spherical adjustable seat after stabilizing at 600 F test temperature for 15 to 30 minutes at a load rate of 30,000 lb/minute.

(2) Skin orientation: (0, ±45, 90)_{2s} 5.7 mils/ply transverse: outer (0) plies transverse to load direction; parallel: outer (0) plies parallel to load direction.

A820129C-11C



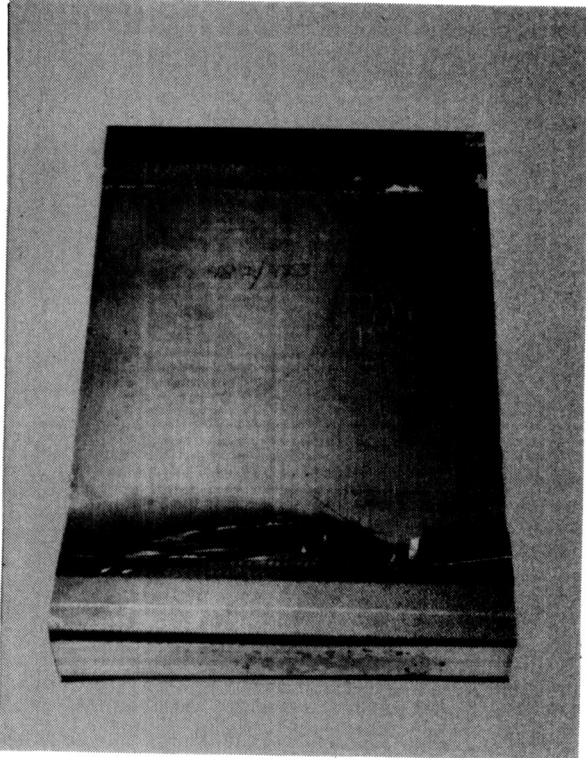
A820129C-12C



FAILURE MODE; SKIN COMPRESSION
ULTIMATE LOAD (LB/INCH): 11,723

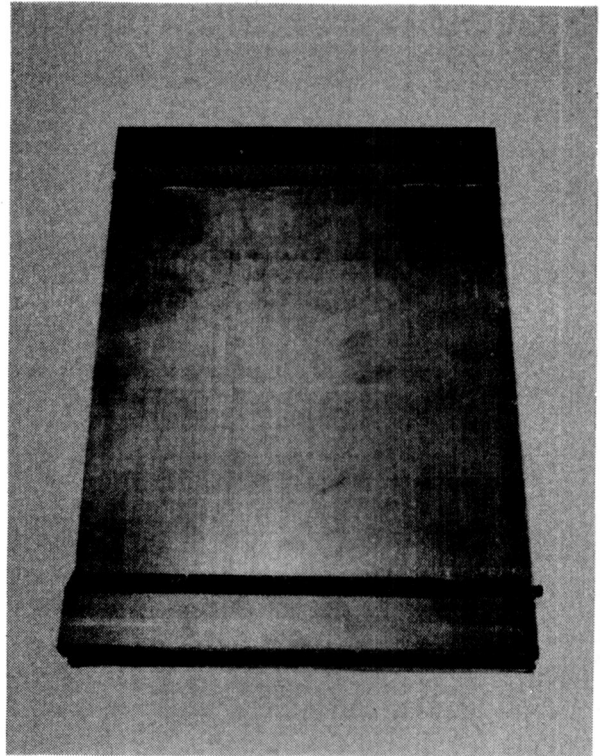
Figure 7-10. Heavily Loaded Sandwich Control Specimen EX482/483-4
(0, ± 45 , 90)_{2s} Transverse-Oriented Outer (0) Fibers--Failure Mode

A820129C-5C



COMPRESSION NEXT TO TAB

A220129C-6C



COMPRESSION INSIDE TAB

ULTIMATE LOAD (LB/INCH): 11,576

Figure 7-11. Heavily Loaded Sandwich Control Specimen EX482/483-5
(0, ± 45 , 90)_{2s} Transverse-Oriented Outer (0) Fibers--Failure Mode

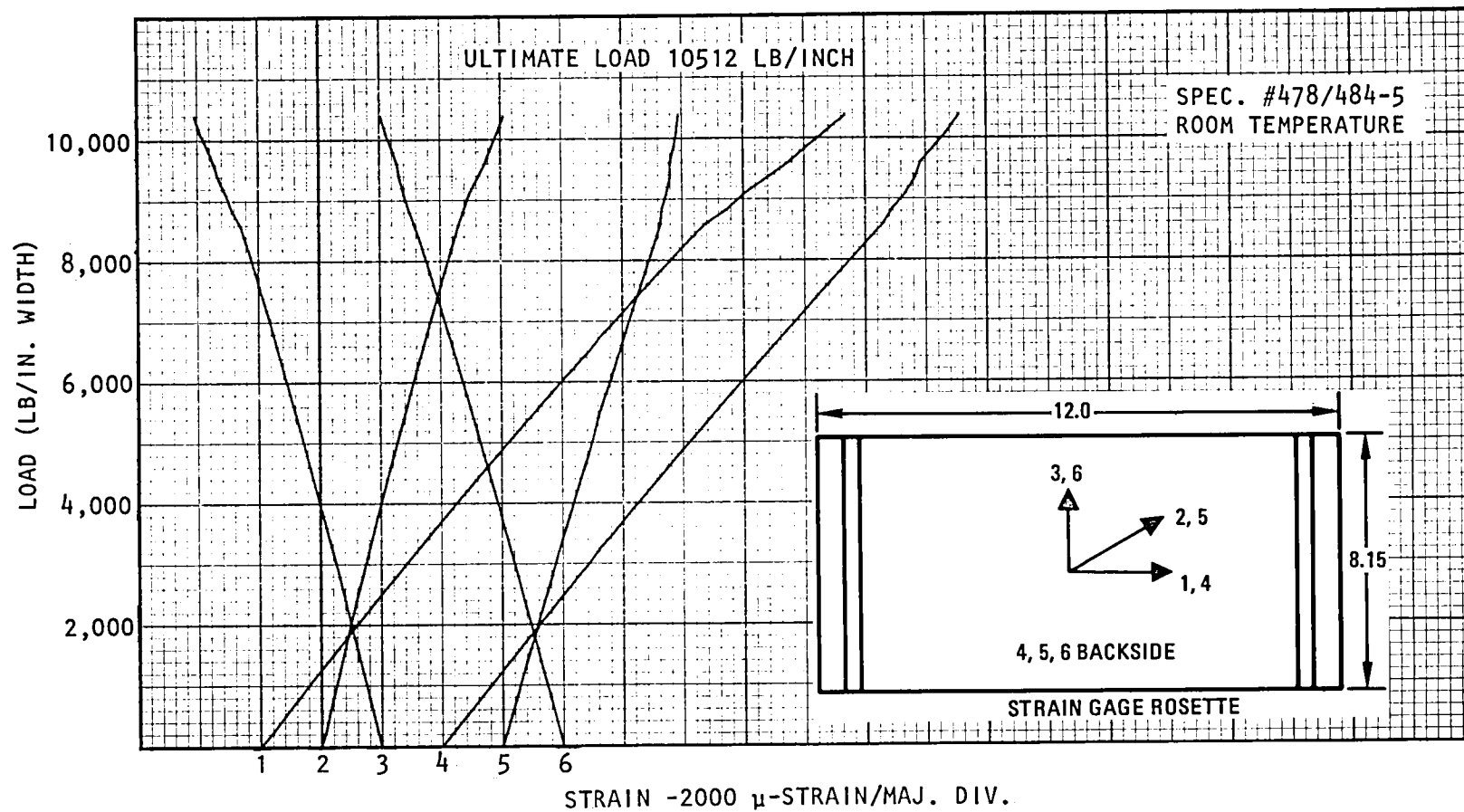
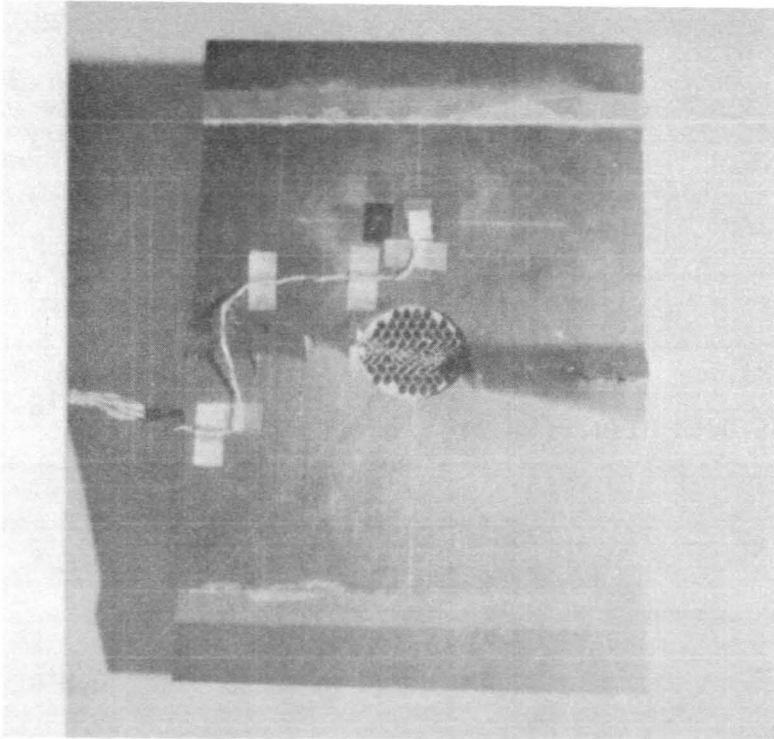
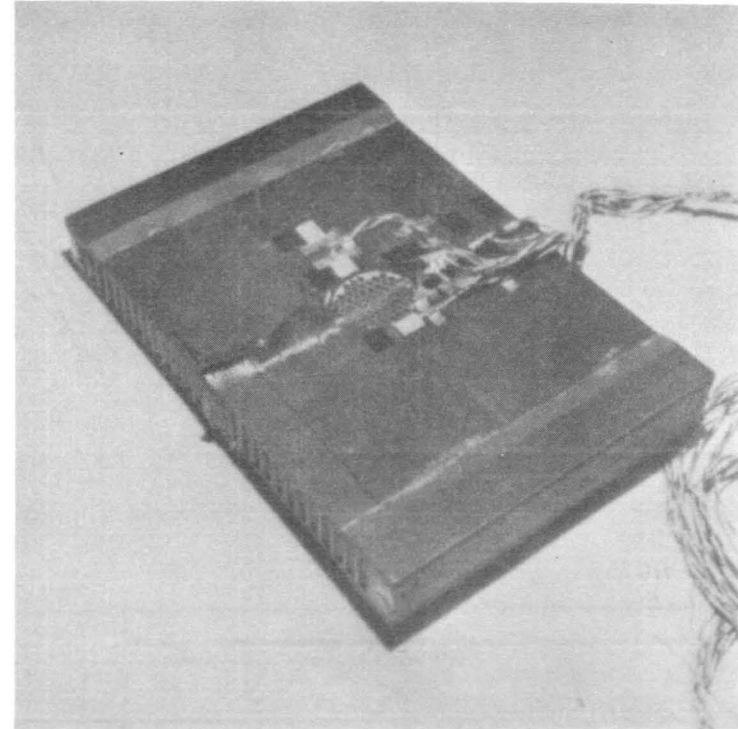


Figure 7-12. Compression Load/Strain Response of Undamaged Control Specimen at Room Temperature, Number 478/484-5

A820402 A-5



A820611 A-9



FAILURE MODE: SKIN COMPRESSION THROUGH NET SECTION
ULTIMATE LOAD, (LB/INCH) 5,580
51% OF CONTROL
SPECIMEN NUMBER, EX478/484-3

Figure 7-13. Heavily Loaded Sandwich Damaged Control Specimen
With 2-Inch Diameter Hole and Parallel Oriented Outer Fibers

81-7

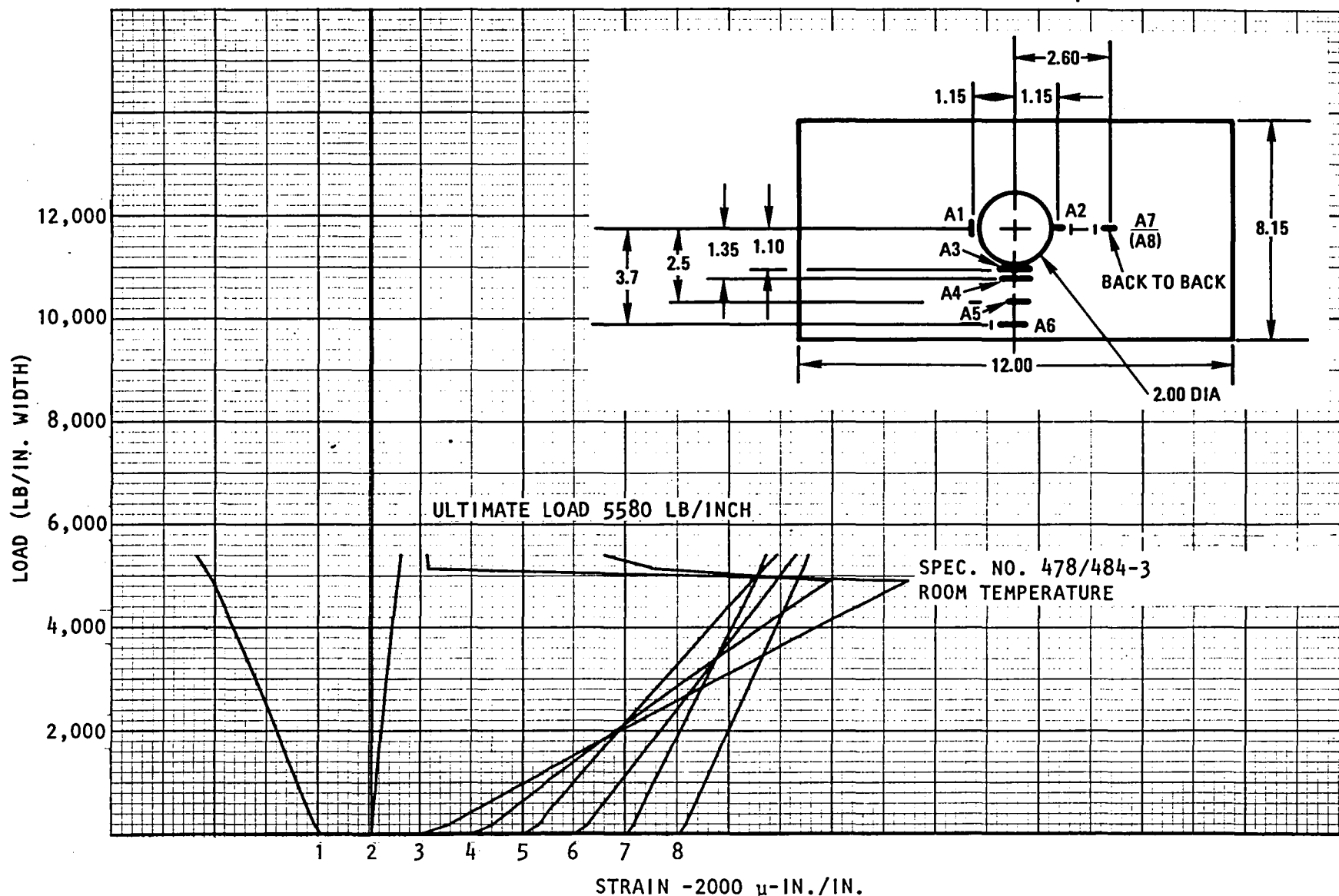


Figure 7-14. Compression Load/Strain Distribution Around 5.08 cm
(2 in.) Diameter Hole at Room Temperature;
Specimen EX478/484-3

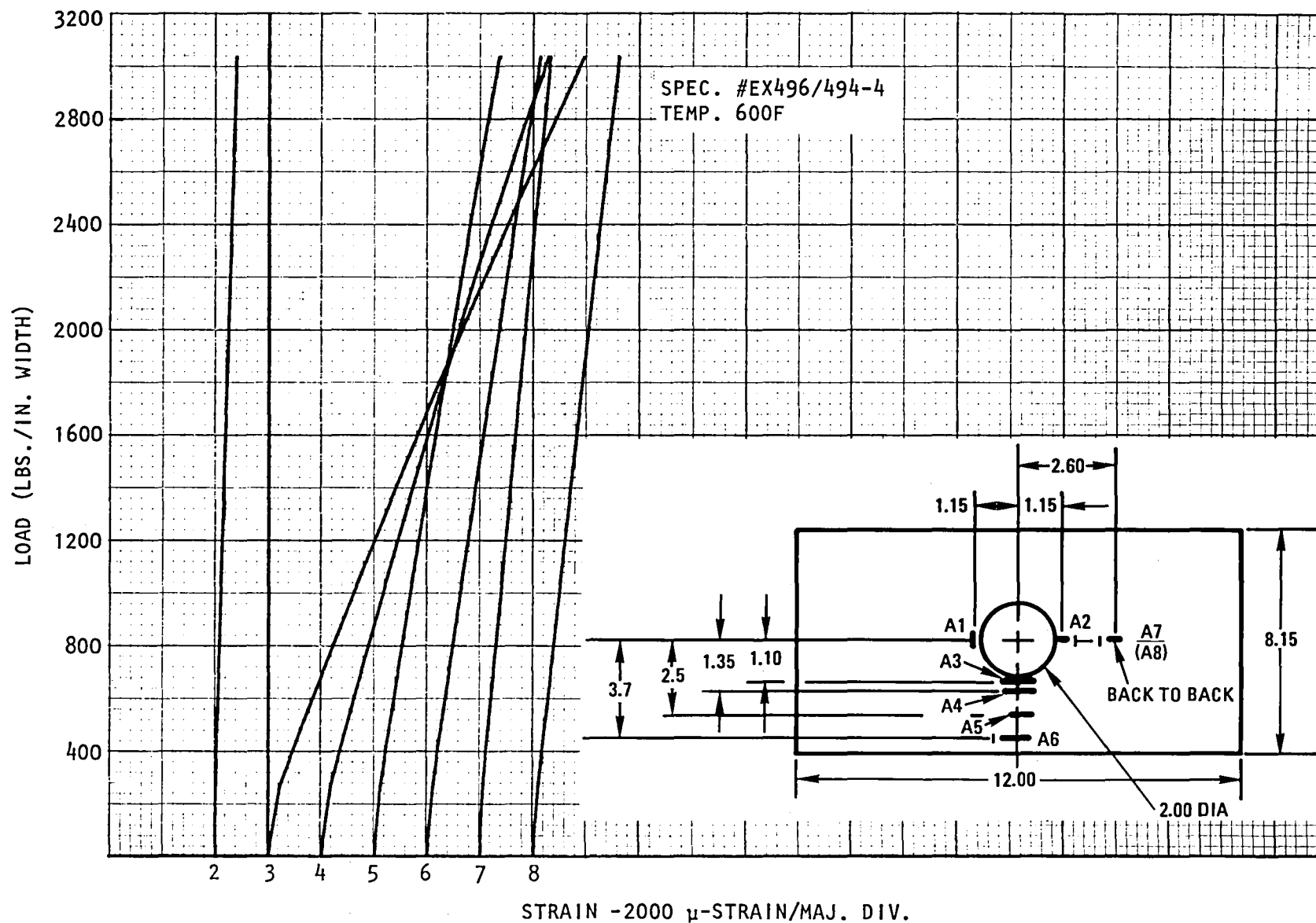


Figure 7-15. Compression Load/Strain Distribution Around 5.08 cm (2.00 in.) Diameter Hole, Specimen EX496/494-4 at 600°F

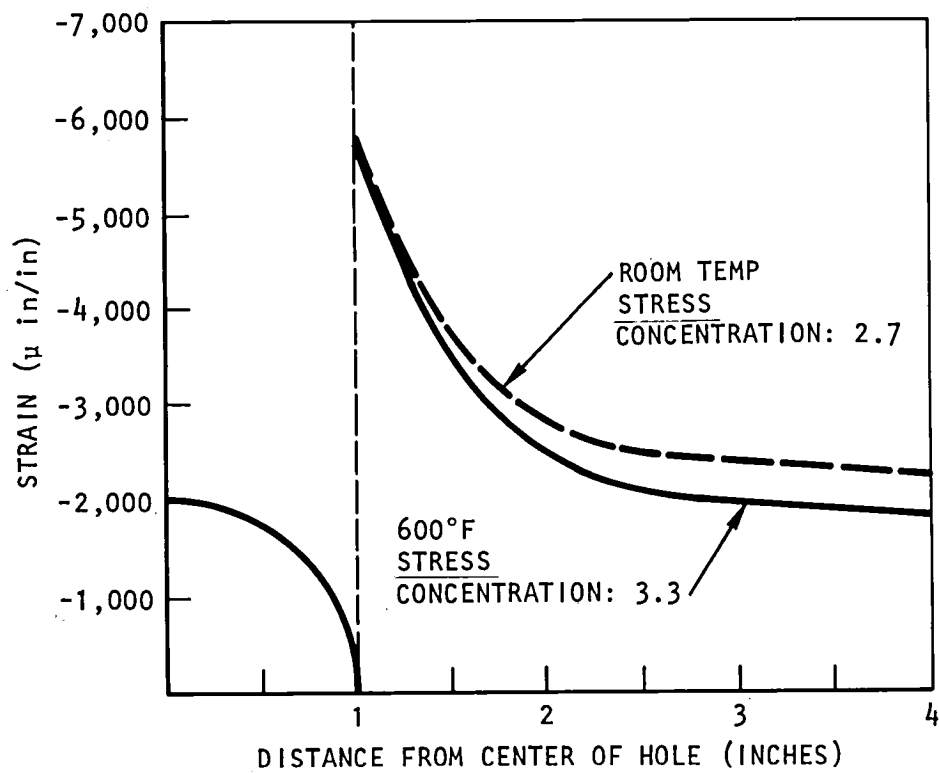


Figure 7-16. Strain Distribution Around 2-Inch Diameter Hole
in Specimens EX478/484-3 and EX496/494-4
(Applied Stress 15 ksi)

Three repaired transverse oriented 0-degree outer fiber specimens were compression tested and joint efficiencies range between 75.7 and 90.6 percent of transverse-oriented fiber undamaged control specimens. Two specimens failed by combined shear-out of the repair patch and compression failure of the repair patch and parent laminate skin. The third and highest load bearing specimen failed by parent laminate skin compression outside the repair area. Photographs showing specimens and modes of failure are presented in Figures 7-17, 7-18, and 7-19.

Two repaired parallel oriented 0-degree outer fiber specimens were compression tested: one each at room temperature and 316°C (600°F). The specimen tested at room temperature failed at 91 percent of the parallel-oriented fiber undamaged control specimens. The specimen tested at elevated temperature, 316°C (600°F), failed at 75 percent of the undamaged control strength. The specimen tested at room temperature failed in the load tabs. The specimen tested at elevated temperature failed through the center of the patch on one skin only as shown in Figure 7-20.

The load-strain response at room temperature and 316°C (600°F) of the repaired heavily loaded honeycomb sandwich panels is presented in Figure 7-21. The repair greatly relieves the stress concentration around the hole, as can be seen by comparison with Figures 7-14 and 7-15. The initial response of the strain gages at 316°C (600°F) is nearly identical to that at room temperature, indicating no reduction in elastic modulus; however, the elevated temperature strength is half the room temperature value.

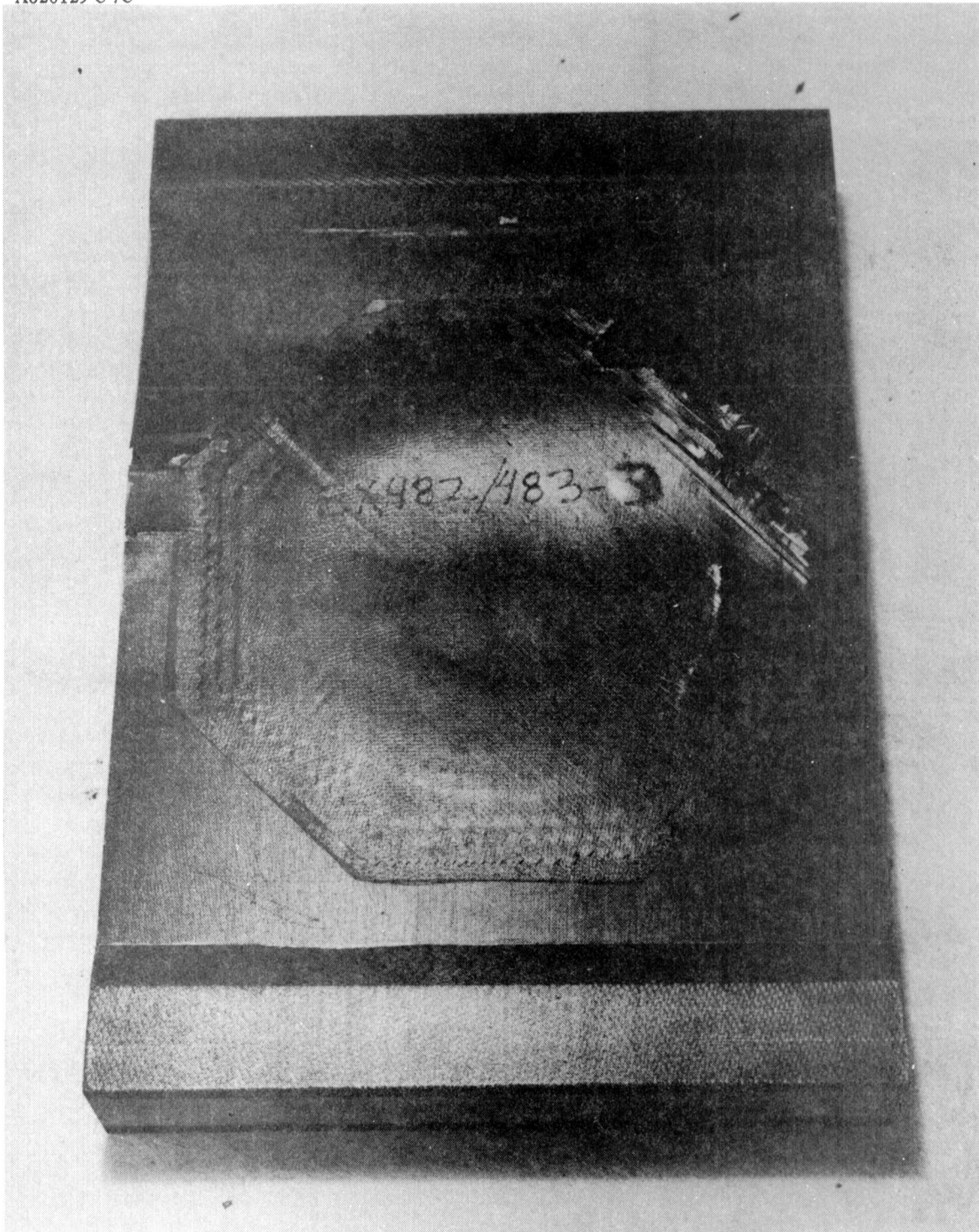
7.1.4 Conclusions - Heavily Loaded Honeycomb Sandwich Repair

A 5.08 cm (2 in.) diameter hole was found to reduce the test specimen strength to 53 percent and 47 percent of the undamaged value at room temperature and 316°C (600°F), respectively. The repairs returned the damaged specimens to 75 to 91 percent of the undamaged strength. Elevated temperature, 316°C (600°F) greatly reduced the strength of the compression test specimens: undamaged strength was 63 percent of room temperature undamaged value; damaged strength, was 56 percent of room temperature damaged value, and repair strength, was 55 percent of room temperature repair value.

7.2 LIGHTLY LOADED HONEYCOMB SANDWICH REPAIR

The Rockwell baseline honeycomb sandwich repair program involved testing of three types of specimens: undamaged control laminates, damaged control laminates with a 5.08 cm (2 in.) diameter hole, and repaired specimens. The undamaged test specimens were designed to carry 0.53 MN/m (3,000 lb/in.). The damaged specimens were expected to fail at 50 percent of the undamaged strength based on the results of the heavily loaded sandwich specimens discussed in the previous paragraphs. The repairs were expected to return 90 percent of the undamaged laminate strength.

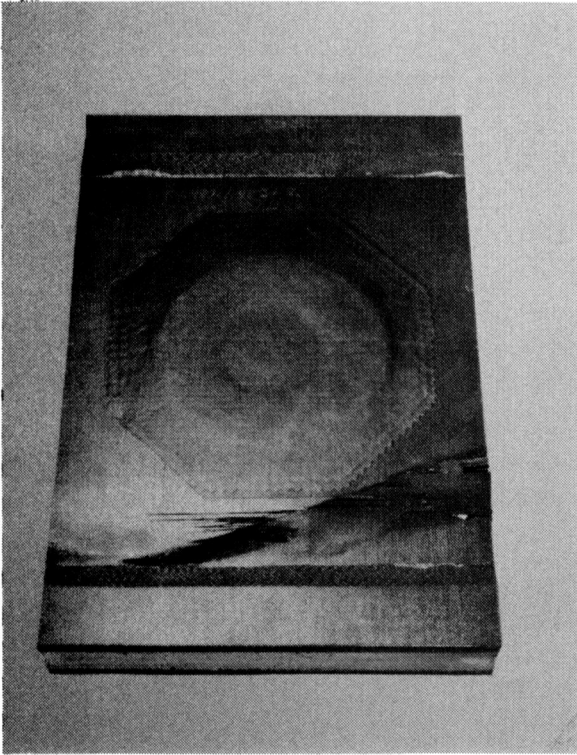
The test element design is presented in Figure 7-1, and consists of 8-ply (0, ±45, 90)_s face sheets on 4.7 cm (1.85 in.) thick glass/polyimide honeycomb core with a nominal density of 57.7 g/m³ (3.6 pcf). The repair designs are



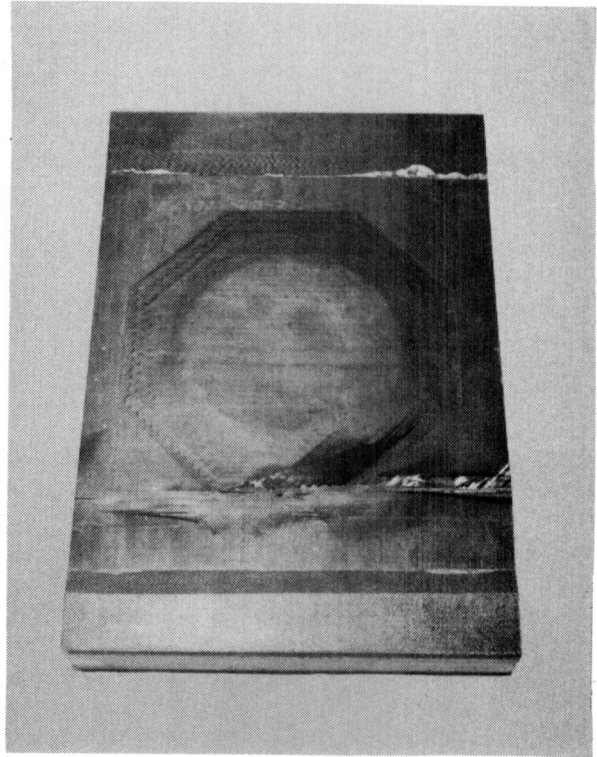
FAILURE MODE: SHEAR FAILURE & SKIN COMPRESSION
ULTIMATE LOAD (LB/INCH): 9,544
81.9% OF CONTROL

Figure 7-17. Heavily Loaded Sandwich Specimen Repair,
EX482/483-3 (0, ± 45 , 90)_{2s} Transverse-Oriented
Outer (0) Fibers--Failure Mode

A820129C-9C



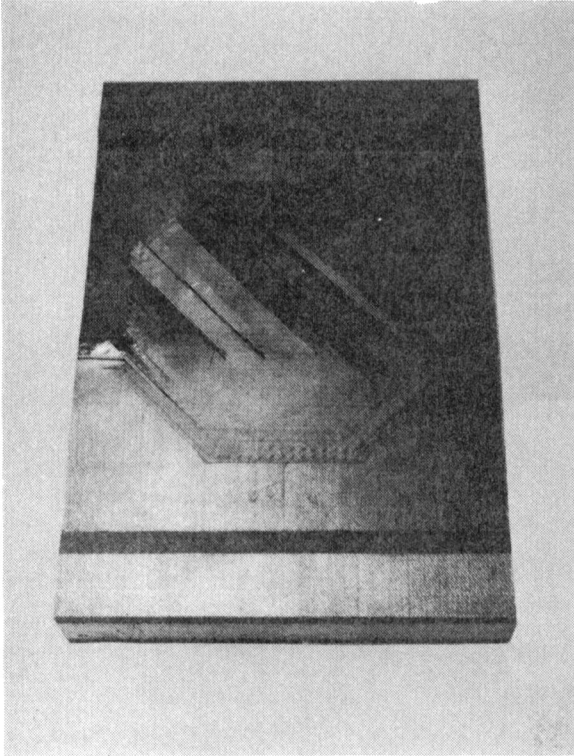
A820129C-10C



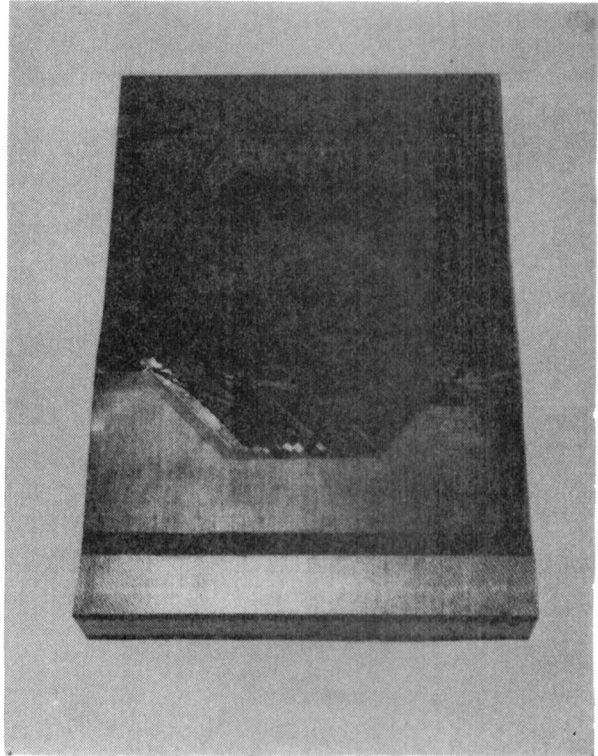
FAILURE MODE: SKIN COMPRESSION OUTSIDE PATCH
ULTIMATE LOAD (LB/INCH) 9,914
85.1% OF CONTROL

Figure 7-18. Heavily Loaded Sandwich Specimen Repair,
EX482/483-2 (0, ± 45 , 90)_{2s} Transverse-Oriented
Outer (0) Fibers--Failure Mode

A820129C-13C



A820129C-14C



FAILURE MODE: SHEAR FAILURE UNDER PATCH AND SKIN COMPRESSION,
ULTIMATE LOAD (LB/INCH): 8,282
71.1% OF CONTROL

Figure 7-19. Heavily Loaded Sandwich Specimen Repair, EX483/483-1
(0, ± 45 , 90)_{2s} Transverse-Oriented Outer (0) Fibers--
Failure Mode; 316°C (600°F) Test

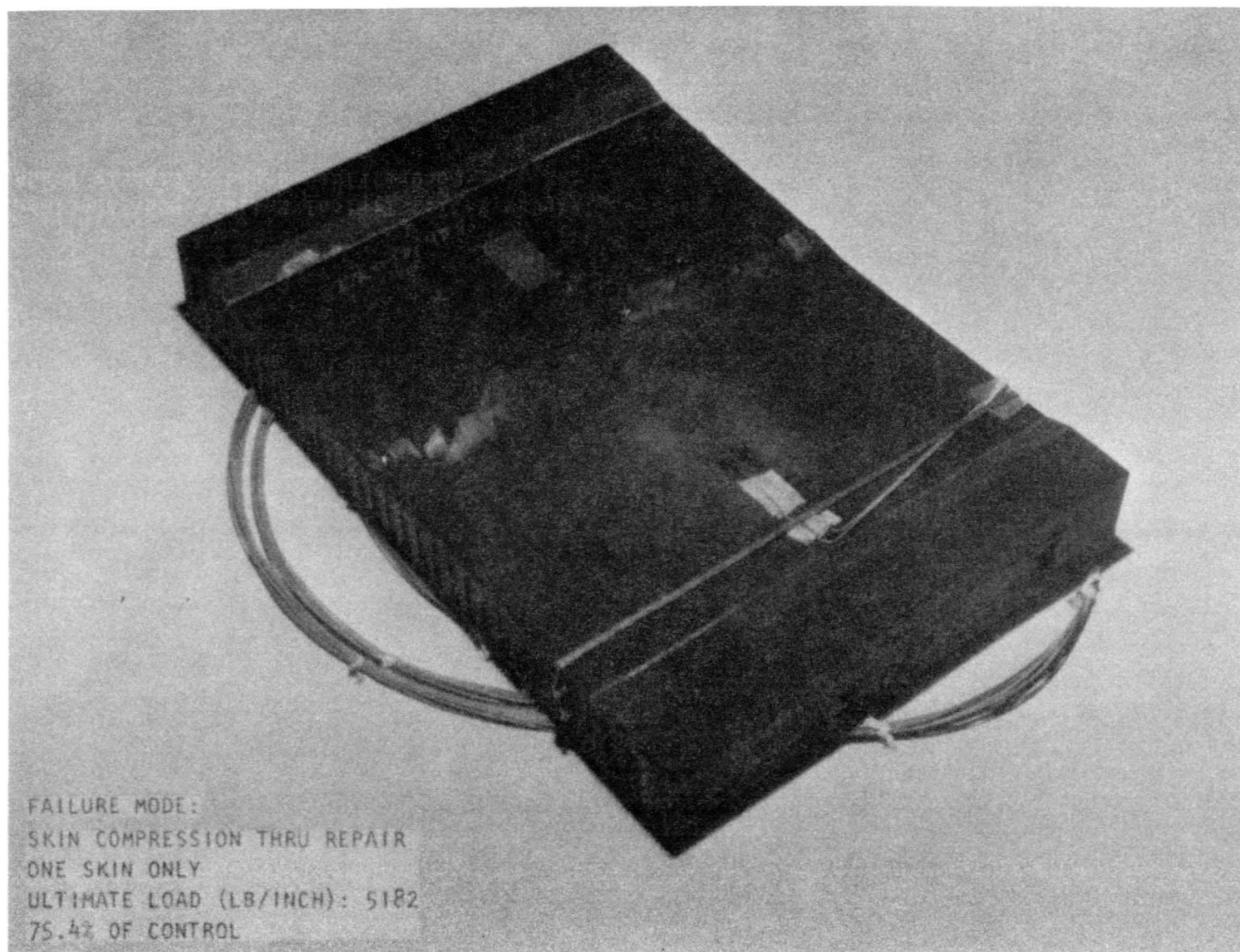


Figure 7-20. Heavily Loaded Sandwich Specimen Repair EX478/484-1--Failure Mode

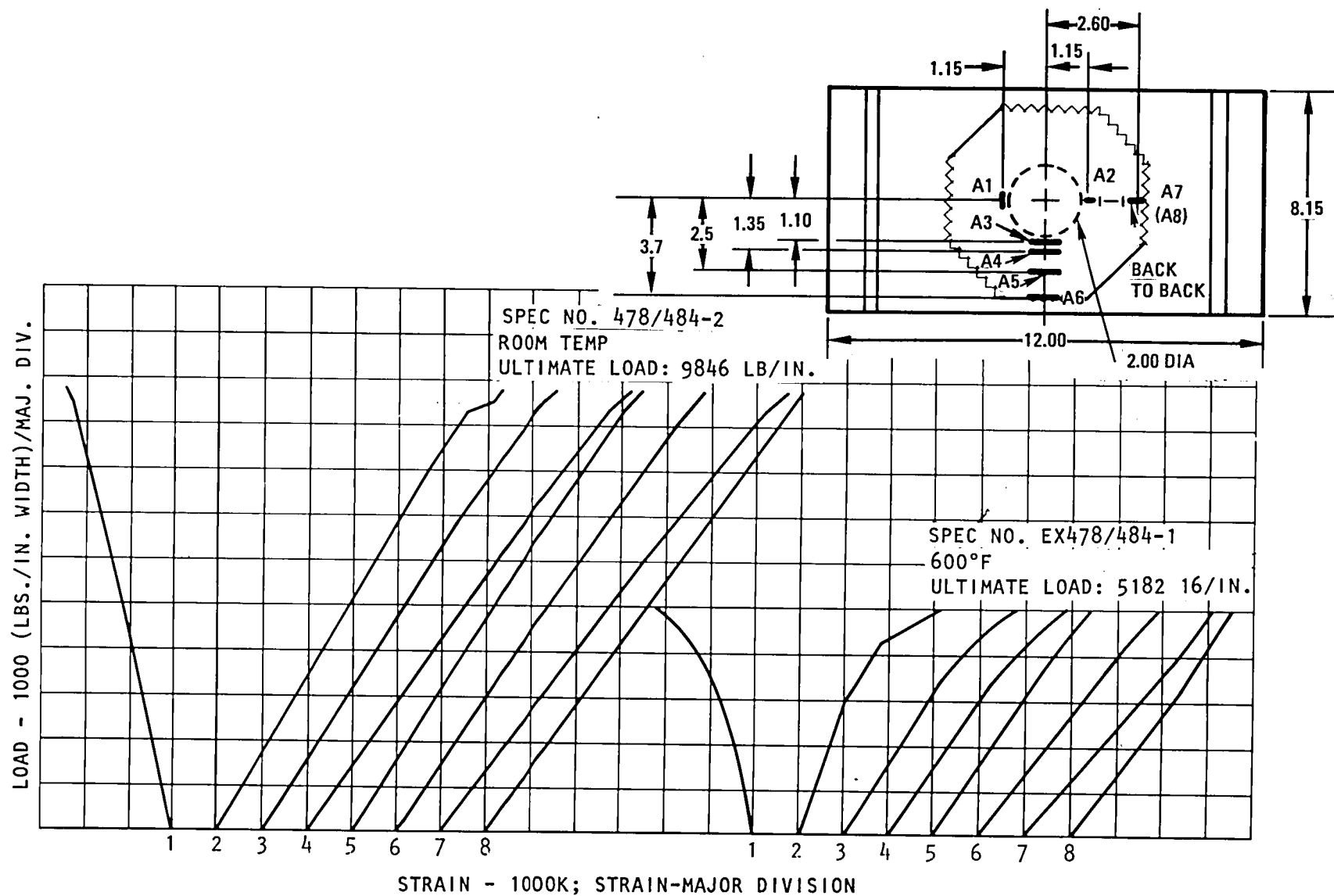


Figure 7-21. Strain Response of Repaired Heavily Loaded Sandwich Specimens at Room Temperature and 600°F

presented in Figures 7-22 and 7-23. The first design is for a secondarily bonded external patch. The second design is a cocure repair similar to that used on the heavily loaded sandwich panels.

7.2.1 Baseline Element Fabrication and Prototype Repair

Control elements, undamaged and with 5.08 cm (2.0 in.) holes, simulating in-service damage areas through both skins were fabricated using standard processes, as per the design of Figure 7-1.

A small prototype sandwich panel of the same cross-section as the baseline elements was repaired per the cocure design shown in Figure 7-22. During the 228°C (550°F) 1,328 KN/m² (200 psi) cure cycle, the HRH 327-3/16 - 3.5 pcf honeycomb core was severely crushed. The repair installations were of excellent aesthetic quality. Core crushing was not expected since data show the stabilized core compression allowable to be 1,708 KN/m² (248 psi) at 288°C (550°F).

7.2.2 Maximum Allowable Bonding Pressure Study

Small sandwich panels comprised of the materials and made by processes employed in fabrication of the baseline compression specimen design were subjected to autoclave curing pressures of 1,033, 689, 517, and 345 KN/m² (150, 100, 75, and 50 psi). Sandwich panels were subjected to these pressures digressively to determine the maximum pressure levels that could be used in either cocure or secondary bonding repair operations at the required minimum 288°C (550°F) curing temperature without crushing or damaging the 3.5 pcf core. These tests proved the maximum allowable curing pressure possible is between 689 and 517 KN/m² (<100 and 75 psi), since elements subjected to pressures of 1,033 and 689 KN/m² (150 and 100 psi) also resulted in crushed cores. The 517 KN/m² (75 psi) pressure had no apparent affect on the core. Concurrently with sandwich isostatic flatwise compression testing, 17.78 by 17.78 by 0.16 cm (7 by 7 by 0.065 in.) midplane single-stage, in-situ imidized, and cocure bonded and secondary bonded panels were made to evaluate the effects of reduced pressure levels on bondline and laminate quality. Results of this study are discussed in Section 4.8.

7.2.3 Low Pressure Secondary Bond Repair of Sandwich Panels

The 35 by 34, 5-harness satin weave Celion/LARC 160 prepreg adhesive system was selected for secondary bonding repair of a lightly loaded sandwich element, based on lap shear and scarf angle shear test results, as discussed in Section 4.8, Table 4-7. Secondary bonding was accomplished per the standard cure cycle described for midplane bonded panels in Table 4-1, except only 517 KN/m² (75 psi) pressure and 288°C (550°F) temperature was used. Initial prototype sandwich panel repairs were made on (0, ±45, 90)_s skins with the outer zero plies oriented 90 degrees to the load direction using the tooling arrangement, shown in Figure 7-24. The transverse fiber loading configuration was evaluated for two reasons in the prototype repair development phase: to develop and evaluate repair application techniques on sandwich panel stock that

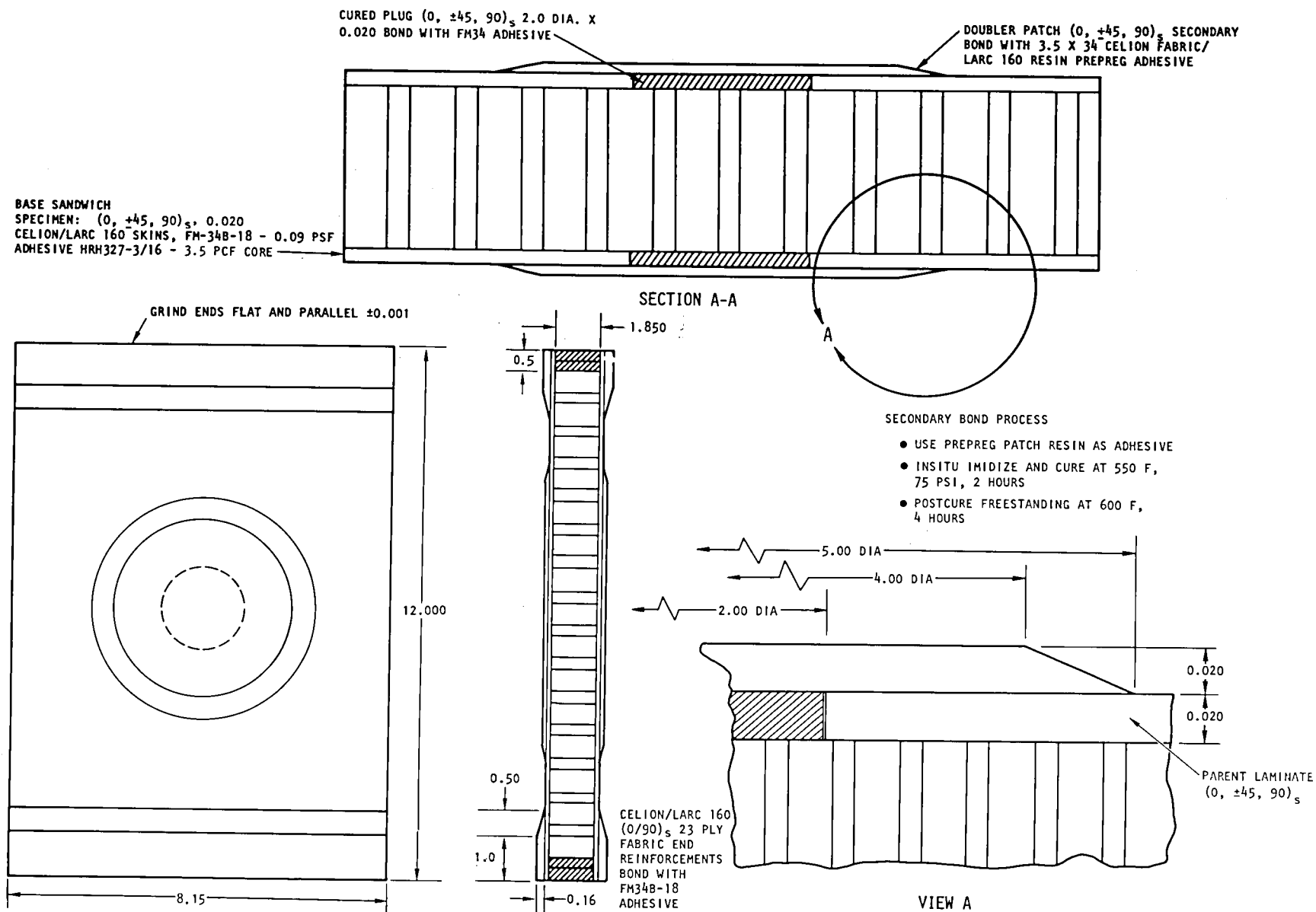


Figure 7-22. Secondary Bond Repair, Lightly Loaded Sandwich Structure Compression Element Design Concept

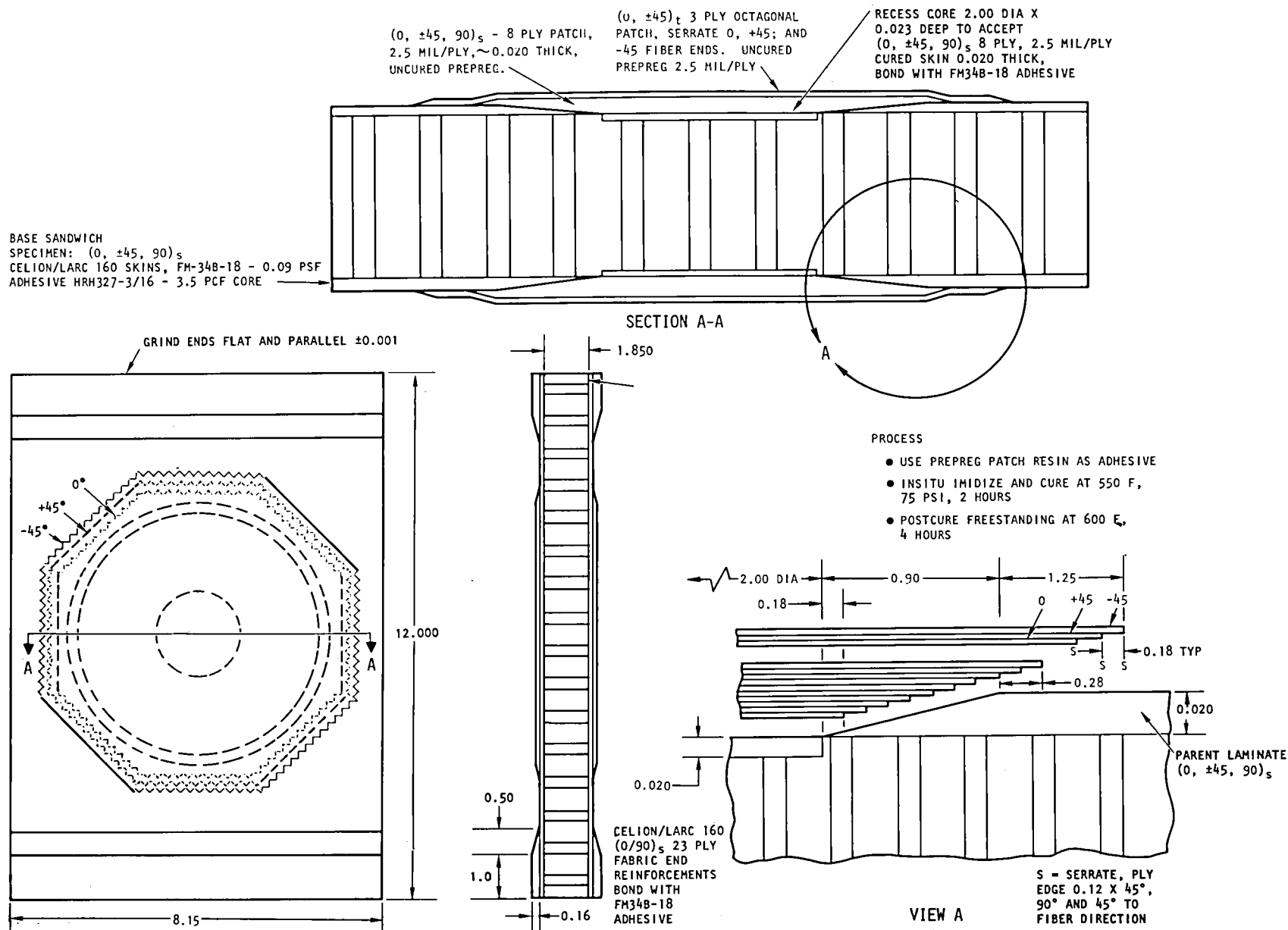


Figure 7-23. Cocure Repair, Lightly Loaded Sandwich Structure Compression Element Design Concept

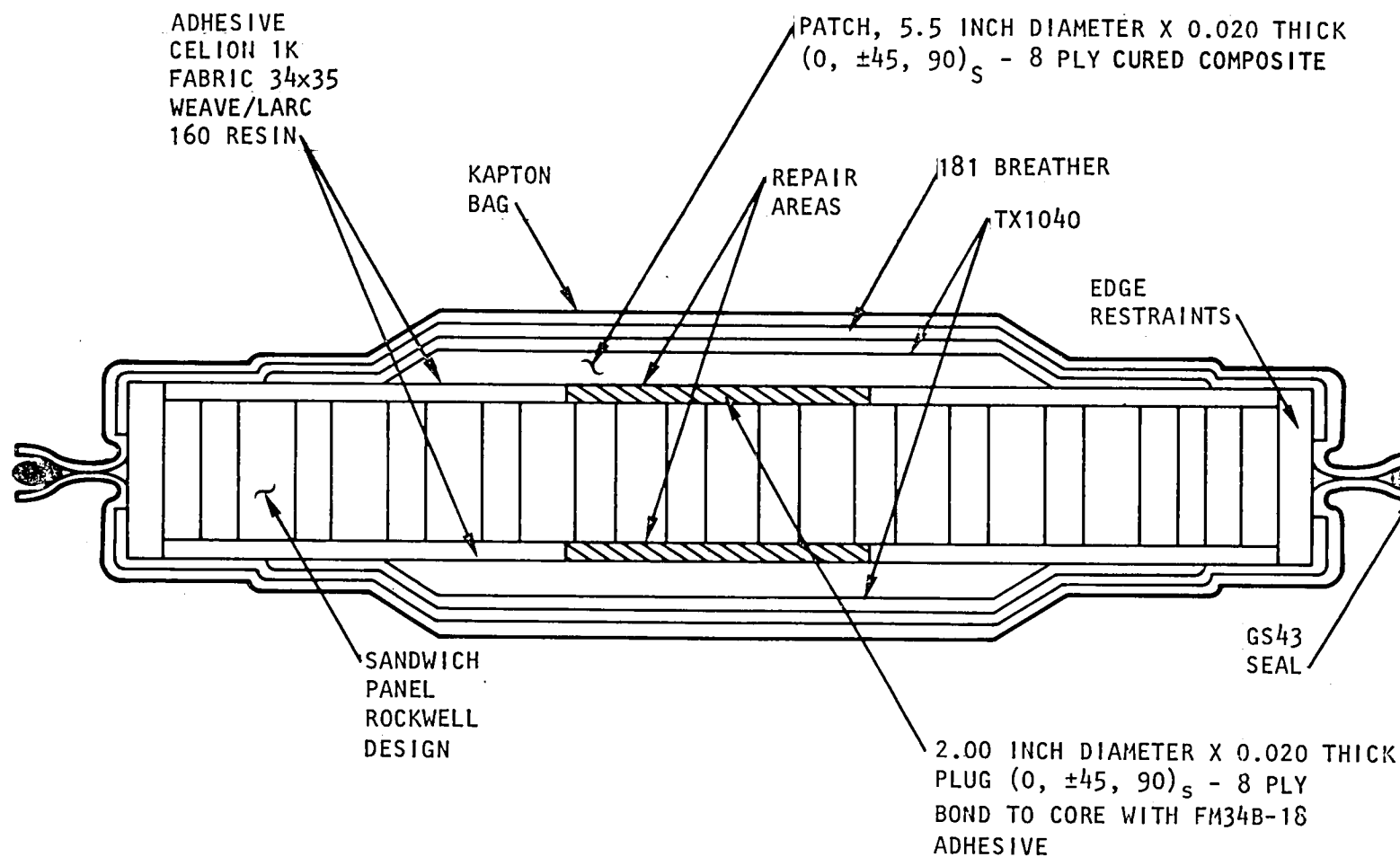


Figure 7-24. Secondary Bond Sandwich Repair Application
Technique - Lightly Loaded Design

would otherwise not be utilized because of waste from overall panel configuration, and to evaluate load transfer characteristics of the repair into the 0-degree transverse-oriented plies of the baseline element (worst case condition).

There were no core crushing or other problems during the 517 KN/m² (75 psi) 288°C (550°F) secondary bonding repair process; however, NDI C-scan recordings showed bondline void areas in approximately 50 percent of both patch areas.

7.2.3.1 Low Pressure Cocure Bonding Repair of Sandwich Panels. The prepreg resin, in-situ imidizing cocure process was used to repair two prototype sandwich elements, as described for heavily loaded elements and as shown in the design Figure 7-23. The repair tooling arrangement is typical to that used in repair of heavily loaded design elements, Figure 7-3.

One element was repaired with skin 0-degree outer plies oriented parallel to the load direction, and one was repaired with 0-degree plies transverse to load direction. There were no problems observed in cocure repair operations. Visually, the skin patches appeared well compacted and had high aesthetic quality; however, NDI C-scan recordings showed a high porosity condition through the 5.08 cm (2.0 in.) center section of the repair and satisfactory condition outside the center section.

7.2.4 Repair Process Selection

Both secondary and cocure low pressure 517 KN/m² (75 psi) bonding processes resulted in random voids in bond lines and cocured laminates. Further process development in modifying cure cycles and/or adhesive systems is required to alleviate the void problems. Although repair patch areas showed significant void inclusions in C-scan recordings, the repair installations did not fail in prototype room temperature compression tests (refer to Section 7.3, Table 7-3); therefore, the repair designs and low pressure processing techniques are considered adequate for the lightly loaded sandwich elements until optimized processing techniques can be achieved. The cocure process has advantages over the secondary bonding process since fit-up problems that would occur with cured laminate patches are eliminated; therefore, the cocure process, as per the design of Figure 7-22, was selected as the best technique for repair of lightly loaded sandwich elements.

7.3 LIGHTLY LOADED HONEYCOMB SANDWICH REPAIR TESTING AND RESULTS

7.3.1 Compression Testing

Control repair elements were compression tested at room temperature and 316°C (600°F) using the same MTS test setup described for heavily loaded honeycomb sandwich design elements. Typical control and repaired specimens were instrumented with strain gages to establish load/strain distribution through parent laminate, around simulated damaged areas and load transfer characteristics into the repair installation. Strain gage installation layouts are presented in Figures 7-25 and 7-26. Specimens were tested at a load rate of 54 KN (12,500 lb) per minute.

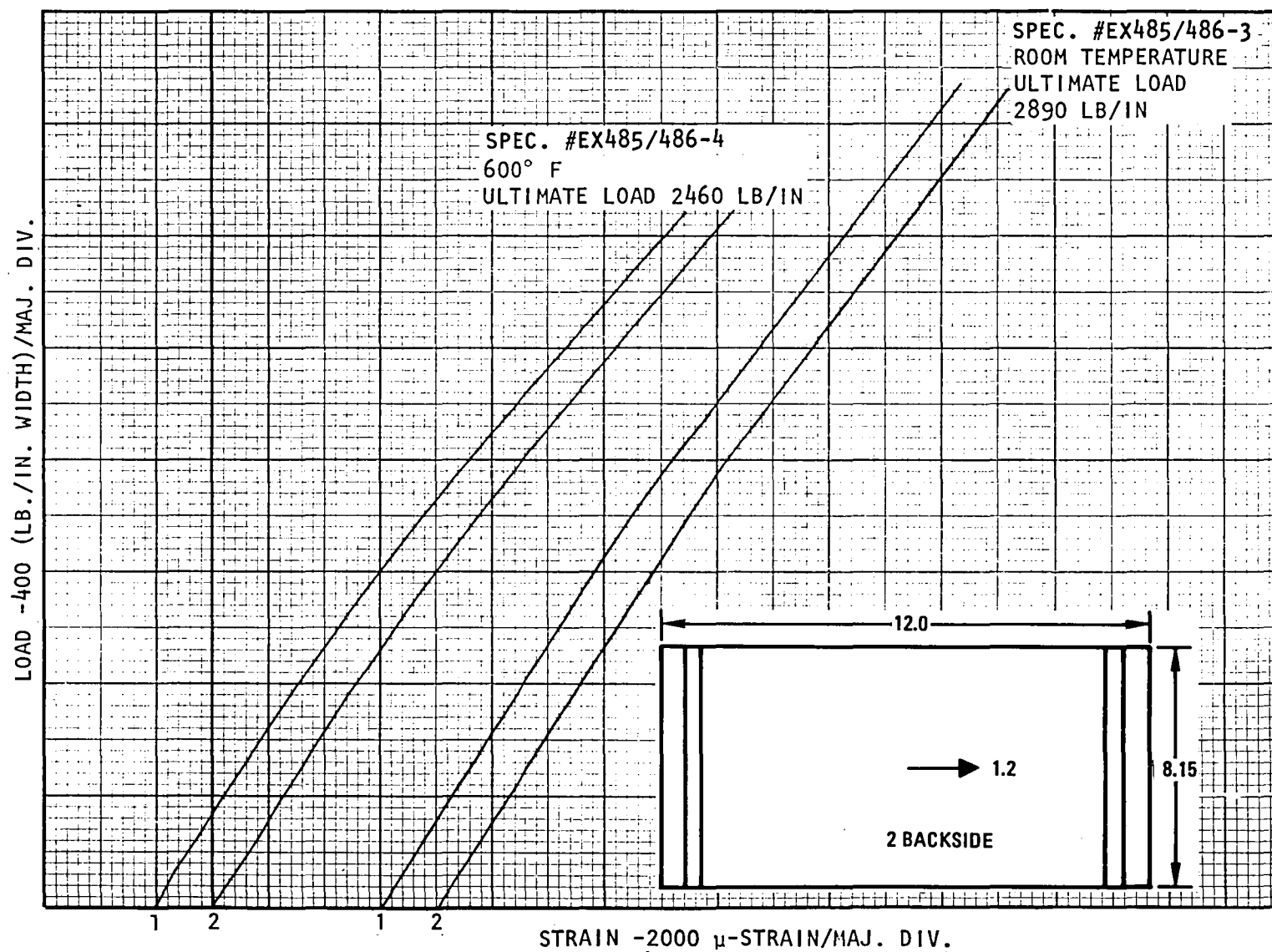


Figure 7-25. Compression Load/Strain Response of Lightly Loaded Sandwich Panels (Undamaged Control) at Room Temperature and 600°F

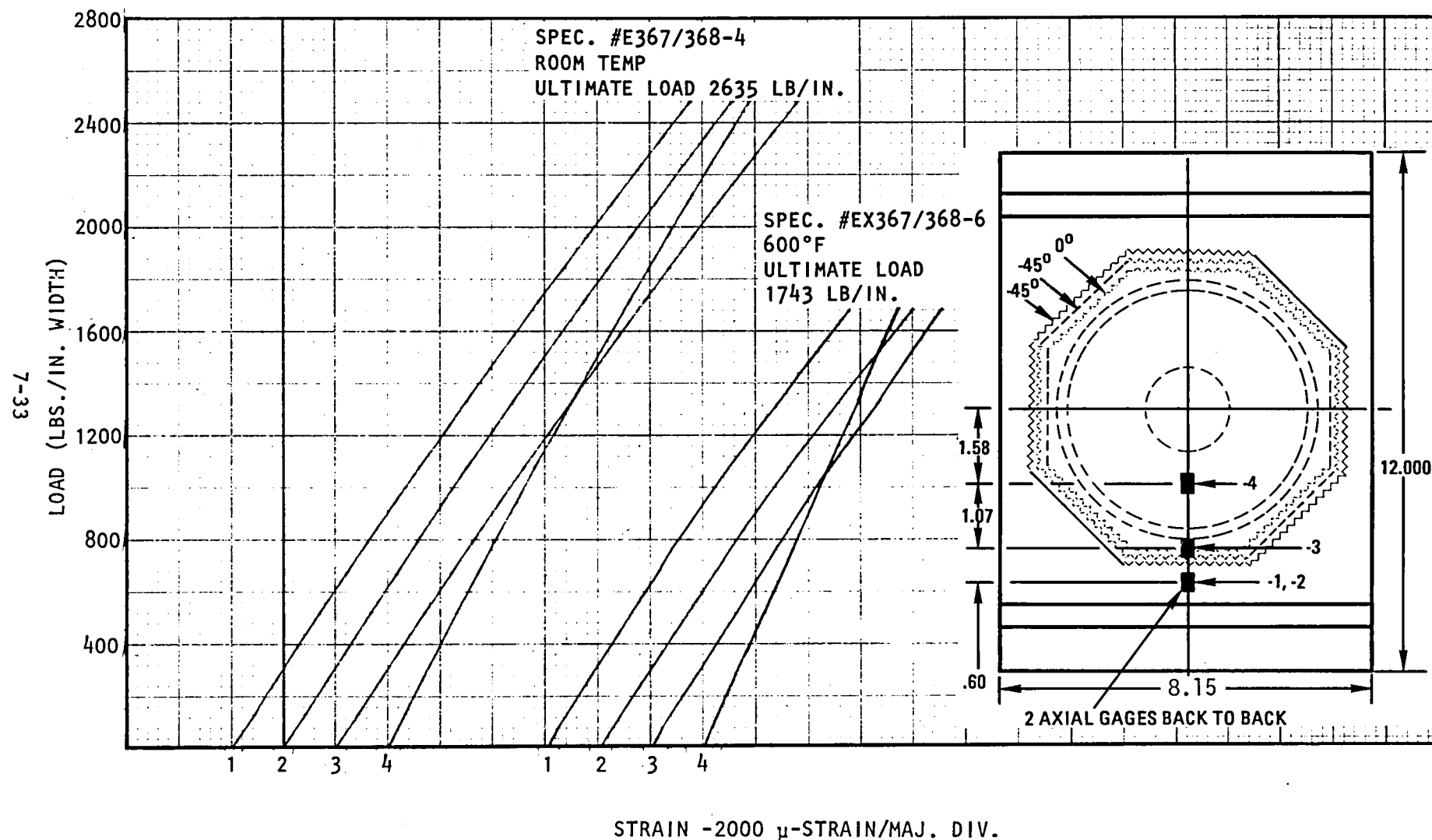


Figure 7-26. Strain Response of Cocure Repaired Lightly Loaded Sandwich Panels at Room Temperature and 600°F

7.3.2 Control Element Results

The test results for the lightly loaded honeycomb sandwich panels are presented in Table 7-2. One undamaged control specimen was tested at room temperature, and one at 316°C (600°F). The room temperature strength was 306 kN/m (2,892 lb/in.) or 96.5 percent of the target design strength. The elevated temperature strength was 85 percent of the room temperature strength. A photograph showing the failure mode of the specimen tested at room temperature is presented in Figure 7-27. Note the combined 45- and 90-degree compression fractures. The specimen tested at elevated temperature failed in a similar manner. The load-strain response for these undamaged control specimens is presented in Figure 7-25. A compression modulus of 49.6 GN/m² (7.2 msi) at room temperature, and 46.2 GN/m² (6.7 msi) at 316°C (600°F) was obtained from the strain gage data.

Next, a specimen with a 5.08 cm (2 in.) diameter hole was tested to determine the amount of strength reduction associated with a hole. This specimen failed at 51.5 percent of the undamaged strength. The failure mode can be seen in Figure 7-28. The specimen had no strain gages.

7.3.3 Repaired Element Results

The failure mode for secondarily bonded repair specimen EX485/486-1T, is shown in Figure 7-29. The specimen failed in face sheet compression near the load tabs. There was no bond or repair failure, but the specimen failed at 75 percent of the undamaged strength.

Four cocure flush repairs were tested, three at room temperature and one at 316°C (600°F). Two of the specimens tested at room temperature failed near the load tabs as shown in Figure 7-30. One of the specimens tested at room temperature, and the specimen tested at elevated temperature failed in the repair area, as shown in Figure 7-31. The failure was by compression and interlaminar delamination. There was no bond failure. The repaired specimens tested at room temperature failed at 82 to 102 percent of the undamaged strength. The repaired specimen tested at 316°C (600°F) failed at 70 percent of the elevated temperature undamaged strength.

Typical load-strain response at room temperature and 316°C (600°F) of the cocure repaired lightly loaded honeycomb sandwich panels is presented in Figure 7-26. The strain distribution along the patch is relatively uniform. Strain gages 1, 2, and 3 have nearly identical strain levels, with gage 4 somewhat lower. The initial response of the strain gages at 316°C (600°F) is nearly identical that at room temperature, which indicates no reduction in elastic modulus; however, the elevated temperature strength is 66 percent of the room temperature value.

Specimen Configuration		Specimen No.	Skin (2) Orientation to Load Direction	Test Temperature C (F)		Compressive Properties ⁽¹⁾								ΔZ of Damaged Specimen	Failure Mode/Remarks
						Net Section Stress		Total Section Stress		Ultimate Load		Repair Efficiency (%)			
						MN/m ²	(Ksi)	MN/m ²	(Ksi)	KN/m	lbs/in.				
Control	Undamaged	EX485/486-3P	Parallel	23	75	-	-	476	69.1	507	2,892	100	194	Combined 45° and 90° compression fractures through center of panel and along load tab/skin interface with core crushing. No bond failures.	
		EX485/486-4P	Parallel	316	600	-	-	405	58.8	431	2,461	100	-	Combined 45° and 90° compression fractures through center of panel and along load tab/skin interface with core crushing. No bond failures.	
	2.0 in. Dia. Hole Damaged	EX485/486-2T	Transverse	23	75	325	47.3	-	-	261	1,489	51.5	100	Skin compression through net section	
Repair	Co-Cure Repair	EX485/486-2P	Parallel	23	75	-	-	487	70.7	519	2,960	102	198	Compression, one face along load tab, other face 45° compression fracture starting at load tab. No repair or bond failures.	
		EX485/486-3T	Transverse	23	75	-	-	390	56.6	418	2,384	82.4	160	Compression fractures both faces at load tabs and local core crush, no bond or repair failure.	
	Secondary Bond Repair	EX485/486-1T	Transverse	23	75	-	-	355	51.5	380	2,167	74.9	146	Compression fractures both faces at load tabs and local core crush, no bond or repair failure.	
	Co-Cure Repair	EX367/368-4	Parallel	23	75	-	-	398	57.7	462	2,635	91.0	177	Compression 1.0 inch above center of patch	
		EX367/368-6	Parallel	316	600	-	-	264	38.3	306	1,744	70.9	TBD	Compression 1.0 inch above center of patch	

(1) Specimens were tested in a MTS 500 Kips test machine on a spherical adjustable seat after stabilizing at 600 F test temperature for 15 to 30 minutes at a load rate of 12,500 lb/minute.

(2) Skin orientation: (0,±45,90) 8 ply, 2.7 mils/ply. Transverse: outer (0) plies transverse to load direction. Parallel: outer (0) plies parallel to load direction.

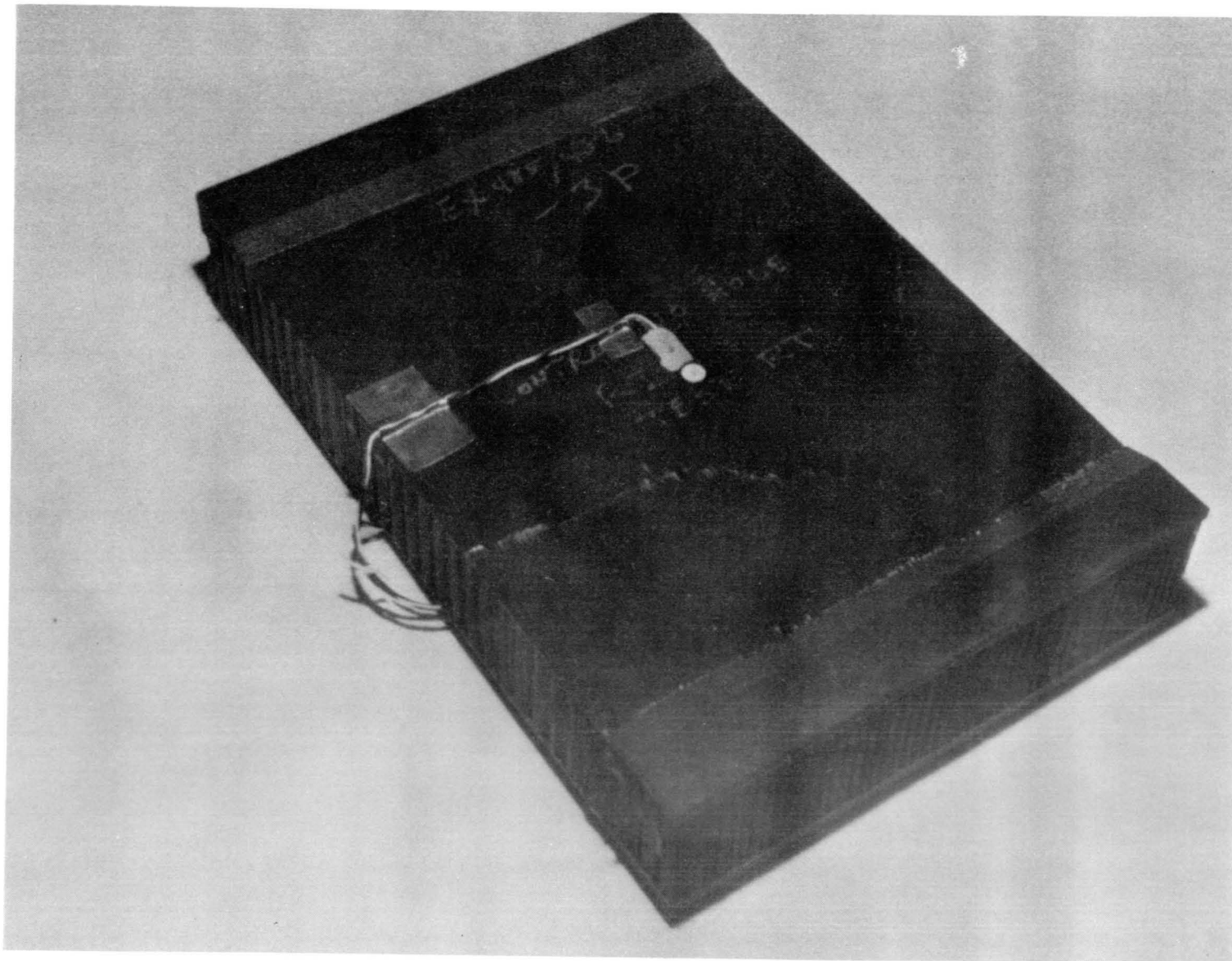
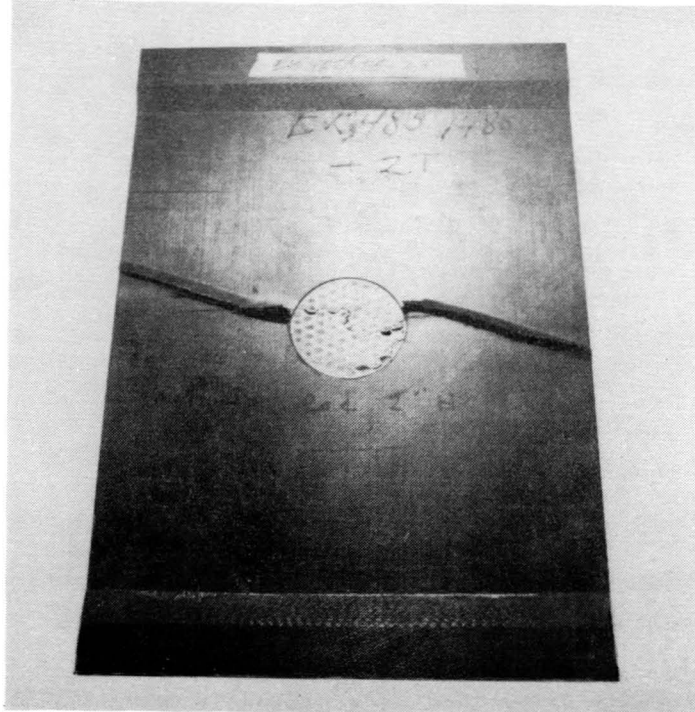


Figure 7-27. Lightly Loaded Sandwich Control Specimen EX485/486-3P--Failure Mode

A820720 C-27 C



A820720 C-28 C

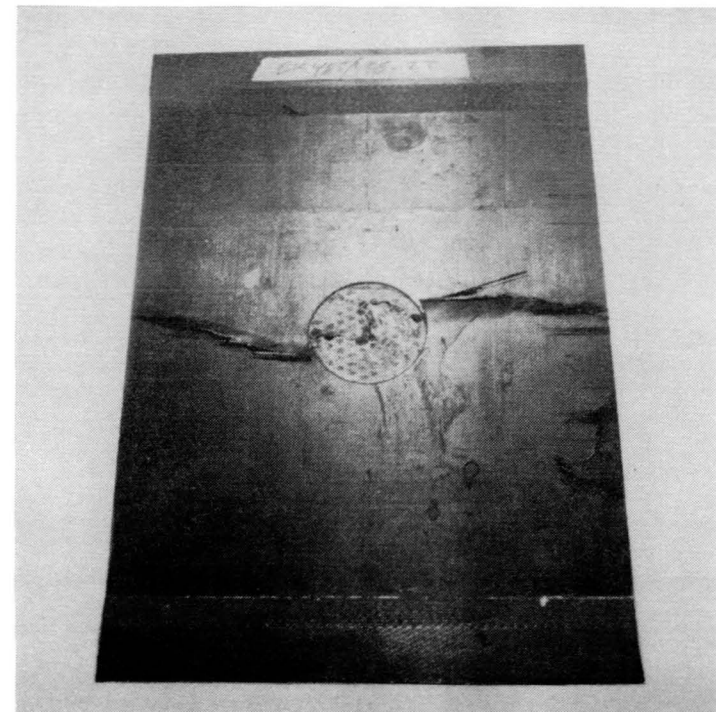


Figure 7-28. Lightly Loaded Sandwich Panel--Room Temperature Control Specimen With a 5.08 cm (2 in.) Diameter Hole Typical Failure Mode (EX485/486-2T)

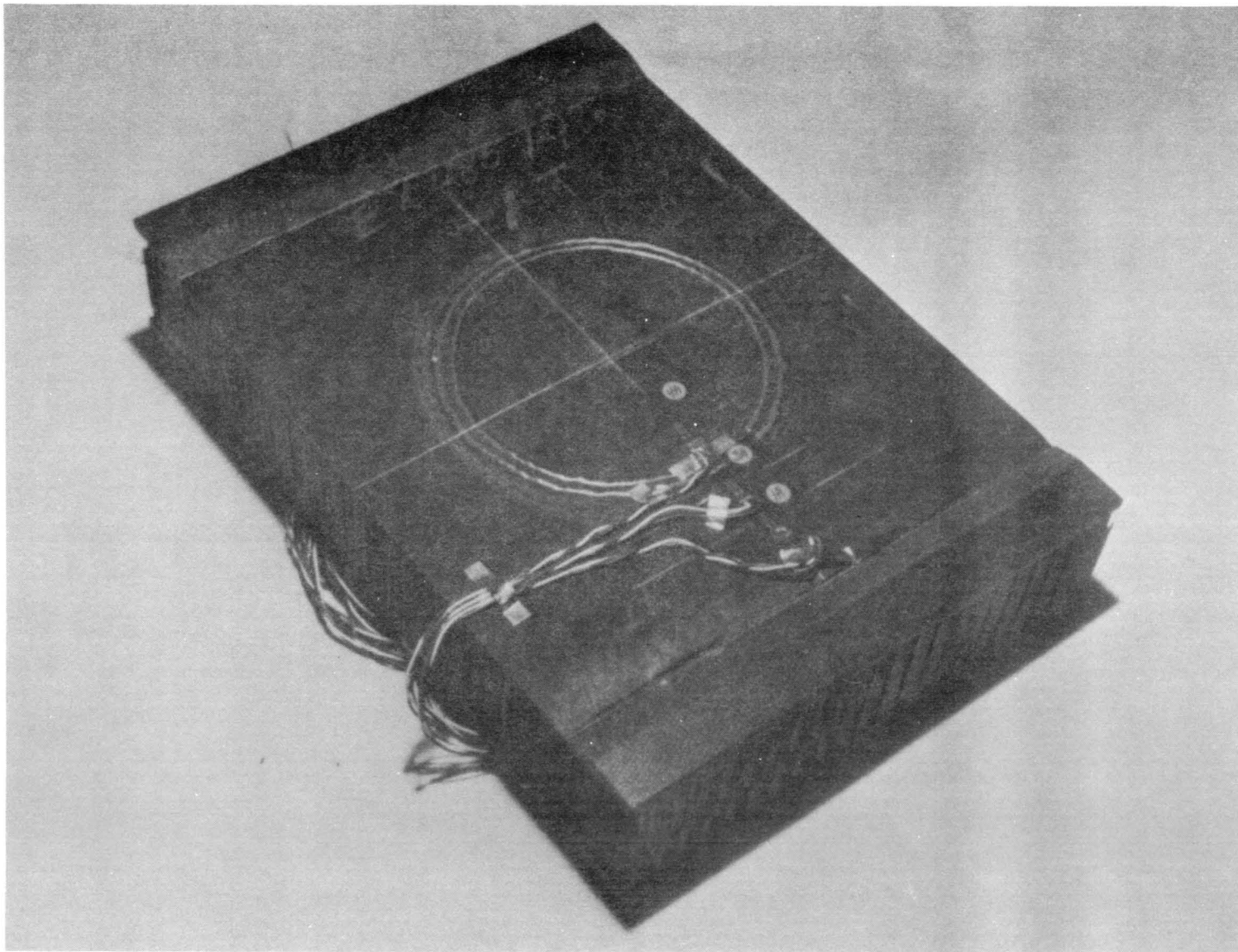


Figure 7-29. Typical Failure Mode Specimen EX485/485-1T, Room Temperature Test, Secondary Bond Doubler Repair, Lightly Loaded Sandwich Panel

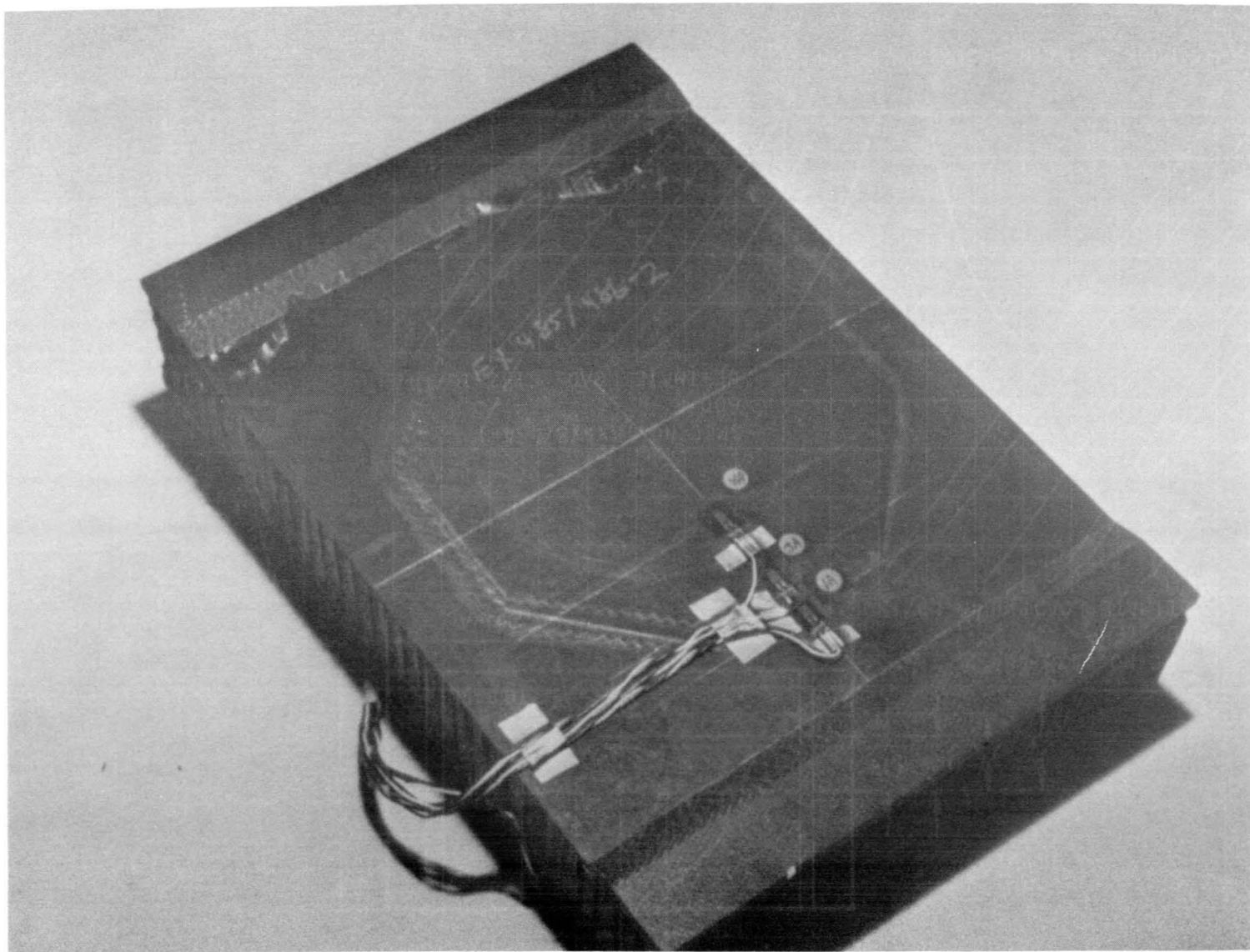
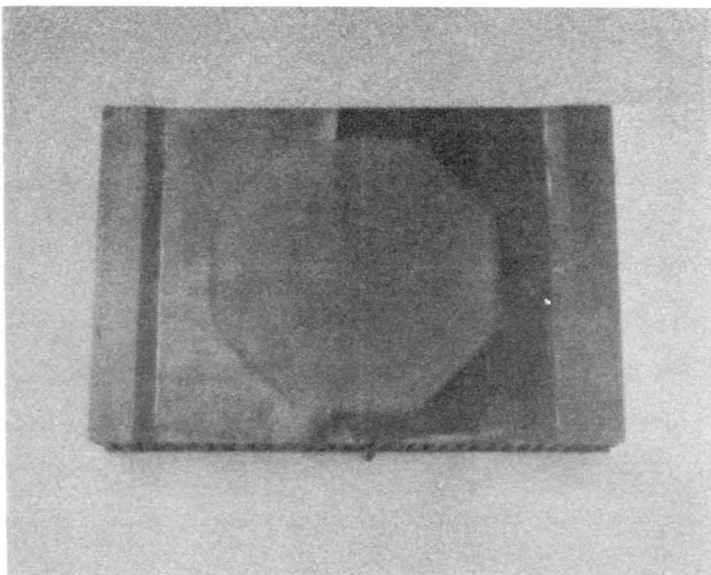


Figure 7-30. Typical Failure Mode Specimen EX485/486-2P Room Temperature Test, Cocure Doubler Repair, Lightly Loaded Sandwich Panel

A820928 G-11 C



A820928 G-12 C

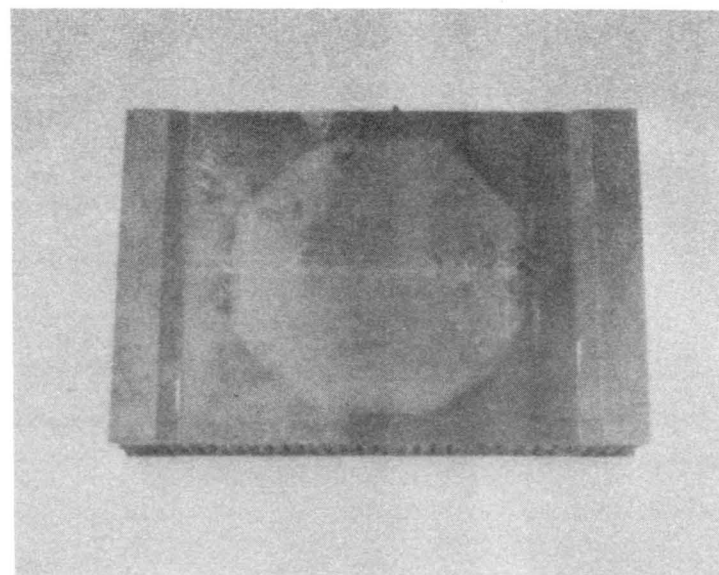


Figure 7-31. Typical Failure Mode Specimen EX367/368-6, 600°F Test,
Cocure Flush Repair, Lightly Loaded Sandwich Panel

7.3.4 Conclusions - Lightly Loaded Honeycomb Sandwich Repair

The undamaged control specimen tested at room temperature failed at 96.5 percent of the 0.57 MN/m (3,000 lb/in.) target design strength. The undamaged control specimen tested at elevated temperature (316°C [600°F]) failed at 85 percent of the room temperature strength. A 5.08 cm (2 in.) diameter hole was found to reduce the specimen strength to 52 percent of the undamaged room temperature value.

Both secondary bond and cocure repairs gave excellent results, returning the specimens to 75 to 102 percent of the undamaged strength. Most of the low strength failures occurred in the load tab area, indicating a high stress concentration possibly caused by misalignment, load path eccentricity, or stiffness imbalance between the thick load tabs and the thin face sheets. The repaired specimen tested at 316°C (600°F) failed at 70 percent of the elevated temperature undamaged strength. This specimen failed in the repaired section caused by combined compression and interlaminar delamination.

8. HAT-STIFFENED SKIN-STRINGER REPAIR

Two types of hat-stiffened skin-stringer panel configurations were used for repair development and demonstration. The first type is a heavily loaded NASA LaRC design consisting of 16-ply skin, 8-ply web, and a 6-ply cap. The second type is a lightly loaded Rockwell design consisting of 8-ply skin, 4-ply web, and a 16-ply cap. The detailed designs for the baseline elements are presented in Figure 8-1. The elements are 15.24 cm (6.0 in.) wide and 30.48 cm (12.0 in.) long. The NASA baseline panel was designed to carry 1.05 MN/m (6,000 lb/in.), while the Rockwell baseline was designed to carry 0.33 MN/m (1,900 lb/in.).

8.1 HAT-STIFFENED SKIN STRINGER ELEMENT REPAIR DEVELOPMENT

8.1.1 Initial Repair Technique and Tooling Approach, Lightly Loaded Skin Stringer

Repair technique development was directed to hat-stiffened skin structure, where the hat element has been damaged. The primary problem in making repairs to this type of structure is providing internal support to the hat stringer while applying external pressure in the repair bonding operation. External pressures can range between 345 KN/m² (50 psi) (secondary bonding) and 1,378 KN/m² (200 psi) (cocure laminating and bonding). The initial approach to resolving this problem was by the use of a molded internal bladder that offsets the external pressure. The bladder material is comprised of the fluoro elastomer, FMCl65, which is described in the process development Section 4.4.

A small prototype element was prepared with a simulated cocure repair installation to develop tooling concepts using the following procedures.

8.1.1.1 Tooling Concept Number 1. The initial tooling concept evaluated is shown in Figure 8-2. Tooling was installed on a lightly loaded prototype hat-stringer/skin structural element. A simulated, repair, without patch was performed to establish performance of the FMCl65 internal bag. The simulated repair was accomplished per the insitu imidizing cure cycle defined in Section 4.4, Figure 4-8; maximum temperature was 288°C (550°F), and 1,378 KN/m² (200 psi) pressure.

A leak occurred in the bladder seams where bagging wrinkles protruded through the rubber during the bladder cure process. Additional problems occurred by cold flow of FMC 165 rubber under the external shim-clamp seals resulting from local intensified pressure, which caused additional leaks. The simulated repair installation cure successfully demonstrated the bladder application by supporting the hat-stringer/skin element with no eccentric deflections.

8.1.1.2 Tooling Concept Number 1, Modified. Bladder and seals were modified by eliminating the external shims and hose clamp seals that caused cold flow in the rubber during the previous cure. The new seal was made by utilizing external bag pressure only. A simulated patch was prepared by

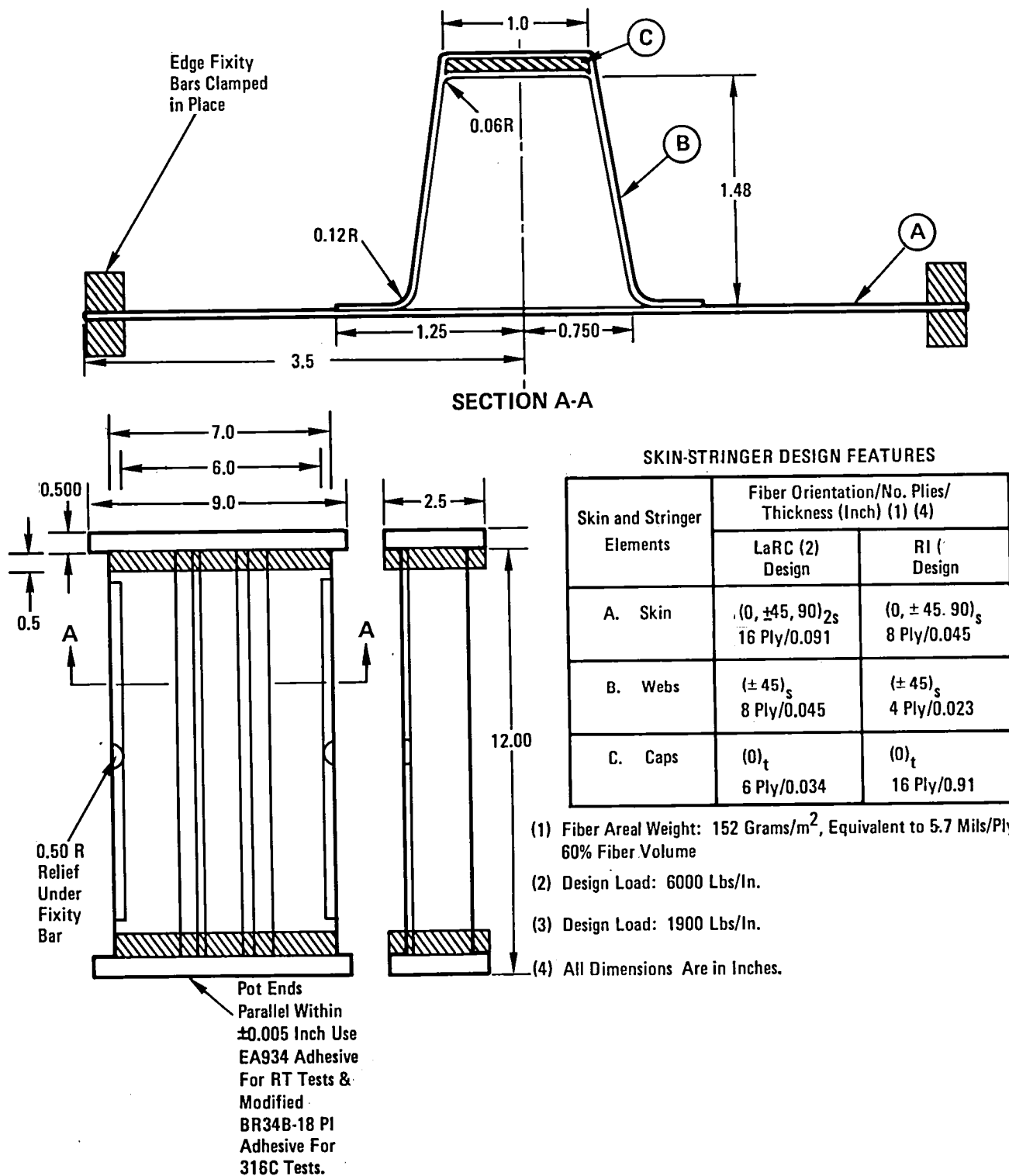


Figure 8-1. Hat-Stiffened Skin Subelement Specimen Design

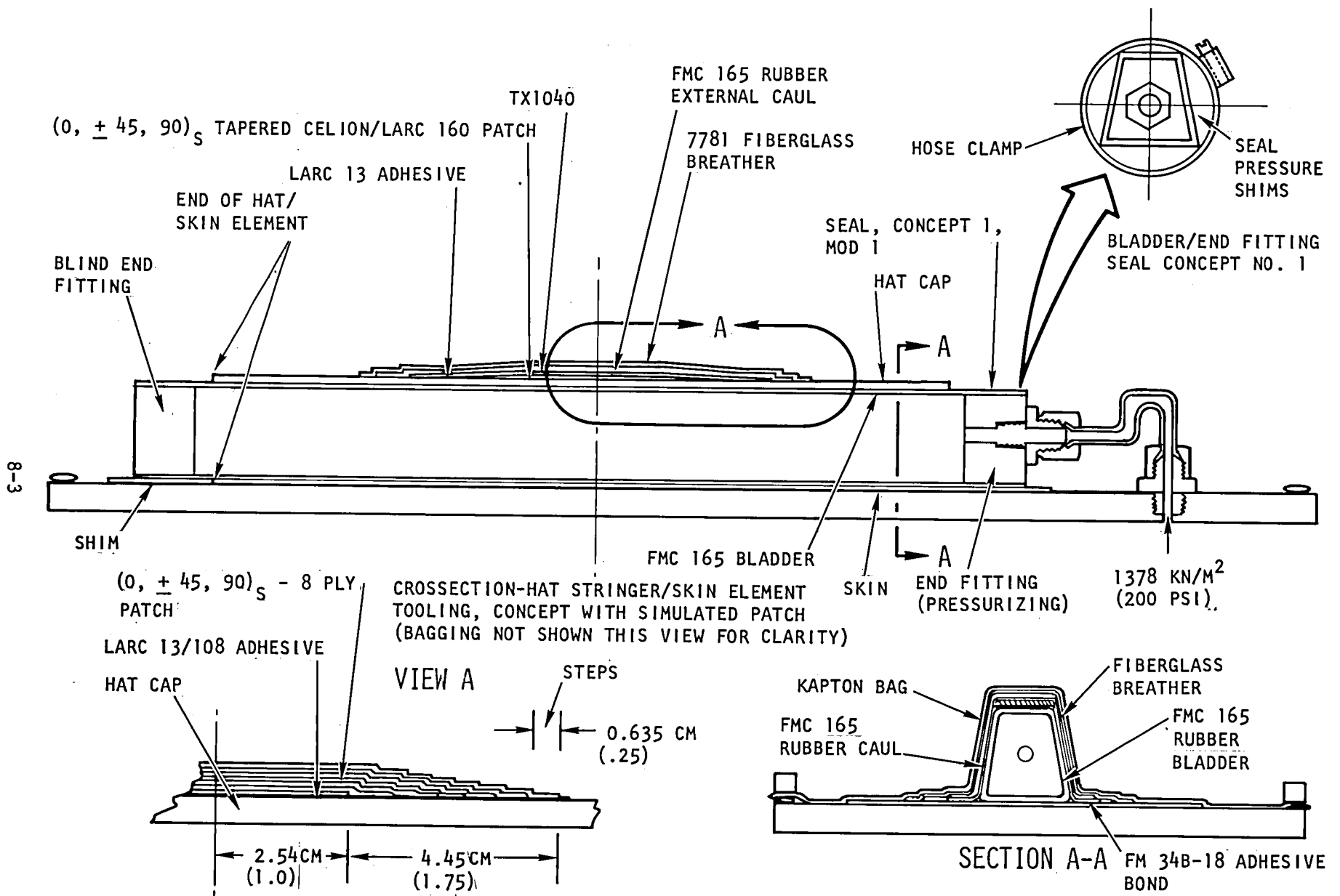


Figure 8-2. Initial Hat-Stringer Repair Bagging Concept

laying up a (0, +45, 90) 8-ply flat perform. Preform ends were tapered by stepping back in 0.64 cm^s (0.25 in.) increments to a 5.08 cm (2.0 in.) long, 8-ply section. The preform was vacuum formed over a hat-section simulator, imidized at 218°C (425°F) for one hour, and then removed.

Hat section faying surfaces were prepared for bonding by abraising and MEK solvent cleaning. Unstaged LARC-13/108 adhesive film was affixed to hat-element faying surfaces. The imidized repair patch was installed over the LARC-13 adhesive surface, simulating a typical installation.

Cocure of the patch installation was accomplished as previously described in concept number 1. A leak occurred during cure, again where bag wrinkles had protruded through the bladder during its cure. Examination of the tooling installation and part after cure showed the following results.

1. Bladder seal-to-end fittings showed no cold flow in the FMC165 rubber.
2. There was a smooth transition between bladder end seals, bladder, and internal surfaces of the hat element.
3. The part maintained its original shape.
4. The patch installation conformed to the contour of the hat and appeared to be soundly adhered to the hat surfaces.
5. There was no evidence of LARC-13 adhesive penetrating to the patch surface.

NDI A sensitivity C-scan tests were performed on the hat element LARC-13/Celion/LARC-160 cocure simulated repair installation. Results showed poor ultrasound through transmission, indicating a porous laminate and/or adhesive bondline. Probable cause of porosity was leakage that occurred in the prototype FMC165 rubber bladder during repair cure and/or Celion/LARC-160 prepreg-LARC-13 solvent incompatibility, Refer to Section 4.4.

8.1.1.3 Repair and Tooling Concept Development Run Number 3. A new FMC165 rubber bladder, 122 cm (48 in.) long was molded using the matched tooling shown in Figure 8-3. There were no molding anomalies and an excellent quality molded bladder was achieved.

A tooling system test was performed using the new bladder, illustrated by the schematic described in Figure 8-3. A bead of General Sealants, Inc. GS-43 sealant was installed between bladder and end plugs to ensure a positive seal. The systems test was performed initially at room temperature, 1,378 KN/m², (200 psi) and then at 288°C (550°F), 1,378 KN/m² (200 psi). System test results were typical to normal flat panel molding operations with no anomalies. There was no part distortion or seal leakage during test.

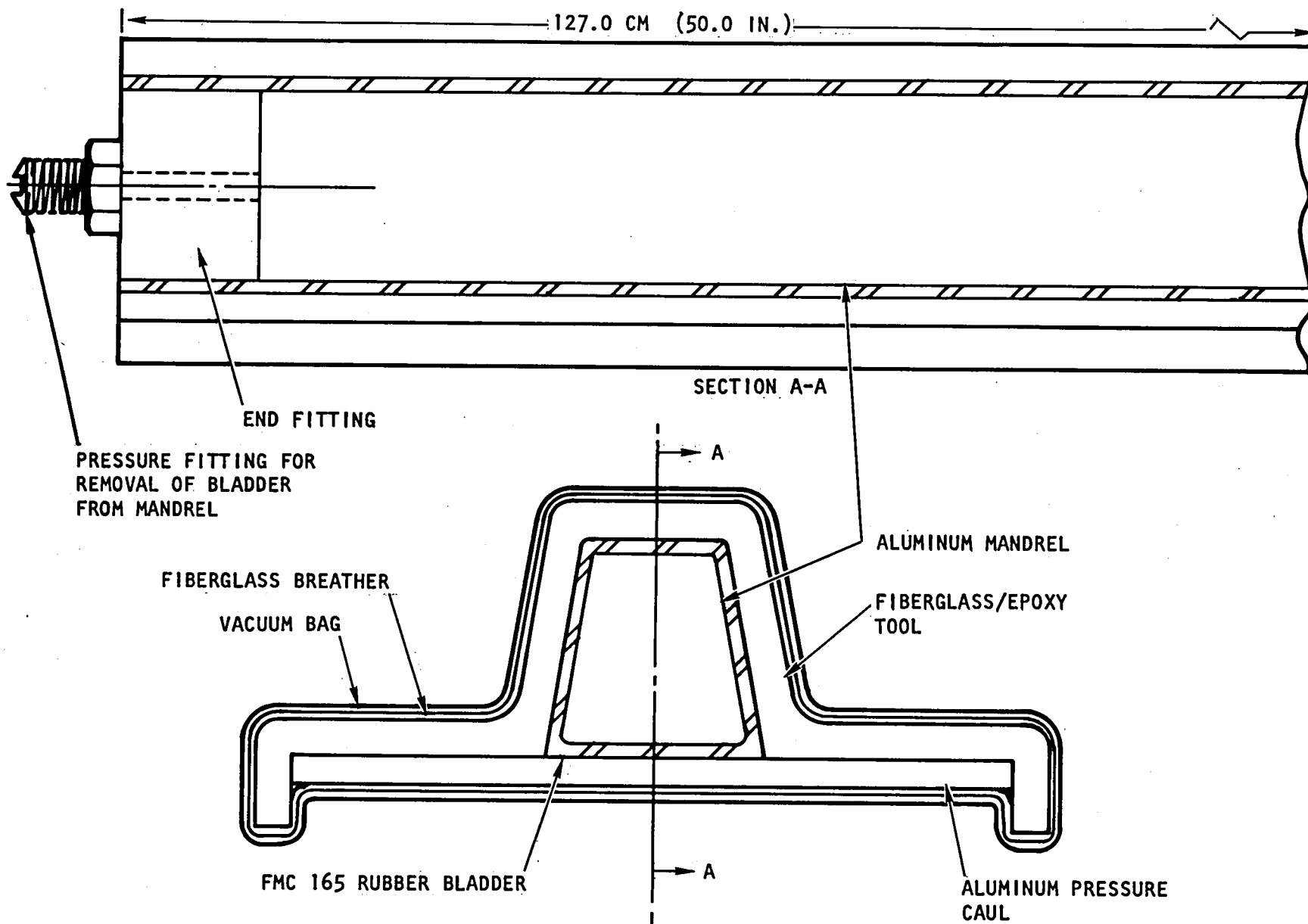


Figure 8-3. Cross-Section - FMC165 Rubber Bladder Molding Concept

8.1.1.4 Repair and Tooling Concept Development Run Number 4. A non-optimized demonstration repair was performed on a hat-stringer element using the match-molded FMC165 fluoro elastomer bladder illustrated in Figure 8-3.

The repair installation involved removing a 5.08 cm (2.0 in.) section of a lightly loaded hat element defined in Figure 8-1 from the $(0, +45, 90)_s$ 8-ply skin. The 16-ply, 0-degree cap and 4-ply, $(+45)_s$ web section was replaced with a Celion/LARC-160 vacuum formed and imidized preform plug of the same configuration as the material removed. A vacuum formed, tapered $(0, +45, 90)_s$ 8-ply imidized preform doubler was applied over the plug and adjacent LARC-13 adhesive film surface of the parent hat element. Cocure of the LARC-13 adhesive and Celion/LARC-160 imidized preforms was accomplished using the second stage of the two stage cure cycle, per Figure 4-8, at $1,378 \text{ KN/m}^2$ (200 psi), 288°C (550°F). There were no anomalies during the cure process.

Results of the repair operation showed good conformance of the repair plug and doubler in the hat 16-ply unidirectional cap and $(+45)_s$ upper webs; however, the base of the webs were depressed outward because of excessive expansion of the rubber bladder showing the bladder did not provide adequate support.

8.1.2 Improved Repair Techniques and Tooling Concept Development; Repair Technique Approach

Since the fluoro rubber pressure membrane did not provide uniform support to prepreg preform patches during the cocure process, Section 8.1.1, the approach to repair of hat elements was revised for improvement. The improved concept is based on installing a split internal insert within the hat element to provide a solid base for applying the repair patch without distortion. The insert can be secondary bonded concurrently during the prepreg patch cocure operation or separately bonded. The repair concept is illustrated schematically in Figure 8-4 through 8-8, and in photographic sequence, Figures 8-9 through 8-17. For repair, the damaged hat is cut away, leaving the skin intact. The edges of the cap repair area are ground to a scarf angle to specific design and webs and flanges blended to fit, as shown in Figures 8-9 and 8-10. A two piece split insert, with midpoint scarf overlap per the schematic, Figure 8-6 and photograph, Figure 8-11 is required for installation within the small opening in the hat. The insert provides a solid base for the external prepreg preform patch during subsequent cocure bonding operations. The external patch installation consists of a $(0)_{20}$ imidized tapered plug in the cap, molded imidized $(0)_n$ fillets in the two radii at the insert base, an overlapping stepped $(+45)_s$ 4-ply preform web, and 3-ply $(0, +45)_n$ outer doubler with serrated edges, which are shown in photographs Figures 8-14 and 8-15. A molded fluoro rubber caul is placed over the outside of the patch as shown in Figure 8-16 to ensure that smooth surfaces are imparted during the cocure molding operation. For the cure operation, Kapton film bags are installed inside and outside the hat and skin assemblies that provide uniform isostatic pressure to all surfaces during the cocure process. The same

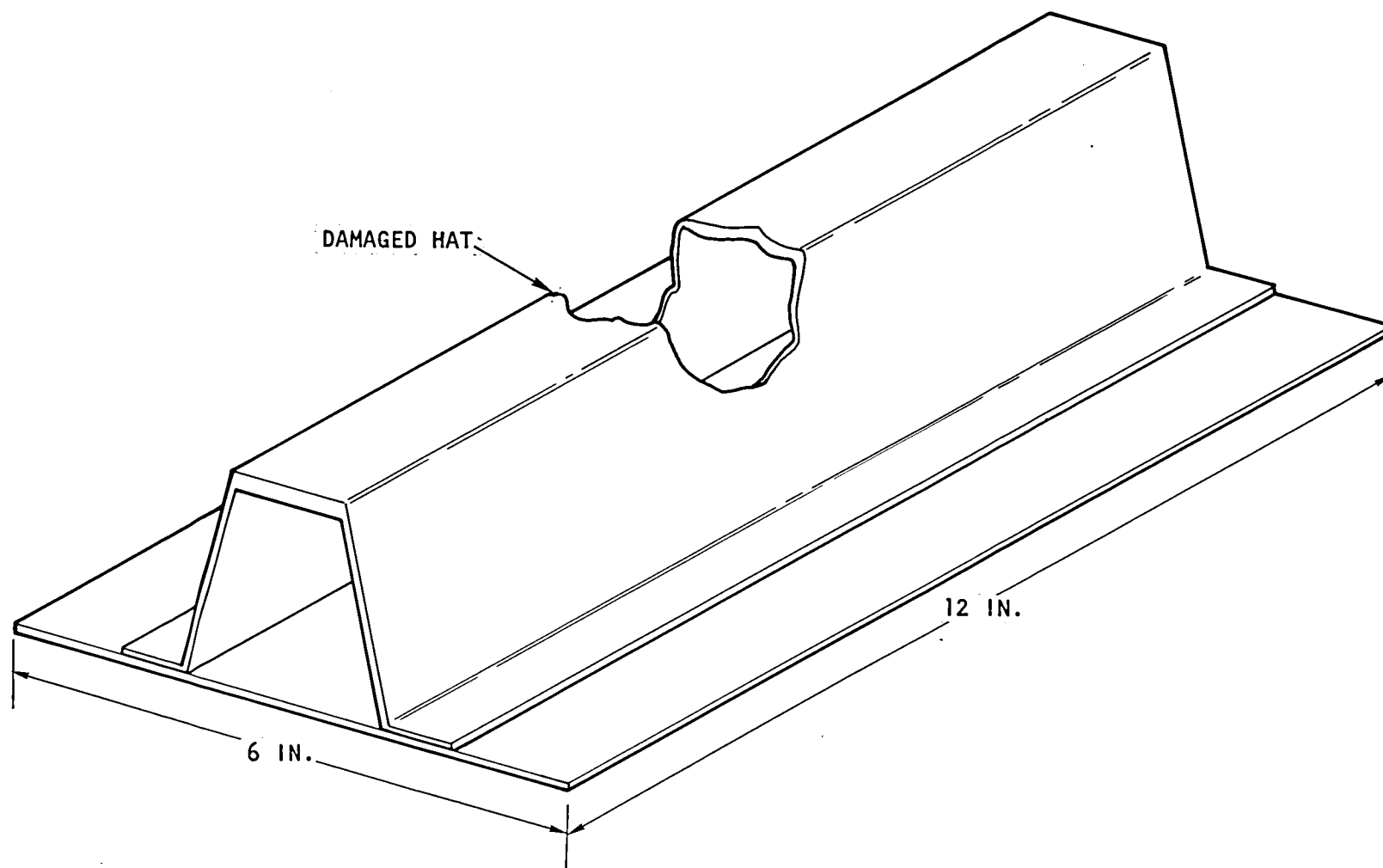


Figure 8-4. Damaged Hat

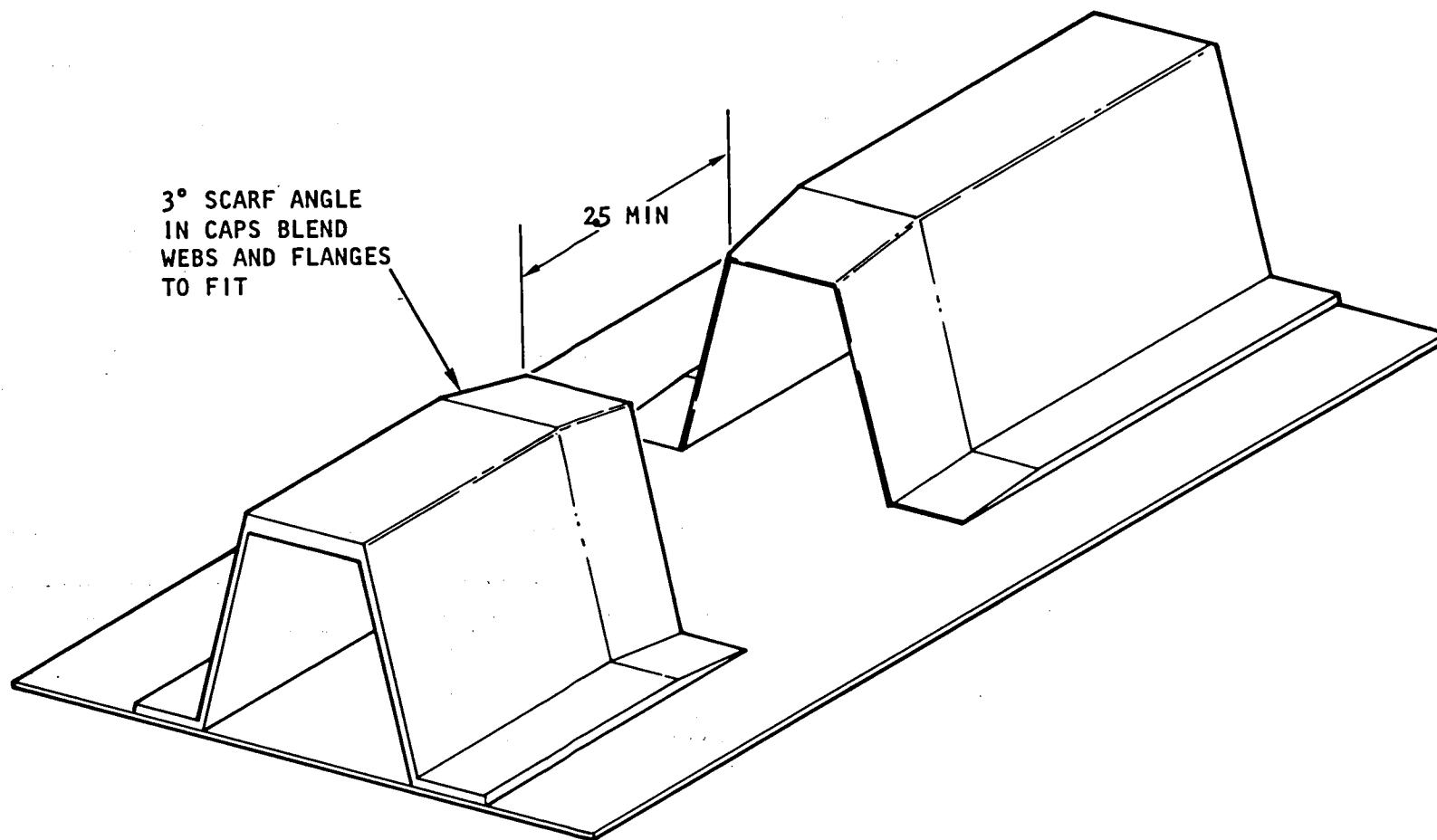


Figure 8-5. Machined 3-Degree Taper for Scarf Joint

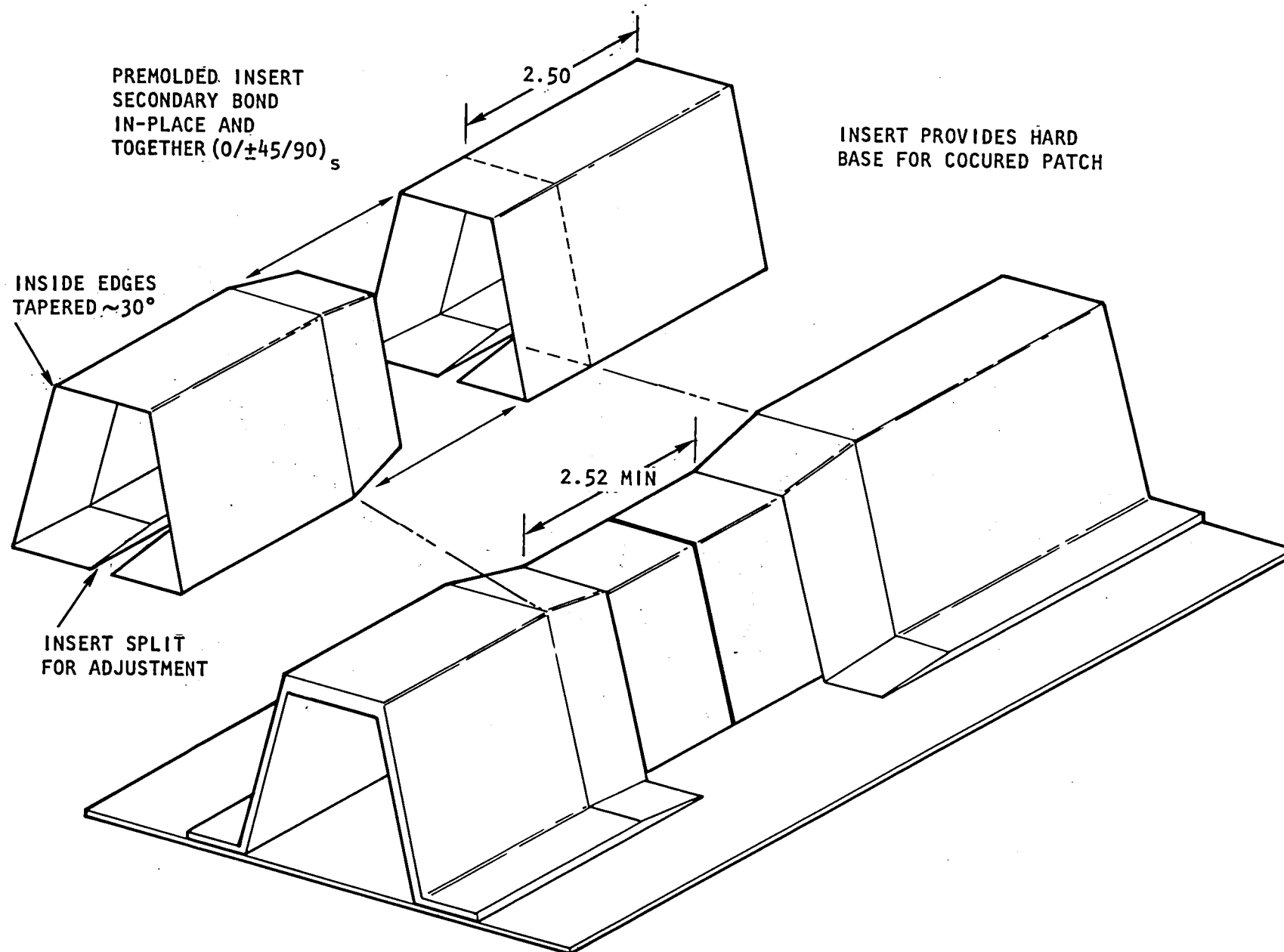


Figure 8-6. Secondary Bond Premolded Internal Support

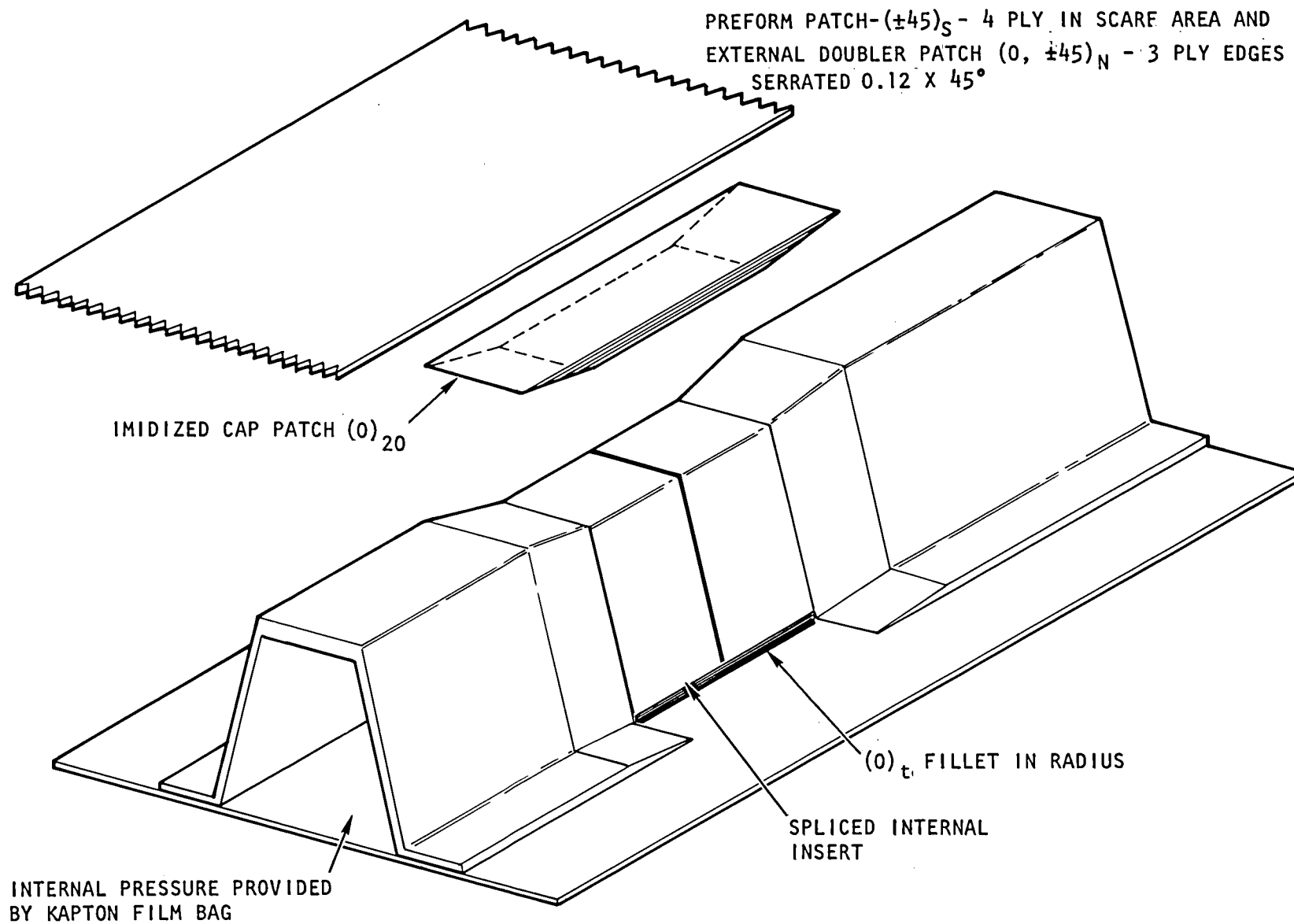


Figure 8-7. Application of Vacuum Formed Flat Preforms and Cap Elements

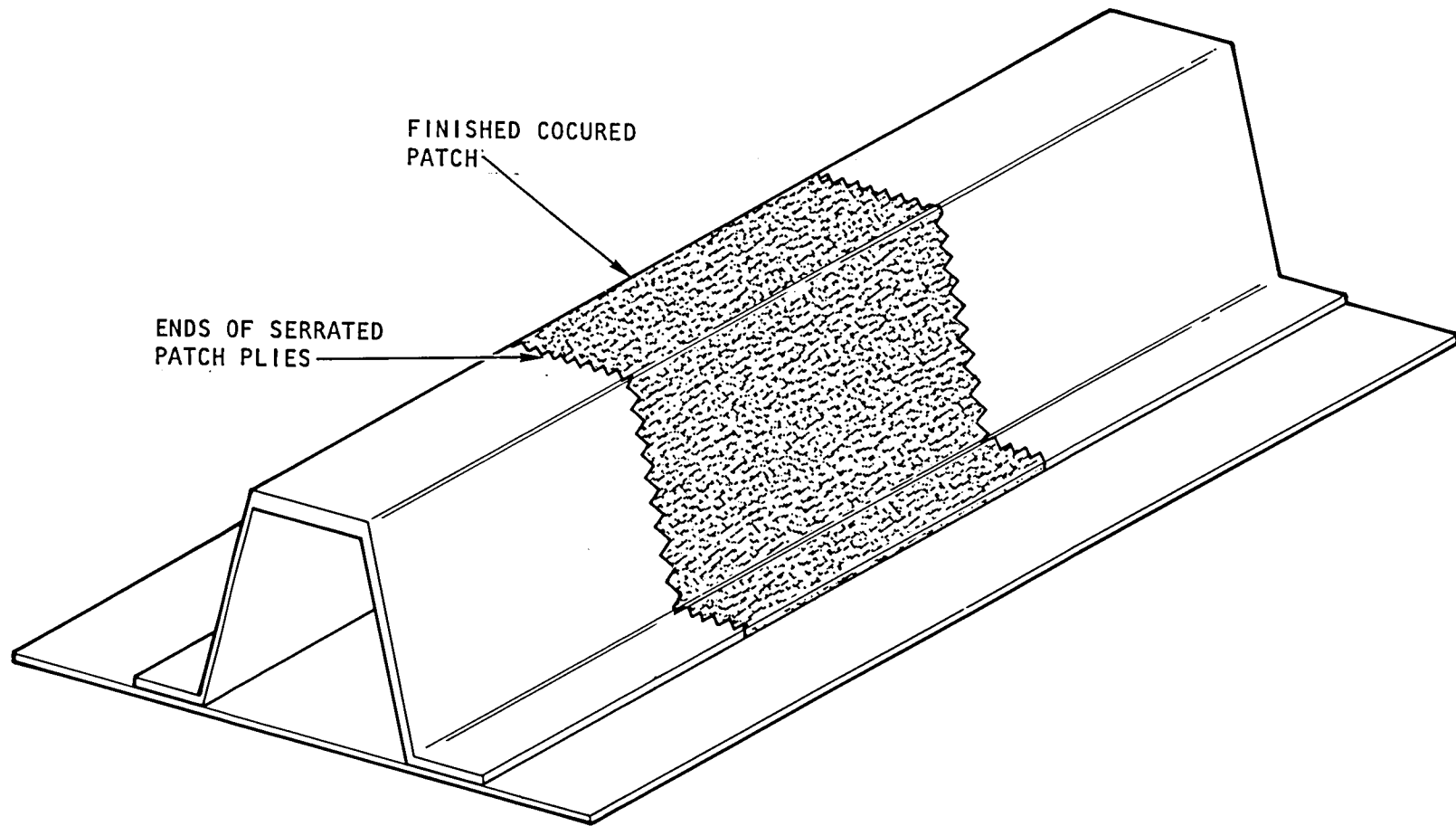


Figure 8-8. Repaired Hat Section

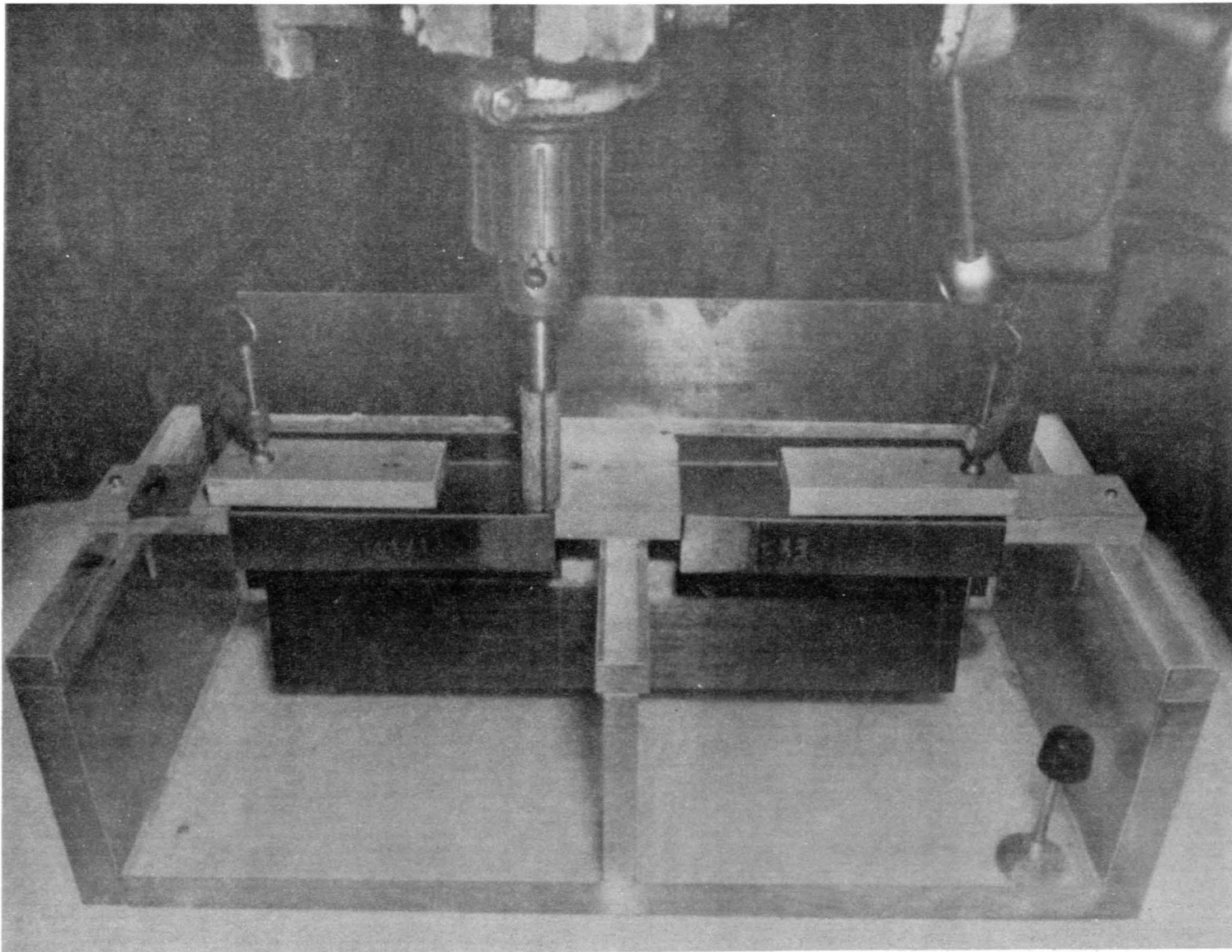


Figure 8-9. Lightly Loaded Hat-Stiffened Skin Stringer Element
Hat Web Scarf Angle Grinding Operation

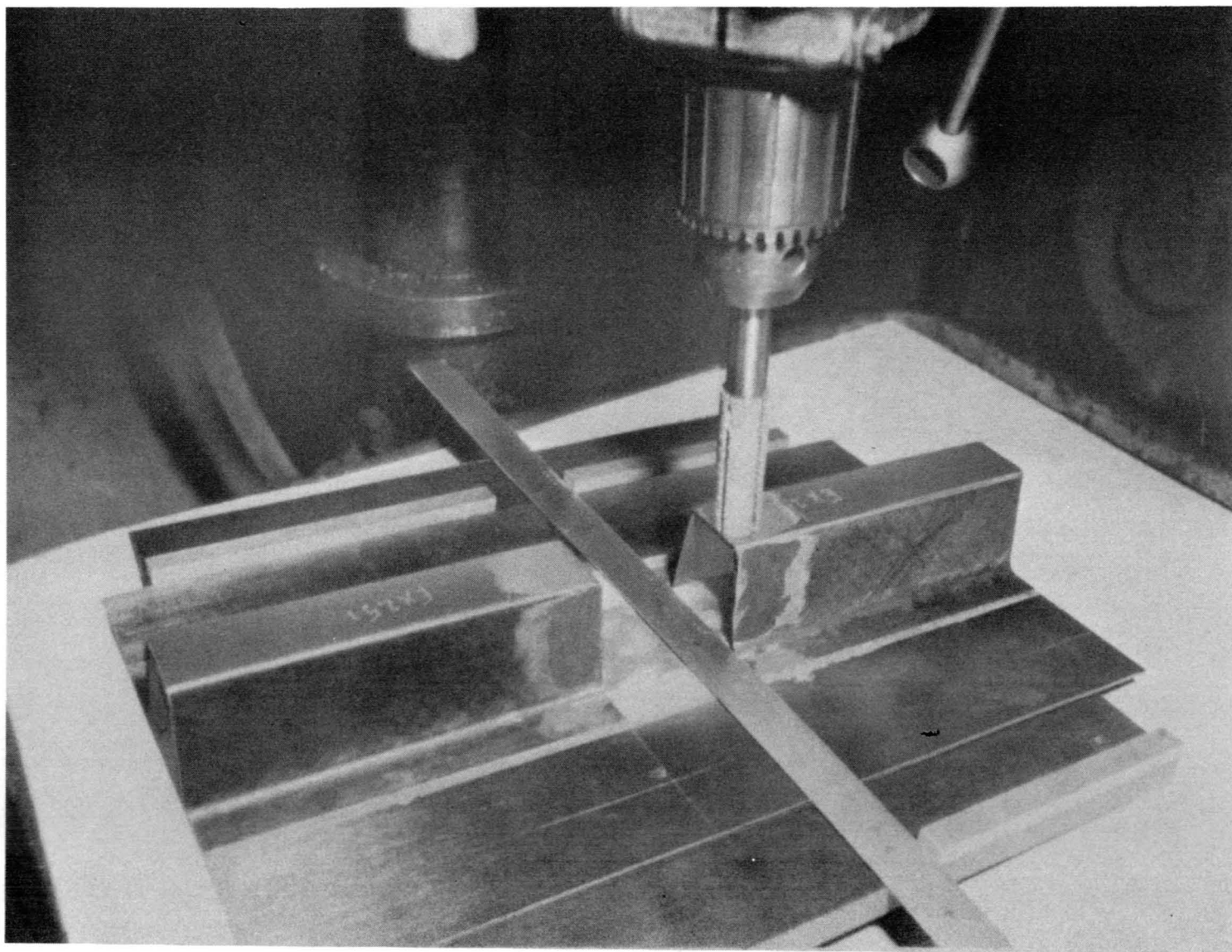


Figure 8-10. Lightly Loaded Hat-Stiffened Skin Stringer Element
Hat Cap Scarf Angle Grinding Operation

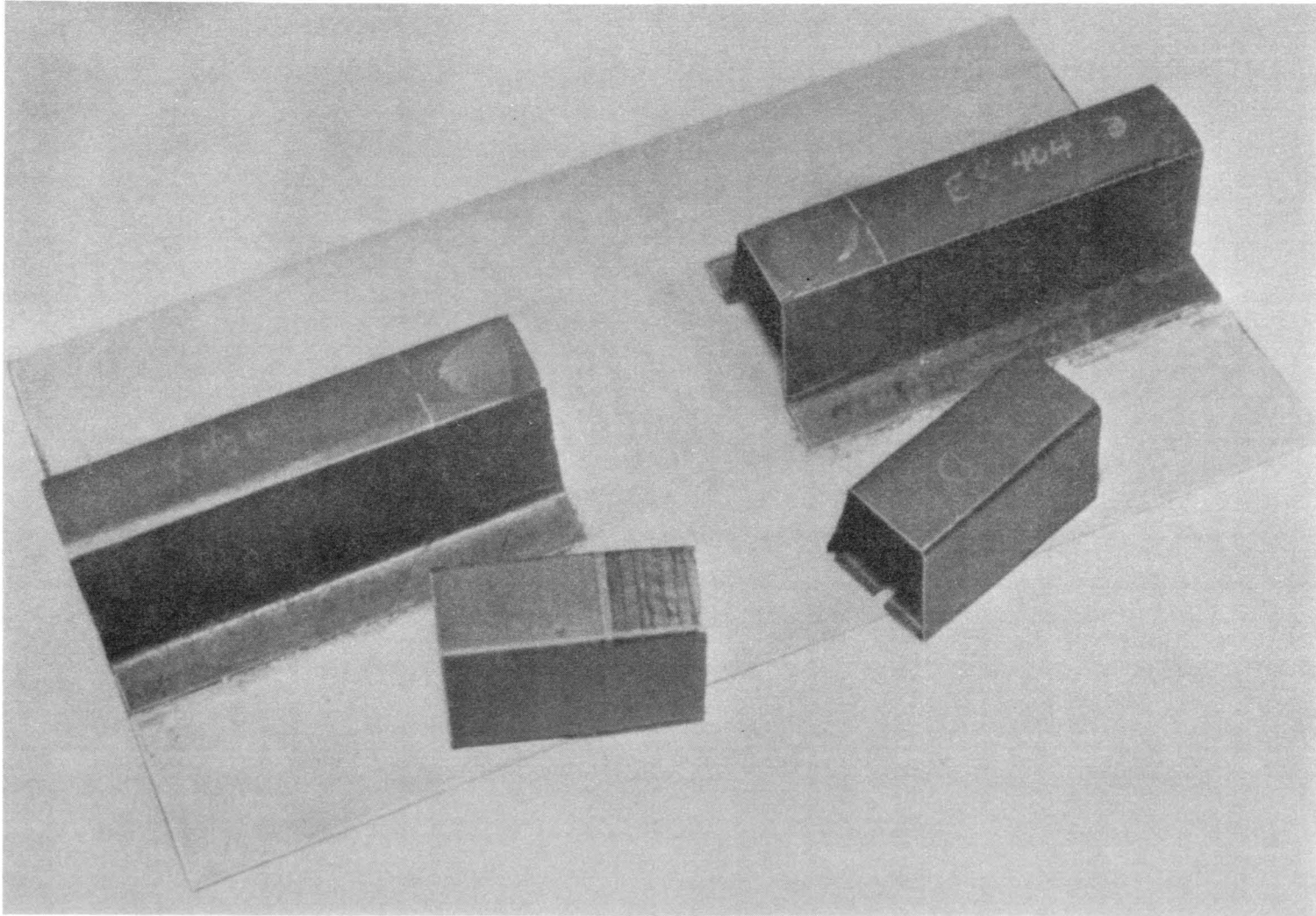


Figure 8-11. Split Internal Hat Support Ready Job Assembly

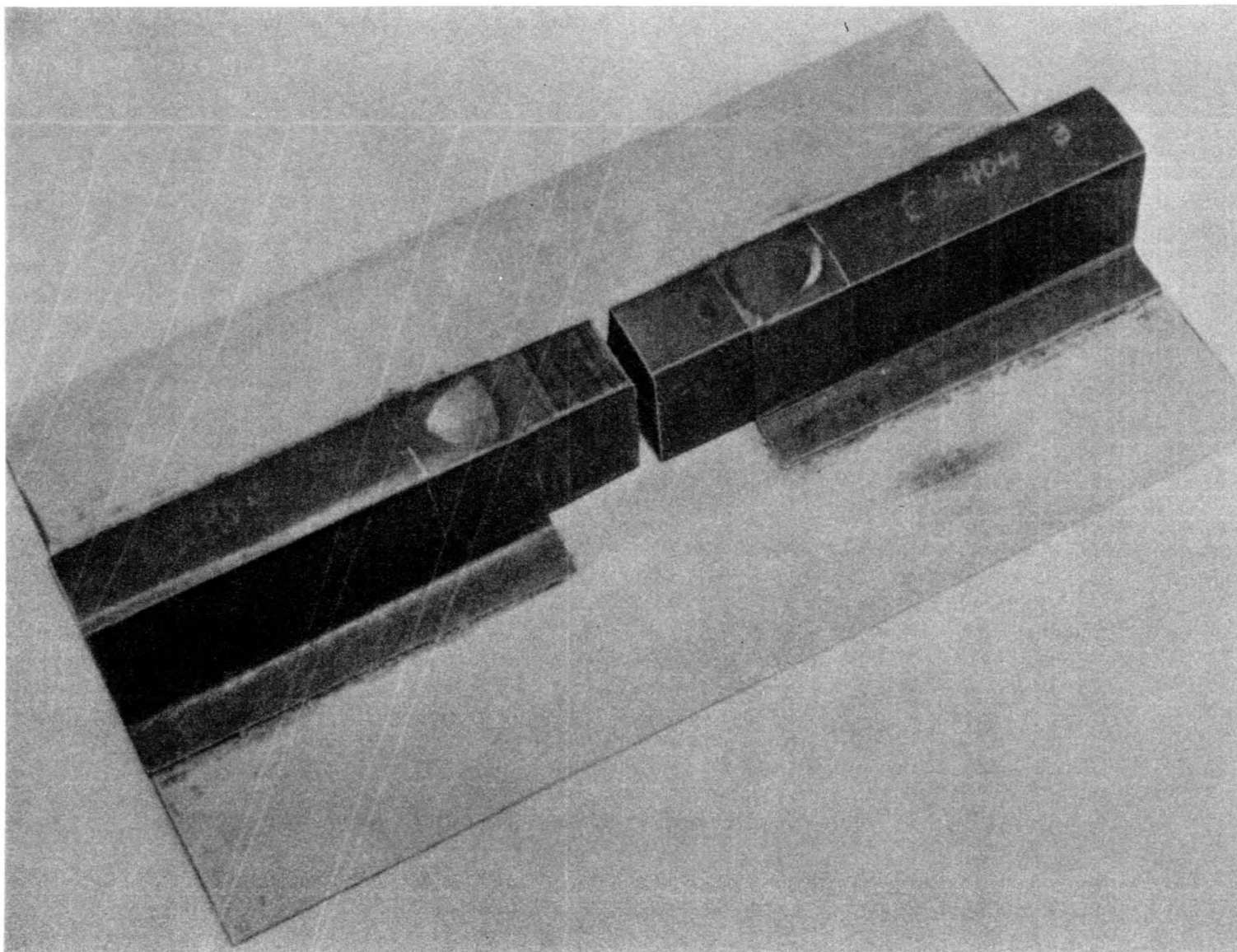


Figure 8-12. Split Internal Hat Support Installed, Ready to Close

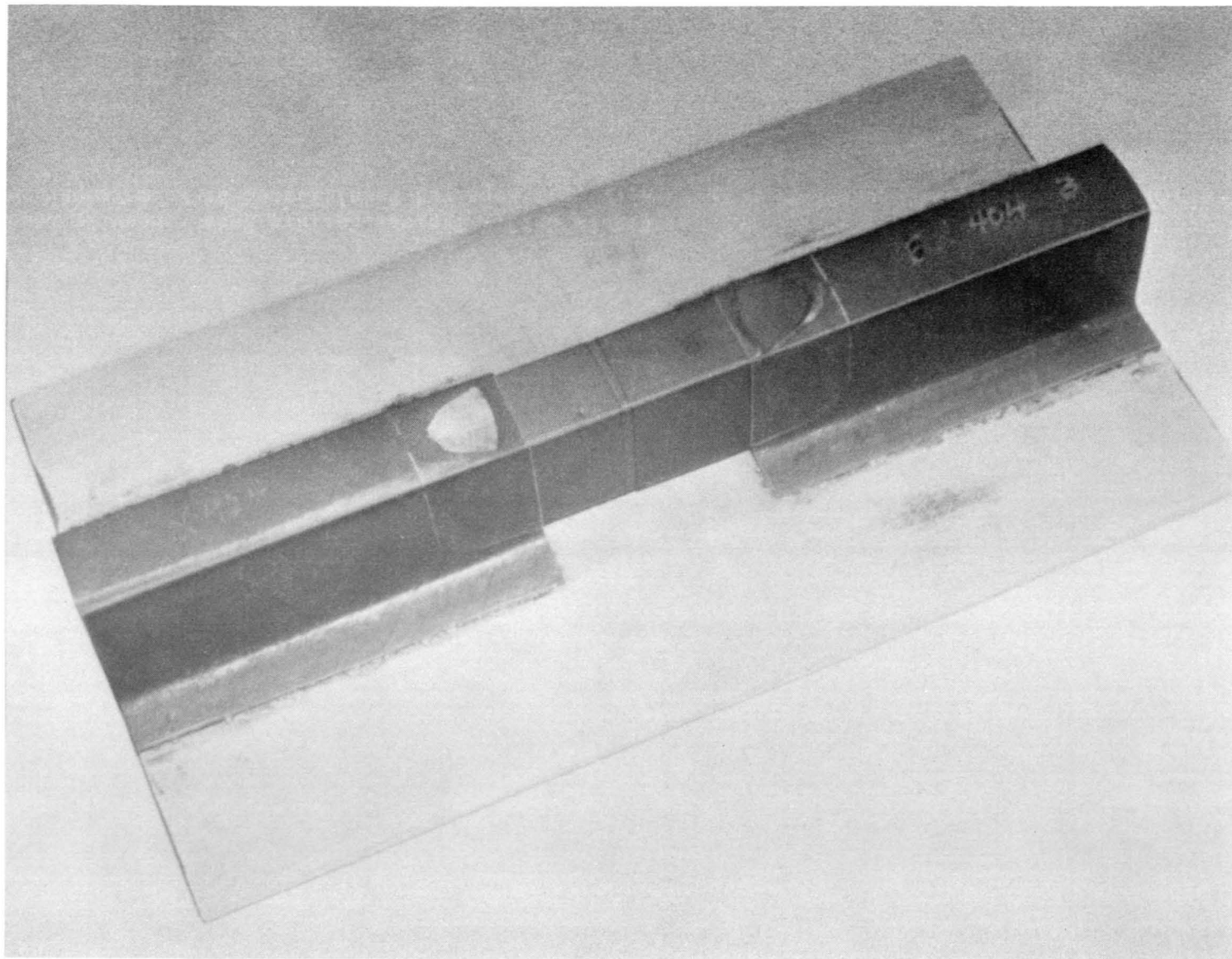


Figure 8-13. Split Internal Hat Support Installation Complete

A820316C-2C

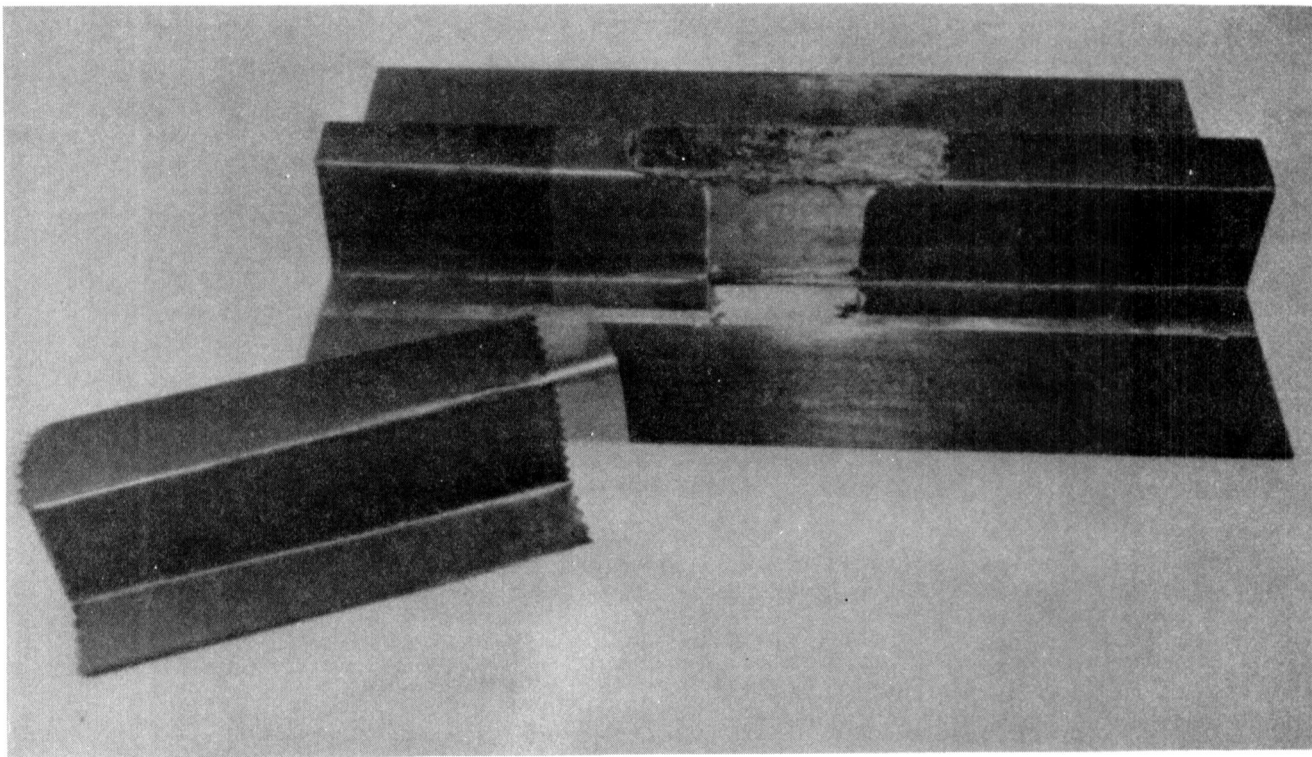


Figure 8-14. 0 Degree Cap Element and Preformed Flat Doubler
Ready for Installation

A820316C-3C

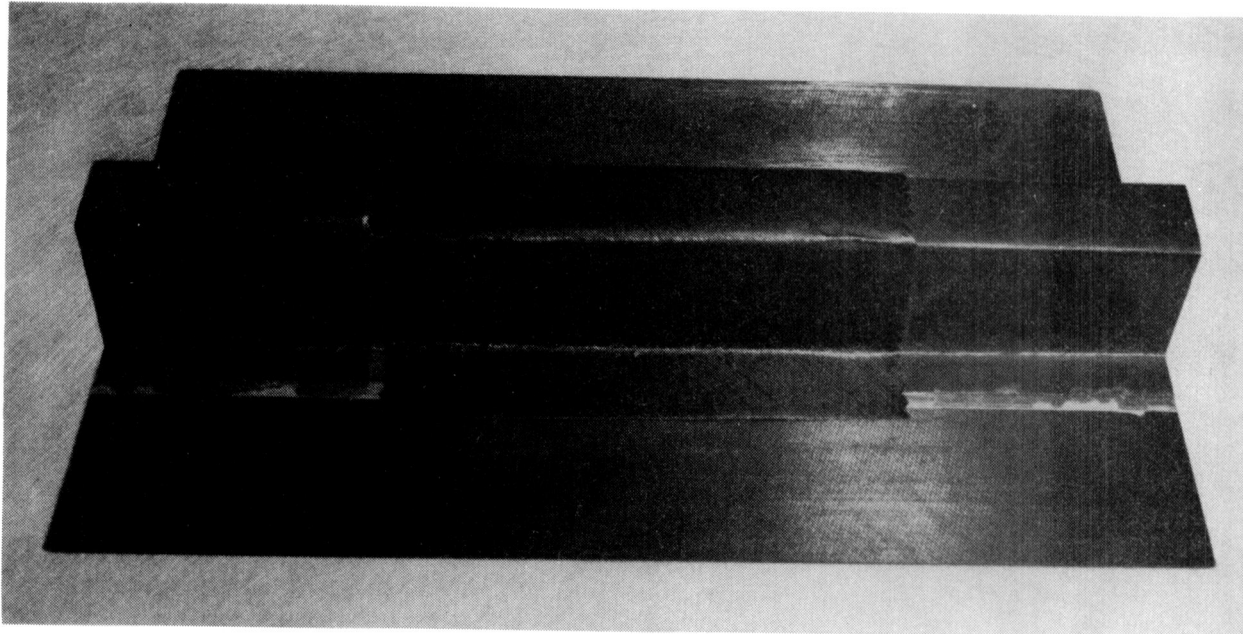


Figure 8-15. Hat Doubler Preform Installed

A820316C-4C

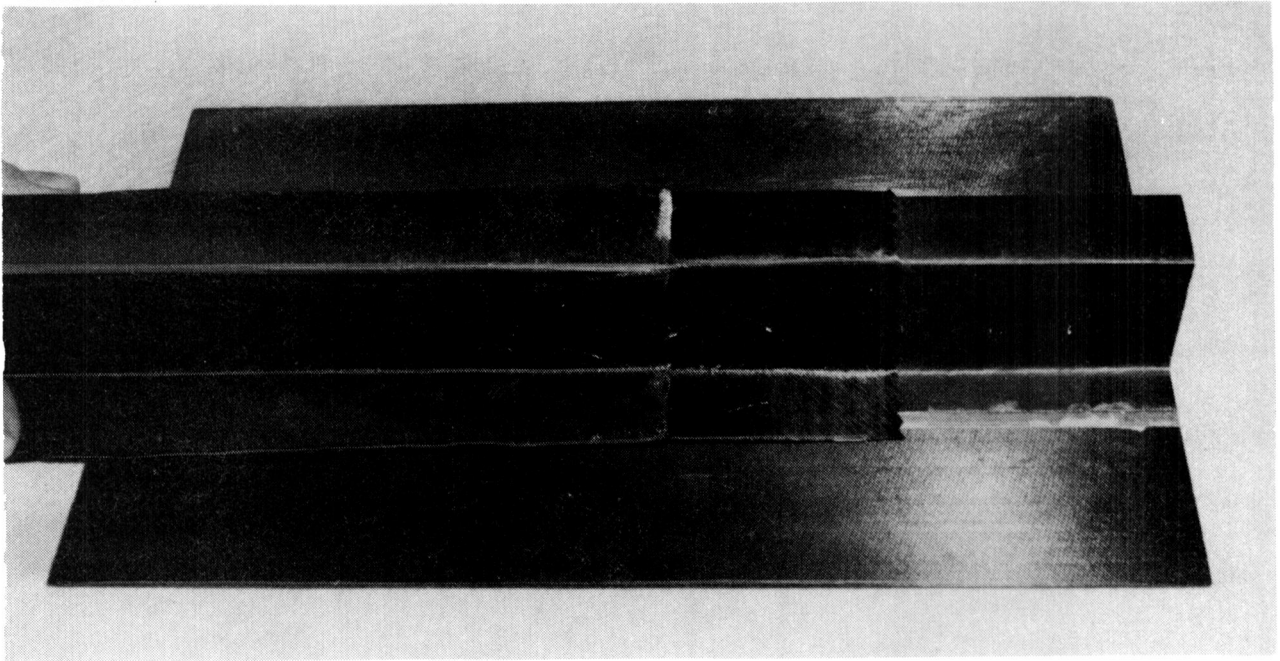


Figure 8-16. Fluoro Rubber Pressure Caul Being Installed
Over Hat Doubler Patch

A820316C-5C

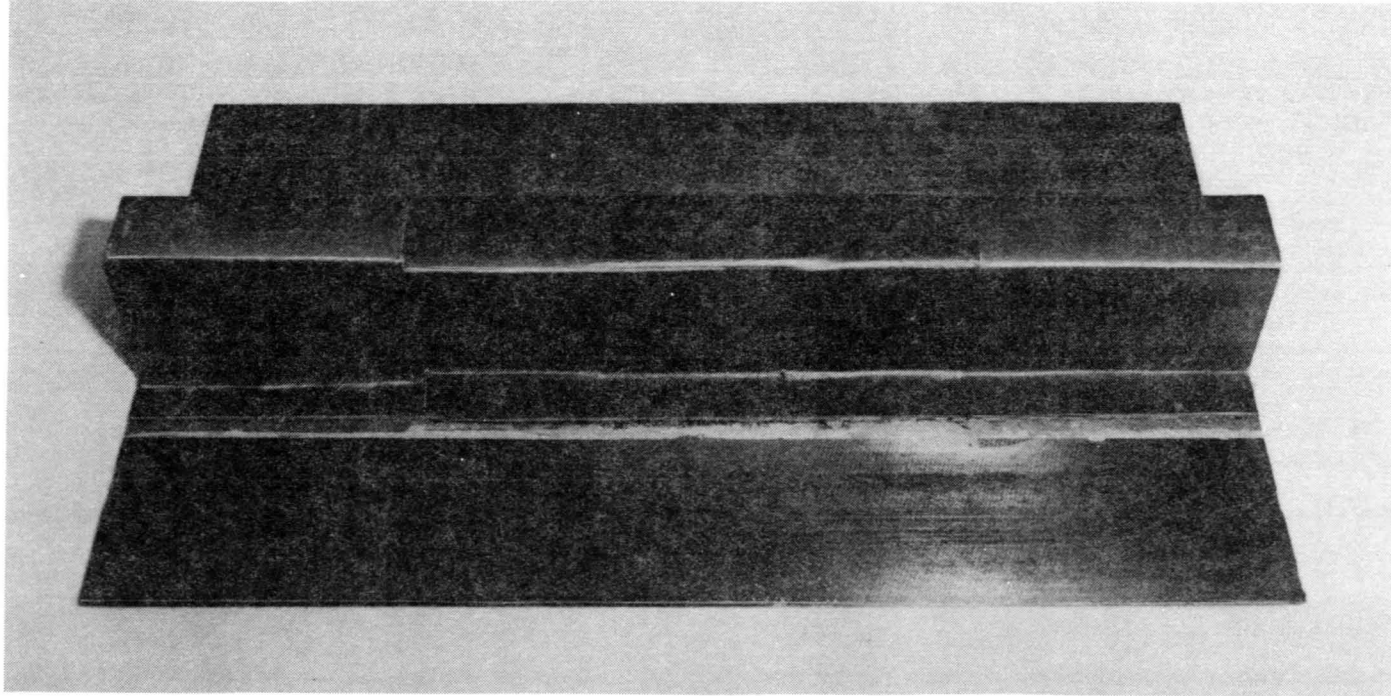


Figure 8-17. Completed Repair of Hat-Stiffened Element,
Lightly Loaded Design

prepreg adhesive, single-stage in-situ imidizing cocure cycle developed for repair of flat laminates and sandwich structures is employed in this operation.

8.1.3 Results of Improved Repair Installations

Prototype heavily and lightly loaded design elements per the respective designs, Figures 8-18 and 8-19, were repaired using the above techniques. Repair installations had an excellent aesthetic appearance with smooth transition between the repair area and parent material. The serrated edges terminating the external doubler plies showed good definition and all layers were well compacted. The repair installations conformed well to the baseline element configuration without distortion. A repair element is shown in Figure 8-17. NDI C-scan A-sensitivity test recordings showed low void in the web and flange areas. The 20-ply 0-degree cap repair area showed some voids in the tapered bond section. Based on the successful results of repair installations on both lightly and heavily loaded hat-stiffened skin-stringer elements, this method of repair was selected for repair verification testing.

8.2 HEAVILY AND LIGHTLY LOADED HAT-STIFFENED SKIN-STRINGER ELEMENT REPAIR TECHNIQUE AND RESULTS

The same basic techniques and curing processes used in the process development elements were employed in repair of remaining heavily and lightly loaded elements per the design shown in Figures 8-18 and 8-19. The same good results attained in repair of prototype baseline elements were achieved in repair of the remaining skin-stringer elements. NDI C-scan recordings showed some voids in random areas of cap, web, and flanges.

8.3 HEAVILY LOADED HAT-STIFFENED ELEMENT REPAIR TESTING AND RESULTS

8.3.1 Compression Testing

Control and repaired specimens were tested in compression at 54 KN (12,500 lb) per minute at room temperature and 316°C (600°F) in the test setup, Figure 8-20, to establish the structural integrity of the repair. Elements were clamped between ground steel parallel bars on each edge to provide fixity during testing, as shown in Figures 8-1 and 8-20.

8.3.2 Control Element Test Results

The test results for the heavily loaded hat-panels are presented in Table 8-1. Undamaged control elements were tested one each at room temperature and 316°C (600°F). The room temperature strength was 0.904 MN/m (5,167 lb/in.) or 86 percent of the target strength. The elevated temperature strength was 77 percent of the room temperature value. The failure modes for these control specimens are shown in Figure 8-21. Compression failure occurred in the cap, web, and skin about 7.6 cm (3.0 in.) from the base.

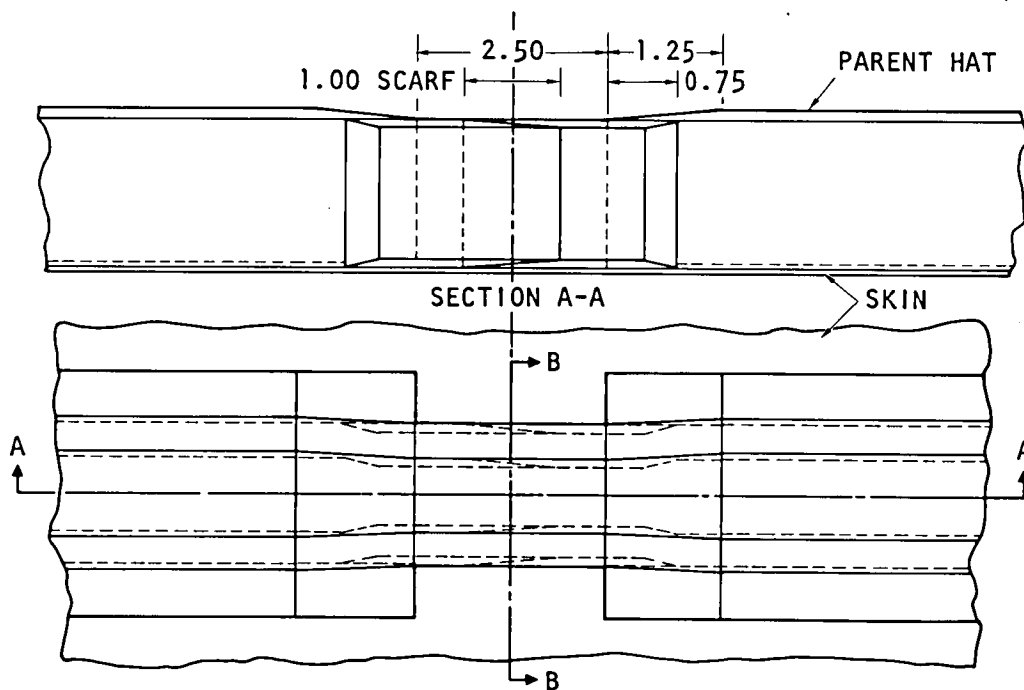
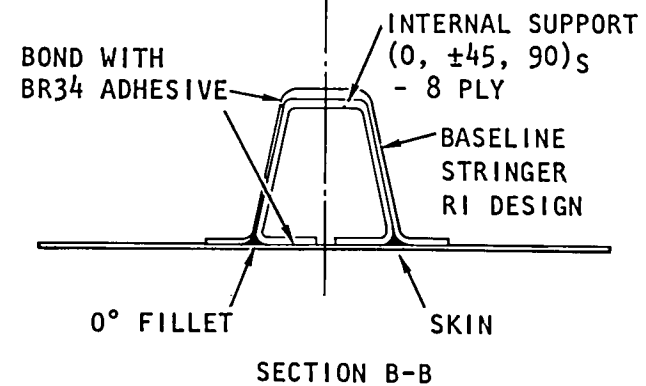
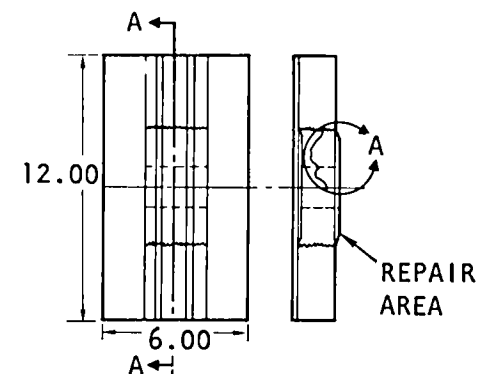
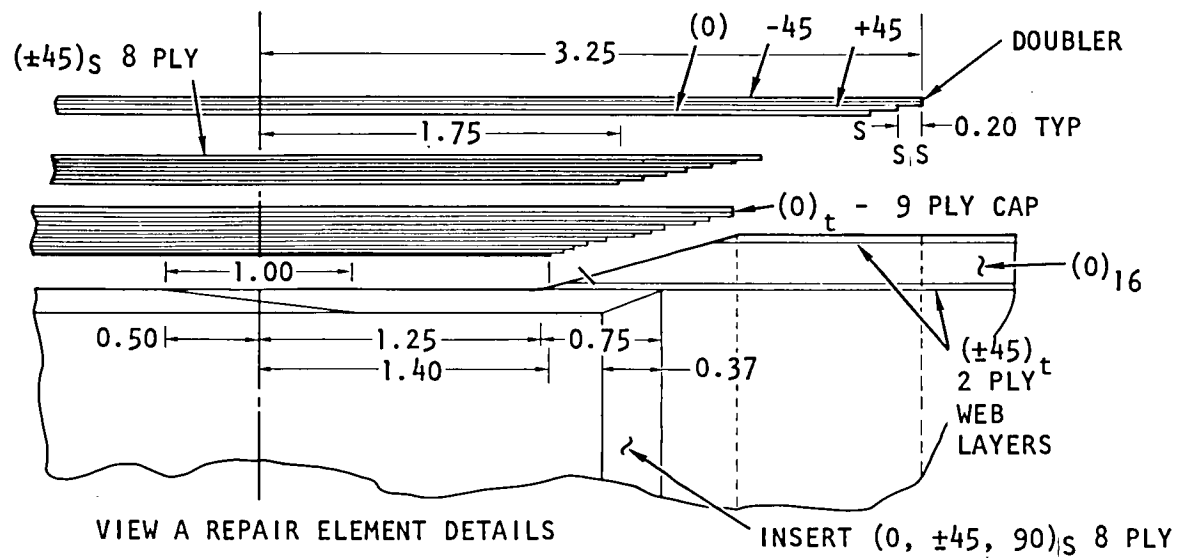


Figure 8-18. Heavily Loaded Stringer Repair - Internal Support and Patch Design

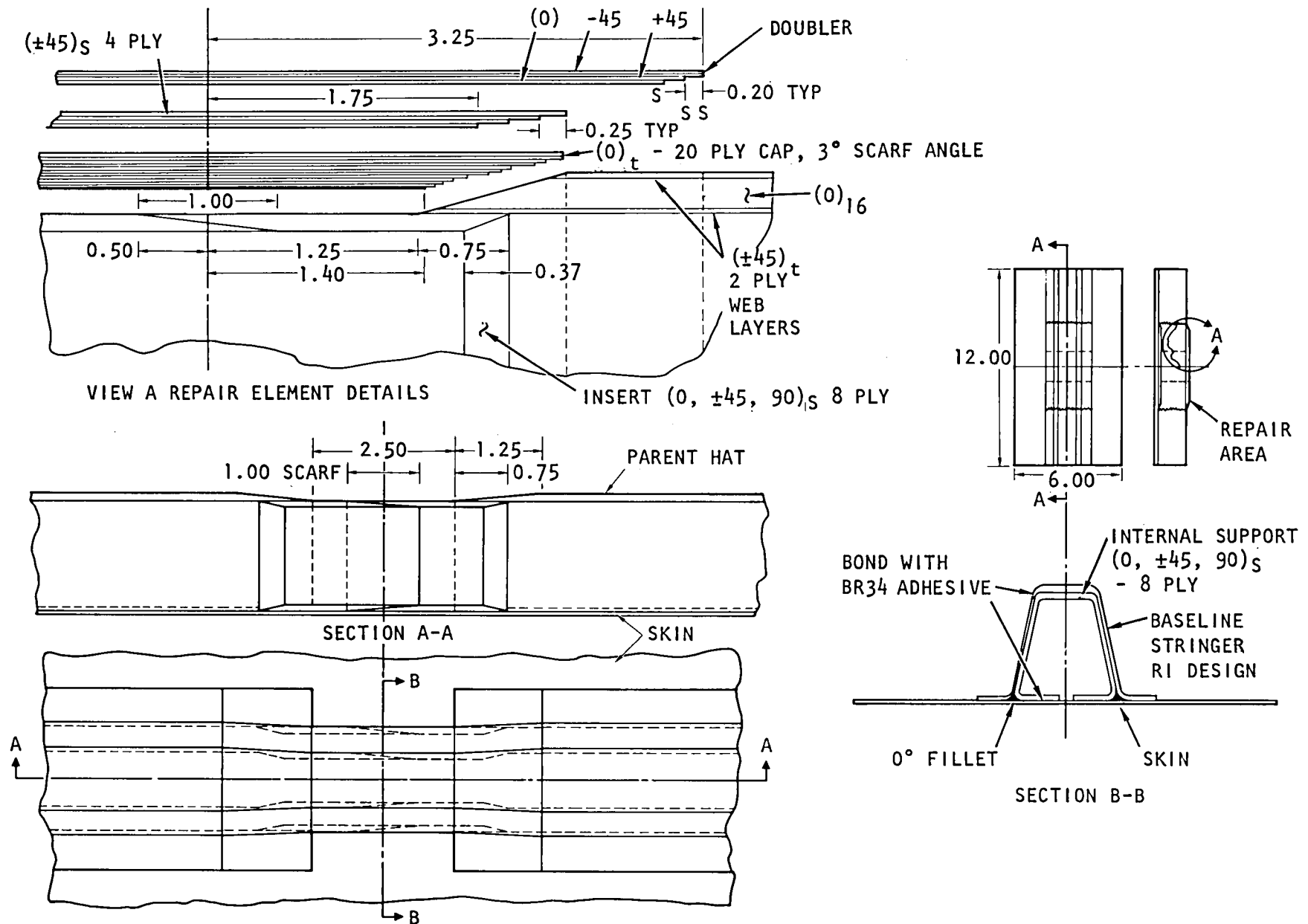
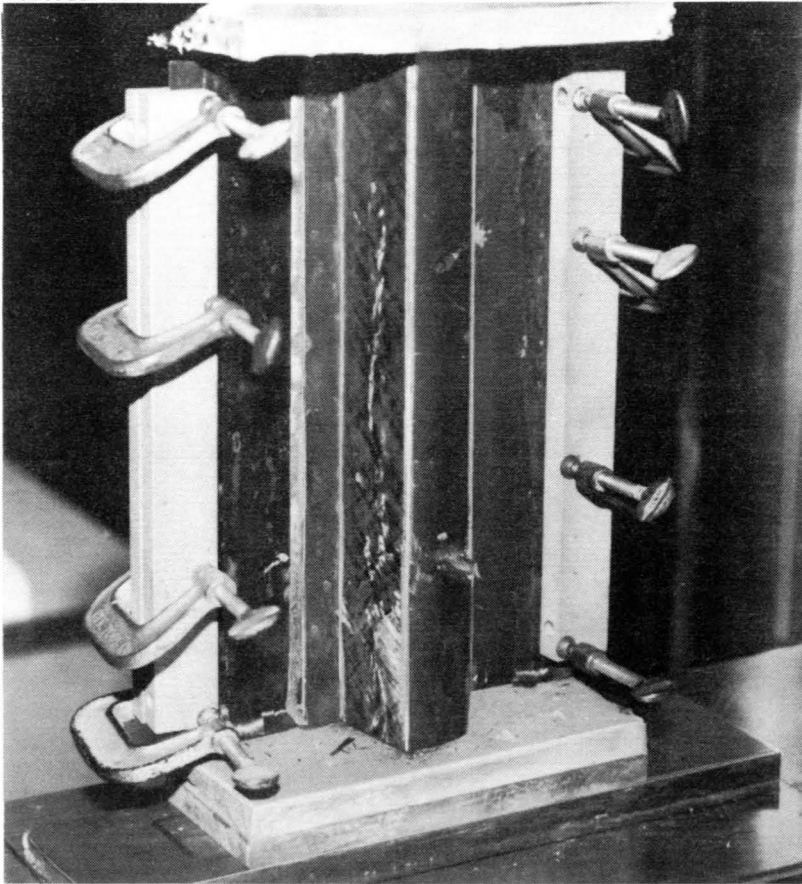


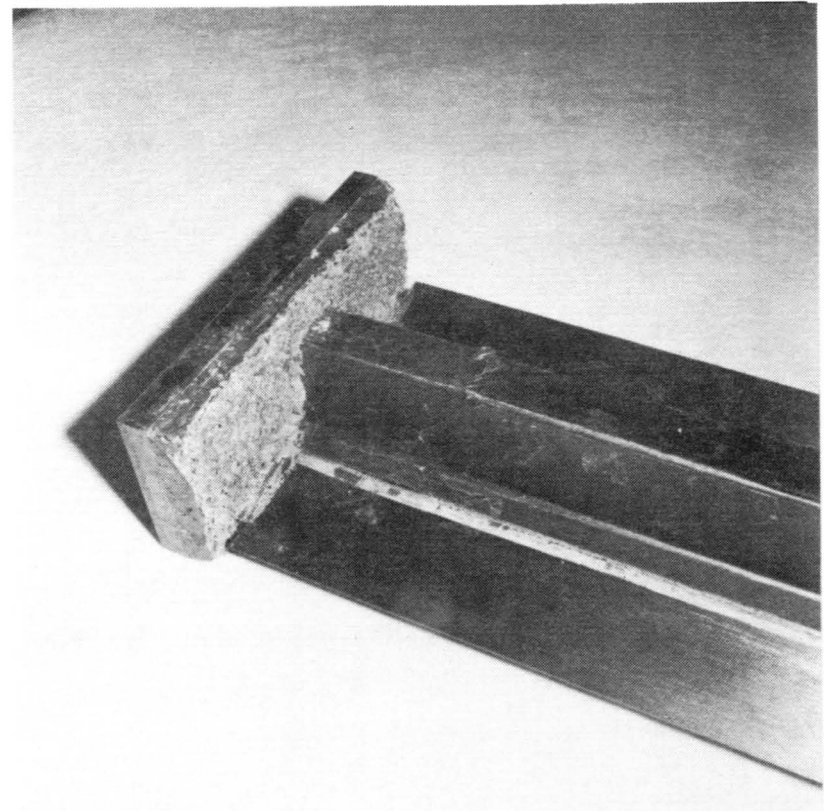
Figure 8-19. Lightly Loaded Stringer Repair - Internal Support and Patch Design

A820311F-22C



a) Specimen Number EX135-1 Tested
at Room Temperature

A820507 D-5 C



b) Specimen EX247-3 Tested at 600°F

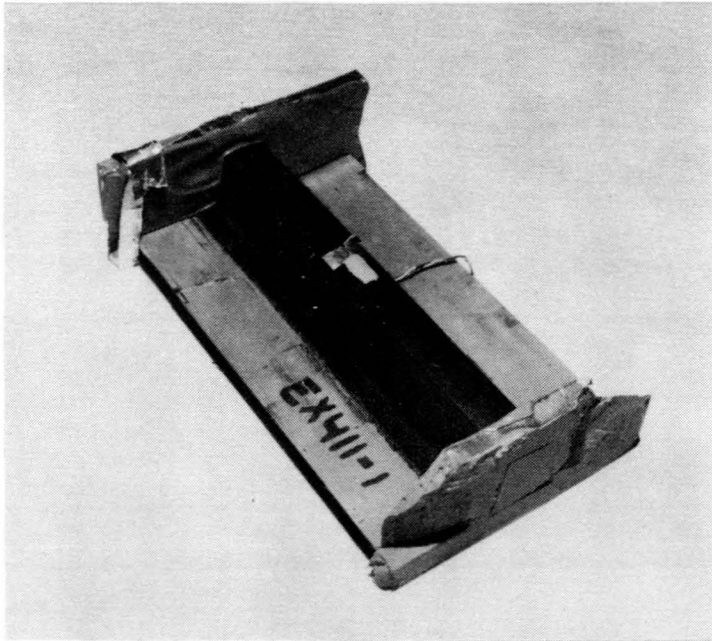
Figure 8-20. Lightly Loaded Hat-Stiffened Skin Stringer
Undamaged Control Specimen, Typical Failure Mode

Table 8-1. Test Results for Heavily Loaded Hat-Stiffened Skin-Stringer Control and Repaired Elements

Specimen Configuration ⁽¹⁾	Specimen No.	Test Temperature		Compressive Properties ⁽¹⁾			
				Ultimate Load		Repair Efficiency (%)	Failure Mode/Remarks
		C	(F)	KN/m	lb/in.		
Undamaged control.	EX411-1	23	75	904	5,167	100	Compression in cap, webs and skin; skin and web secondary.
Undamaged control.	EX411-2	316	600	700	4,000	100	Compression in cap, webs and skin; skin and web secondary.
Co-cure repair, split insert co-cure	EX411-3	23	75	846	4,833	94	Compression in cap, webs and skin; skin and webs secondary, outside repair
Co-cure repair, 1 piece insert, 16 ply cap, 4 ply webs/Rockwell repair design	EX493-1	23	75	861	4,196	81	Compression in cap, webs and skin; skin and webs secondary, outside repair
Co-cure repair, split insert	EX493-2	23	75	832	4,750	92	Compression in cap, webs and skin; skin and webs secondary, outside repair.
Co-cure repair, 1 piece insert, co-cure patch	EX493-3	316	600	664	3,792	95	Compression in cap, webs and skin; skin and webs secondary, outside repair.
Co-cure repair, split insert	EX493-4	316	600	489	2,791	70	Compression in cap, webs and skin; skin and webs secondary, outside repair.

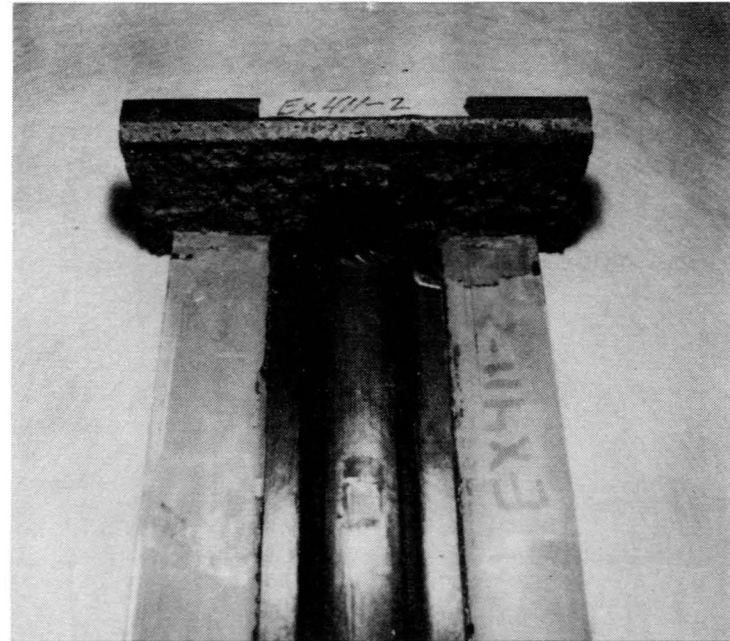
(1) Specimens were tested in a MTS 500 Kips test machine on a spherical adjustable seat after stabilizing at 600 F test/temperature for 15 to 30 minutes at a load rate of 12,500 lb/minute.

A820611 A-13



a) SPECIMEN EX411-1 TESTED
AT ROOM TEMPERATURE

A820720 C-14



b) SPECIMEN EX411-2 TESTED
AT 316°C (600°F)

Figure 8-21. Heavily Loaded Hat-Stiffened Skin-Stringer Undamaged
Control Specimens - Typical Failure Mode

The load-strain responses for the heavily loaded control specimens are presented in Figure 8-22. The test specimens were placed in the test fixture and adjusted to give equal initial strains in the cap and skins. As shown in the figure, these strains remained nearly equal to failure. The specimen tested at 316°C (600°F) had nearly identical initial response as the specimen tested at room temperature, indicating no reduction in elastic modulus; however, the elevated temperature ultimate strength was 77 percent of the room temperature value.

8.3.3 Repaired Element Test Results

A 5.08 cm (2 in.) section of the hat stiffener was removed from five test specimens. These specimens were repaired per Figure 8-18. Three of the specimens were tested at room temperature, and two were tested at 316°C (600°F). As shown in Table 8-1, the specimens tested at room temperature failed at 81 to 94 percent of the undamaged control strength, while the specimens tested at elevated temperature failed at 70 and 95 percent of the control strength. Both the room and elevated temperature tested specimens failed in a similar manner. The typical failure mode for these specimens is shown in Figure 8-23. The failure mode was compression in the cap, web, and skin approximately 7.62 cm (3 in.) from the base. Failure occurred outside the repair area at the edge of the patch. Initial failure analysis indicated a stress concentration at this point because of the scarf repair; however, the undamaged control specimens failed in the same location (Figure 8-21).

The typical load-strain responses at room temperature and 316°C (600°F) for the repaired heavily loaded hat-stiffened panels are presented in Figure 8-24, and the 316°C (600°F) failure mode is presented in Figure 8-25. Referring to the response of the specimen tested at room temperature, the strain in the cap (gage 1) is somewhat larger than in the skin (gage 2), indicating that the specimen was not placed precisely square in the test fixture. This could result in premature failure in the cap. The load transfer into the patch is shown by strain gages 3 and 4. Strains are about 17 percent higher at the edge of the patch than 2.54 cm (1.0 in.) from the edge. During the elevated temperature test, the cap and skin were strain balanced, but this particular specimen failed at 58 percent of the room temperature repair strength, although it was outside the repaired section.

8.3.4 Conclusions: Heavily Loaded Hat-Stiffened Panel Repair

The undamaged control specimen tested at room temperature failed at 86 percent of the 1.05 MN/m (6,000 lb/in.) target design strength. The undamaged control specimen tested at elevated temperature (316°C [600°F]) failed at 77 percent of the room temperature value. The repairs gave excellent results, returning the damaged specimens to 70 to 95 percent of the undamaged control strengths at room and elevated temperatures. All failures were outside the repair area, and the repaired specimens failed in the same location as the undamaged specimens.

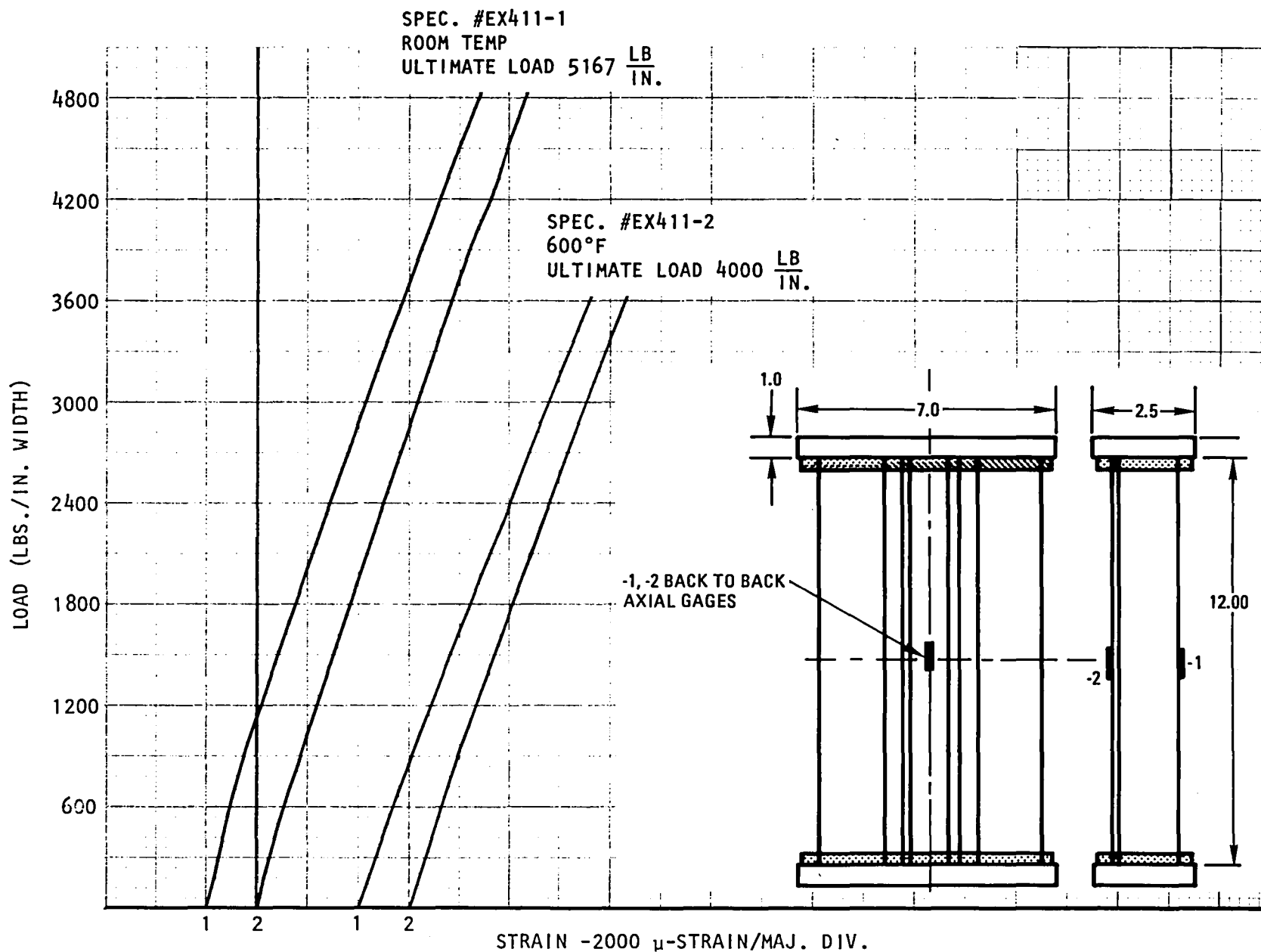
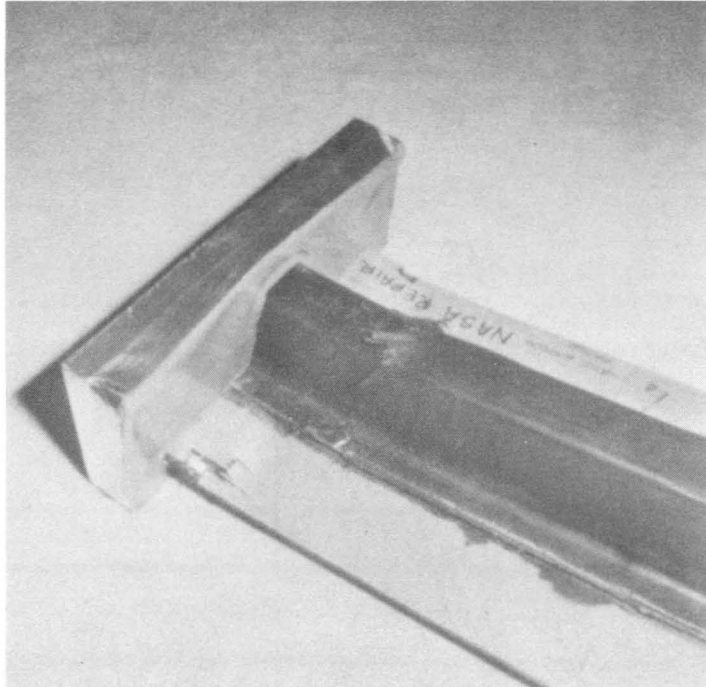


Figure 8-22. Compression Load/Strain Response of Heavily Loaded Hat-Stiffened Panels (Undamaged Control) at Room Temperature and 600°F

A820507 D-1 C



A820507 D-2 C

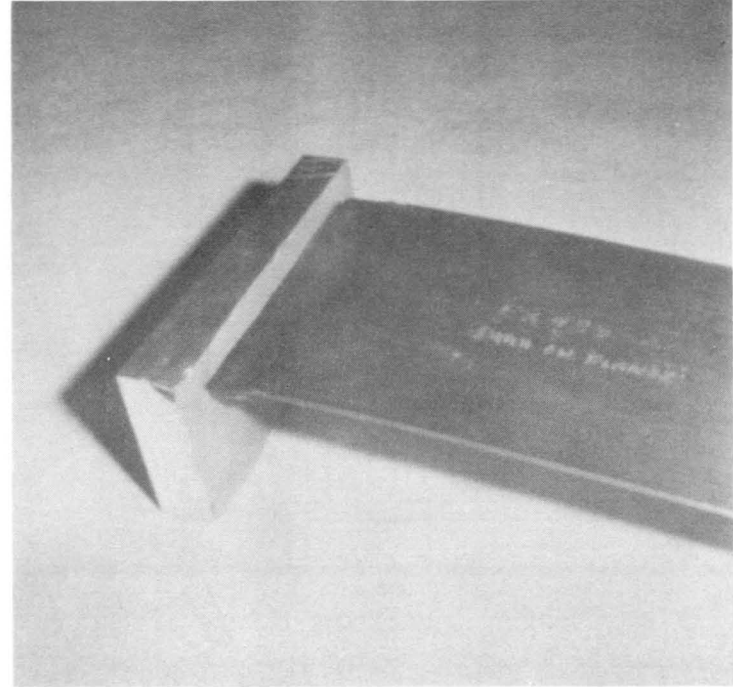


Figure 8-23. Typical Failure Mode - Heavily Loaded Hat-Stiffened Skin-Stringer Repaired Panel Tested at Room Temperature, Specimen EX493-2

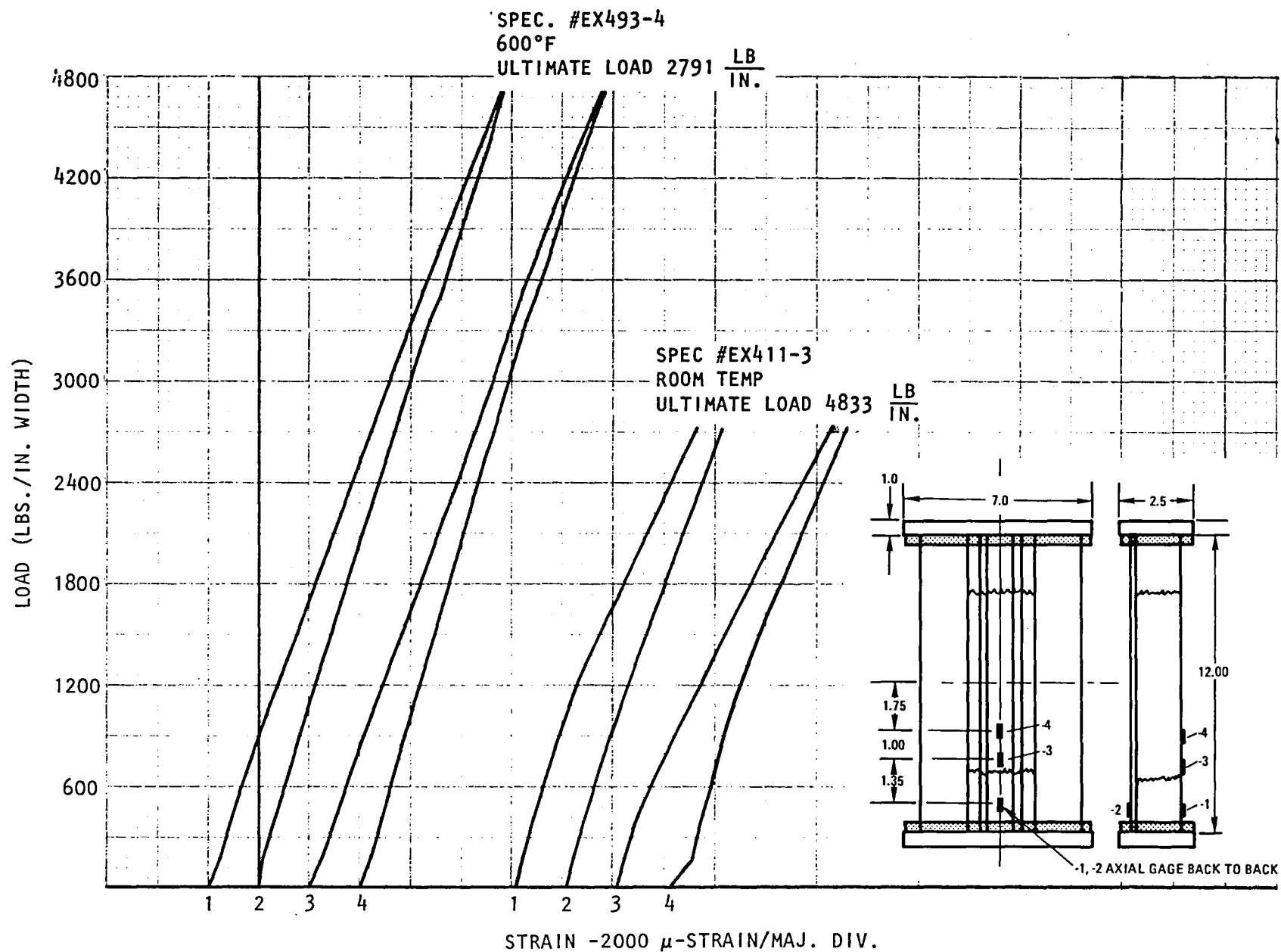


Figure 8-24. Compression Load/Strain Response of Repaired, Heavily Loaded Hat-Stiffened Panels at Room Temperature and 600°F



Figure 8-25. Failure Mode of Heavily Loaded Repaired Hat Stringer
Element Tested at 316°C (600°F)

8.4 LIGHTLY LOADED HAT-STIFFENED ELEMENT REPAIR TESTING AND RESULTS

The lightly loaded hat-stiffened panel repair program involved testing two types of specimens: undamaged control specimens and repaired specimens. The test results are summarized in Table 8-2.

8.4.1 Control Element Test Results

Undamaged control elements were tested at room temperature and 316°C (600°F). The average room temperature strength achieved was 0.268 MN/m (1,533 lb/in.) or 20 percent less than predicted. The average elevated temperature strength was 94 percent of the room temperature value. The elevated temperature strength was expected to be 75 percent of the room temperature strength, indicating the room temperature specimen had a premature failure and the analysis was not in error. As discussed in the following, the repaired specimens tested at room temperature all failed at levels greater than the undamaged control. The failure modes for these control specimens are shown in Figure 8-20. Failure occurred because of compression in the cap, web, and skin about 7.6 cm (3.0 in.) from the base. Also shown in Figure 8-20, is the room temperature test setup. Note the stabilizer bars clamped to the edges of the specimens to prevent premature buckling.

8.4.2 Repaired Element Test Results

A 5.35 cm (2.45 in.) section of the hat-stiffener was removed from seven test specimens. These specimens were repaired per Figure 8-19. Four of the specimens were tested at room temperature and three were tested at 316°C (600°F). As shown in Table 8-2, the specimens tested at room temperature failed at 111 to 135 percent of the undamaged control strength; however, the undamaged control had premature failure. The repaired specimens failed at 90 to 110 percent of the predicted control strength (0.33 MN/m, 1,900 lb/in.). The specimens tested at elevated temperature failed at 72 to 103 percent of the control strength. Both the room temperature and elevated temperature tested specimens failed in a similar manner, as shown in Figure 8-26. The failure mode was by compression in the cap, web, and skin, approximately 7.62 cm (3.0 in.) from the base. Failure occurred in the undamaged section at the edge of the repair. Initial failure analysis indicated a stress concentration at this point caused by the scarf repair; however, the undamaged control specimens failed in the same location (Figure 8-20).

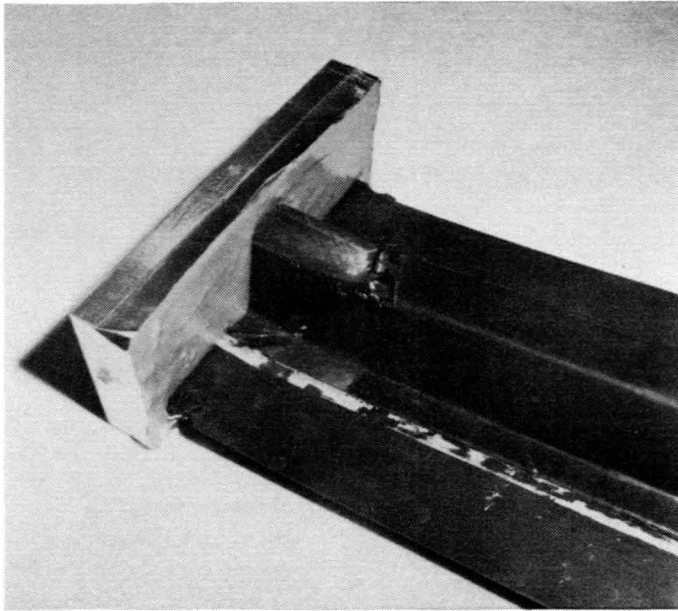
Typical load-strain responses of the lightly loaded hat-stiffened panels are presented in Figure 8-27. In both the room and elevated temperature tests, the strains at each point were nearly equal, except for gage 4, which was located in the total thickness repair area. The material at that point in the cap has a higher elastic modulus because of the added 0-degree plies (see Figure 8-19). The specimen tested at 316°C (600°F) failed at 67 percent of the room temperature repair strength. A typical failure mode is shown in Figure 8-28.

Table 8-2. Test Results for Lightly Loaded Hat-Stiffened Skin-Stringer Control and Repaired Elements

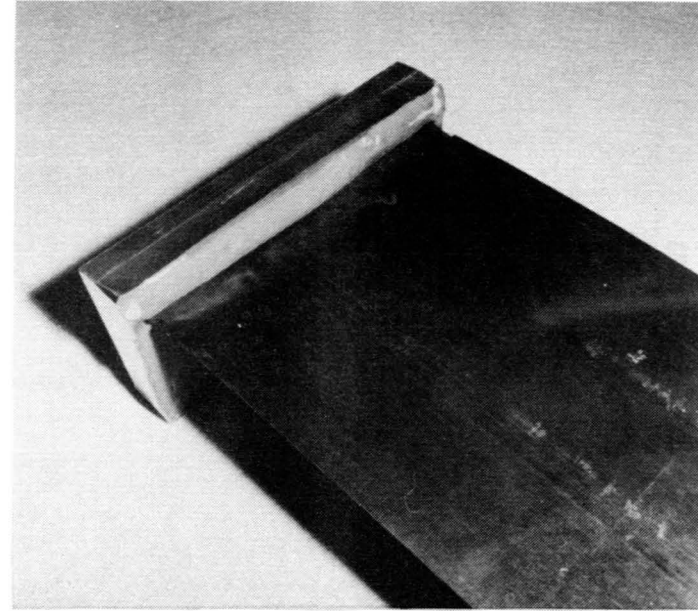
Specimen Configuration	Specimen No.	Test Temperature		Compressive Properties ⁽¹⁾				Failure Mode/Remarks
				Ultimate Load		Repair Efficiency (%)		
		C	(F)	KN/m	lb/in.			
Undamaged control	EX135-1	23	75	268	1,533	100	Compression in cap webs and skin	
Undamaged control	EX247-3	316	600	253	1,442	100	Compression in cap, skin compression secondary	
Cocure repair	EX246-1	23	75	265	2,083	135	Compression outside repair in cap, skin compression secondary	
Cocure repair	EX246-4	23	75 -	353	2,016	132	Compression outside repair in cap, skin compression secondary	
Cocure repair	EX247-1	23	75	299	1,708	111	Compression outside repair at edge of cap serrations and in webs and skin	
Cocure repair	EX247-2	23	75	299	1,708	111	Compression outside repair in cap, skin compression secondary	
Cocure repair	EX251-2	316	600	180	1,025	72	Compression outside repair in cap, skin compression secondary	
Cocure repair	EX246-2	316	600	255	1,458	103	Compression outside repair in cap, skin compression secondary	
Cocure repair	EX246-3	316	600	245	1,400	99	Compression in serrated doubler overlap area in cap, skin compression secondary	

(1) Specimens were tested in a MTS 500 Kips test machine on a spherical adjustable seat after stabilizing at 600 F test temperature for 15 to 30 minutes at a load rate of 12,500 lb/minute.

A820402 D-7 C



A820402 D-8 C



A820402 D-9 C

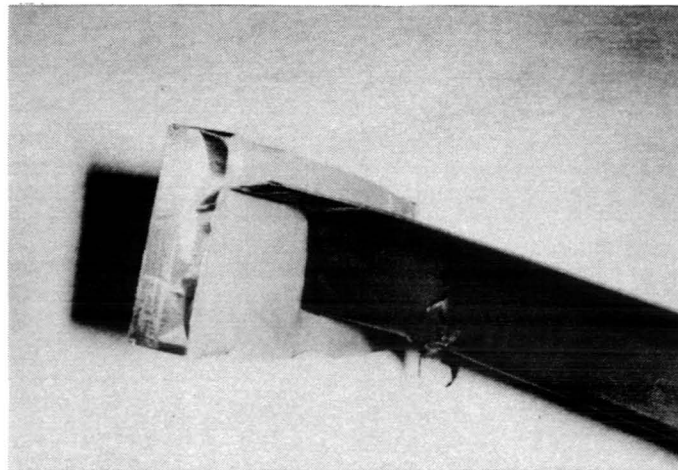


Figure 8-26. Room Temperature Compression Failure Modes of Repaired Lightly Loaded Hat-Stiffened Skin - Stringer Panel EX247-2

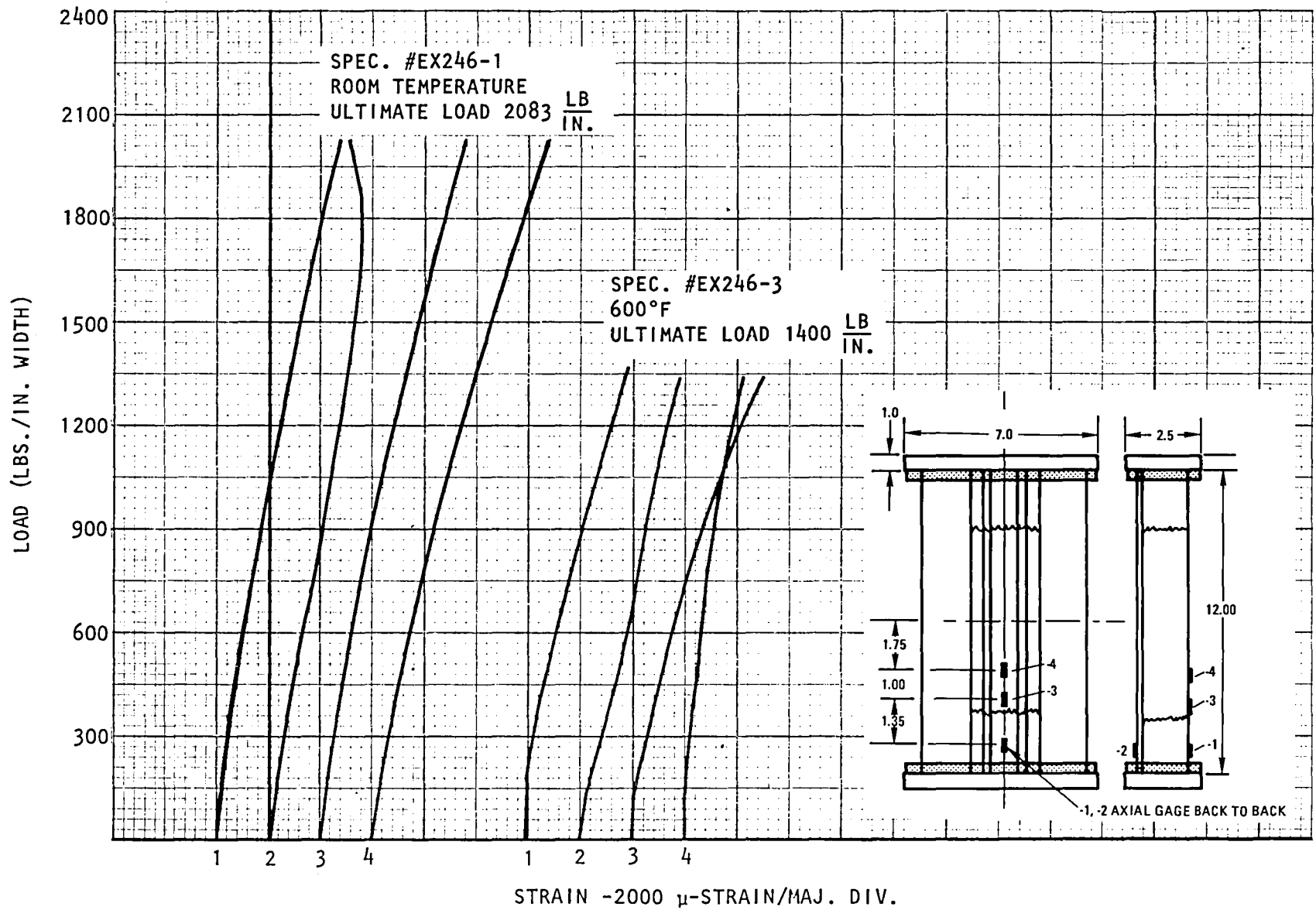


Figure 8-27. Compression Load/Strain Response of Repaired Lightly Loaded Hat-Stiffened Panels at Room Temperature and 600°F



Figure 8-28. Failure Mode of Lightly Loaded Repaired Hat-Stringer
Element Tested at 316°C (600°F)

8.4.3 Conclusions - Lightly Loaded Hat-Stiffened Panel Repair

The undamaged control specimen tested at room temperature failed prematurely at 80 percent of the 0.33 MN/m (1,900 lb/in.) target design strength. The undamaged control specimen tested at elevated temperature (316°C [600°F]) failed at 94 percent of the room temperature value. The repairs gave excellent results, returning 72 to 135 percent of the undamaged strengths at room temperature and 316°C (600°F). All failures were outside the repair area, and the repaired specimens failed in the same location as the undamaged control specimens.

9. SUMMARY AND CONCLUSIONS

Viable factory-type repair techniques have been developed for Celion/LARC-160 GR/PI structure. The repair methodology was achieved through advances in materials processing, adhesive bonding, NDI, fabrication techniques, and design concepts. The repairs were implemented on flat laminates, honeycomb sandwich panels (lightly and heavily loaded), and hat-stiffened skin-stringer panels (lightly and heavily loaded). The repair methodology was verified through compression testing at room temperature and 316°C (600°F). The repairs returned 70 to 95 percent of the undamaged control component ultimate strength at room and elevated temperatures. Specific results of the developmental program are summarized in the following.

9.1 ADHESIVE BONDED JOINT PROCESSING AND ANALYSIS DEVELOPMENT

Adhesive bonding was chosen as the primary repair method because bolted repairs have high stress concentrations, high weight penalty, and thermal incompatibility problems for 316°C (600°F) repairs. The repairs can consist of secondarily bonded precured patches, or cocured patches. Ideally, large area repairs would be made with relatively low temperatures (less than 350°F) and low pressures (less than 50 psi). Commercially available FM34B-18 adhesive cures at low temperatures and pressures, but is not suitable for large area bonding. It was determined that other adhesives capable of large area bonding, such as LARC-13 (peroxide catalyst) and LARC-160 require a minimum 288°C (550°F), 689 KN/m² (100 psi) cure cycle. Results of the secondary bonding and cocure bonding development study follow.

9.1.1 Secondary Bonding Development

Secondary bonding processes were developed for large area midplane laminate bonding using three candidate adhesives based on diglyme solvent: LARC-13, LARC-13 (peroxide catalyst), and LARC-160. Initially, inconsistent NDI C-scan test results were attained using these adhesives. Continued processing studies with the three adhesives produced consistent low void bond lines as determined by C-scan testing. Processing limits were established at 316°C (600°F), 689 KN/m² (100 psi) for the LARC-13 adhesive, and 288°C (550°F), 689 KN/m² (100 psi) for the LARC-13 (peroxide catalyst) and LARC-160 adhesives.

Results of notched lap shear tests on midplane bonded panels were inconsistent with C-scan results; often high void bonds had higher strengths than low void bonds. Relatively low lap shear strengths attained were attributed to eccentric loading during testing, which imposed a high peel moment on the joint. This resulted in interlaminar shear failure in the laminate, and not fully stressing the adhesive in true shear. This problem was resolved in later cocure bonding studies by the use of FED STD 406, Method 1042 antipeel clamps, which resulted in a near true shear stress application during testing.

Later studies determined the best secondary bonding results were attained with LARC-160 laminating resin coated on Celion unidirectional tape and bidirectional fabric. The LARC-160 adhesive was found to be superior in strength and more consistent in processing, yielding low void large area bonds with a 689 KN/m^2 (100 psi) and 288°C (550°F) cure cycle.

9.1.2 Cocure Bonding Development

The LARC-13, LARC-13 (peroxide catalyst), and LARC-160 adhesives evaluated for secondary bonding were evaluated as auxiliary adhesives in cocure process development studies. Two-stage preimidizing, cure, and single-stage in-situ imidizing cure processes were evaluated in accomplishing the cocure bond of Celion/LARC-160 preform laminates to cured laminate stock in fabrication of large area midplane bonded panels and flush-scarf angle bond joint panels. Inconsistent C-scan recordings were attained with each process, some panels having zero void and others high voids. The cause of the high void was traced to entrapment of the auxiliary adhesive high temperature boiling diglyme solvent in prepreg and bondline during cure. Correlation of lap shear strength with C-scan recording was inconclusive since high lap shear values were attained in some high void specimens.

Based on a suggestion from NASA LaRC, the Celion/LARC-160 prepreg resin in the stacked preform was used directly (no auxiliary adhesive) as the adhesive in the cocure operation. A single-stage in-situ imidizing and cure process was used. Consistent zero void, large area midplane cocure bonded laminates and bond lines were attained using $1,378 \text{ KN/m}^2$ (200 psi) and 288°C (550°F) cure parameters. Antipeel clamps were used in lap shear tests to eliminate peel and promote true shear in test. Resultant lap shear strengths were double those attained without antipeel clamps, 22.4 MN/m^2 and 21.8 MN/m^2 (3,978 and 3,156 psi) at room temperature and 316°C (600°F).

The cocure approach yielded significantly higher tensile shear strengths than specimens fabricated using the secondary bonding technique. The cocure technique was found to be more adaptable to repair operations than secondary bonding methods since prepreg preform patches will conform uniformly to complex-shaped structures more readily than precured laminate patches.

9.1.3 Cocure Scarf Joint Development (Standard and Improved)

The prepreg adhesive, in-situ imidizing and cocure process was applied to 3-degree, 4.5-degree, and 6-degree scarf angle joint panel cocure bonds. NDI C-scan recordings showed consistent zero void bonds were attained; however, bond strength was lower than the target 90 percent of parent laminate strength.

An improved repair cocure bond joint was developed following the basic approach used by Northrop Corp. for graphite/epoxy repairs. The repair design consists of a scarf angle patch overlapped externally with three-stepped plies of (0, +45) oriented unidirectional tape. Edges of the external tape plies are serrated. Northrop tests show the external doubler plies reduced peel loads into the scarf joint and the serrations provided uniform load transfer

from parent laminate into the doubler. Tests on tensile specimens following the concept verified Northrop results and yielded 99 percent joint efficiency in 4.5-degree scarf angle specimens at room temperature and 91 percent efficiency at 316°C (600°F). Maximum joint efficiencies attained in corresponding identically processed 3-degree flush scarf angle specimen tests were 59 percent at room temperature and 58 percent at 316°C (600°F).

Test equipment limitations precluded the use of the improved repair concept on the flat laminate elements; however, the improved technique was implemented on the prototype sandwich and hat-stiffened element specimens. These results are discussed in a following section.

9.1.4 Low Pressure Bonding Development

Low pressure secondary and cocure bonding techniques were investigated for repair of₂ lightly loaded sandwich structures. Low bonding pressures, less than 551 KN/m² (80 psi), were required to prevent crushing the HRH-327-3/16 -3.5 pcf glass/polyimide honeycomb core during the cure process.

Satisfactory room and elevated temperature 316°C (600°F) secondary bond lap shear strengths were achieved using 517 KN/m (75 psi) autoclave pressure and standard processing at 288°C (550°F). Relatively high void areas were detected in NDI C-scan tests. The three adhesives evaluated were LARC-160/AL123/ETOH/108 carrier, LARC-160/Celion unidirectional tape, and LARC-160/Celion fabric. The LARC-160/Celion fabric adhesive was selected for prototype sandwich repairs based on the best overall balance in strength and NDI C-scan characteristics.

Cocure midplane bonded specimens cured at 517 KN/m (75 psi) and employing the LARC-160 prepreg resin adhesive concept produced large voids in bond lines and laminates. Lap shear tests were not performed.

9.1.5 Tooling Development

During process development studies, a tooling concept was developed for both secondary and cocure bonding operations. One key feature of the tooling is a flexible pressure caul that applies uniform pressure to the repair areas. The pressure caul is comprised of a fluoro rubber elastomer, capable of service in the 316°C (600°F) range. The tooling concept allows uniform removal of prepreg volatiles using the prepreg adhesive single-stage in-situ imidizing cocure process.

9.1.6 Analytical Methods Development

Simple analytical models were developed to determine the optimum scarf angles and doubler overlaps for the repair designs. The models were based on existing adhesive bonded joint studies, and applicability of the models was based on correlation of the coupon test data from the adhesive bonding study. Because of the large scatter in the test data caused by materials, processing,

and test variables, more complex analytical models would not yield better results. The simple models yield useful, general answers that were used to design working repairs.

9.2 FLAT LAMINATE REPAIR

Several flush and doubler repair design concepts were implemented on 15.2 by 30.5 by 0.23 cm (6.0 by 12.0 by 0.091 in.) flat laminate elements (0, +45, 90)_{2s} orientation using the LARC-160 prepreg resin cocure processed developed on coupon specimens. NDI C-scan tests performed on 3- and 6-degree scarf angle flush repaired elements showed zero void cocure bonds and laminate patches were achieved. Cocure repaired elements with external doublers showed some void areas. Elements were tested in compression at room temperature but not at 316°C (600°F) because of potential test fixture constraints. A flush repair with a 3-degree scarf angle was found to yield the best results, returning nearly 80 percent of the undamaged laminate strength. An improved cocure repair design, which added serrated patch plies, was fabricated but could not be tested in the special test fixture. This improved design was predicted to return over 90 percent of the laminate original strength.

9.3 HONEYCOMB SANDWICH REPAIR

Two types of honeycomb sandwich panel configurations were used for repair development and demonstration. The first type is a heavily loaded panel designed by NASA/LARC to carry a compression load of 2.1 MN/m (12,000 lb/in.). The second type is a lightly loaded panel designed by Rockwell to withstand 0.53 MN/m (3,000 lb/in.). The honeycomb sandwich repair program involved testing of three types of specimens: undamaged control laminates damaged control laminates with a 5.08 cm (2 in.) diameter hole, and repaired specimens. The test element measured 20.7 by 30.5 cm (8.15 by 12.00 in.). The heavily loaded design consists of 16-ply (0, +45, 90)_{2s}, 0.23 cm (0.091 in.) Celion/LARC-160 face sheets bonded to 2.54 cm (1.00 in.) thick HRH-327 3/16-6.0 pcf core. The lightly loaded design consists of 8-ply (0, +45, 90)_s 0.051 cm (0.02 in.) face sheets bonded to 4.69 cm (1.85 in.) core. In the sandwich repair, the processes developed for the repair of flat laminates were directly extended to the repair of honeycomb sandwich panels. The repair consists of a precured solid laminate plug bonded into a recess in the core. This plug provides the base for cocuring the patch plies on the face sheet laminate and prevents dimpling. The patch has a 4.5-degree scarf with three external serrated octagonal patch plies added.

Control, damaged and repaired elements were compression tested at room temperatures and 316°C (600°F). Repair efficiency of the heavily loaded elements at room temperature ranged between 75.7 and 90.6 percent of control element strength, and 75.4 percent of control strength at 316°C (600°F). Elevated temperature, 316°C (600°F), significantly reduced the laminate compressive strength: undamaged strength, 63 percent of room temperature value; damaged strength, 56 percent of room temperature damaged value; and repaired strength, 53 percent of repaired room temperature value.

There were no problems observed in 288°C (550°F), 517 KN/m² (75 psi) cocure repair operations on lightly loaded elements. Visually, the skin patches appeared well compacted and had high aesthetic quality; however, NDI C-scan recordings showed a high void condition through the 5.08 cm (2.0 in.) center section of the repair and a satisfactory condition outside the center section.

Cocure bond repairs, using the improved design concept demonstrated on flat laminates and highly loaded sandwich elements that were compression tested at room temperature, yielded efficiencies of 82.4 and 102 percent of undamaged control elements. Two elements tested, one each at room temperature and 316°C (600°F), failed in the repair area at 91 and 70.9 percent efficiency of control element strengths, respectively. Compression strengths of undamaged control specimens and repaired specimens at 316°C (600°F) were 85 percent and 67 percent of respective elements tested at room temperature.

A secondary bond repair implemented on a lightly loaded design element yielded 75 percent repair efficiency in room temperature compression tests. Compression failures occurred outside the repair area in the parent laminate skins.

9.4 HAT-STIFFENED SKIN-STRINGER REPAIR

Two types of hat-stiffened skin-stringer panel configurations were used for repair development and demonstration. The first type is a heavily loaded NASA LaRC design consisting of 16-ply skin, 8-ply web, and a 6-ply cap. The second type is a lightly loaded Rockwell design consisting of 8-ply skin, 4-ply web, and a 16-ply cap. The elements were 15.24 cm (6.0 in.) wide and 30.48 cm (12.0 in.) long. The heavily loaded panel was designed to carry 1.05 MN/m (6,000 lb/in.), while the lightly loaded panel was designed to carry 0.33 MN/m (1,900 lb/in.). Hat-stringer repairs were developed on elements with a simulated 5.08 cm (2.00 in.) damage area in the hat assembly. A variation of the cocured flush scarf angle patch with external serrated edged doubler was implemented in repair of hat-stringer details. A unique feature of the repair concept is a premolded insert that is installed and secondary bonded inside the hat stringer to provide a solid support backup for the cocured patch during the repair operation. The insert also provides additional shear area in the repair bond joint, thus adding strength to the repair. Repair installations had an excellent aesthetic appearance with smooth transition between the repair area and parent material. The serrated edges terminating the external doubler plies showed good definition and all layers were well compacted. The repair installations conformed well to the baseline element configuration without distortion. NDI C-scan A-sensitivity test recordings showed low void in the web and flange areas. The 0-degree cap repair area showed some voids in the tapered bond section. Control and repaired elements were compression tested at room temperature and 316°C (600°F).

Repair efficiency of the heavily loaded repaired elements ranged between 81 and 94 percent at room temperature, and 70 and 95 percent at 316°C (600°F). All specimens failed in the same location just outside of the repair area. Compressive strength of undamaged control specimens tested at 316°C (600°F) was 77 percent of the element tested at room temperature.

Repair efficiencies of the lightly loaded element ranged between 111 and 135 percent at room temperature. All failures occurred outside of the serrated edged doubler in the same location as the control specimens. However, the undamaged control specimen failed prematurely at 80 percent of the target design strength. Three elements tested at 316°C (600°F) yielded 72, 103, and 99 percent joint efficiency, respectively. Two failures occurred outside the serrated edged doubler and one in the doubler overlap area. Compression strength of undamaged control specimens at 316°C (600°F) tested yielded 94 percent of the room temperature tested element.

10. REFERENCES

1. Development and Demonstration of Manufacturing Processes for Fabricating Graphite/LARC-160 Polyimide Structural Elements. NASA CR-165809, Dec. 1981.
2. Labor, J.D. and Myhre, S.H. Large Area Composite Structure Repair. AFFDL-TR-79-3040 (Mar. 1979).
3. Engineering Design Handbook, Joining of Advanced Composites. DARCOM-P 706-316 (Mar. 1979).
4. Hart-Smith, L.J. Adhesive-Bonded Single-Lap Joints. NASA CR-112236 (Jan. 1973).
5. Hart-Smith, L.J. Adhesive-Bonded Double-Lap Joints. NASA CR-112235 (Jan. 1973).
6. Hart-Smith, L.J. Adhesive-Bonded Scarf and Stepped-Lap Joints. NASA CR-112237 (Jan. 1973).
7. Hart-Smith, L.J. Analysis and Design of Advanced Composite Bonded Joints. NASA CR-2218 (Aug. 1974).
8. Develop, Demonstrate, and Verify Large Area Composite Structural Bonding With Polyimide Adhesives. NASA CR-165839, May 1982.
9. Ashton, J.E., et al. Primer on Composite Materials: Analysis, Technomic Publication Company (1969).
10. Jones, J.S. Celion/LARC-160 Graphite/Polyimide Composite Processing Techniques and Properties. SAMPE 14th National Technical Conference (Oct. 1982).
11. Advanced Composites Design Guide. AFML Wright-Patterson Air Force Base, United States Air Force, Vol. II, Analysis, Third Edition (Jan. 1973).
12. Beck, C.E. Advanced Composite Structure Repair Guide. AIAA 21st Conference (1980). AIAA-80-0774.
13. Myhre, S.H. and Beck, C.E. Repair Concepts for Advanced Composites Structures. AIAA Journal (Oct. 1979).
14. Lugin, G. et al. Repair Technology for Boron/Epoxy Composites. AFML-TR-71-270 (Feb. 1972).
15. Studer, V.J., and LaSalle, R.M. Repair Procedures for Advanced Composite Structures. AFFDL-TR-76-57 (Dec. 1976).

16. McCarty, J.E., Horton, R.E., et al. Repair of Primary Bonded Structure. AFFDL-TR-78-79 (June 1978).
17. Foreman, C., McGovern, S.A., and Knight, R. S-3A Graphite/Epoxy Spoiler Fabrication of Ten Shipsets and Damage Repair Study. NADC-76234-30, Final Report (May 1976).
18. Chatterjee, S.N., Hashin, Z. and Pipes, R.B. Definition and Modeling of Critical Flaws in Graphite Fiber Reinforced Resin Matrix Composite Materials. NADC-77278-30 (Aug. 1979).
19. Labor, J.D., et. al. Structural Criteria for Advanced Composites, Vol. I Summary. AFFDL-TR-76-142 (Mar. 1977).
20. Joining of Advanced Composites. Alexandria, Virginia: United States Army Material Development and Readiness Command, NTIS AD72362.
21. Dreger, D.R. Design Guidelines for Joining Advanced Composites. Machine Design (May 8, 1980), Vol. 52, No. 10, P89-93
22. Lehman, E.M., Hawley, A.V., et. al. Investigation of Joints in Advanced Fibrous Composites for Aircraft Structures. AFFDL-TR-69-43 (June 1969).
23. Peterson, J. Toward Rational Design of Adhesive Joints. SAMPE Quarterly, July, 1971.
24. Hart-Smith, L.J. Bolted Joints in Graphite/Epoxy Composites. NASA CR-144899 (June 1976).
25. Ashton, J.E., and Witney, J.M. Theory of Laminated Plates. Progress in Materials Science Series, Technomic Publ. Co., c.(1970).
26. Bohlmann, R.E., Glaser, D.A., and Watson, J. Field Repair of Composite Structural Components. NADC-78073-60 (Feb. 1980).
27. Horton, R.E. and McCarty, J.E. Adhesive Bonded Aerospace Structures Standardized Repair Handbook. AFML-TR-77-206, AFML-TR-77-139 (Dec. 1977).
28. Knight, R.C., and Rosenzweig, E.L. S-3A Composite Spoilers Service Experience. 12th National SAMPE Conference (Oct. 1980).
29. Stone, R.H. Development of Repair Procedures for Graphite/Epoxy Structures on Commercial Transports. 12th National SAMPE Conference (Oct. 1980).
30. Scow, A.L. Large Area Composite Structure Repair. AFFDL-TR-77-5, (May 1977).
31. Kiger, R.W. and Myhre, S.H. Large Area Composite Repair. Second Interim Report, AFFDL-TR-77-121 (Nov. 1977).
32. Kiger, R.W. and Beck, C.E. Large Area Repair Concepts for Composite Aircraft Structures. ASTM 5th Conference (Mar. 1978).

33. Myhre, S.H., and Labor, J.D. Repair of Advanced Composite Structures.
AIAA 21st Conference (1980).

APPENDIX A
MATERIAL SPECIFICATIONS AND
BASELINE LAMINATE FABRICATION PROCESSES

A.1 MATERIAL PROCUREMENT SPECIFICATIONS

A.1.1 Celion/LARC-160 Unidirectional Prepreg Tape Materials

U.S. Polymeric, Inc. was selected as the supplier for prepreg tape materials used in this program. U.S. Polymeric, Inc. prepreg material physical properties certification data are given in Table A-1. Requirements were as follows.

1. Nominal 0.007/cm (0.0028 in.)/ply at 60 percent composite fiber volume
 - Fiber type: Celion 3000, NR150-B2 sized
 - Resin type: LARC-160
 - Fiber areal weight: 76 grams/m² +3
 - Resin solids: 34 +4/-0
 - Volatile content: 12% +3
 - Tape width: 15.24 cm (6.0 in.)
2. Nominal 0.0145 cm (0.0057 in.)/ply at 60 percent composite fiber volume
 - Fiber type: Celion 6000m NR159B2 sized
 - Resin type: LARC-160
 - Fiber areal weight: 152 grams/m² +3
 - Resin solids: 34 +4/-0
 - Volatile content: 12% +3
 - Tape width: 15.24 cm (6.0 in.)
3. Prepreg material procurement

A.1.2 Adhesives

Adhesive requirements were as follows.

1. American Cyanamid Co.: FM34B-18 440 grams/m² (0.09 psf) adhesive film supported on 104 fiberglass
2. American Cyanamid Co.: BR34B-18, aluminum filled adhesive paste, 82 percent solids
3. LARC-13 and LARC-160 aluminum-filled adhesives based on ester processing and diglyme solvents developed in ref. 8 adhesive materials prepared by Rockwell were coated on 108-style fiberglass carriers

Table A-1. Prepreg Physical Properties⁽¹⁾

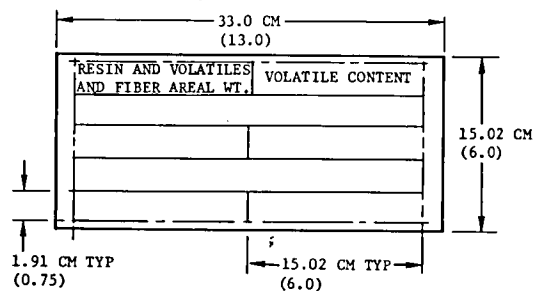
Prepreg Batch No.	Resin Batch	Fiber Data (4)			Fiber Areal Weight (gram/m ²)	Calc Ply Thick., 60% Fiber Vol		Resin Solids Cont. (%)	Volatile Cont. (%)	Roll Weight Kilograms (lb)	Defects No.	Remarks
		Batch/ No. Filaments	Tensile Strength, MN/m ² (ksi)	Tensile Modulus GN/m ² (msi)		CM	(mils)					
					U.S.P. Data (3)							
					Rockwell Data (2)							
		Length Cross Meters (feet)	Meters (feet)									
2W4885 R1	WR 7039	HTA-7 9X31/3K	3190 (463)	233 (33.8)	75.6 73.2 70.5 73.0 72.2	.0071 .0069 .0066 .0069 .0069	(2.8) (2.7) (2.6) (2.7) (2.7)	36.8 39.5 42.7 40.8 41.0	12.4 11.4 12.5 11.8 11.9	4.9 (10.8) 233 (777)	9 3.45 (11.5)	Good fiber collimation, surface smoothness and handling tack
2W4886 R1	WR 7039	HTA-7 9522/6K	3280 (476)	237 (34.4)	144 154 141 148 148	.0132 .0147 .0147 .0190 .0140	5.2 (5.8) (5.3) (5.5) (5.5)	37.6 36.9 39.1 36.6 37.5	11.6 11.2 12.2 10.6 11.3	4.4 (9.6) 107 (358)	13 5.1 (17.0)	Good fiber collimation, surface smoothness and handling tack
2W4886 R2	WR 7039	HTA-7 9522/6K	3280 (476)	237 (34.4)	145 151 137 152 147	.0132 .0142 .0130 .0145 .0140	5.2 (5.6) (5.1) (5.7) (5.5)	38.0 34.5 37.9 35.1 35.1	11.6 11.6 13.3 12.3 12.4	3.9 (8.6) 89.4 (298)	16 2.8 (9.5)	Good fiber collimation, surface smoothness and handling tack
2W4886 R3	WR 7039	HTA-7 9522/6K	3280 (476)	237 (34.4)	146 148 141 149 146	.0147 .0140 .0147 .0142 .0140	5.3 (5.5) (5.3) (5.6) (5.5)	38.0 36.1 37.6 35.9 36.6	11.5 12.2 12.9 12.2 12.4	4.8 (10.5) 117 (389)	20 4.0 (13.5)	Good fiber collimation, surface smoothness and handling tack

(1) Prepreg specification requirements:

Batch 2W4885R1: Fiber areal weight, 76 ± 3 grams/m²; calculated thickness/ply, 0.0074 cm (2.85 mils) resin solids, $34 \pm 4\%$; volatiles $12 \pm 3\%$

Batch 2W4886R1, R2, R3: Fiber areal weight, 152 ± 3 grams/m²; calculated thickness/ply, 0.0148 (5.70 mils); resin solids, $34 \pm 4\%$; volatiles, $12 \pm 3\%$

(2) Prepreg Sampling Plan



(3) U.S. Polymeric Inc. material certifications

(4) Celanese fiber certification

4. U.S. Polymeric, Inc. Celion 6000/LARC-160 unidirectional tape, 152 grams/m 0.007 cm (5.7 mils) per ply
5. Fiberite Corp.: Celion 1000/LARC-160 fabric, 35 by 35 5-harness satin weave, epoxy size
6. Rockwell; LARC 160 resin/AL 123/ETOH solvent/108 fiberglass carrier, 440 grams/m (0.09 psf)

A.1.3 Honeycomb Core

Honeycomb core requirements are as follows.

1. Hexcel fiberglass/polyimide, type HRH-327, 3/16 - 3.5 pcf, 4.70 cm (1.85 in.) thick
2. Hexcel fiberglass/polyimide, type HRH-327, 3/16 - 6.0 pcf, 2.54 cm (1.00 in.) thick

A.2 CELION/LARC-160 UNIDIRECTIONAL TAPE MATERIAL QUALIFICATION

Unidirectional prepreg tape material batches 2W4885 and 2W4886 purchased from U.S. Polymeric, Inc., were evaluated for conformance to procurement specifications using the following procedures.

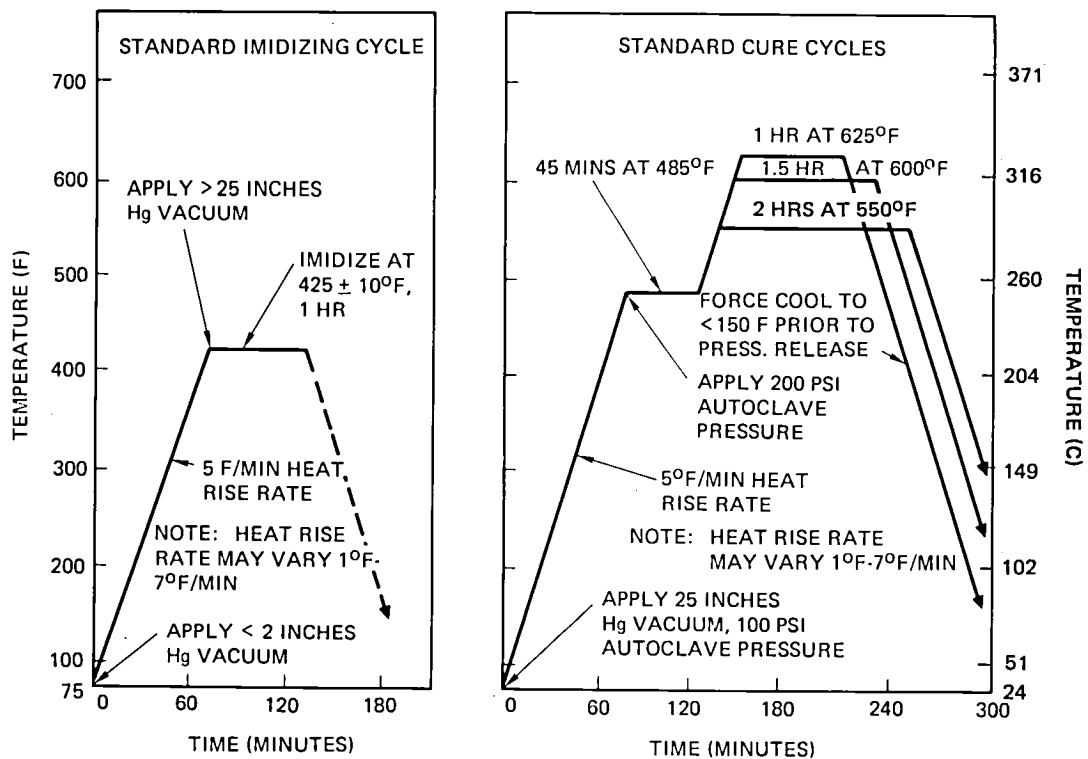
A.2.1 Initial Prepreg Testing and Results

Initial prepreg testing and results include:

1. Prepreg physical properties test results showed the four individual rolls of material to have excellent cosmetic quality and good handling tack
2. The requirements for resin solids (34 percent ± 4) and fiber areal weight (76 grams/m² ± 3) were not achieved on batch 2W4885 while the volatile content was within requirements (12 percent ± 3).
3. Batch 2W4886 R1, R2, and R3 achieved the target resin solids requirement of 34 percent ± 4 on an average basis. The fiber areal weight requirement of 152 grams/m ± 3 was not achieved, ranging between 145 and 147 grams/m. The volatile requirement of 12 grams/m ± 3 was achieved.
4. Detailed prepreg physical properties are presented in Table A-1

A.2.2 Laminate Fabrication

Unidirectional laminates, 15.2 by 15.2 cm (6.0 by 6.0 in.) 24 plies, batch 2W4885 R1, and 14 plies, batch 2W4886 R1, were prepared using the lay-up, two-step imidizing and cure cycles described in Figure A-1, except



STANDARD 2 STAGE CELION/LARC 160 IMIDIZING AND CURE CYCLE

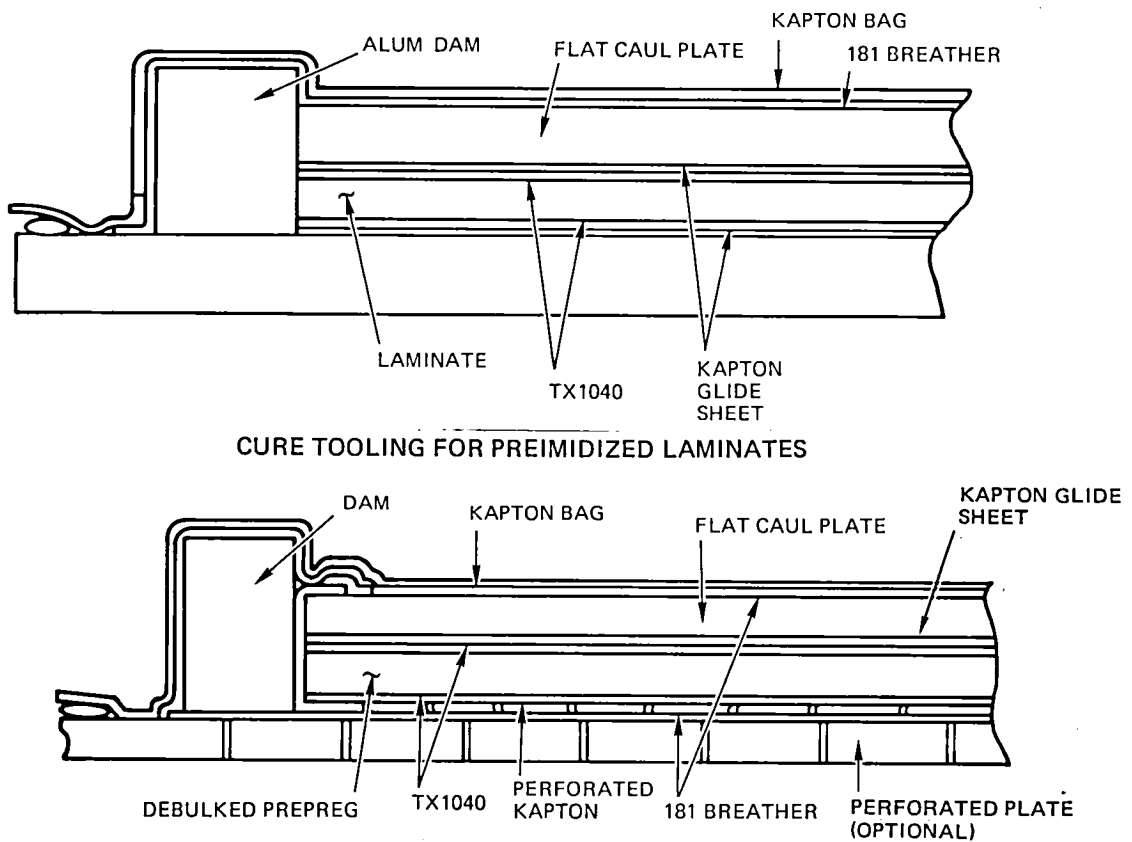


Figure A-1. Celion/LARC-160 Laminate Two-Stage Cure Cycle and Tooling Concept

EX 345

Figure A-2. NDI-C Scan A Sensitivity Recording of USP Prepreg
Batch 2W4885R1 24-Ply Qualification Panel -
210°C (410°F) Imidizing Cycle

imidizing was accomplished at 191°C (375°F) for 1 hour. Cure was accomplished by applying 689 KN/m² (100 psi) at the start, raising the part temperature to 288°C (550°F) at 1.6° to 3.9°C (3.0° to 7.0°F)/per minute, and curing for 3 hours.

A.2.3 Results of Laminate Fabrication

Excessive resin flow was noted from laminate edges and mass fiber washing between parts and edge dams. Laminate edges were tapered, centers crowned, and considerable warpage noted because of fiber washing. Composite physical properties were not run because of poor quality of the laminate; however, NDI C-scan A-sensitivity ultrasound transmission was very good (greater than 98 percent) considering the tapered, warped condition of the laminates.

A.2.4 Problem Resolution

High resin flow problems were reduced by raising the imidizing temperature to 199°C (390°F) and staging for 60 to 90 minutes. Further staging was accomplished at 252°C (485°F) during the cure cycle to ensure complete imidization occurs.

This same higher imidizing temperature approach was employed in making four additional laminates from prepreg batches 2W4885 and 2W4886. Laminates EX342 and EX343, imidized at 199°C (390°F) for 90 minutes, showed some reduced resin flow and fiber washing from the 191°C (375°F) imidized laminates, but edge tapering and warping conditions were still present. Laminates EX345 and EX346, imidized at 218°C (425°F) for 1 hour, demonstrated minimum resin flow, with small resin beads formed at panel ends. Minimum edge tapering was noted and panels were flat. NDI C-scan A sensitivity tests showed 100 percent ultrasound transmission (Refer to a typical recording, Figure A-2). Composite physical properties tests verified high quality by NDI C-scan recordings 60 percent ± 2 fiber volume and calculated less than 0.5 percent void contents. Target values are detailed physical properties are presented in Table A-2. TMA-Tg tests were performed to determine thermal stability of postcured laminates. Results showed good stability was attained: 334°C (633°F) for both EX345 and EX346 composites; TMA-Tg curves are shown in Figure A-3. Flexural strength, elastic modulus, and short beam shear tests were performed at room temperature and 316°C (600°F) to determine basic mechanical properties of the postcured laminates. Lower than target results were realized in flexural strength and elastic modulus values in both laminates. Short beam shear properties were in line with those attained in previous tests. Since the tape materials have good overall cosmetic quality, handling tack, prepreg, and composite physical properties are within reasonable limits, the materials was considered acceptable for repair technique development efforts.

Table A-2. Celion/LARC-160 Composite Physical and Mechanical Properties, Prepreg Qualification

Properties	Laminate	EX 345	EX 346
USP Prepreg Batch No.		2W4885R1	2W4886R1
<u>Composite Physical Properties</u>	<u>Target Property</u>		
1. Specific gravity (grams/cc)	1.579 - 1.561	1.570	1.553
2. Resin weight content (%)	31.29 - 34.98	32.01	35.46
3. Fiber volume (%)	62 - 58	60.9	57.3
4. Void volume (%)	<2	0.31	0.35
5. Barcol hardness (ASTM 2583)	>70	72-73	75-78
6. Weight loss in postcure (%)	<1	0.57	0.28
7. TMA-Tg °C (°F)			
Postcured 4 hr at 316°C (600°F)	>340 (644)	334 (633)	334 (633)
8. C-Scan ultra sound transmission			
Postcured 4 hr at (600°F) (%)	>95	100	100
<u>Composite Mechanical Properties⁽²⁾</u>		MN/m ² (ksi)	MN/m ² (ksi)
1. Flexural strength	MN/m ² (ksi)	(193)	—
RT		(208)	(206)
		(203)	(199)
	Avg	<u>1385</u>	<u>1399</u>
		(201)	(203)
Avg normalized strength, 60% F/V	>1571 (>228)	1364 (198)	1455 (211)
316°C (600°F)		(104)	(111)
		(107)	(116)
		(116)	(120)
	Avg	<u>751</u>	<u>799</u>
		(109)	(116)
Avg normalized strength, 60% F/V	>937 (>136)	740 (107)	831 (121)
2. Flexural modulus	GN/m ² (msi)	GN/m ² (msi)	GN/m ² (msi)
RT		(16.2)	—
		(16.1)	(16.1)
		(16.6)	(15.8)
	Avg	<u>112</u>	<u>110</u>
		(16.3)	(16.0)
Avg normalized modulus, 60% F/V	>124 (>18)	110 (16.1)	114 (16.6)
316°C (600°F)		(14.4)	(14.1)
		(14.5)	—
		(15.5)	(15.0)
	Avg	<u>102</u>	<u>101</u>
		(14.8)	(14.6)
Avg normalized modulus, 60%, F/V	>124 (>18)	101 (14.6)	105 (15.2)
3. Short beam shear strength	MN/m ² (ksi)	MN/m ² (ksi)	MN/m ² (ksi)
RT	>103 (>15)	(17.0)	(15.0)
		(16.9)	(15.7)
		(16.6)	(15.6)
	Avg	<u>116</u>	<u>106</u>
		(16.8)	(15.4)
316°C (600°F)	>48 (>7)	(6.9)	(5.3)
		(6.5)	(5.1)
		(5.7)	(4.9)
	Avg	<u>44.1</u>	<u>35.1</u>
		(6.4)	(5.1)

(1) NDI-C-Scan Tests were performed using the NASA-LaRC established "A" sensitivity standards

(2) Specimens were tested after stabilizing at 600°F for 10 minutes at a load rate of 0.127 cm (0.05 inch)/minute.

SAMPLE: <i>PI Laminates</i> BATCH 2W4885R1, 24 PLIES BATCH 2W4886R1, 14 PLIES POSTCURED 4 HOURS AT 316C (600F) ORIGIN:	SAMPLE HEIGHT <i>() mls</i>	X-AXIS SCALE <i>50</i> $\frac{^{\circ}\text{C}}{\text{DIV.}}$	RUN NO. _____
	LOADING ON TRAY <i>5g.</i>	Y-AXIS SCALE <i>.008</i> $\frac{\text{MV}}{\text{IN.}}$	DATE <i>1-6-81</i>
	PROBE: <u>EXPANSION/PENETRATION</u>	Y-AXIS SENSITIVITY _____	OPERATOR <i>[Signature]</i>
	HEATING RATE <i>5</i> $\frac{^{\circ}\text{C}}{\text{MIN}}$	_____ $\frac{\text{IN. PROBE DISPL.}}{\text{IN. OF CHART}}$	

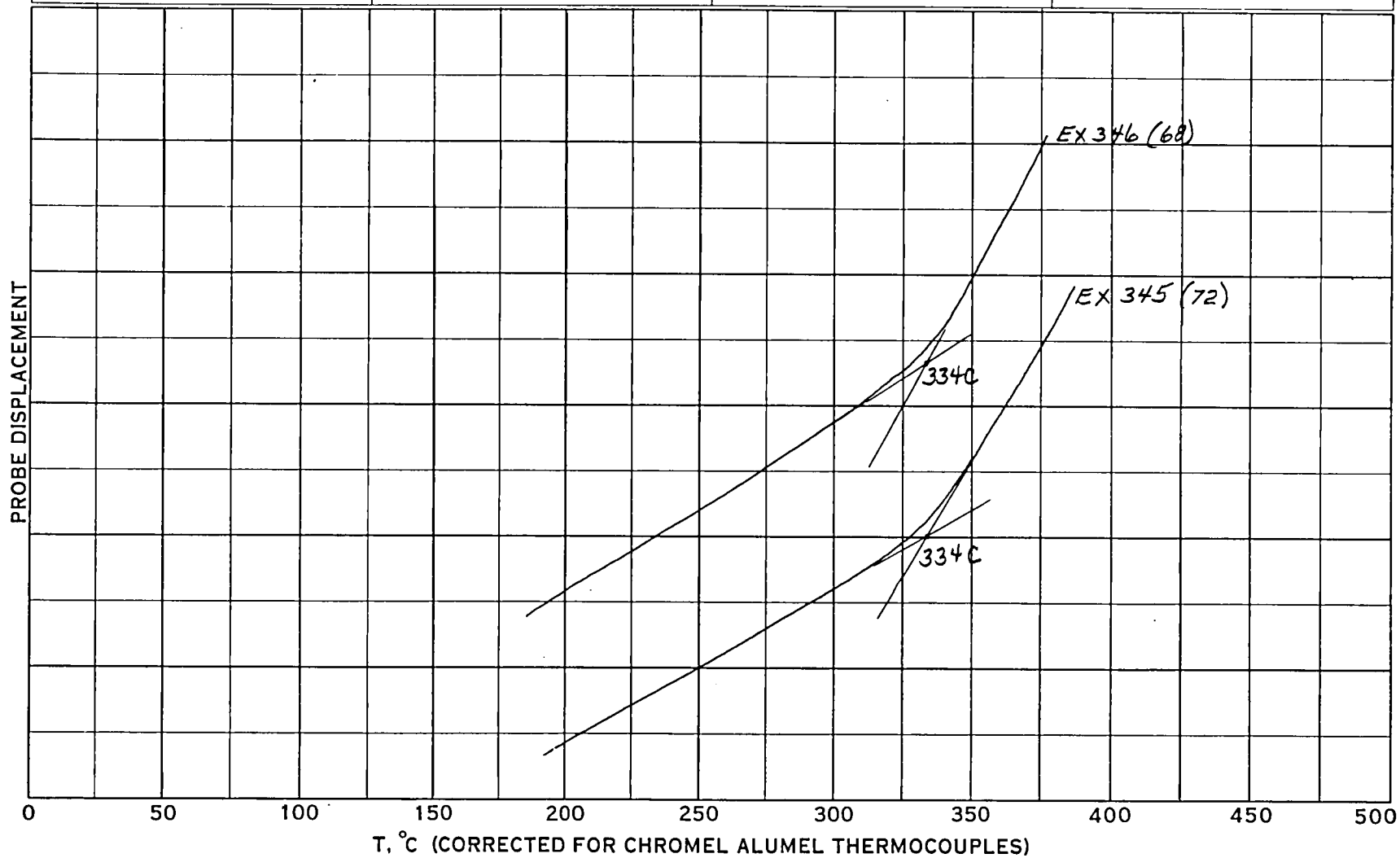


Figure A-3. TMA-T_q Characteristics of Celion/LARC-160 Laminates -
 Batches 2W4885R1 and 2W4886R1

A.3 BASELINE FLAT LAMINATE AND STRUCTURAL ELEMENT FABRICATION PROCESSES

A single step in-situ imidizing autoclave cure cycle was developed under a process improvement study. This cure cycle and concurrently developed tooling concepts were used on this program in fabrication of subsequent quality control laminates, flat laminates, and hat elements used in coupon specimens and baseline structural elements. These process and tooling techniques are described in Figure A-4.

A.3.1 Objectives of the Process Improvement Study

The primary objective of the process improvement study was to develop a simplified, reliable in-situ imidizing and autoclave molding process that would consistently yield laminates with high and uniform quality. The in-situ imidizing process was accomplished by imidizing the laminate preform under low-vacuum bag pressure to 218°C (425°F) during the initial phase of the cycle, which increased hot melt resin viscosity, and thereby reduced the flow. After imidization was complete, 1,378 KN/m² (200 psi), augmented pressure was applied, and hot melt resin flow occurred normally in the 273°C to 288°C (525°F to 550°F) temperature range when the part was taken to ultimate cure temperature 288°C to 316°C (550°F to 625°F).

A.3.2 Process and Tooling Improvements

To further process and tooling improvements, it was desired to employ a bleederless molding technique, which requires near net resin solid in the prepreg material. Net resin solids required in a 60 percent ± 2 fiber volume laminate is 33.1 percent ± 1.8 ; therefore, unidirectional prepreg tapes were purchased from U.S. Polymeric, Inc., to a 34 ± 3 resin solid content, which would yield the target fiber volume with compensation for small resin losses into the breather material.

A.3.3 Volatile Release

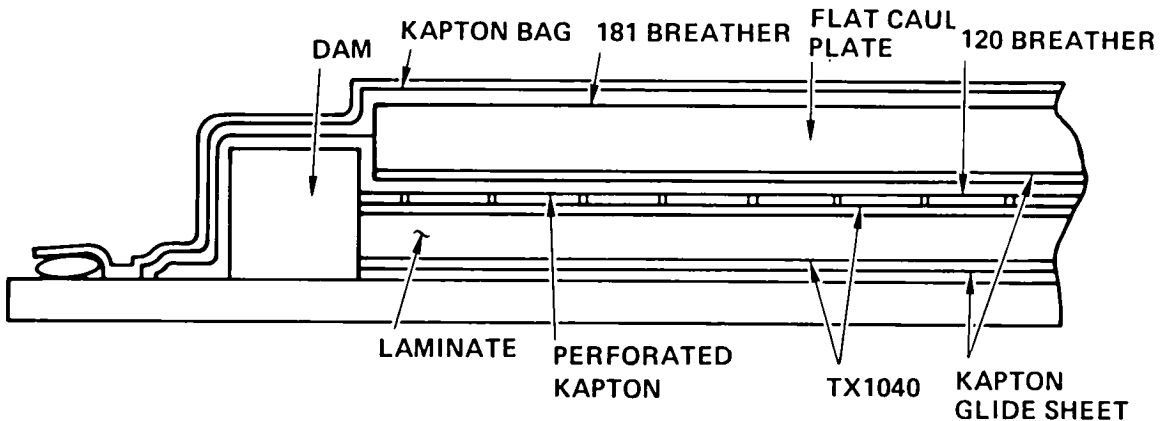
Kapton film with random needlepoint perforations, which were located approximately 1.0 inch on centers, was utilized as the porous separator. Satisfactory resin flow control and uniform volatile removal through the perforated Kapton film into the breather layer were achieved. Perforated tooling cauls were eliminated and volatiles were removed laterally across the breather material. Later studies on small area parts demonstrated that the perforated Kapton film and breather materials could also be eliminated.

A.3.4 Complex Shaped Parts

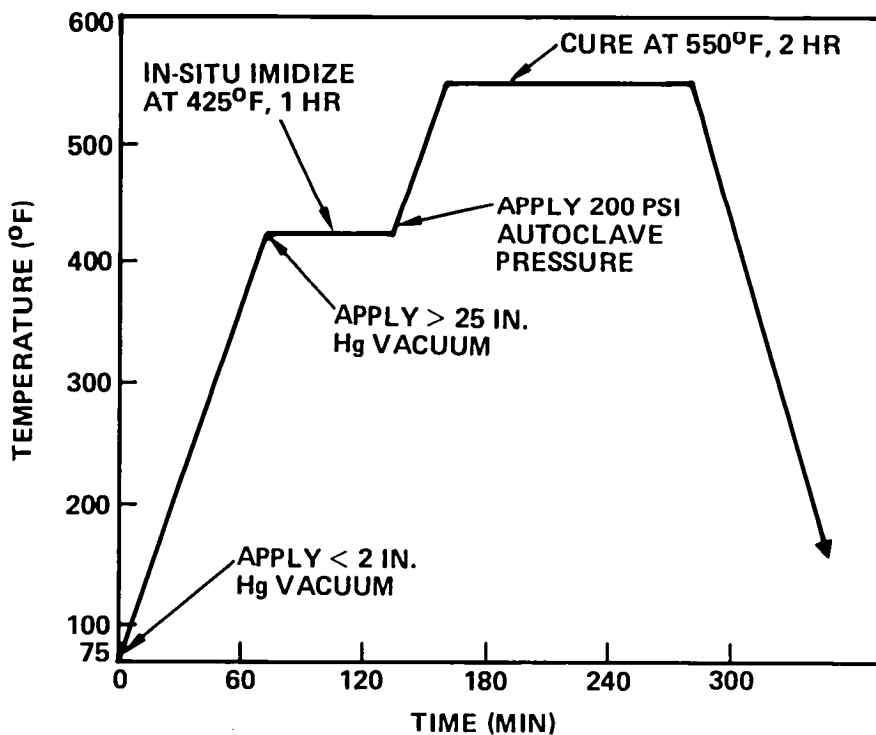
The autoclave molding process must be applied to complex, compound contoured parts. Aluminum or steel have been demonstrated satisfactorily as hard baseline tools; however, the bag, or soft tooling side created a problem because of the wrinkling caused by the Kapton film bag and the inability to conform to tight radii; therefore, molded silicone and a new fluoro rubber compound (D Aircraft SMC 250 and FMC 165) were evaluated for the pressure intensifier caul application.

IMPROVED SINGLE STAGE CURE

- INSITU IMIDIZE AT 425 F, < 2 INCHES Hg VACUUM; REMOVES VOLATILES < 1%
- APPLY 200 PSI AFTER IMIDIZING – NO FLOW
- RESIN SEEKS NATURAL HOT MELT FLOW AT ~ 525 F – 550 F
- PREPREG NET RESIN CONTENT. CONTROLLED RESIN FLOW, BLEEDER LESS MOLDING ACHIEVED
- POSTCURE FREESTANDING AT 600 F, 4 HOURS



INSITU IMIDIZING CURE CYCLE TOOLING



IMPROVED CELION/LARC-160 INSITU IMIDIZING CURE CYCLE

Figure A-4. Standard Celion/LARC-160 Cure Cycle and Tooling

Results of this study showed that:

1. Both SMC 250 silicon rubber and FMC 165 fluoro rubber caults imparted the desired wrinkle-free, sharply defined laminate surfaces.
2. The silicon rubber reverts in proximity of LARC-160 curing by-products.
3. The fluoro₂ rubber does not revert and has been utilized in multiple 1,378 KN/m² (200 psi) autoclave cures in the (288°C to 316°C) 550°F to 625°F temperature range.

A.3.5 Single-Stage Process

The basic imidizing and cure cycle parameters (Section A.2.2) that were used in the two-stage cure cycle were combined into the single-stage in-situ curing process, as illustrated in Figure A-4. The in-situ imidizing and cure flat laminate tooling concept is also shown in Figure A-4. Laminates require a freestanding oven postcure at 310°C, 600°F for 4 hours to achieve the required TMA-TG of greater than 330°C. This simplified process, in combination with tooling innovations, yielded the following advantages over previous cure cycles:

1. Chance of error in prediction resin flow point is eliminated when augmented pressure is applied immediately after completion of the imidizing cycle, because the LARC-160 resin is in a solid form.
2. The LARC-160 resin is allowed to seek its normal hot melt flow point in the temperature range of 288°C (525°F to 550°F) while under constant augmented pressure, causing detrimental effects of varying part thickness or tooling mass are eliminated.
3. The process is simplified and less costly since the separate imidizing process is eliminated and parts can be imidized and cured in a single operation, thus eliminating multiple bagging and debagging operations.
4. Tooling improvements eliminated the perforated caul plates, and thus eliminated the uncontrolled loss of resin through perforations during the in-situ imidizing and cure process.
5. Bleederless molding techniques allowed the use of almost net resin solids in prepreg tapes and fabrics, thus eliminating the need for cumbersome and costly bleeder material.
6. Fluoro rubber pressure intensifier caults provide the technique for imparting smooth surfaces to complex-shaped parts.

To qualify the process, unidirectional laminates were molded, and flexural and short beam shear (SBS) tests were performed at room temperature and 600°F.

Test results showed the process to yield laminate mechanical properties that were at least equivalent to laminates typically produced using the FY 1980 IR&D two-stage and ref. 1 processes. Laminate flexural and SBS test values obtained from the three processes are shown graphically in Figure A-5.

A.4 CONTROL SPECIMEN FABRICATION, TEST, AND EVALUATION

Tensile coupon control specimens $(0, \pm 45, 90)_{2s}$ fiber orientation were required to establish baseline tensile strength values for an undamaged laminate. This 16-ply laminate configuration, 0.229 cm (0.091 in.) thickness was employed in the NASA LaRC flat laminate, sandwich, and a hat-stiffened skin-stringer baseline elements. Strength data were used as target criteria for repair joint efficiencies at room temperature and 316°C (600°F) test temperatures.

A.4.1 Fabrication Procedures and Results

A $(0, \pm 45, 90)_{2s}$ - 16-ply laminate EX349 63.5 by 53.5 by 0.23 cm (25 by 25 by 0.09 in.) was processed from prepreg batch 2W4886 R1 by preimidizing at 218°C (425°F) for 45 minutes and then rebagging and autoclave curing at 316°C (600°F), 1,378 KN/m² (psi) for 2 hours using procedures described in Section 12. The panel was postcured freestanding at 316°C (600°F) for 4 hours.

Small resin beads formed at laminate edges indicating desired flow occurred during cure. Laminate surfaces were smooth and uniform with the exception of three 5.08 cm (2.0 in.) long tow splices noted on one surface. NDI C-scan A sensitivity tests showed approximately 96 percent ultrasound through transmission after cure. This void area appeared to increase after postcure, yielding approximately 90 percent ultrasound transmission. A C-scan recording of the postcured laminate is shown in Figure A-6.

A.4.2 Testing Procedures

Tension coupons were machined to the configuration shown in Figure A-7. Specimens were tested at room temperature and 316°C (600°F) at a load rate of 0.127 cm (0.05 in.) per minute after stabilizing 10 minutes at 316°C (600°F).

A.4.3 Evaluation

Tensile strength of the $(0, \pm 45, 90)_{2s}$ laminate averaged 392 and 450 MN/m² (56.9 and 65.2 ksi) or 951 and 1,072 KN/m (5,429 and 6,127 lb/in.). Values were used as target strength levels for repair bond joints during the program. Detailed tensile strength, elastic modulus, elongation, and laminate physical properties are presented in Table A-3.

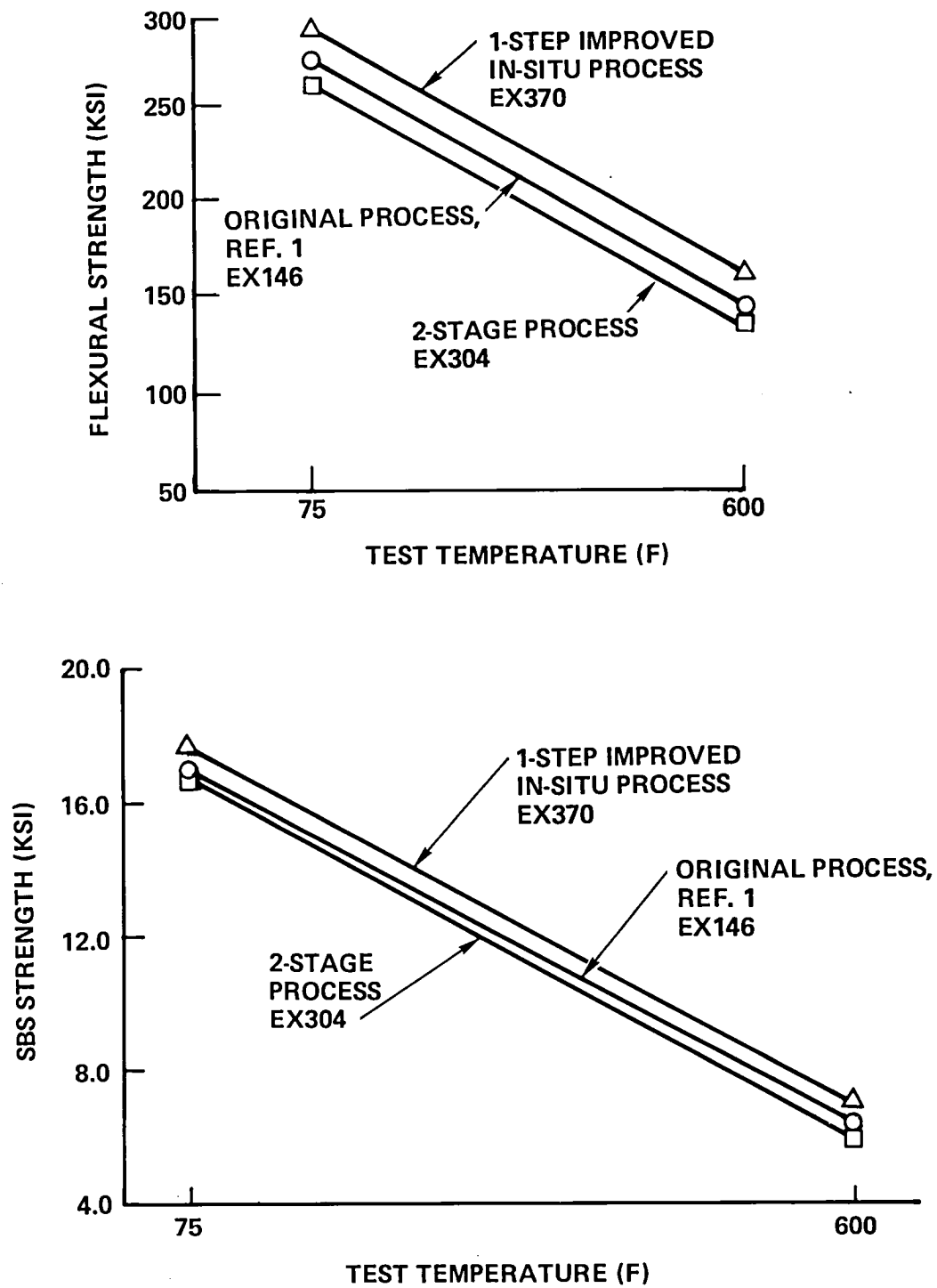


Figure A-5. Mechanical Properties of Celion/LARC-160 Laminates - Three Different Cure Cycles

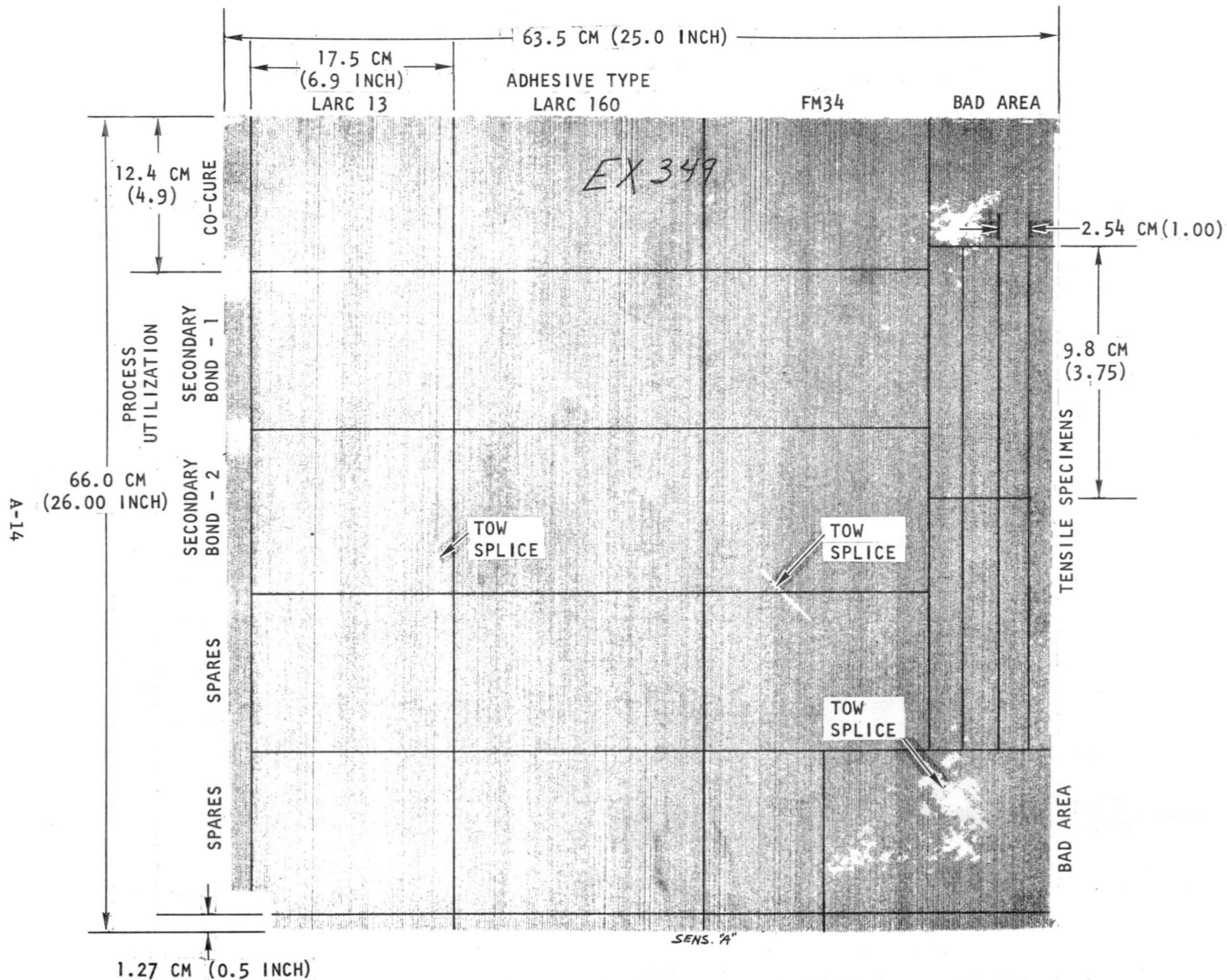


Figure A-6. NDI C-Scan A Sensitivity Recording of Adhesive Screening Adherend Panel Stock and Utilization Plan

A-15

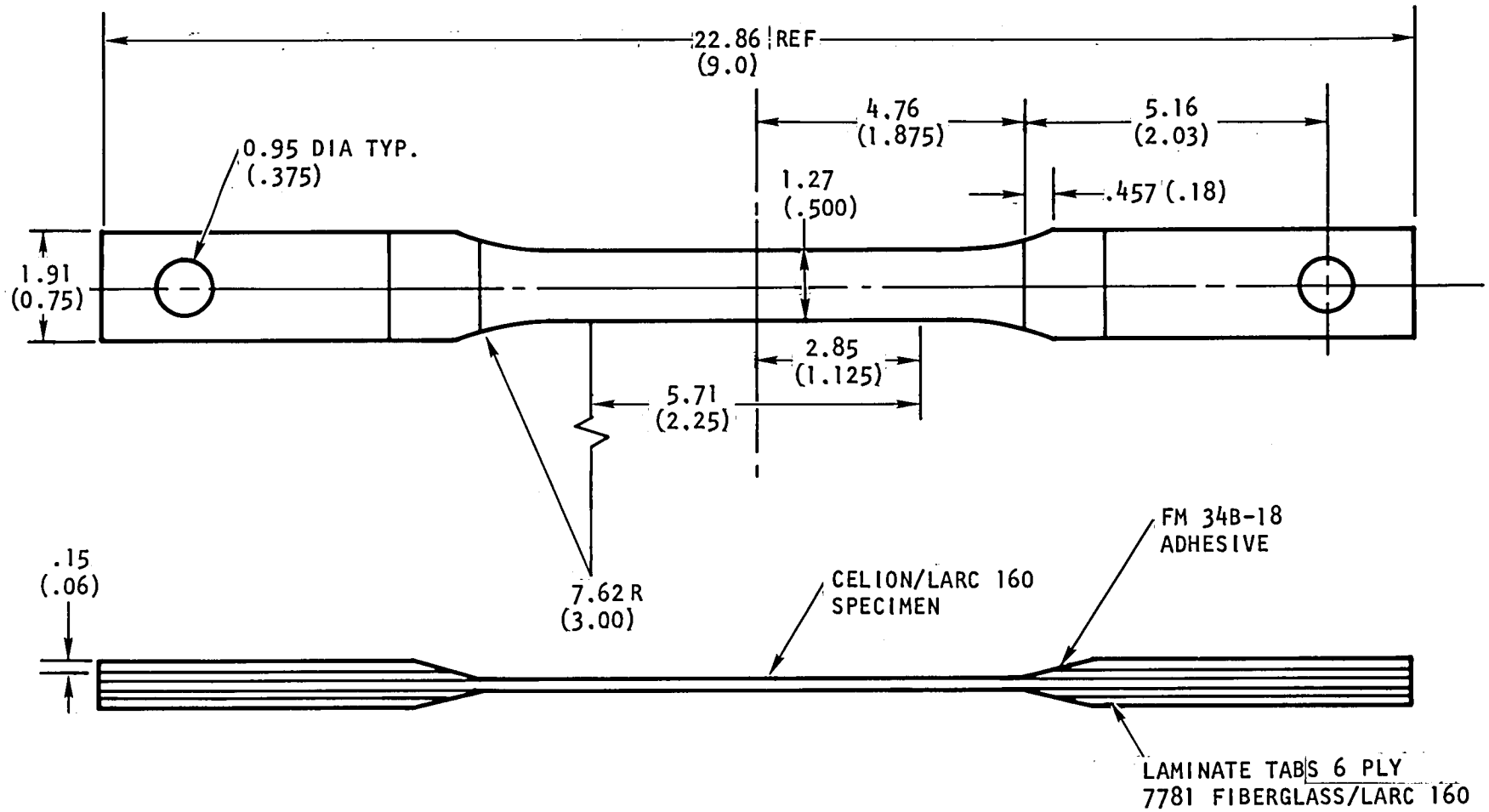


Figure A-7. Tensile Specimen Configuration

A-16

Table A-3. Tensile Properties of Celic LARC-160
(0, +45, 90)_s Oriented Quality Assurance Panel

Specimen No.	Test (1) Temperature C (F)	F _{tu}		E _t		Ult (%)	Ultimate Load	
		MN/m ²	(KSI)	GN/m ²	(MSI)		KN/m	(lb/in.)
EX349-1	24		53.7		5.2	1.10		4,293
-2	(75)		58.2		6.5	0.95		6,834
-3			58.3		5.9	1.05		5,795
-4			60.5		5.9	1.05		4,792
	Avg	392	56.9	40.7	5.9	1.05	951	(5,429)
	Average Normalized Property, 60% F/V	404	(58.7)	41.9	(6.08)			
EX349-5	316		70.8		7.3	1.05		7,083
-6	(600)		66.0		5.7	1.12		6,323
-7			63.4		5.8	1.15		6,113
-8			62.6		5.5	1.12		4,990
-9			63.0		5.9	1.10		6,127
	AVG	450	65.2	41.3	6.0	1.10	1,072	(6,127)
	Average Normalized Property, 60% F/V	464	(67.2)	42.5	(6.18)			

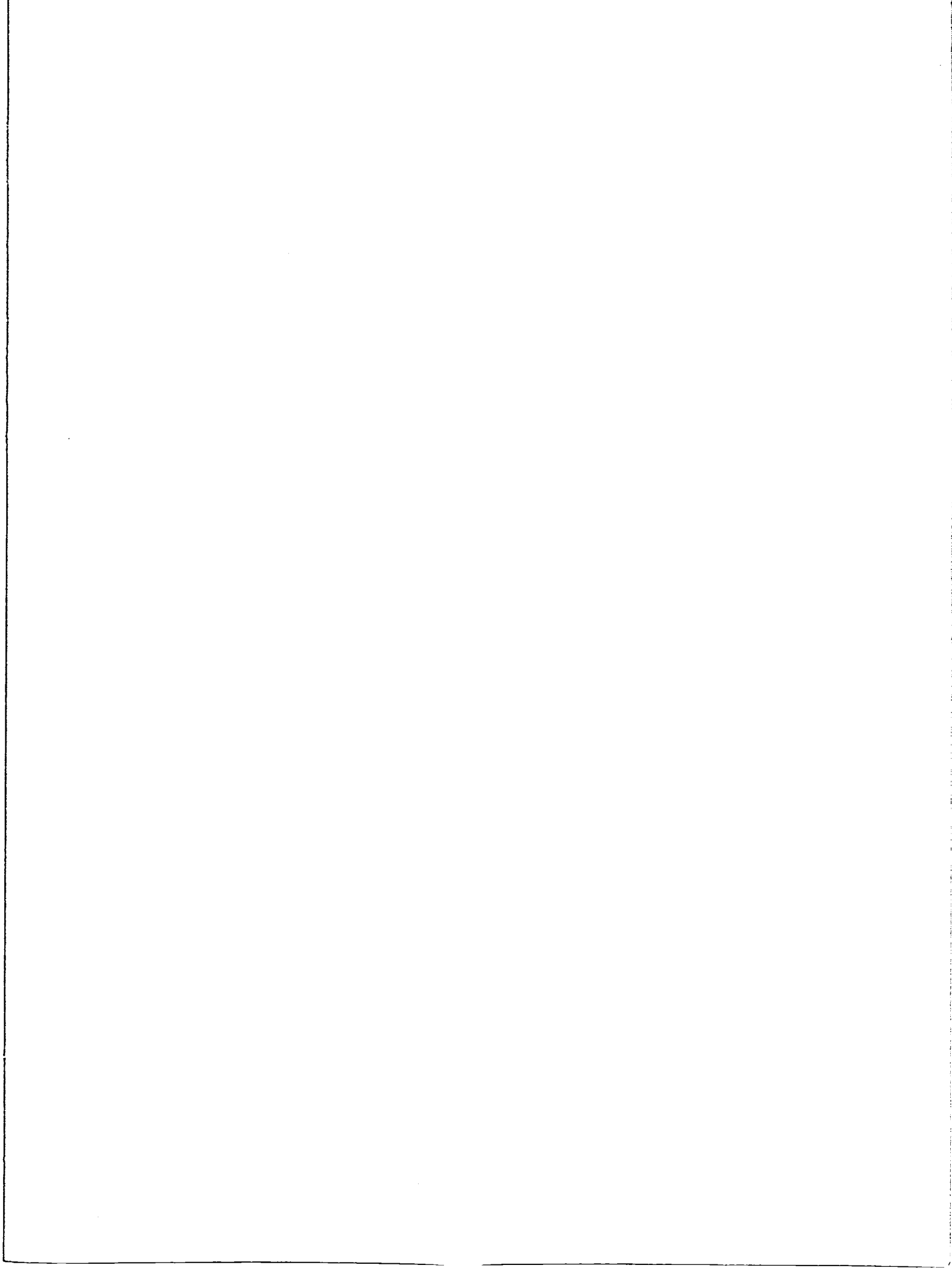
PHYSICAL PROPERTIES LAMINATE

Density (gram/cc)	Resin Content (%)	Fiber Vol (%)	Void Vol (%)	Thickness (2)		C-Scan Transmission (%)
				Calculated cm (mils)	Actual cm (mils)	
1.562	34.61	58.2	-0.01	0.225 (88.6)	0.203-0.239 (80-94)	95

(1) Specimens were tested after stabilizing at test temperatures for 10 minutes +5 at a load rate of 0.05 inch/minute.

(2) Calculated composite thickness based on USP batch 2W4886R1 prepreg Areal fiber weight of 148 grams/m²;

1. Report No. NASA CR-3794		2. Government Accession No.		3. Recipient's Catalog No.	
4. Title and Subtitle REPAIR TECHNIQUES FOR CELION/LARC-160 GRAPHITE/POLYIMIDE COMPOSITE STRUCTURES				5. Report Date June 1984	
				6. Performing Organization Code	
7. Author(s) J.S. Jones and S.R. Graves				8. Performing Organization Report No. STS 81-0352-12	
9. Performing Organization Name and Address Rockwell International Space Transportation and Systems Group 12214 Lakewood Blvd., Downey, CA 90241				10. Work Unit No.	
				11. Contract or Grant No. NAS1-16448	
12. Sponsoring Agency Name and Address National Aeronautics and Space Administration Washington, D.C. 20546				13. Type of Report and Period Covered Contractor Report	
				14. Sponsoring Agency Code	
15. Supplementary Notes Langley Technical Monitor: Jerry W. Deaton Final Report					
16. Abstract Operational feasibility of the next generation of reusable space vehicles requires the development of a structural material system that is significantly lighter than the conventional aluminum structure presently employed on the Space Shuttle orbiter. Utilization of graphite filament reinforced polyimide matrix composite material, capable of 600°F service, can achieve this goal. The large stiffness-to-weight and strength-to-weight ratios of graphite composite in combination with the 600°F structural capability of the polyimide matrix can reduce the total structure/TPS weight by 20-30 percent. In order for the graphite/polyimide (GR/PI) material system to be acceptable for use in advanced space transportation systems, it is necessary that manufactured components be maintained in a safe and economical manner. It is inevitable that with planned usage of GR/PI structural components, damage will occur either in the form of intrinsic flaw growth or mechanical damage. Research and development programs were initiated to develop repair processes and techniques specific to Celion/LARC-160 GR/PI structure. The study was directed toward highly loaded and lightly loaded compression critical structures for factory type repair. Repair processes included cocure and secondary bonding techniques applied under vacuum plus positive autoclave pressure. Viable repair designs and processes were developed for flat laminates, honeycomb sandwich panels, and hat-stiffened skin-stringer panels. The repair methodology was verified through structural element compression tests at room temperature and 315°C (600°F).					
17. Key Words (Suggested by Author(s)) Graphite/polyimide structures repair, laminates, sandwich, hat-stringer, design, analysis, techniques, adhesives, composite processing, compression testing RT and 600°F, results.			18. Distribution Statement Unclassified - Unlimited Subject Category 24		
19. Security Classif. (of this report) Unclassified	20. Security Classif. (of this page) Unclassified	21. No. of Pages 209	22. Price A10		



National Aeronautics and
Space Administration

Washington, D.C.
20546

Official Business

Penalty for Private Use, \$300

SPECIAL FOURTH CLASS MAIL
BOOK

Postage and Fees Paid
National Aeronautics and
Space Administration
NASA-451



Wesley Stewart

NASA

POSTMASTER: If Undeliverable (Section 158
Postal Manual) Do Not Return
